UNIVERSIDAD AUTONOMA DE NUEVO LEON

SCHOOL OF BIOLOGICAL SCIENCES

STUDY OF THE MECHANISM AND IMMUNOGENICITY OF THE CELL DEATH INDUCED BY PKHB1 AND IMMUNEPOTENT-CRP IN BREAST CANCER
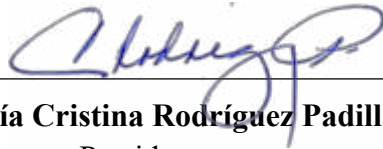
BY

KENNY MISAEL CALVILLO RODRÍGUEZ

IN PARTIAL FULFILMENT OF THE REQUIREMENT FOR THE DEGREE OF

DOCTOR OF SCIENCE
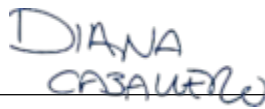WITH ORIENTATION IN IMMUNOBIOLOGY

2023

STUDY OF THE MECHANISM AND IMMUNOGENICITY OF THE CELL DEATH INDUCED BY PKHB1 AND IMMUNEPOTENT-CRP IN BREAST CANCER
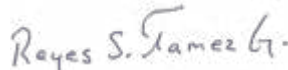

Dr. María Cristina Rodríguez Padilla.
Presidente

Dr. Diana E. Caballero Hernández.
Secretario

Dr. Reyes S. Taméz Guerra.
Vocal 1

Dr. Diana Reséndez Pérez.
Vocal 2
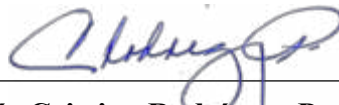

Dr. Philippe Karoyan.
Vocal 3

Dr. Katiuska Arévalo Niño.
Subdirector de posgrado

STUDY OF THE MECHANISM AND IMMUNOGENICITY OF THE CELL DEATH INDUCED BY PKHB1 AND IMMUNEPOTENT-CRP IN BREAST CANCER

Dirección de Tesis

Dr. María Cristina Rodríguez Padilla.
Director

Dr. Philippe Karoyan.
Director externo

SPECIAL ACKNOWLEDGEMENTS

ACKNOWLEDGEMENTS

To Dr. Cristina Rodríguez Padilla, for their support, advice and for the effort they make to ensure that the laboratory, researchers, and students have the necessary tools to work and continue contributing to science.

Dr. Philippe Karoyan, thank you for supporting and trusting my work, for your words of encouragement, for inspired me with your scientific spirit. Thank you for allowing me to work in your laboratory in Paris, and for helping me to think out of the box.

Thanks to the members of my thesis committee.

To Dr. Diana E. Caballero Hernández, for her great guide in the handling of the *in vivo* model and for always being willing to support me.

To Dr. Reyes Taméz, thank you for the great technical support provided by you and your lab.

To Dr. Diana Reséndez Peréz for her advice during the writing of my thesis and her motivation to continue working hard.

To my friends from Lab 14, with whom I have shared many good and bad things, who every day inspire me with their desire to do science and motivate me to keep working, from whom every day I learn something new. Thank you to each one of you, María, Rodolfo, Rafa, Ana, Mizael, Daniel, Blanca, and Andrea. Helen thank you for fighting with me, as sometimes I need it. Alejandra Reyes, thank you for always questioning me and not believing everything I say. Thank you, L-14, for your trust and unconditional support.

To my friend Luis, thank you for always supporting me during my thesis work.

To my friend Karla and Alejandra who are an example of perseverance and dedication, and who despite the distance continue to support me and show me their affection.

To my friends (SCs), Erick, Fernando (freezer), Adrian, Victor, Luis (güero), Paco, Mario, Michel, Augusto, Alex (keko) and Brandon (friend, I will always give the 100%). Thank you for being with me in good and in bad times and that, despite the years, the distance, and the circumstances, I am sure that I can always count on you in any situation.

To my family.

Mom and Dad (Flor and Juan) all my life I will be grateful to you for give me your unconditional love and for guiding me to be the person I am today. I will always be proud to be your son.

Thank you to my brothers Kenya and Toño, for being who you are with me, for understanding me, for trusting me, for making me angry.... and above all for making me proud to be his brother.

To my love, Carolina there are not enough words to express my gratitude to you. Thank you for challenging me and for listening to my ideas. Thank you for sharing with me your experiences in the work and life, you can't imagine how much they helped me. Thank you for getting up when I failed and for helping me have confidence in myself, thank you for making me see that my limits are further away than I thought. Thank you for loving me and for always supporting me, you are my inspiration. Thank you for our beautiful baby, Kenny Elian and for our princess Amelie and Citlalli, I will work for to be a good researcher and above all to be the best father and husband, I always want to enjoy the life with you.

I love you family; this is all for you.

INDEX

ABSTRACT

Breast cancer is the most diagnosed cancer and the main cause of cancer death in women worldwide. The latest advances in immuno-demonstrate the beneficial immunostimulatory effects of the induction of immunogenic cell death (ICD). ICD increases tumor infiltration by anti-tumor cells and is associated with improved prognosis in different types of cancer including triple negative breast cancer (TNBC). The aim of this thesis was to evaluate the antitumoral effect and the immunogenicity of the cell death induced by PKHB1, a thrombospondin-1 peptide mimic, and the effect of the bovine leukocyte extract Immunepotent-CRP (ICRP) against breast cancer cells *in vitro*, *ex vivo*, and *in vivo*. Results showed that PKHB1 and ICRP induce mitochondrial alterations, ROS production, intracellular Ca^{2+} accumulation, as well calcium-dependent cell death in breast cancer cells, including triple negative subtypes, additionally ICRP induce a ROS dependent type of cell death. PKHB1 has antitumor effect *in vivo* leading to a reduction of tumor volume and weight and promotes intratumorally CD8 + T cell infiltration. Furthermore, *in vitro*, PKHB1 and ICRP induces calreticulin (CALR), HSP70, and HSP90 exposure and release of ATP and HMGB1. Additionally, killed cells obtained after treatment with PKHB1 (PKHB1-KC) or ICRP (ICRP-KC) induced dendritic cell maturation, and T cell antitumor responses, *ex vivo*. Moreover, PKHB1-KC and ICRP-KC *in vivo* were able to induce an antitumor response against breast cancer cells in a prophylactic application, whereas in a therapeutic setting, PKHB1-KC and ICRP-KC induced tumor regression; both applications induced a long-term antitumor response. Altogether our data shows that PKHB1 and ICRP, induce *in vivo* antitumor effect and promote immune system activation through immunogenic cell death induction in breast cancer cells.

RESUMEN

El cáncer de mama es el cáncer más diagnosticado y la principal causa de muerte por cáncer en mujeres a nivel mundial. Avances recientes en el campo de inmunooncología demuestran los beneficiosos efectos inmunoestimuladores de la inducción de la muerte celular inmunogénica (MCI). La MCI aumenta la infiltración de células T al tumor y se asocia con un mejor pronóstico en pacientes afectados por diferentes tipos de cáncer, incluyendo el cáncer de mama triple negativo (TNBC) con enfermedad residual. El objetivo de esta tesis fue evaluar el efecto antitumoral y la inmunogenicidad de la muerte celular inducida por PKHB1 y el extracto dializable de leucocitos bovinos, Immunepotent-CRP (ICRP), en células de cáncer de mama, *in vitro*, *ex vivo* e *in vivo*. Los resultados mostraron que PKHB1 e ICRP inducen alteraciones mitocondriales, producción de ROS, acumulación de Ca^{2+} intracelular, así como muerte celular dependiente de calcio en células de cáncer de mama, incluidos los subtipos triple negativos, además observamos que el ICRP induce muerte celular dependiente de ROS. El PKHB1 tiene un efecto antitumoral *in vivo* que conduce a la reducción del volumen y peso tumoral, promoviendo la infiltración de células T CD8+ intratumorales. Además, *in vitro*, PKHB1 e ICRP inducen la exposición de calreticulina (CALR), HSP70 y HSP90 y la liberación de ATP y HMGB1. Además, las células muertas obtenidas después del tratamiento con PKHB1 (PKHB1-KC) o ICRP (ICRP-KC) indujeron la maduración de células dendríticas y activaron la respuesta antitumoral de células T, *ex vivo*. Además, PKHB1-KC e ICRP-KC *in vivo* indujeron una respuesta antitumoral contra las células de cáncer de mama en una aplicación profiláctica, mientras que en un entorno terapéutico, PKHB1-KC e ICRP-KC indujeron la regresión tumoral; ambas aplicaciones promovieron una respuesta antitumoral a largo plazo. En conjunto, los datos muestran que PKHB1 e ICRP tienen un efecto antitumoral *in vivo* e inducen la activación del sistema inmunológico a través de la inducción de muerte celular inmunogénica en células de cáncer de mama.

BACKGROUND

Cell death

Every day, our cells carry out an endless number of processes that are essential for the organism's maintenance and the appropriate functioning. Within these processes the cell death, which mainly occur in cells with physical damage, infected with pathogenic agents or with genetic abnormalities which make impposible the maintaining of their functions. Thus, the irreversible cessation of essential cellular processes might be referred to as cell death. To precisely identify a dead cell, the Cell Death Nomenclature Committee (NCCD) has set three criteria:

1. The plasma membrane's irreversible loss of its barrier properties.
2. The fragmented breakdown of the cell.
3. Intake of the cells by cells with phagocytic activity (L Galluzzi et al. 2012).

Cell death can by triggered by different pathways and use different cellular mechanisms, which complicate the classification of a certain type of cell death, for this reason the Nomenclature Committee on Cell Death (NCCD), define different priciples for the interpretation of all aspects of cell death (Lorenzo Galluzzi et al. 2018). Currently, the NCCD classifies cell death into two broad categories, described below and schematized in Figure 1.

Accidental cell death (ACD)

ACD is a type of immediate death, caused by physical (high temperatures or pressures), chemical (variations in pH, detergents) or mechanical damage, unresponsive to pharmacological or genetic interventions.

Regulated cell death (RCD)

RDC comprise of a molecular machinery genetically encoded, which can be modulated pharmacologically or genetically, using the key components of this machinery as a target, as caspases, calpains, ROS, among others. Regulated cell death can be activated during immune responses, tissue homeostasis and among all during embryonic development. Programmed cell death is the term to describe the completely physiological cases (L Galluzzi et al. 2012). Pyroptosis and necroptosis, which are seen during development or in the context of viral infections, are examples of subtypes of RCD that can be categorized based on their molecular characteristics. Other subtypes of RCD, such as ferroptosis, netotic cell death, entotic cell death, parthanatos, lysosome dependent cell death, autophagy-dependent cell death, oxeiptosis, and alkaliptosis, are less studied and may be limited to cellular responses to specific molecules (as toxins) that do not reflect normal physiology (Tang et al. 2019). Genetic or pharmaceutical interventions are now employed to interrupt the lethal cascade that conclude in cell death for finally describe or classify the cell death mechanism (Tang et al. 2019).

Programed cell death (PCD)

It's a pathway conserved for the embryonic development and tissue homeostasis. PCD operate as a typical physiological response to different stimuli that results in the elimination of aberrant cells, infected or dysfunctional cells (Sjostrom 2001).
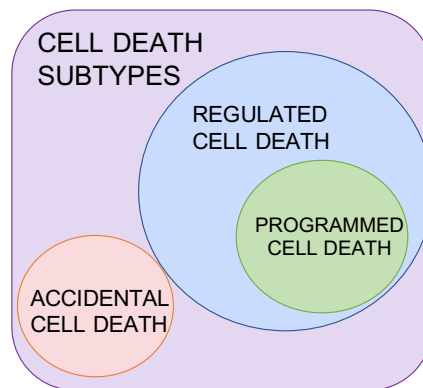
Figure 1. Cell death subtipes. Extreme mechanical stressors, physical or chemical, cause cells to virtually instantly die and losing their structural integrity at the same time. Accidental cell death

(ACD) is the name given to this form of cell death. On the other hand, regulated cell death (RCD) refers to cell death that is initiated by a molecular machinery that is genetically encoded. Programmed cell death (PCD) refers to instances of RCD that take place as part of a physiological process to preserve tissue homeostasis (L. Galluzzi et al. 2015).

Classification of RCD

Modulation of intracellular signaling is crucial for cell survival or death. Signaling for cell death can be activated after stimulation of damage to cellular structures, death receptors, deregulation of the system that controls ion movements across cell membranes or other stimuli. The main actors in the signaling pathway determine the type of cell death that would be triggered. In this sense, apoptotic cell death is determined by caspases (cysteine-dependent aspartate-directed proteases), while the autophagic machinery rules autophagic cell death. Moreover, executors of cell death may also participate in cell survival; for example, some caspases are involved in inflammation, proliferation, among others, also autophagosome formation is crucial for the removal of damaged or unnecessary organelles (Galluzzi et al. 2018). Thus, it is thought that the decision of die or survive relies on the nature of the stimuli, and in the status of the cell. The inhibitory and promoting-RCD signals coexist and balance one another, and at some stage one predominates over the other. The NCCD has also classified the different cell death modalities described until now, based on the molecular aspects that are essential for the process (Table 1). However, it is important to mention that an interconnection can exist between different cell death modalities (Galluzzi et al. 2018).

Hallmarks of major types of RCD
Type	Biochemical characteristics	Major regulators	Major inhibitors
Apoptosis	Activation of caspases; DNA fragmentation; $\Delta\Psi m$ disruption; Phosphatidilserine exposure	Positive: initiator caspase (2, 8, 9, and 10), effector caspase (3, 6, and 7); pro-apoptotic BLC2 family (e.g. BAK, BAX, BOK, BCL2L11, BBC3, PMAIP1, and BID) TP53 Negative: anti-apoptotic BCL-2 family (BCL2, BCL2L1, MCL1, BCL2L2 and BCL2L10)	Inhibitors of pan caspases Z-VAD-FMK; emricasan; QVD-OPh; Z-VAD (OH)-FMK Z-DEVD-FMK (Caspases 3, 6, 7, and 10) Z-VDVAD-FMK (CASP2); ivachtin (CASP2)
Necroptosis	Activation of RIPK1, RIPK3, and MLKL; cytosolic necrosome formation	Positive: RIPK1, RIPK3 and MLKL. Negative: ESCRT-III, cIAPs, LUBAC, PPM1B, and AURKA	Necrostatin-1 (RIPK1); GSK872 (RIPK3); HS-1371 (RIPK3); necrosulfonamide (MLKL)
Pyroptosis	Activation of CASP1, CASP3, and GSDMD; GSDMD cleavage; GSDMD-N-induced pore formation	Positive: CASP1, CASP11, and GSDMD Negative: GPX4, ESCRT-III, PKA	AcYVAD-cmk (CASP1); Z-YVAD(OMe)-FMK (CASP1); wedelolactone (CASP11); Ac-FLTD-CMK (GSDMD cleavage); MCC950 (NLRP3-inflamosome)
Ferroptosis	Iron accumulation; lipid peroxidation; $\Delta\Psi m$ dissipation; MAP1LC4B-I to MAP1LCEB-II conversion; glutaminolysis; caspase-independent	Positive; TFRC, ACSL4, LPCAT3, ALOX15, GLS2, DPP4, NCOA4, BAP1, BECN1, PEBP1, CARS, VDAC2/3, RAB7A, HSP90, and ALK4/5 Negative; SLC7A11, GPX4, NFE2L2, HSPB1, HSPA5, FANCD2, NFS1, ITGA6, ITGB4, and OTUB1 Dual: TP53	Deferoxamine (Fe); cyclopirox (Fe); deferiprone (Fe); Ferrostatin-1 (ROS); liproxatin-1 (ROS); β-mercaptoetanol (ROS), vitamin-E (ROS); β-carotene (ROS), NAC (ROS), XJB-5-131 (ROS); zileuton (ROS) vildagliptin (DPP4), alogliptin (DPP4); thiazolidinedione (ACSL4); rosiglitazone (ACSL4); selenium (GPX4)
Parthanatos	Excesive activation of PARP1; $\Delta\Psi m$ dissipation; caspase-independent; NAD+ and ATP depletion; accumulation; accumulation of poly ADP-ribose (PAR) polymers; AIFM1 release from mitochondria to nucleus	Positive; PARP1, AIFM1, MIF, and OGG1 Negative; ADPRHL2 and RNF146	BYK204165 (PARP1); AG-14361 (PARP1); iniparib (PARP1)
Entotic cell death	Activation of adhesion proteins and actomysin; LC3associated phagocytosis	Positive: CDH1, CTNNA1, AMPK, RHOA, ROCK, myosin, ATG5, ATG7, PI3KC3, BECN1, CYBB, UVRAG, and RUBCN	C3-toxin (RHOA), Y-27632 (ROCK), bebbistatin (myosin)

Table 1. Hallmarks of major types of RCD (adapted from Tang, D. et al 2019).

Calcium and cell death

It has been shown that the depletion of the ER Ca^{2+} pool or ER-Ca^{2+} overload results in disturbances that can lead to endoplasmic reticulum stress and cell death (Figure 2) (Zhivotovsky and Orrenius 2011). As Ca^{2+} is a highly versatile second messenger, it regulates broad cellular functions, and disturbances in Ca^{2+} homeostasis can lead to cell death (Monteith, Prevarskaya, and Roberts-Thomson 2017). Ca^{2+} alterations can lead to the activation of different cell death effectors and the induction of distinct types of regulated cell death mechanisms, such as caspase-dependent and caspase-independent cell death modalities, in different cancer types (figure 2) (Danese et al. 2021).
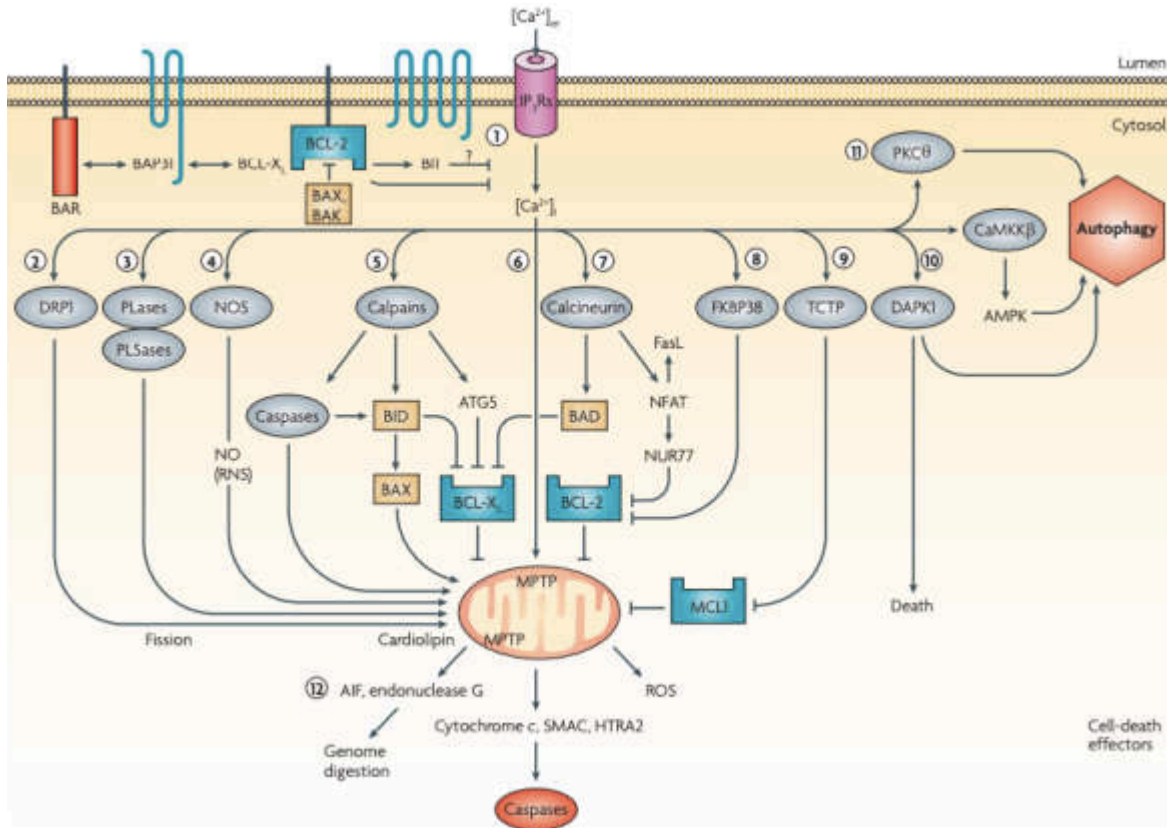
Figure 2. Calcium pathways related to cell death. Calcium could be a central mediator for the activation of diverse molecules related to the inhibition or stimulation of cell death such as: DRP-1, PLases, NOS, caspases, calpains, calcineurin, FKBP38, TCTP, DAPK1, PKC, CaMKK and AIF. The result of the signaling induced by the different molecules, depends on the context and the trigger. Also, mitochondrion have an important role for the cell death induction. (Danese et al. 2021).

Deregulation of cell death and associated pathologies

Two main physiological mechanisms that control homeostasis in the body are cell division and death. Deregulation of these processes increase the pathogenesis of different diseases, such as neurological conditions, myocardial infarction, atherosclerosis, cerebrovascular accidents, cancer, among others. Therefore, recently the research focus on the search of cell cycle and cell death modulators for develop new therapeutic approaches to treat these diseases.

Furthermore, deregulation in the cell death machinery can result in death resistance, which is associated with carcinogenesis. In fact, the cell death-resistance is one of the hallmarks of cancer cells, as well one of the principal targets of anti-cancer therapies (Hanahan and Weinberg 2011).

Cancer

Cancer is a generic term for a wide group of diseases that can affect several parts of the body. They are characterized by uncontrolled growth of abnormal cells, which can migrate to nearby organs and spread to other parts of the body, this process is known as metastasis and is the main problem to attend and the principal cause of death from cancer (Cancer n.d.). Nearly 10 million deaths caused by cancer and 19.3 million of new cases were expected to be occurred globally in 2020, with 28.4 million cases expected in 2040. The most commonly

diagnosed cancer in 2020 were breast, lung, colorectal, prostate and stomach cancers being lung cancer the most lethal type of cancer (Figure 3) (Sung et al. 2021).
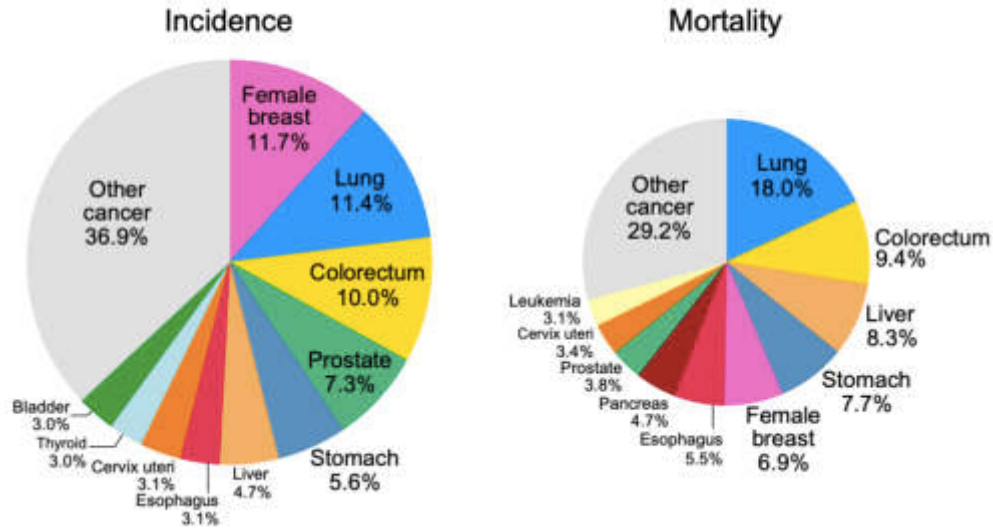
Figure 3. Distribution of cases and deats for the top 10 cancers in 2020 (Sung et al. 2021).

Despite its heterogeneity, all cancer diseases share different characteristics or hallmarks. This Hallmarks are characteristics or capabilities acquired by cancer cells and are crucial for their capacity to form malignant tumors (Figure 4). This hallmarks are: cell death resistance, growth suppressor evasion, angiogenesis induction, sustaining proliferative signaling, avoidance of immune destruction, replicative immortality, tumor-promoting inflammation, deregulation of cellular energetics, activation of metastasis and invasion, genome instability (Hanahan and Weinberg 2011) and recently added: polymorphic microbiomes and senescent cells, non-mutational epigenetic reprogramming, unlocking phenotypic plasticity (Hanahan 2022). As the hallmarks are important characteristics for the cancer development, this could represent treatment strategies to combat cancer diseases.
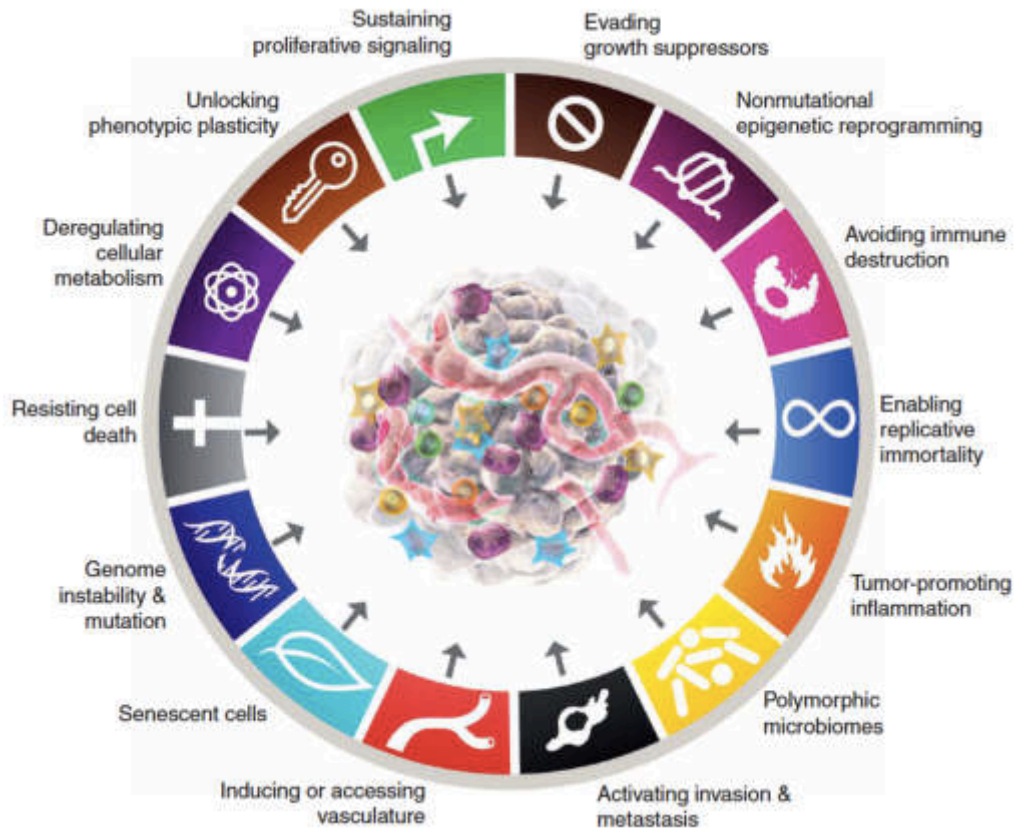
Figure 4. Hallmarks of Cancer. (Hanahan 2022)

Breast cancer

The most common type of cancer in women and the main cause of cancer-related deaths is breast cancer (Sung et al. 2021); The main challenge in treating BC is its innate and acquired treatment resistance to conventional therapies (figure 5). As the 5-year survival rates drop from 99% in localized disease to 27% when the cancer has spread to other organs, advanced metastatic cancer is the main cause of deaths of BC (Dias et al. 2019).

Figure 5. Global cancer incidence and mortality in women. (Sung et al. 2021).

Breast cancer comprises different tumor subtypes that present cellular and molecular heterogeneity. According to the presence or absence of the hormone receptors for estrogen and progesterone, and the epidermal growth factor receptor 2 (HER2) status it can be classified in different subtypes: luminal A, luminal B, HER2-enriched and the Triple negative breast cancer (TNBC) (Fig. 6). Additionally, the presence or absence of these receptors influences whether treatment should be employed. (Dias et al. 2019).

Figure 6. Breast cancer's molecular subtypes, including basal, claudin-low, normal-like, and metaplastic breast cancer (MBC), as well as their corresponding incidence, including luminal A, luminal B, HER2-enriched, and triple-negative breast cancer (TNBC). (Dias et al. 2019).

11

Cancer and the immune system

The dynamic interaction between the immune system and cancer cells has been observed for decades. Paul Ehrlich was the first to propose the hypothesis that host defense may combat the cancer cells in 1909. This hypothesis after was included in the "immune surveillance theory" by Lewis Thomas and Frank Burnet which suggest that the immune system constantly detect and eliminate cancer cells throughout the body. Until 2002, Dunn and Schreiber described that if mutated cells survive to the immune surveillance, they continue to interact with immune cells, initially in equilibrium, and finally escaping of the immune control to develop a tumor, and named this process as "cancer immunoediting" (Dunn et al. 2002; Gicobi, Barham, and Dong 2020).

Cancer immunoediting

Cancer immunoediting is a concept that describe the host-protective and the pro-tumor activities of the immune system, which could lead to the tumor rejection (elimination), control of residual tumor cells (equilibrium), or cancer-immune evasion (escape) (Gubin and Vesely 2022). Thus, the cancer immunoediting is a complex process that function to control or promote cancer (Figure 5). The innate and adaptive immune cells recognized and eliminate tumor cells to return to homeostasis of tissues during the elimination phase. However, if the immune system is unable to eliminate the tumor, the residual tumor variants could enter in the equilibrium phase, where adaptive immunity prevent tumor outgrowth. Finally, in the escape phase the cancer cells variants could acquire mutations and result in the evasion of

the immune attack or recognition, leading to the development of the tumor (figure 7) (Vesely et al. 2011).
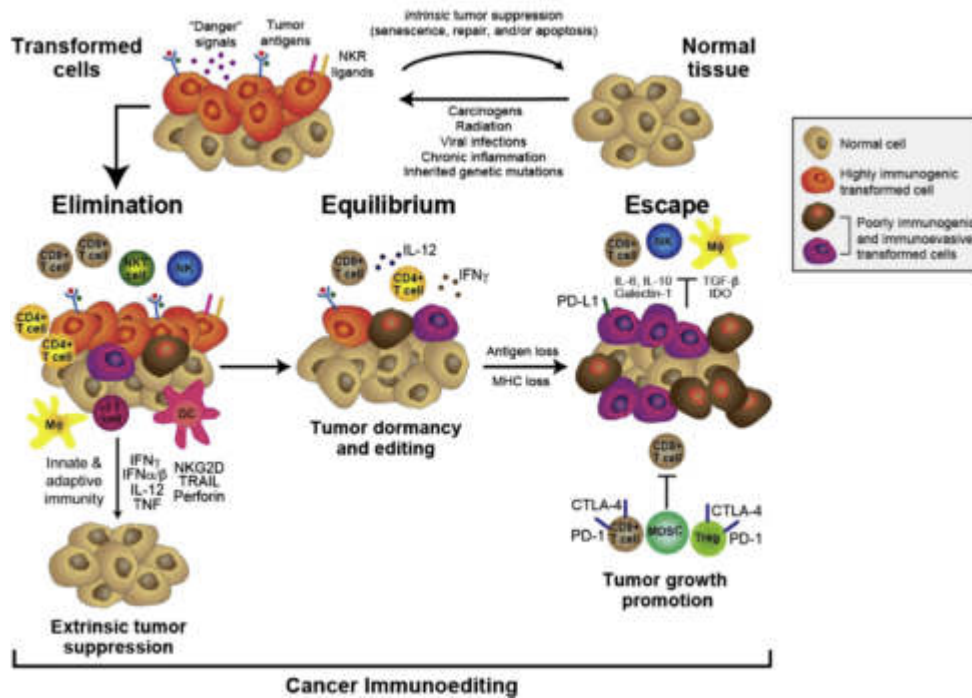
Figure 7. Cancer immunoediting. Schematic representation of the cancer immunoediting process (Lussier and Schreiber 2016).

Elimination

This phase considers that innate and adaptive immune system detect and eliminate cancer cells before it becomes clinically apparent. The immunologic elimination of a growing tumor involves the innate and adaptive antitumor response and initiate when the developed tumor disrupts the tissue surrounding leading to the emission of damage signals which alerted to the immune system.

The immune system could be alerted by different mechanisms, 1) tissue damage which can produce proinflammatory molecules that occurs because of the remodeling processes for the tumor microenvironment construction, the angiogenesis and tissue-invasive growth (two of the hallmarks of cancer), 2) release of danger or damage signals (DAMPs) by dying or

stressed cancer cells or 3) by the expression of stress ligands or tumor antigens in the surface of malignant cells (Dunn, Old, and Schreiber 2004; Schreiber, Old, and Smyth 2011).

After recognition of tumor cells, innate and adaptive immune cells could eliminate tumor cells by different mechanisms (figure 8) (Zitvogel, Tesniere, and Kroemer 2006). The mechanisms in the elimination phase are based in the general immune activation through antigen processing, presentation and T cell priming and effector responses (Maiorino et al. 2022).

Also, the innate immune system has antitumorigenic functions additionally to the antigen presentation and activation of adaptive responses, such as the direct cell death induction of tumor cells by NK, NKT, IKDC, γδT cells, among others, and the cytokine secretion's role in the augmentation of the immune responses (figure 8) (Maiorino et al. 2022).
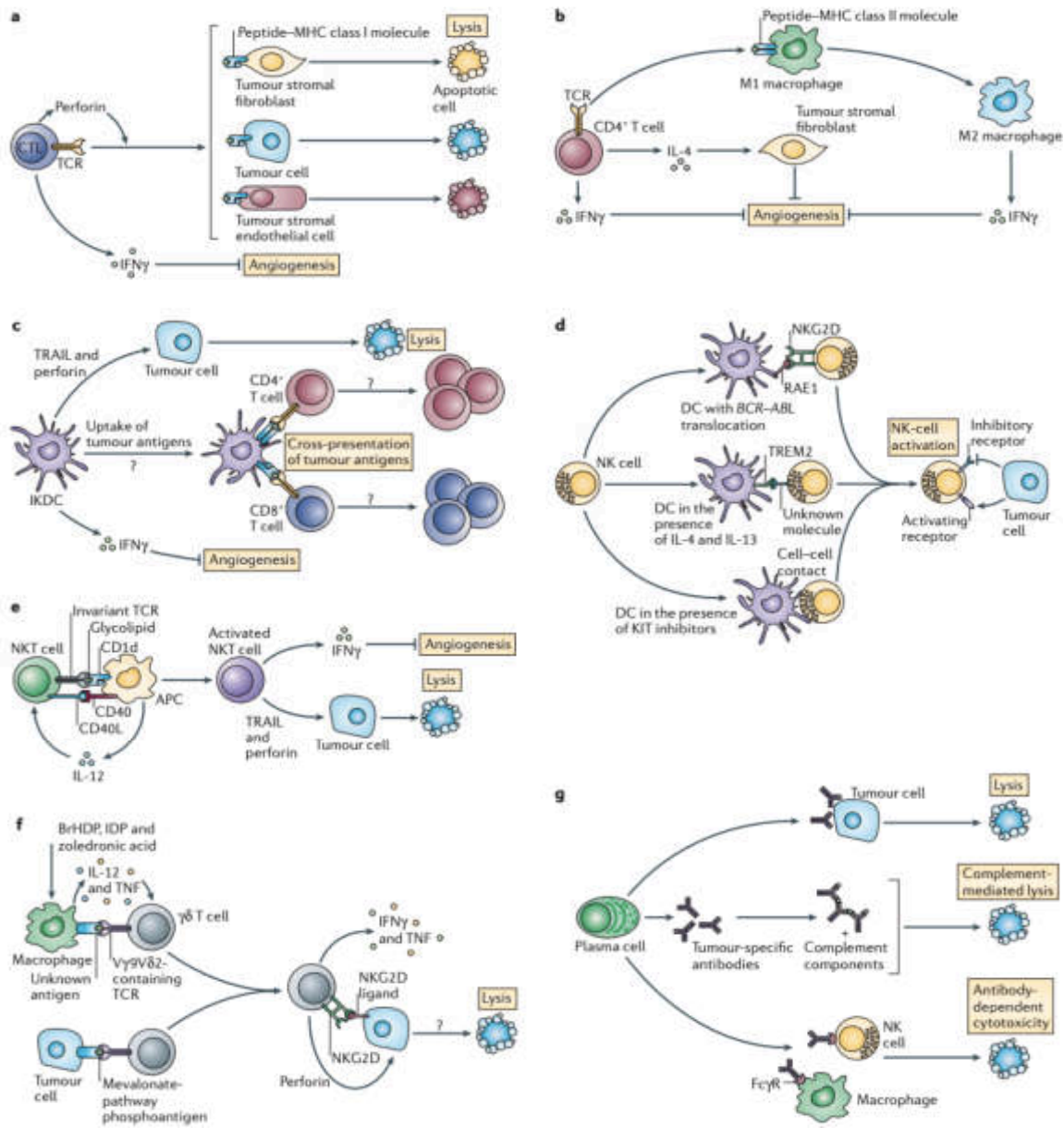
Figure 8. Elimination of tumor cells by innate and adaptive immune system. a) CD8+ cytotoxic T lymphocytes (CTLs) identify and eradicate cancerous or stromal cells while releasing IFN. b) Tumor-infiltrating macrophages are found by activated CD4+ T cells, which causes them to polarize into M2 macrophages. c) TRAIL (tumor-necrosis factor (TNF)-related apoptosis-inducing ligand) and perforin are required for IFN-producing killer dendritic cells (IKDCs) to kill tumor cells. d) Glycolipids linked to CD1d in DCs, KIT inhibitors, or TREM2 (triggering receptor expressed on myeloid cells 2) were used by DCs to stimulate NK-cell activation. e) IFN is secreted by activated NKT cells, which then lyse tumor cells. f) IFN is secreted by activated NKT cells, which then lyse tumor cells. f) Tumor cells or APCs present the F1-ATPase–apolipoprotein-A complex or phosphoantigens to γδ T cells with a Vγ9Vδ2-containing T-cell receptor (TCR), and these γδ T cells produce cytokines or kill tumor cells. g) Tumor-specific antibodies have a tumoricidal function by increasing antiproliferative effects either directly or by causing complement-mediated lysis or antibody-dependent cytotoxicity.

However, the surviving tumor variants that where resistant and poor immunogenic to the elimination phase could enter in the equilibrium phase.

Equilibrium.

During this phase, the immune system applies a strong "selection pressure" to the malignant cells which is sufficient to maintain the tumor cells in an equilibrium between cell death and cell growth, but not to completely eradicate it (Dunn, Old, and Schreiber 2004). Despite most of the initial tumor cells variants are eliminated, new variants with distinct mutations could appear, and this mutations can provide different aggressive characteristics to tumor cells, such as the cell death resistance, evading growth suppressors, among other hallmarks of cancer, which confer higher resistance to immune attack (Hanahan 2022).

One unfortunate result during the equilibrium process is the generation of a new population of tumor clones with poor immunogenicity, because of the "selection pressure" of the immune system. Also, it has been proposed that the immune system could sustain the equilibrium phase over a period of many years and may be the longest phase, which is the interval between first carcinogen exposure and the clinical detection of the tumor (Dunn, Old, and Schreiber 2004).

Finally, after tumor enters to the latent period of equilibrium, there are three possible outcomes: (1) eventual immune system elimination; (2) the maintenance in the equilibrium phase by the immunity control; or (3) escape from the "selection pressure" and progression to the final escape phase of the immunoediting process (Smyth, Dunn, and Schreiber 2006).

Escape

During this phase, the immune system fails to control or eliminate cancer cells, allowing that the remaining or residual tumor cell variants could proliferate in an immunologically unrestricted manner. The constant interaction between cancer cells variants and the immunological pressure serves as a Darwinian selection of the most fit tumor variants, which

acquire the necessary characteristics to avoid immune system recognition or elimination (Vesely et al. 2011).

Tumor escape mechanisms

The immune system targets tumor cells through several mechanisms, including the elimination of tumor cells by NK, NKT or CD8+ T lymphocytes which lead to the elimination of the most immunogenic cells, resulting in the selection of tumor cell variants that can evade the immune attack.

During development, tumors acquire different characteristics to evade the immunity system (Figure 9), such as the downregulation of antigen presentation molecules (MHC), the lack of Molecules involved in cell death (such as caspases, calpains, among others), the upregulation of cell death inhibitors (Bcl-XL, FLIP, among others), or the expression of inhibitory molecules (PD-L1, FasL, CTLA-4). Additionally, tumor cells can secrete anti-inflammatory cytokines and factors that favors the immune inhibition (IDO, IL-10, VEGF, TGF-β LXR-L, gangliosides, among others) and promote the recruitment of regulatory cells for the construction of the immunosuppressive microenvironment (PGE2, GM-CSF, IL-4, IL-13, IL-1β, VEGF). Regulatory cells induce pro-tumor immunity by releasing immunosuppressive cytokines and changing the microenvironment's nutrient composition. The recruitment and polarization of M2 macrophages from myeloid progenitors, which produce TGF-, IL-10, and PDGF that suppress T cells, is induced by the production of IL-13 and IL-4 in the microenvironment. When tumor cells secrete colony-stimulating factors such as IL-1, VEGF, or PGE2, promote the MDSCs recruitment and inhibit T cell activity by secreting TGF-, ARG1, and iNOS (Vesely et al. 2011).
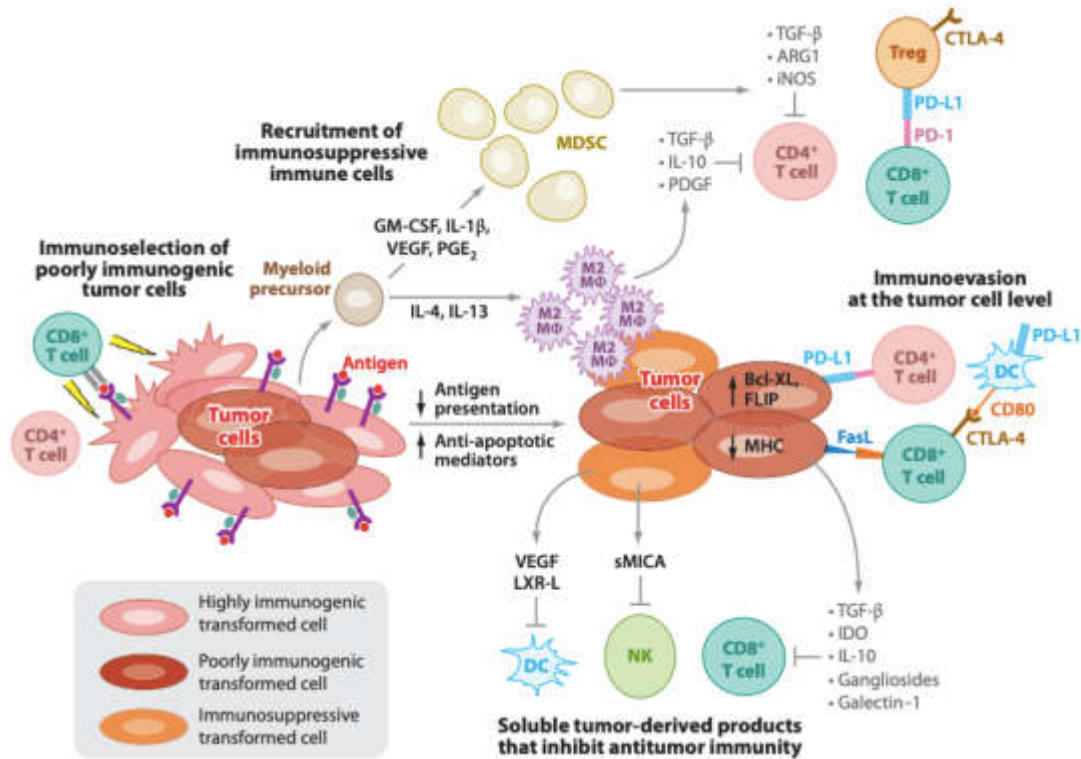
Figure 9. Tumor escape mechanisms. Although there are many ways for tumors to avoid immune detection and destruction, they may typically be divided into two categories: cell-autonomous alterations and immune cell modifications induced by tumor cells **(Vesely et al. 2011).**

Cancer immunoediting and tumor microenvironment

Tumors establish an immunotolerant environment named tumor microenvironment (TME) which is a complex and continuously evolving entity that comprise: tumor cells, fibroblasts, endothelial and immune cells, and the non-cellular components such as fibronectin, collagen, hyaluronan, laminin, among others. Now it's clear that the TME is a crucial component for the tumor development and progression as well as an indicator of treatment response. The TME inhibits the function of the antitumor immune system and promotes the recruitment of (pro-tumor) regulatory immune cells to avoid the immune attack (as shown in figure 10 for the TME of breast cancer) (Chang and Beatty 2020; Soysal, Tzankov, and Muenst 2015). Additionally, the diverse interactions between cancer cells and immune system induced changes in the TME leading to tumor growth, angiogenesis, and metastasis, among others.

18

BREAST TUMOR MICROENVIRONMENT
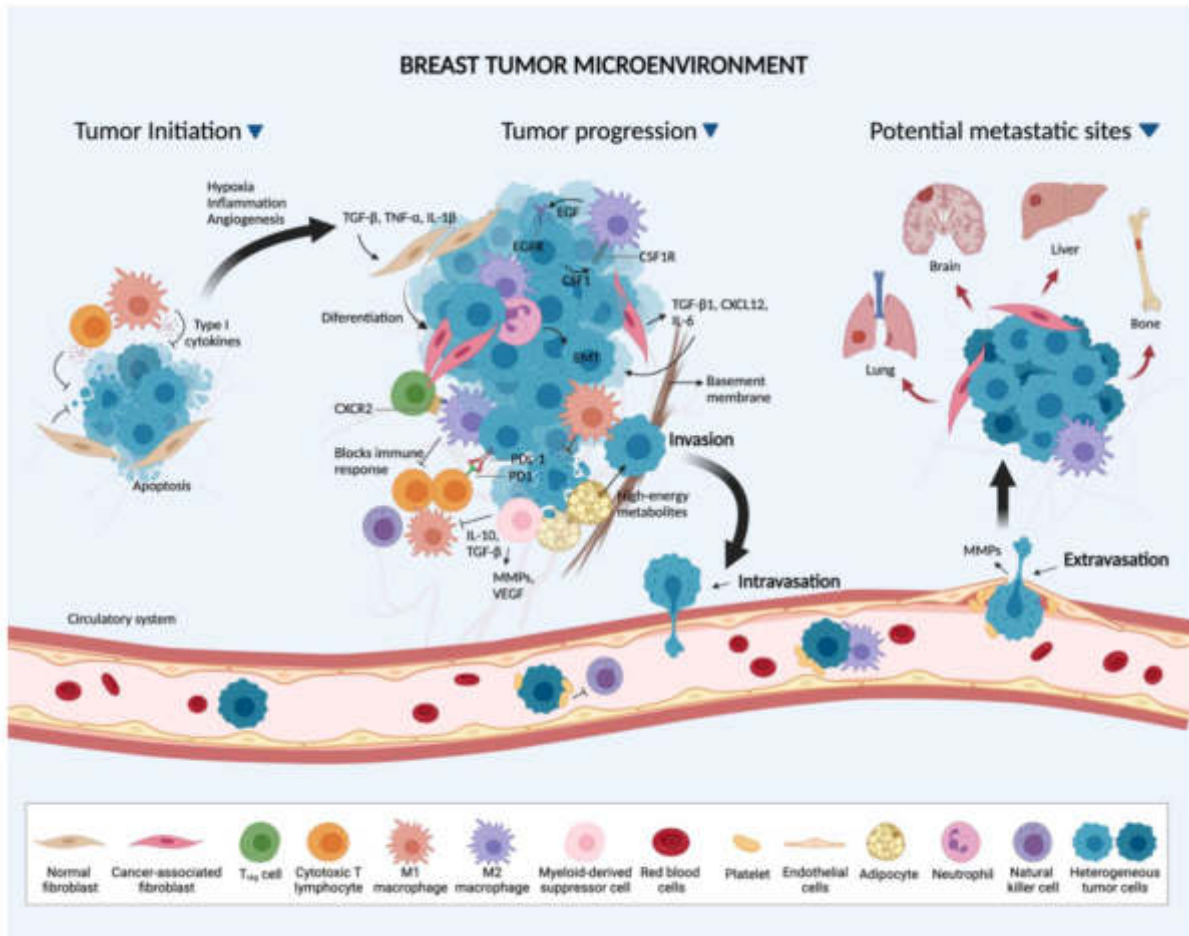
CFigure 10. The development of breast cancer and the tumor microenvironment (TME). Inflammatory signals that are predominantly regulated by cytotoxic T-lymphocytes, M1 macrophages, and fibroblasts are exposed to the growing tumor at the time of tumor start. Breast cancer cells overcome the antitumor mechanisms through instructing host stroma cells to develop pro-tumorigenic characteristics. The differentiation of healthy fibroblasts into cancer-associated fibroblasts (CAFs) is then modulated by cytokines (TGF-, IL-1, and TNF-) generated during the inflammatory phase. CAFs release extracellular matrix proteins and soluble factors (TGF-, CXCL12, IL-6) that promote tumor development and growth through the epithelial to mesenchymal transition (EMT). Neutrophils can cause EMT and advance tumor growth. High-energy metabolites are secreted by adipocytes to promote tumor development. By secreting pro-tumorigenic cytokines and growth factors, tumor-associated macrophages (mainly M2 macrophages) promote several activities inside the TME, including BC development and invasion. Myeloid-derived suppressor cells (MDSCs) and regulatory T cells (Treg) are recruited when the tumor grows because of activated cytokines in the environment (CXCL5-CXCR2, TGF-), which also inhibit natural killer cells, M1 macrophages, and cytotoxic T lymphocytes. By overexpressing the PD-L1 ligand, BC cells can also evade immune monitoring. Secreted substances like MMPs and VEGF make it easier for tumor cells intravasation into the circulation. There, platelets and M2 macrophages engage with BC cells to help them survive by preventing immunological identification. Additionally, platelets escort tumor cells to distant sites and promote extravasation (Soysal, Tzankov, and Muenst 2015).

Furthermore, immune cells in the microenvironment can release chemokines and cytokines that attract innate cells, such as myeloid-derived suppressive cells (MDSC), neutrophils and macrophages which help to the development of tumors and are related to immunosuppression and poor prognosis is. On the other hand, NK cells, another type of innate immune cell, are a sign of a positive prognosis and tumor clearance in the TME (Table 2) (Shihab et al. 2020).

Table 2. Cells in the tumor microenvironment		
Cells	**Primary functions in TME**	**Main Citokine / chemokine**
CD8+ T lymphocytes	Recognize and kill stromal and/or tumor cells in an MHC-restricted and perforin-dependent manner	IL-2, IFN-γ
Treg	They can suppress a wide range of immune cells, including CD8+ T cells, natural killer cells, B cells and antigen-presenting cells	IL-4, IL-10, TGFβ
Myeloid derived suppressor cells (MDSC)	Induce processes related to cancer invasion, such as the epithelial mesenchymal transition (EMT), promoting tumor invasiveness by impairing anti-tumor innate and adaptive responses	IDO, CCL3, CCL4, CCL5, Arg1, PGE2, IL-4, IL-10, TGFβ
NK cells	NKs employ death receptor mediated apoptosis and perforin/granzyme-mediated cytotoxicity to target tumor cells and limit primary tumor growth	IFN-γ, TNF-α, IL-2, IL-12
Tumor associated Macrophages (TAMs)	Display a characteristic phenotype oriented towards promoting tumor growth and angiogenesis, tissue remodeling and suppressing adaptive immunity	TGFβ, IL-10, VEGF, CCL22, Arg1
Cancer associated fibroblast (CAF)	Constitute one of the most abundant cells in TME, enhance tumor progression and metastasis by promoting cancer cell growth, pro-tumor immune responses, extracellular matrix (ECM) remodeling and angiogenesis	TGFβ, CXCL12, PDGF, IL-6
Regulatory dendritic cells	Support the tumor progression inducing tolerogenicity and immunosuppressive activities (suppress of T cell responses)	TGFβ, IL-10
B lymphocytes	They contribute to the regulation of tumor cell survival and proliferation and the development of treatment resistance.	IL-10
Tumor associated Neutrophils	Support cancer cell proliferation, angiogenesis, and immunosuppression	MMP-9, CXCL1/8/3/6, Collagenase IV, Heparanase, TGF-β, PGE2

Adapted from (Li et al. 2021; Ma et al. 2013; Soysal, Tzankov, and Muenst 2015).

The notion of cancer immunoediting incorporates the diverse and controversial effects of the immune system on the emergence and spread of tumors. On the other hand, understanding the cellular and molecular processes that contribute to cancer immunoediting and tumor microenvironment, it's important to found targets for therapeutic intervention, including the interaction with the TME, and it should be possible to develop new safer and efficacious

cancer therapies than the current treatments. (Schreiber, Old, and Smyth 2011; Vesely et al. 2011).

Nowadays it's clear that the generation of anti-tumor immunity will require treatment strategies able to overcome the physiological barriers that control immune responses against tumor cells. However, most of the tumor regulatory mechanisms limits the development of anti-cancer immune responses. Immune control may be inherent to immune effector cells or may result from the release of immunosuppressive agents and the activation of regulatory cells in the microenvironment of growing malignancies. To strengthen the anti-tumor immunity, immunotherapy employs techniques that target specific immune-regulatory mechanisms.

Immunotherapy: a strategy to overcome the cancer immunoediting and tumor microenvironment.

Immunotherapy it's a type of therapy that use materials or substances that improve or restore the immune system's capacity to prevent and fight disease. Cancer immunotherapy aims to promote the elimination of cancer cells by the immune system cells without triggering off-target effects or uncontrolled autoimmune inflammatory reactions that restrict its therapeutic potential (Background of Immunotherapy). To accomplish these goals, different immunotherapy modalities are being investigated.

Types of immunotherapies

There are different developed strategies of immunotherapies, comprising but not restricted to; (I) adoptive cell therapy approaches involving *ex vivo* treated tumor-specific lymphocytes or tumor cells; (II) therapeutic administration of monoclonal antibodies; (III) strategies that block or eliminate different immunosuppressive mediators (immune check point inhibitors)

such as PD-1, CTLA-4, or MDSCs; (IV) vaccine approaches which promotes specific antitumor-immune responses (Schreiber, Old, and Smyth 2011).

Monoclonal antibodies

Monoclonal antibodies (mAbs) are a class of anticancer treatments with a wide range of mechanisms of action. Figure 11 shows the different methods that monoclonal antibodies attack cancer cells, including, immune checkpoints inhibition, immune-mediated destruction, direct death of cancer cells among others. When MAbs attach to tumor-associated antigens with antigen specificity, they induce different cytotoxic effects (figure 11). Additionally, other monoclonal antibody strategy named antibody drug-conjugated (ADCs) employs mAbs attached to a cytotoxic drug for induced cell death. ADC have three components: the monoclonal antibody (mAb), the linker, and the cytotoxic or cytostatic/cytotoxic drug (Mishra et al. 2022).
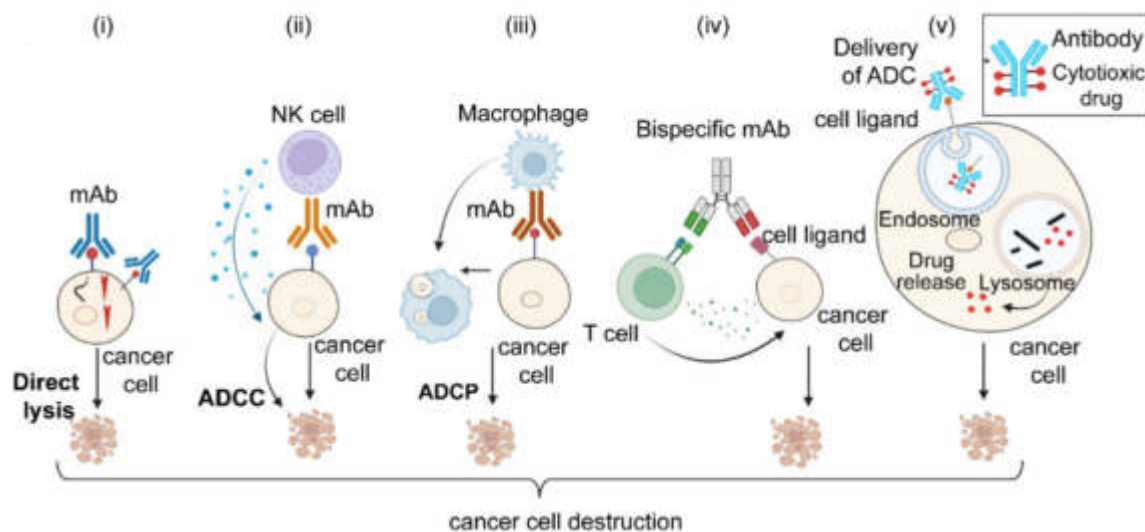
Figure 11. Model illustrates the different ways in which cancer immunotherapy uses therapeutic monoclonal antibodies. (i) Direct cell death induction. (ii) Antibody-dependent cell-cytotoxicity (ADCC), (iii) Antibody-dependent cellular phagocytosis (ADCP) (iv) Bispecific antibodies promotes the interaction between immune and cancer cells leading to tumor cell induction (v). The ADC (antibody-drug conjugate) interact with

their receptor in cancer cells, promote their endocytosis for the drug release and the cell death induction (Mishra et al. 2022).

Adoptive cell therapy (ADC)

ACT is an immunotherapy that promote the elimination of tumor cells that express a specific surface marker using immune cells using: CAR-NK (NK cell-based treatments), TILs (tumor-infiltrating lymphocytes), synthetic TCRs (engineered T-cell receptors), as cell-based adoptive therapies (Cha et al. 2020; Mishra et al. 2022).

Tumor-infiltrating lymphocytes (TIL) are effector T cells that recognized tumor antigens and induce cancer-cell death, but they are insufficiently numerous to destroy the tumor. The patient receives the expanded TILs (ex vivo) cells that have been extracted from the donor or patient.

Adoptive cellular therapy based on synthetic TCRs employs genetically modified cells which can directly recognized antigens presented by the major histocompatibility complex (MHC). Chimeric antigen receptor (CAR) T cells are lymphocytes obtained from patients which are genetically modified for to express an hybrid receptor which comprise: an extracellular domain that detect a tumor antigen, and usually is composed of an antibody single-chain variable fragment (scFv), and an intracellular signaling domain, which provide activation

signals, this is generally derived from the co-stimulation molecules CD28 or 4-1BB (Cha et al. 2020; DePeaux and Delgoffe 2021).
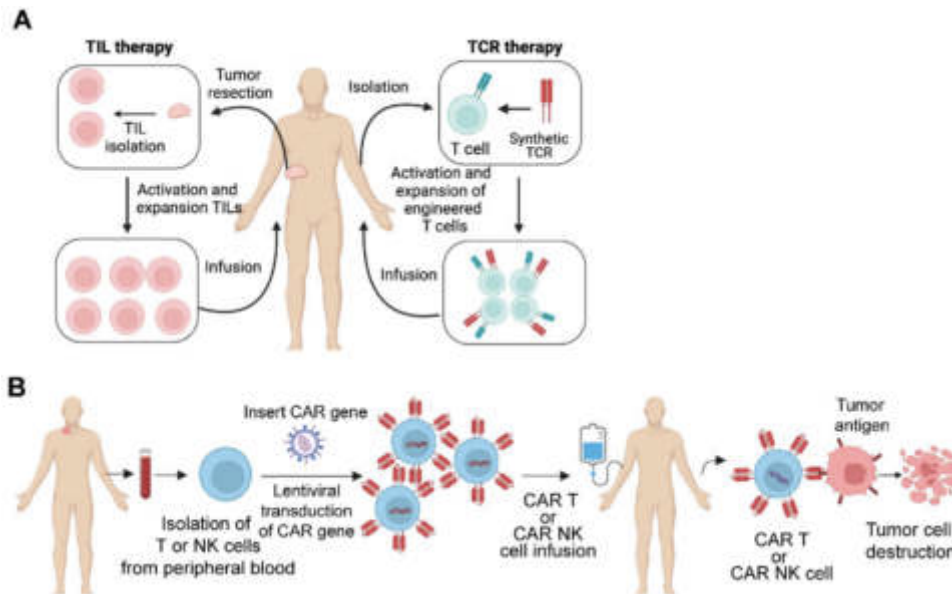
Figure 12. Adoptive cell therapy. (A) TIL and TCR therapy involve the obtention of cells from patients which are treated *ex vivo* and reinjected to patients. (B) Schematic outline of CAR T or CAR NK therapy. (Mishra et al. 2022).

Immune checkpoint inhibitors (ICIs)

A group of molecular effectors known as immunological checkpoints are proteins expressed in the surface of immune cells that interact with their ligands to finally regulate immune homeostasis and prevent autoimmune disease. Through the immunoediting process, tumor cells may exploit this homeostatic mechanism by overexpressing ligands for immunological checkpoints. Due to their critical involvement in cancer immunity, these checkpoint proteins have been utilized as significant therapeutic strategies in anticancer immunotherapy (Mishra et al. 2022).

In the priming and effector stages, respectively, the interaction between CTLA-4 and B7-1, PD-1 and PD-L1 are significant immunological checkpoints that compromise cell activation (figure 13). The TCR pathway is down-regulated, and T-cell activities are inhibited as a result of interactions between PD-1 and PD-L1, CTLA-4 and B7-1, and Src homology region 2 domain-containing phosphatases (SPH2) and the protein phosphatase 2 (PP2A) respectively (Cha et al. 2020). The immune responses that prevent healthy tissues from exacerbated

immune attack are dependent of the immune checkpoint's molecules. T cells expressed PD-1 upon activation and allows the identification of abnormal and cancerous cells. PD-L1 is expressed in tumor, which binds to PD-1 on T cells to prevent T cells activation and prevent the recognition of tumor cells. As a result, T cell-mediated tumor cell killing is enabled by inhibiting this interaction using mAbs that target either PD-L1 or PD-1.

On the other hand, the degree of T cell activation is controlled by the co-inhibitory protein CTLA4, another immunological checkpoint. The interaction between CTLA4 and its ligands, CD80 and CD8 prevents T cell activation promoting tumor progression, by preventing their interaction T cells can continue to be active, detect, and destroy tumor cells (Riley et al. 2019).
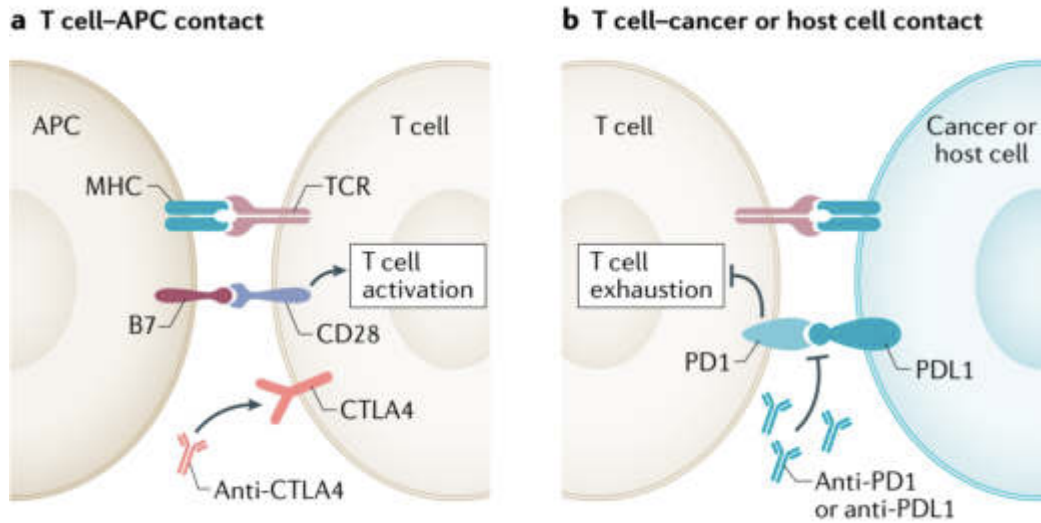
Figure 13. Mechanism of action of ICIs. (a) T cell activation comprise: 1) engagement of a T cell receptor (TCR) with the antigen presented in a major histocompatibility complex (MHC) on antigen-presenting cells (APC); and 2) a co-stimulatory signal such as CD28 on T cells that binds to B7 on APCs. On the other hand, the antigen known as CTLA4 blocks the second signal attaching to B7 with a greater affinity than CD28 blocking the second signal. Thus, blocking CTLA4 pharmacologically with ICIs, restoring the CD38-B7 interaction. (b) T cell exhaustion is the result of a series of T cell inhibitory mechanisms that are triggered when the T cell receptor PD1 contacts its ligand PDL1, which is expressed on a range of cells, including tumor cells and tumor-infiltrating macrophages. With PD1- or PDL1-targeting antibodies, blocking either side of this interaction inhibits this engagement, which delays T cell depletion and promotes anti-tumor T cell activity. (Wright, Powers, and Johnson 2021).

Vaccines

A crucial stage in cancer immunosurveillance (elimination phase of immunoediting) is the immune system's ability to detect aberrant or altered cells. The antitumor immune system cells infiltration in the TME is crucial to find tumor neoantigens expressed by cancer cells. However, cancer cells can downregulate the exposure of neoantigens to reduce their immunogenicity preventing the presence anti-tumor immune cells in the TME. In this sense, the vaccination approach based on tumor antigens could reactivate the immunosurveillance and promote the intratumorally infiltration of immune cells (also known as the "hot condition") (Cha et al. 2020).

The ideal antigens for cancer vaccines need to be: (1) selectively expressed in cancer cells, (2) prevalent in a wide variety of cancers, (3) necessary for cancer growth, and (4) highly

immunogenic. Although not all antigens may achieve these objectives, they can still significantly trigger the anticancer immune response in cancer patients (Cha et al. 2020).

Therapeutic cancer vaccines can be classified into four groups accordingly with their formulation techniques and delivery mechanisms: and cell-based vaccines, virus-based vaccines, DNA or RNA-based vaccines and peptide-based vaccines (Figure 14).
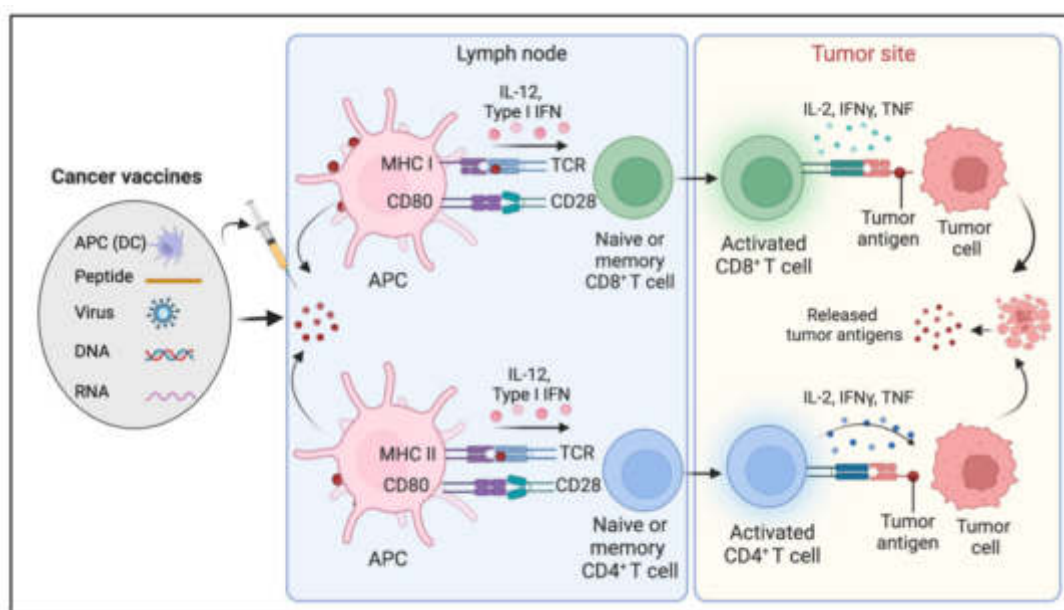
Figure 14. Schematic representation of cancer vaccines therapy function. Following the administration of a cancer vaccine, APCs uptake and process the tumor antigen to display them on MHC-I or II, to stimulate cytotoxic or helper T cells. Antigen-specific CD4+ or CD8+ T lymphocytes that are activated can migrate to the tumor microenvironment trigger cancer cell death (Mishra et al. 2022).

Nucleic acids-based vaccines

In contrast to traditional vaccinations, nucleic acid treatments, such as RNA or DNA-based vaccines, involve the intracellular transport of nucleic acids.

In this approach, the APCs uptake the DNA or mRNA leading to the expression of TAAs or TSAs. Finally, the antigens are presented to T cells for activate the antitumor response (Riley et al. 2019).

Cancer DNA vaccines uses bacterial plasmids for to induce the expression of tumor antigens in different cells, which activate the antitumor immune system. However, there are three key mechanisms for this strategy: 1) after translation of tumor antigens, this are loaded in MHC-

I molecules to activate CD8+ cells, 2) the antigen released by somatic cells (that integrated the DNA) is phagocyted, processed and presented to CD4+ T cells in MHC-II molecules by APCs, 3) APCs could also express the tumor antigen for after processed and presented them to CD8+ and CD4+ T cells to activate humoral and cellular responses (Liu et al. 2022). mRNA-based cancer vaccines directly induce the expression of antigens in APCs. The mRNA molecules present different advantages such as the easy production, their half-life could be improved by different modifications, among others. However, mRNA requires transfections agents or systems for their delivery in the cells (Riley et al. 2019)

Virus-based vaccines

Many viruses have *per se* immunogenic properties and could be used as cancer vaccine-platforms, also, it is possible to modify their genetic material to include sequences that encode tumor antigens. Also, the immune system effectively responds to viruses, with both innate and adaptive systems working together to create a robust and durable response which is one of the main advantages for virus-based vaccines. Pattern recognition receptors (PRRs), which are triggered by viral pathogen-associated molecular patterns, promote APC activity. For safety reasons, replication-defective or attenuated variants of the most widely used viral vaccine vectors—poxviruses, adenoviruses, and alphaviruses—are favored (Hollingsworth and Jansen 2019).

Peptide-based vaccines

Peptide-based vaccines aims to promote the antitumor response against tumor-associated antigens (TAAs) or tumor-specific antigens (TSAs) using purified, synthetic, or recombinant peptides. Personalized cancer vaccines are being created using peptide vaccination methods and synthetic peptides. Upon administration, and uptake by APCs antigenic peptides are displayed on the cell surface in combination with HLA molecules for stimulate T cells and promotes the anticancer-specific responses. Recently, peptide-based cancer vaccines are typically composed of 20–30 amino acids and contain certain epitopes from antigens that are known to be highly immunogenic in order to activate the immune response (Miao, Zhang, and Huang 2021).

Cell-based vaccines

Cell-based anticancer vaccines are usually prepared with whole cells or cell fragments, which provide TAAs or TSAs to induce a robust antigen immune response (Liu et al. 2022). Cell-based vaccines are divided in two categories: 1) tumor cells vaccines and 2) immune cell-based vaccines.

Tumor cell vaccine

One of the vaccination approaches under evaluation uses the patient's own cancer cells to create an autologous tumor cell vaccine. This approach presents different advantages such as that whole cells lysates provide a source of all immunogenic antigens and avoids the need to select the best antigen. Also, it is possible to simultaneously target numerous tumor antigens, eliciting immune responses against multiple tumor antigens, and avoiding problems with tumor antigen loss.

When a whole cell vaccine is created using autologous tumor cells, patients are immunized with cells that express the same tumor antigens as their tumor. However, this strategy has

certain technical limitations, including the inability to collect patient's tumor cells (Keenan and Jaffee 2012).

Dendritic cells-based vaccines

Dendritic cells (DCs) are attractive targets for immunotherapies, due to their different mechanisms used to ingest and present tumor-associated antigens (TAAs), which trigger potent antitumor responses (Liu et al. 2022).

In addition, DCs possess essential capabilities needed for the establishment of antitumor effects such as the antigen presentation capabilities, their capacity to migrate in lymphoid and non-lymphoid tissues, their role in cytokine and chemokines release for immune regulation and tissue homing of immune cells. Recently, autologous DCs vaccines have been extensively evaluated (Figure 15), these personalized vaccines are derived from patient's precursor of DCs such as monocytes or hematopoietic stem cells (HSPCs) which are differentiated and stimulated with tumor antigens *ex vivo* (Perez and De Palma 2019; Sadeghi Najafabadi, Bolhassani, and Aghasadeghi 2022). The main benefits of this approach are that (1) allows the presentation of multiple antigen epitopes on MHC molecules, leading to the stimulation of both CD4+ and CD8+ T cells, and (2) the mechanism of processing of the antigen allow a prolonged antigen presentation (Sabado, Balan, and Bhardwaj 2017).

Also, antigens could be obtained from different sources such as cell lysates, tumor-derived peptides, antigens packaged within viral vectors, among others.
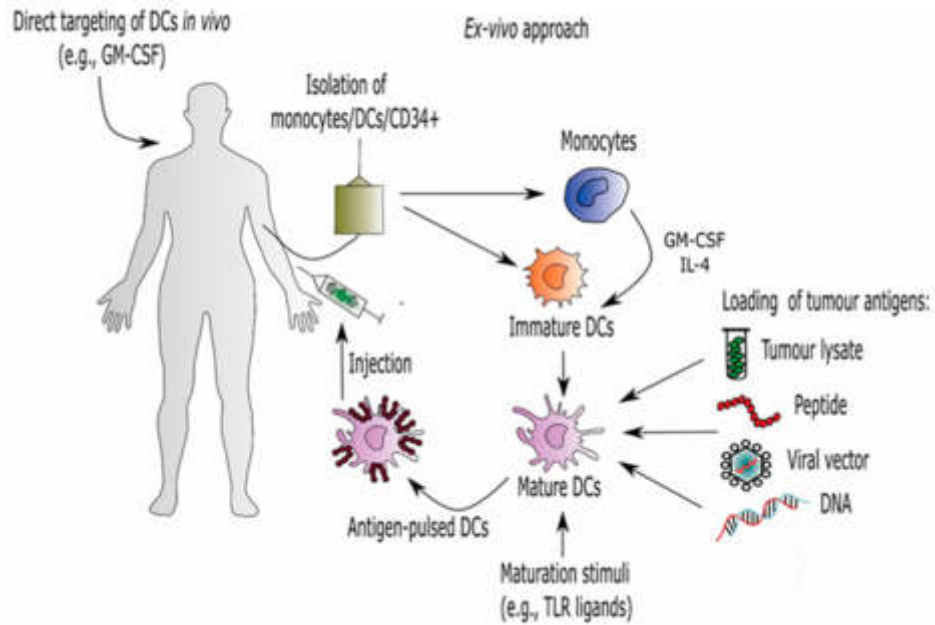
Figure 15. Dendritic cells-vaccines. Different approaches are used for generating DCs-vaccines: direct growth of circulating DCs, isolation of circulating DC subsets, differentiation from progenitor cells. Immature DCs are stimulated with different maturation stimuli after differentiation. Finally, patient is then given an injection of prepared antigen-loaded DCs (Tešić, Poženel, and Švajger 2021)

The influence of adjuvants

Adjuvants promotes the recruitment of immune cells to the site of inoculation, while also stimulates the antigen uptake and maturation of APCs. An effective therapeutic cancer vaccine is characterized for efficiently induce the presentation of antigens that led to the antitumor immune system activation, which depends mainly on DCs. However, cancer cells inhibit the DCs maturation and function and induce through the release of anti-inflammatory cytokines in the TME. Therefore, cancer vaccine approach without DC activators (adjuvants) could result in a tolerant immune response.

In this sense, the stimulation of DCs with immunostimulatory adjuvants is a crucial step in the antitumor response establishment. Adjuvants can activate different pattern recognition receptors such as: Nod-like receptors (NLRs), Toll like receptors (TLRs), stimulator of interferon genes (STING), CD40 agonists, among others, which upon activation induced inflammatory responses. Without enough stimulation signals, the immune system is unable

to elicit a potent anti-tumor response, because of defective co-stimulation and antigen presentation by DCs (Morse, Gwin, and Mitchell 2021)

Immunotherapy and immunoediting

Cancer immunoediting could occur in response to immunotherapy as well as during the development of tumors. In this sense, immunotherapy may present a secondary (acquired) resistance, which manifests as a clinical response, followed by progression (secondary escape) of cancer.

In general, the resistance of most cancers to immunotherapies highlights the necessity of better understanding both, the cancer immune-evasion mechanisms and the antigenic targets to stimulate cancer-specific effectors cells (T, NKT cells, among others)(Gubin and Vesely 2022). Thus, the future of immunotherapies need focus in overcome the immunosuppressive microenvironment, improve the immunogenicity of malignant cells and elucidate new targets for overcome these characteristic, and not only focus on the stimulation of untargeted immune response (Tan, Li, and Zhu 2020). In this sense, immunogenic cell death is an interestingly strategy to overcome the tumor microenvironment, due to this type of cell death induce the anti-tumor immune system responses and remodeling the tumor microenvironment.

Immunogenic Cell Death: a novel approach to overcome cancer immunoediting

It has been determined that an essential factor in the development of anti-cancer therapies is the immunogenicity of cancer cells. Therefore, research has started to concentrate on the general immunobiology of tumors to overcome the immunosuppressive function of TME and to increase the immunogenicity of the cancer cells, (Kroemer et al. 2013). Currently, it is understood that some anti-cancer treatments can induce a peculiar type of cell death known as Immunogenic Cell Death (ICD), which is characterized by the presence of damage associated molecular patterns (DAMPs) and the increased immunogenicity of tumor cells

(which act as a tumor vaccine) leading to the generation of immunological memory (Kroemer et al. 2013).

Immunogenic cell death (ICD)

ICD is a type of cell death that promote the antitumor immune response and induce immunological memory against endogenous (cellular) or exogenous (viral) antigens. The ability of ICD to stimulate adaptive immunity comprise two major parameters: antigenicity and adjuvanticity. **Antigenicity** is the capacity for a molecule, protein, among others to be detected as an antigen and promotes an inflammatory response. This, is provided by the production and presentation of antigens in the setting of central tolerance in a particular host that do not result in clonal deletion, suggesting that the host has naive T cell clones that can recognize such antigens. **Adjuvanticity** is mainly provided by the release or exposure of danger signals such as DAMPs due to cell damage or stress and by phatogen-associated molecular patterns (PAMPs) in pathogen-derived ICD which promotes the recruitment and maturation of DCs. These molecules have non-immunological effects within the cell, however, there are present on the cell membrane or there are released in the extracellular matrix because of cellular stress allow their binding to receptors in immune cells (Lorenzo Galluzzi et al. 2018; Garg and Agostinis 2017; Kroemer et al. 2013).

Damage associated molecular patterns (DAMPs)

Through the release or exposure of DAMPs by dying cells, ICD favors the establishment of the antitumor immune system responses (Kroemer et al. 2013).
Under normal circumstances, the immune system does not identify intracellular molecules known as DAMPs. However, under cellular stress or tissue injury, these molecules are exposed in dying cells or released into the extracellular space, thus allowing their binding to receptors in immune cells. DAMPs are recognized by different innate pattern recognition receptors (PRRs) (Toll-like receptors (TLRs) and NOD-like receptors (NLRs)), promoting the establishment of the anti-tumor immune responses. Altogether, this effects are typically

associated with immunological memory which promotes the long-term efficacy of anticancer drugs (Ahmed and Tait 2020).

It is remarkable that depending on the context in which they are detected by the host, DAMPs can activate pro- and anti-inflammatory effects in addition to tissue remodeling effects (Land 2015). The most notable DAMPs identified to date, together with their method of emission, linked cell death pathway, and related receptors, are included in Table 3 (Garg et al. 2015). However, it's important to remember that not all DAMPs have the potential to serve as immunogenic signals. Table 2 demonstrates that several DAMPs, such as Annexin A1 (ANXA1), Death Domain 1 (DD1), and different extracellular matrix molecules, are essential for the preservation of tissue homeostasis and the suppression of autoimmune reactions because they have immunosuppressive effects (Garg et al. 2015).

Table 3. Damage-associated molecular patterns (DAMPs)

DAMPs	Receptors	Localization and mode of emission	Relevant cell death pathway	Functions
Annexin A1	FPR-1	Surface exposed or actively	Apoptosis	Guides the final approach of APCs to dying cells
Adenosine Triphosphate	P_2Y_2 and P_2Y_7	Actively or passively released	ICD, Apoptosis / Necrosis	Favours the recruitment of APCs and their activation
Calreticulin	LPR1 (CD91)	Mostly surface exposed sometimes passively released	ICD	Promotes the uptake of dead cell-associated antigens
Cellular RNA, dsRNA, ssRNA, dsDNA	TLR3, TLR7, CDSs	Passive release	ICD/Necrosis	Promotes the synthesis of pro-inflammatory factors including type I IFNs
Type I IFNs	IFNAR	-	ICD	Promote CXCL10 secretion by cancer cells and exert immunostimulatory effects
Thrombospondin 1 and its heparin-binding domain	αvβ3 integrin	Passively released or surface associated	Apoptosis	Mediates the protein's interaction with calreticulin, and integrins during cellular adhesion. Low-density lipoprotein receptor-related protein during uptake and clearance
Heat shock proteins (HSP70/90,60,72)	LRP1,TLR2, TLR4 SREC-1 and FEEL-1	Surface exposure, active secretion or passive release	ICD, Apoptosis / Necrosis	Stimulates the uptake of dead cell-associated antigens
High-mobility group box	TLR2, TR4, RAGE and TIM3	Mostly passively relesed; sometimes actively released	ICD/Necrosis	Promotes the synthesis of pro-inflammatory factors including type I IFNs

Adapted from (Lorenzo Galluzzi et al. 2017; Garg et al. 2015)

Calreticulin (CALR), the main DAMP related with ICD, is normally found in the endoplasmic reticulum (ER) lumen, but it has been shown to act as a potent "eat me" signal when it is exposed in the plasma membrane (Garg et al. 2015) which allow the phagocytose of stressed or dying tumor cells DCs. The production of tumor necrosis factor (TNFα) and IL-6 can also be stimulated by CRT, and it also enhances the antigen presentation of T lymphocytes by DCs, leading to the polarization of Th1 lymphocytes (lymphocytes that activate NK cells, dendritic cells, and macrophages). For this reason, CALR is the main protein related to immunogenic cell death (Garg et al. 2015)

High mobility group 1 protein (HMGB1) is a non-histone chromatin binding protein that is associated to different nuclear functions (Tesniere et al. 2008). Once in the extracellular space, HMGB1 can be recognized by a variety of receptors, such as toll-like receptors (TLR2 or TLR4) and the receptor for advanced glycosylation end products (RAGE) on DCs, leading

to the stimulation of inflammatory responses. Also, HMGB1 can promote the release of pro-inflammatory cytokines and assists in the correct antigen presentation (Garg et al. 2015).

Extracellular ATP is a strong "find me" signal (Elliott et al. 2009), it promotes the recruitment and differentiation of immune cells at ICD sites, this effect depends on the P2Y purinergic receptor (coupled to a G protein). Extracellular ATP also promotes the activation of DCs (Ghiringhelli et al. 2009) which in turn activates the NLRP3 inflammasome and causes the production of pro-inflammatory cytokines including IL-18 and IL-1 (Garg et al. 2015).

On the other hand, during ICD, heat shock proteins (HSP) 70 and 90 could be exposed in the cell surface of dying or stressed cells (Showalter et al. 2017). HSP70 and HSP90 can be transported to the plasma membrane during tumor cell death induction, facilitating the absorption and processing of antigens from dead tumor cells by DCs and the presentation of "cross-linked" peptides derived from tumors to CD8+ T cells, which triggers a cytotoxic immune response. Since HSPs exposure occurs after CALR exposure, it may just be a supporting factor in DCs' choice to take up and processing the antigens (Kepp et al. 2011).

Overall, the exposure or release of DAMPs provides the adjuvanticity in the ICD and is essential for dead cancer cells' immunogenicity, figure 16 shows the role of DAMPs in the antitumor immune system establishment (Garg et al. 2015).
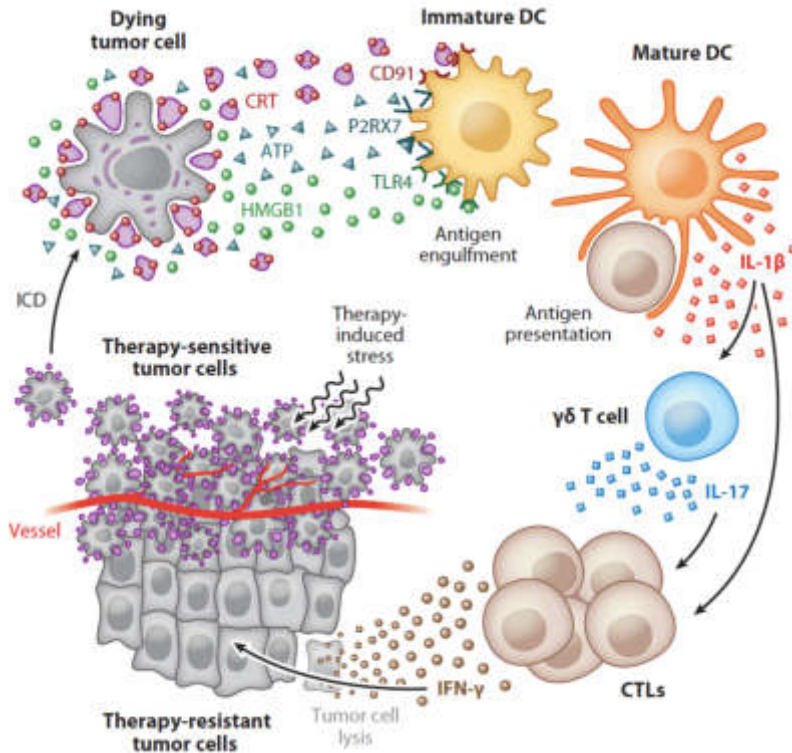
Figure 16. Immunogenic cell death characteristics. In response to ICD inducers, cancer cells expose CRT in their plasma membrane and release ATP and HMGB1 leading to the engaged of their receptors in immune cells CD91, P2RX7, and TLR4. This supports the efficient recruitment of DCs into the tumor site, DC engulfment of tumor antigens and the antigen presentation to T lymphocytes. This process led to a powerful immune response activation which result in the destruction of tumor cells and resistant tumor cells.

Immunogenic capacity of treatments

Some of the conventional anti-tumor therapies used with success for decades (chemotherapy and radiotherapy) can induce immunogenic cell death, however defects in the immune system involved with the capacity to perceive a cell death as immunogenic, also, the side effects due the lack of specificity that can lead to the immunosuppression, influence negatively among cancer patients treated with ICD inductors (Kepp et al. 2014).

Among different DAMPs, the CRT exposure is universally present in all ICD inductors, therefore it is the principal DAMP related with ICD, while ATP, HMGB1 or HSP70/90 can or not be present. Therefore, the analysis of DAMPs is not determinant for the ICD description. In this sense, the evaluation of DAMPs should be secondary to the *in vivo* and *ex vivo* evaluations of the antitumor immune response, to conclude that a treatment induced

ICD (Garg et al. 2015). For this reason, the **gold standard** for evaluating the capacity of antitumor treatments to induce ICD involve vaccination trials that show the tumor rejection capabilities of the immunized host (Garg et al. 2015).

In this context, as described in Figure 17, the gold standard consists in treated cancer cells *in vitro* with the treatment, modality, or agent to be evaluated and then dying tumor cells obtained after treatment, are injected subcutaneously or intradermally in the flank of syngeneic mice. Seven days later, mice received a new challenge with living cells of the same type of cancer in the opposite flank. The percentage of mice that are resistant to the development of tumors indicates the degree of immunogenicity or the cell death (Garg et al. 2015; Kepp et al. 2014). If these strict conditions are maintained, it might be possible the adequate characterization of novel ICD inducers while preventing false positives (Garg et al. 2015).
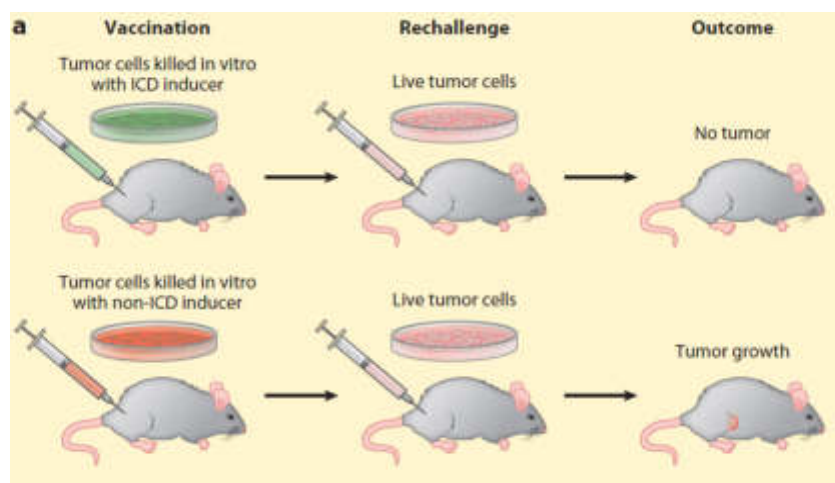
Figure 17. Gold standard of immunogenic cell death. The death of cancer cells can be defined as immunogenic, based on the prevention of tumor establishment. The injection of dying tumor cells that succumb to ICD in immunocompetent mice should present protective specific antitumor response, in the absence of any adjuvant. Adapted from (Kroemer et al. 2013).

ICD inductors classification

Several ICD inductors, including as conventional chemotherapy, targeted anticancer drugs, and other biological and physicochemical treatments, have been identified recently. However, the main obstacle to the development of novel ICD-inducing treatments is the lack

of a universal structure-function relationship capable of classify all the known ICD inductors and predicting the emergence of new ones. Nevertheless, the characteristic of ICD inductors to induce ER stress, has been used as the most peculiar feature (Garg et al. 2015). This is because the simultaneous induction of ER stress and oxidative stress is essential for evoking danger signaling pathways leading to the emission of DAMPs. These observations allowed the classification of ICD inductors, based on the form of ER stress induction for cell death. According to this classification (Figure 18), ICD type I inductors cause cell death through non-ER-associated targets and trigger ICD-related immunogenicity via secondary or "collateral" ER stress. While the type II ICD inductors are cytotoxic agents that target the ER both for the induction of cell death and for danger signaling. This demonstrates how the ICD inductor type I / II can help to find and categorize new ICD inductors based on their preferred orientation to the ER (Garg et al. 2015; Kepp et al. 2011).

Figure 18. Classification of immunogenic cell death inductors. Type I ICD inductors induce cell death through targets unrelated to ER. Type II ICD inductors preferentially target ER for induce cell death (Garg et al. 2015) (Garg et al. 2015).

CD47

CD47 is a ubiquitously expressed transmembrane receptor that plays diverse biological functions (Oldenborg 2013). It contains a highly glycosylated IgV-like extracellular domain, a five-transmembrane spanning domain, and a small intracellular

domain. It is acts as a counter-receptor of the signal regulatory protein alpha (SIRPa) and is a receptor of the matricellular protein thrombospondin-1 (TSP1) another transmembrane protein. It has been reported that large amounts of CD47 are expressed in diverse types of cells including chronic myeloid leukemia (CML), acute lymphoblastic leukemia (ALL), acute myeloid leukemia (AML), Hodgkin's lymphoma (LH), bladder cancer, among other solid tumors (Chao, Weissman, and Majeti 2012), to avoid their recognition by the innate immune system, promoting the progression of the disease (Barclay and Van den Berg 2014; Jaiswal et al. 2009; Majeti et al. 2009). Consequently, it has been proposed that <u>CD47 blockade</u> with monoclonal antibodies can disrupt its interaction with SIRPα, restoring programmed tumor elimination. However, has been demonstrated that, in contrast with its blockade, **CD47 activation** by certain antibodies or TSP-1-mimic peptides, is involved in cell death of cancer cells (Mateo et al., 1999; Oldenborg & Per-Arne, 2013; Martinez-Torres et al., 2015; Uscanga-Palomeque 2019; Denefle et al., 2019).

CD47 participates in diverse physiological processes, including migration, adhesion, and proliferation, among others, by its interaction with proteins like integrins, and thrombospondin-1. In addition, the functions of CD47 is a phagocytosis inhibitor when interacts with the signaling regulatory protein alpha (SIRPα) expressed in phagocytes, leads to the activation of a tyrosine phosphatase and the inhibition of myosin accumulation in the phagocytic synapse (Chao, Weissman, and Majeti 2012). Thus, CD47 fuction as a "don't eat me" signal that helps at the recognition of the own. The main ligands of CD47, TSP-1 and SIRPα, are described in detail below.

CD47 structure and interactions

CD47 consists of an N-terminal domain of extracellular IgV type (Figure 19), followed by a presenilin domain that contains five transmembrane segments and a variable cytoplasmic sequence (Chao, Weissman, and Majeti 2012). It has been shown that the IgV domain of CD47 interacts with diverse ligands or counter-ligands in the extracellular matrix or anchored to the plasma membrane. The main ligand of CD47 is TSP-1, a homotrimeric glycoprotein, which its C-terminal domain mediates CD47 binding (Isenberg et al. 2009). The interaction

of TSP-1-CD47 is also carried out in different organism such as murine, bovine, porcine and rats, which indicates that this interaction is not specie-specific within mammals. The family of SIRPα, known as CD47 counter-receptors, is formed by three members: SIRPα binds with greater affinity to CD47, SIRPγ with lower affinity and SIRPβ does not bind to CD47(Soto-Pantoja, Kaur, and Roberts 2015).
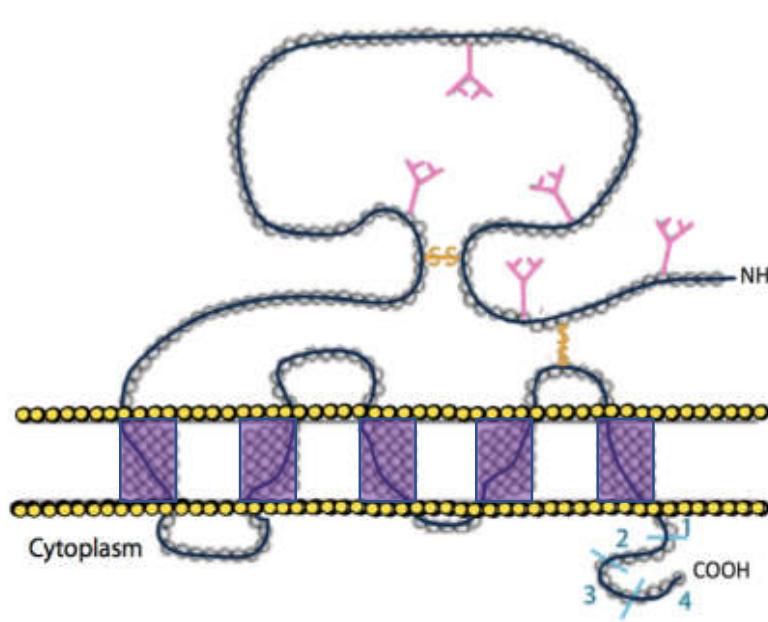

Figure 19. Structure of CD47. CD47 has an extracellular IgV domain, with 5 glycosylation sites (in pink), followed by 5 transmembrane segments (MMS) (in purple), disulfide bonds (s-s in orange) and finally the carboxyl terminal cytoplasmic domain with 4 possible alternative splicings, where the isoform 4 is the complete molecule.

SIRP-α

SIRPα (also known as SHPS-1, BIT, CD172a, or p84) is a counter-receptor of CD47, whose interaction has been demonstrated to mediate cell adhesion. It is a member of the family of membrane proteins involved in the control of leukocyte activity. SIRPα is expressed in myeloid cells such as granulocytes, myeloid dendritic cells, mast cells, macrophages, and hematopoietic stem cells (Subramanian, Boder, and Discher 2007). SIRPα has two

immunoreceptor tyrosine-based inhibitory motifs (ITIM) in its cytoplasm and three immunoglobulin-like domains in its extracellular area (Figure 20).

CD47 and SIRPα regulate phagocytosis

In the instance of SIRPα, which interprets CD47 on the cell's surface as a "don't eat me" signal, APCs express receptors that regulate their activities, including phagocytosis (Navarro-Alvarez and Yang 2011). This signal results in the recruitment of phosphatases SHP-1 and -2, activation of SIRPα-ITIMs, and inhibition of phagocytosis.
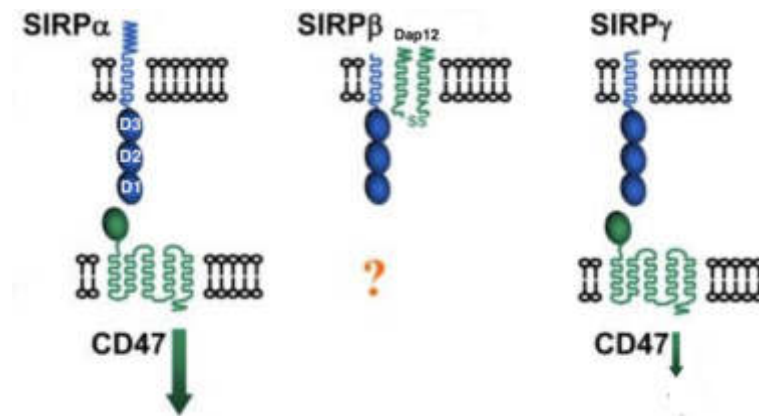
Figure 20. Interactions of SIRPs with CD47. The forms of SIRP have three Ig-like domains (blue ovals), of which only the D1 domain of SIRPα and SIRPγ interact with the Ig domain (green oval) of CD47, inducing signals of activation (green arrow). SIRPβ its activation only in the presence of the adapter protein Dap12 but doesn't bind to CD47. Obtained from (Barclay 2009).

Thrombospondin-1

Thrombospondin (TSP) belongs to a family of five multifunctional proteins that can be divided into two subgroups: first, TSP-1 and TSP-2, homotrimers with a region of procollagen type and repetitive regions, and a second group TSP-3, TSP-4 and TSP-5, which conform homopentamers (Martínez-Torres, 2013).

TSP-1 is a protein that is expressed mainly on the cell surface, and transiently in the extracellular matrix in a soluble manner. It modulates cellular functions by involving cell surface receptors and other components of the extracellular matrix. In adults, the TSP-1 expression is limited to tissue remodeling sites where it resides in the extracellular space and determines the phenotype, structure, and composition of the extracellular matrix. TSP-1 promotes the migration of vascular smooth muscle cells and suppresses the chemotaxis and motility of endothelial cells with the same potency (Mirochnik, Kwiatek, and Volpert 2008). The subfamily TSP-1 and TSP-2 present anti-angiogenic activities and have been shown to be able of inhibit tumor growth (Isenberg et al. 2009).

In addition, TSP-1 is the main soluble ligand of CD47, that after its interaction promote signals that alter cellular calcium and cyclic nucleotides signaling, integrins and growth factors, controls cell fate, its viability and resistance to stress (Roberts et al. 2012).
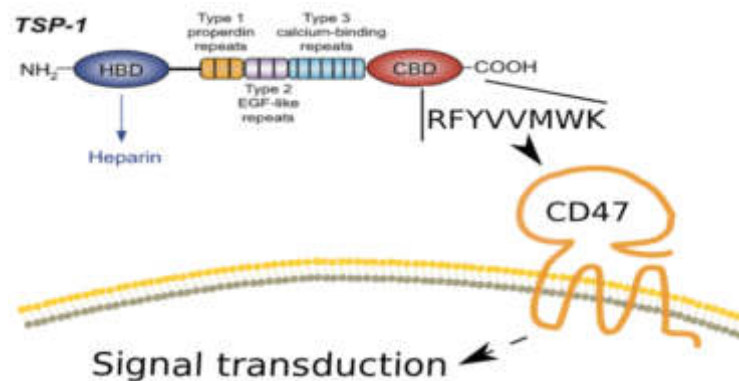

Figure 21. Thrombospondin-1 (TSP-1). TSP1 is composed of a globular N-terminal heparin binding domain (HBD), three chains that contain repeats of properdin (Type 1), epidermal growth factor like repeats (EGF, Type 2), and calcium binding (Type 3), joined by disulfide bonds, and another globular region in its C-terminal domain (CBD), which is the one that interacts with CD47. Adapted from Martínez-Torres, 2013.

As shown in Fig 21, the VVM motif in the carboxyl terminal domain of TSP-1 that binds to CD47 is conserved among the five families, suggesting that the binding to CD47 could be a universal characteristic of these families (Isenberg et al. 2009).

The CD47/TSP-1 interaction is involved in different biological processes. This interaction mediates the inhibitory signal of nitric oxide (NO), on the cardiovascular system leading to the decreases of adhesion molecules in platelets and alters the calcium levels in the vascular smooth muscle cells, among other mechanisms. In addition, vasodilation and chemotaxis are

controlled when TSP-1 inhibits the enzyme that censes and activates NO production, soluble guanylyl cyclase (sCG) in platelets and endothelial cells (Isenberg et al. 2006). Similarly, CD47 / TSP-1 plays an important role in angiogenesis, since it has been shown that peptides derived from TSP-1 inhibit angiogenesis induced by fibroblast growth factor 2 (FGF-2) *in vitro* and *in vivo* (Kanda et al. 1999).

CD47 as a therapeutic target in cancer

According to the diverse biological functions in which CD47 is involved, on the one hand, it exerts the "don't eat me" signal that can be exploited by neoplastic cells and contribute to their survival and progression. On the other hand, it can inhibit angiogenesis by interacting with TSP-1 and induce cell death in chronic lymphocytic leukemia (Mateo et al. 1999b) and breast cancer cells (Manna and Frazier 2004). The understanding of CD47, its ligands and signaling pathways, is fundamental to understanding its role as a therapeutic target.

CD47: induction of RCD in cancer cells

It has been observed that CD47 induces RCD in different cancer cell types. Monoclonal antibodies (mAbs) such as coated B6H12, soluble TSP-1, and peptides such a 4N1K have been used against CD47 to induce RCD in chronic lymphocytic leukemia (CLL) cells (Mateo et al. 1999b). Subsequently, many researchers continued to evaluate the induction of RCD in other cell types, using soluble anti-CD47 mAbs in multiple ALL (CCRF-CEM and Jurkat cells) (Leclair et al. 2018; Uno et al. 2007), breast cancer (MCF-7) (Manna and Frazier 2004) and AML cell lines (NB4-LR1) (Saumet et al. 2005), among others.

Furthermore, TSP-1, or TSP-1-mimic peptides such a 4N1 and 4N1K induced RCD in leukemic and breast cancer cells (Manna and Frazier 2004). The RCD induced by CD47 shared the following characteristics: a rapid cell death, caspase-independent, mitochondrial membrane depolarization without release of proapoptotic proteins, reactive oxygen species production, phosphatidylserine exposure, plasma membrane permeabilization, without DNA fragmentation or chromatin condensation (Martínez-Torres, 2013).

Although it was observed that peptides derived from TSP-1 induced RCD in cancer cells, the difficulty of their administration in a soluble manner limited the potential of their therapeutic use, for this reason most of the CD47 research of recent years reports the induction of RCD with mAbs through different mechanisms. Thus it was until 2015 when the activation of CD47 recovered importance when the first TSP-1-mimic peptide serum stable was synthetized, called PKHB1, which shares the same amino acid sequence of 4N1K, but the natural C- and N-terminal lysines, L-amino acids were replaced by their equivalents D. PKHB1 was shyntetized with the objective of optimizing the poor solubility and serum stability of the peptides 4N1 and 4N1K, which until 2015 were the only the TSP-1-mimic peptides that had been described (A.-C. Martinez-Torres et al. 2015). Therefore, it was demonstrated that the activation of CD47 by PKHB1 selectively induces calcium-regulated cell death in CLL cells from refractory patients, through ER changes, which leads to calcium ion overload (Ca^{2+}) in the cytosol, damaging lethally the mitochondria and inducing the proteases activation (serpases) (A.-C. Martinez-Torres et al. 2015).

On the other hand, the growth of CLL cell tumors (human cells) in xenotransplanted NSG (immunodeficient) mice was significantly reduced when treated with PKHB1 (A.-C. Martinez-Torres et al. 2015). Also, Dènefle et al. demonstrated that PKHB1 is also able to induce cell death of at least lung, colon and breast cancer cell lines, without damaging healthy B and T cells (Denèfle et al. 2016). Additionally, recent results show that PKHB1 selectively kills different types of leukemia cell lines (Jurkat, CEM, HL-60 and K562) and a murine T-cell lymphoblastic cell line (L5178Y-R), but not primary cultures of non-human cancerous or murine cells (Uscanga-Palomeque et al. 2018). PKHB1-Cell death in different types of leukemia apparently occurs through a mechanism similar to that of CLL, since it depends on the influx of calcium (Uscanga-Palomeque et al. 2018).

Possible implications of CD47 agonist peptides in the induction of immunogenic cell death

It is clear that the efficacy of current treatments against cancer, such as different chemotherapies and radiotherapies, is fundamentally based on their ability to stimulate innate and adaptive immune responses and overcome the immunosuppressive signals of the TME, which depend on the immunogenicity and the adjuvant capacity of the tumor (Lorenzo Galluzzi et al. 2017). An interesting feature observed in CLL cells is that PKHB1 caused exposure of CRT to the cell surface (A.-C. Martinez-Torres et al. 2015), which is deeply involved with the immunogenicity of cell death and favors the activation of immunological memory (Obeid et al. 2007).

In addition, CD47 plays critical roles in the immune system, regulates inflammatory responses (Gutierrez, Lopez-Dee, and Pidcock 2011; Sarfati et al. 2008), by mediating the migration of leukocytes to sites of infection (Martinelli et al. 2013) or the resolution of inflammation by the elimination of macrophages (Calippe et al. 2017). Finally, in our laboratory, we used PKHB1 to study its effects on an immunocompetent murine model with a syngeneic tumor of L5178Y-R cells, and we found that treatment with PKHB1 not only reduces the tumor burden in immunocompetent mice, but induces complete regression in most cases (Uscanga-Palomeque et al. 2018) inducing the intratumor T CD8+ cells infiltration, suggesting that the immune system could play a role in the antitumor activity of the TSP-1-mimic peptides. So collectively, the available data highlighted the potential of TSP-1-mimic peptides to induce non-apoptotic immunogenic cell death of cancer cells, which was tested in this thesis.

The bovine dializable leukocyte exctract, Immunepotent-CRP as an immunogenic cell death inducer.

The dialyzable leukocyte extract (DLE) obtained from disrupted spleen IMMUNEPOTENT CRP (ICRP), is a combination of biologically active substances that has numerous applications in human health. Besides, ICRP has now been shown to have immunomodulatory and anti-cancer properties, which I will further describe.

The immunomodulatory effects that has been observed with ICRP include; ICRP improved survival (90%) in BALB/c mice with LPS-induced endotoxic shock, decreasing IL-10, IL-6,

and TNF-α levels in serum (Franco-Molina et al. 2004). In addition, ICRP decreased NO, TNF-α and IL-6 but increased IL-10 production in LPS-stimulated murine peritoneal macrophages (Franco-Molina et al. 2005). Moreover, in LPS-stimulated human macrophages ICRP increased the endogenous antioxidants activity such as catalase, glutathione peroxidase, and superoxide dismutase, and decreased cyclooxygenase-2 activity, PGD2, NO, and TNF-α production (Franco-Molina et al. 2011). Furthermore, ICRP administration improved life-quality and increase the total leukocytes and T-lymphocyte subpopulations (immunomodulatory activity) in lung and breast cancer patients undergoing chemotherapy and-or radiation therapy (Franco-Molina et al. 2008; Lara et al. 2010).

ICRP also has anti-tumor activity, as ICRP induced loss of cell viability in breast (MCF-7, BT-474, MDA-MB-453), lung (A549, A427, Calu-1, INER-51), cervical (HeLa, SiHa), and lymphoid (L5178Y, K562, MOLT-3) cancer cell lines, without affecting the viability of human monocytes and PBMCs, and murine peritoneal macrophages (Franco-Molina et al. 2006; Martinez-Torres et al. 2019; Martínez-Torres et al. 2018; Sierra-Rivera et al. 2016).

ICRP triggered ROS production and caspase-independent cell death, which involves mitochondrial damage, cycle arrest and DNA degradation(Martínez-Torres et al. 2018; A. C. Martinez-Torres et al. 2019) in lung and cervical cancers. Also, in murine melanoma, ICRP decreased the viability of melanoma B16F10 cells, inducing the activation of caspase-3, and *in vivo*, ICRP-treatment induce tumor decrease and dimmish tumor weight, which improved the survival of tumor-bearing mice, showing a decrease in VEGF production and prevention of metastasis (Franco-Molina et al. 2010), moreover, ICRP combined with oxaliplatin increased DAMPs release and the rate of ICD (Rodríguez-Salazar et al. 2017).

In breast cancer cells, ICRP induced caspase-independent, ROS-dependent cell death and ROS-dependent autophagosome formation (Martínez-Torres et al. 2020); furthermore, treated with ICRP decrease tumor volume and increase in survival in breast tumor-bearing mice decrease in comparison with untreated mice. Also, ICRP treatment decreased PD-L1, IDO and Gal-3 expression, IL-6, IL-10, and MCP-1 levels, and increased IFN-γ, and IL-12 levels in the tumor site. Moreover, ICRP treatment increase CD8+ T cells, memory T cells,

and innate effector cells in peripheral blood, where they also observed an increase in IFN-γ, and IL-12 levels (Santana-Krímskaya et al. 2020). These results strongly suggest that ICRP induce an effective immune system stimulation and a TME remodeling which is related with the induction of ICD.

JUSTIFICATION

Cancer is one of the most important public health problems worldwide. Despite the efforts to treat it, innate and acquired treatment-resistance of cancer cells to current therapies remain one of the principal problems to solve in clinical care. Immunogenic cell death (ICD) recently has been recognized as a critical determinant for the efficiency of cancer therapies. Due to this, the current treatments seek to induce ICD in cancer cells through conventional chemotherapeutics, targeted antitumor agents, and other biological and physicochemical therapies. Unfortunately, most treatments are highly nonspecific and cause serious side effects that limit their use.

From this perspective, the use of synthetic peptides and immunotherapies are a promising approach in cancer therapy, since it has been observed that both treatments induced selective regulated cell death (RCD) of cancer cells. Also, the cell death induced by thrombospondin-1 mimic peptides in leukemic cells is characterized by endoplasmic reticulum alterations and CRT exposure, one of the main DAMPs involved in ICD, and the ICRP-cell death induces ROS production and autophagy that are related with ICD-induction.

However, the mechanisms and immunogenicity of the cell death induced by thrombospondin-1 mimic peptides and ICRP has not been evaluated in breast cancer models. Therefore, this study was conceived to expand the knowledge of the immunogenicity of these types of cell death and its effect on the establishment of an antitumor immune response. This might extend its potential application to other types of cancer, and to evidence its possible advantages over the current ICD inducers.

HYPOTHESIS

PKHB1 and IMMUNEPOTENT CRP induce immunogenic cell death in breast cancer cells

OBJECTIVES

General objective

- To evaluate the mechanism and immunogenicity of the cell death induced by PKHB1 and Immunepotent-CRP in breast cancer cells.

Specific objectives

- To determine the mechanism of the cell death induced by PKHB1 and Immunepotent-CRP in breast cancer cells.
- To analyze the immunogenicity and therapeutic potential of the cell death induced by PKHB1 and Immunepotent-CRP in breast cancer cells.

CHAPTER 1.

1. Study of the mechanism and immunogenicity of the cell death induced by PKHB1.

The results in the present chapters gave rise to a patent: EP3650036A1, filed by Sorbonne Université and Universidad Autónoma de Nuevo León.

1.1. Article 1. PKHB1, a thrombospondin-1 peptide-mimic, induces antitumor effect through immunogenic cell death induction in breast cancer cells.

Taylor & Francis
Taylor & Francis Group

ORIGINAL RESEARCH

🔓 OPEN ACCESS | Check for updates

PKHB1, a thrombospondin-1 peptide mimic, induces anti-tumor effect through immunogenic cell death induction in breast cancer cells

Kenny Misael Calvillo-Rodríguez [a,b,c], Rodolfo Mendoza-Reveles[a], Luis Gómez-Morales[a,b,c,d], Ashanti Concepción Uscanga-Palomeque[a], Philippe Karoyan [b,c,d,e,f*], Ana Carolina Martínez-Torres [a*], and Cristina Rodríguez-Padilla[a,g*]

[a]Facultad de Ciencias Biologicas, Laboratorio de Inmunología y Virología, Universidad Autónoma de Nuevo León, San Nicolás de los Garza, Mexico; [b]Sorbonne Université, Ecole Normale Supérieure, PSL University, CNRS, Laboratoire des Biomolécules, LBM, 75005 Paris, France; [c]Sorbonne Université, Ecole Normale Supérieure, PSL University, CNRS, Laboratoire des Biomolécules, DRUG Lab, Site OncoDesign, 25-27 Avenue du Québec, 91140 Les Ulis, France; [d]Kaybiotix, GmbH, Zugerstrasse 32, 6340 Baar, Switzerland; [e]Kayvisa, AG, Industriestrasse, 44, 6300 Zug, Switzerland; [f]χ-Pharma, 25 Avenue du Québec, 91140 Les Ulis, France; [g]LONGEVEDEN SA de CV, Monterrey, Mexico

ABSTRACT

Breast cancer is the most commonly diagnosed cancer and the leading cause of cancer death in women worldwide. Recent advances in the field of immuno-oncology demonstrate the beneficial immunostimulatory effects of the induction of immunogenic cell death (ICD). ICD increases tumor infiltration by T cells and is associated with improved prognosis in patients affected by triple negative breast cancer (TNBC) with residual disease. The aim of this study was to evaluate the antitumoral effect of PKHB1, a thrombospondin-1 peptide mimic, against breast cancer cells, and the immunogenicity of the cell death induced by PKHB1 in vitro, ex vivo, and in vivo. Our results showed that PKHB1 induces mitochondrial alterations, ROS production, intracellular Ca^{2+} accumulation, as well calcium-dependent cell death in breast cancer cells, including triple negative subtypes. PKHB1 has antitumor effect in vivo leading to a reduction of tumor volume and weight and promotes intratumoral CD8 + T cell infiltration. Furthermore, in vitro, PKHB1 induces calreticulin (CALR), HSP70, and HSP90 exposure and release of ATP and HMGB1. Additionally, the killed cells obtained after treatment with PKHB1 (PKHB1-KC) induced dendritic cell maturation, and T cell antitumor responses, ex vivo. Moreover, PKHB1-KC in vivo were able to induce an antitumor response against breast cancer cells in a prophylactic application, whereas in a therapeutic setting, PKHB1-KC induced tumor regression; both applications induced a long-term antitumor response. Altogether our data shows that PKHB1, a thrombospondin-1 peptide mimic, has in vivo antitumor effect and induce immune system activation through immunogenic cell death induction in breast cancer cells.

Background

Breast cancer is the most frequent type of cancer among women; its innate and acquired treatment resistance to current therapies is the principal problem to treat it, causing the greatest number of cancer-related deaths.[1] While systemic therapies have increased the survival rates of breast cancer patients, the dramatic variations in response rates of patients with distinct clinicopathologic parameters,[2] as well as innate or acquired resistance to current therapies,[3] make relevant the search for new effective treatments for the different molecular subtypes of breast cancer, in particular those associated with poor prognosis.

Recently, several clinical studies have demonstrated the beneficial immunostimulatory effects of inducing immunogenic cell death (ICD),[4,5] recognized as a critical determinant for the efficiency of cancer therapies. Indeed, this peculiar type of cell death is capable of stimulating a long-term antitumor

immune response against dead cancer cell antigens.[6,7] Additionally, inducing ICD increases tumor tissue infiltration by T cells, which plays an essential role in mediating a positive response to chemotherapy and is associated with improving clinical outcomes in all subtypes of breast cancer.[5,8]

We recently designed PKHB1 through a structure–activity relationship studies around the C-terminal Binding Domain (CBD) of thrombospondin-1 (TSP-1). PKHB1 is a peptide mimic stable in the serum of mice and human and able to induce a cell death involving CD47 activation in different cancer cells, especially in hematological malignancies.[9–12] The ability of PKHB1 to induce cell death was also observed in leukemic cells from patients with aggressive and chemo-resistant phenotypes, without affecting non-tumoral cells from humans or mice.[9,11,13] Additionally, PKHB1 induces ICD in T cell acute lymphoblastic leukemia.[11,14] If this peptide is currently under

development in pre-clinical studies addressing CLL (χ-Pharma), little is known about the cell death capacity, mechanism, immunogenicity, and the antitumor effect of PKHB1 in solid cancers with different molecular characteristics and poor prognosis such as breast cancer (including the triple negative subtype).

Therefore, the aim of this study was to evaluate the antitumor potential of PKHB1 in breast cancer cells (in vitro and in vivo) including triple negative subtypes and to determine whether it induces antitumor immune system activation through ICD induction (ex vivo and in vivo).

Methods

Peptide synthesis

PKHB1 and 4NGG peptides were synthesized manually, using Fmoc-protected amino acids and standard solid phase peptide synthesis (SPPS) (supplemental material and methods), as described previously.[6]

Cell culture

MCF-7, MDA-MB-231, and 4T1 cell lines were obtained from the ATCC. MCF-7 and MDA-MB-231 cell lines were maintained in DMEM-F12 medium (GIBCO by Life Technologies, Grand Island, NY, USA), while 4T1 cell line was maintained in RPMI-1640 medium, both were supplemented with 10% of fetal bovine serum, 2 mM L-glutamine, 100 U/mL penicillin-streptomycin (GIBCO by Life Technologies, Grand Island, NY, USA), and incubated at 37°C in a controlled humidified atmosphere with 5% CO_2. Cell count was performed following the ATCC's standard protocols.

Cell death induction and inhibition analysis

5×10^4 cells were plated in 24 wells dishes and left untreated or treated for 2 h with 100 µM, 200 µM, 300 µM, or 400 µM of PKHB1 (*KRFYVVMWKK*), or 300 µM of 4NGG (KRFYGGMWKK). Annexin-V-allophycocyanin (Ann-V-APC 0.1 µg/ml; BD Pharmingen, San Jose CA, USA), and propidium iodide (PI, 0.5 µg/ml Sigma-Aldrich) were used to assess phosphatidylserine exposure, cell death, and cell viability quantification, respectively, in a BD AccuryC6 flow cytometer (BD Biosciences, Franklin Lakes, NJ, USA) (total population 10,000 cells). Data was analyzed using FlowJo software (LLC, Ashland, OR, USA).

The calcium chelator BAPTA (5 mM), the pan-caspase inhibitor Z-VAD-FMK (Z-VAD, 50 µM), the antioxidant N-Acetyl Cysteine (NAC, 5 mM), the necroptotic inhibitor Necrostatin-1 (Nec-1, 50 µM), the phospholipase C (PLC) inhibitor U73122 (1.25 µM) and the ER receptor inhibitors dantrolene (50 µM) and 2-aminoethoxydiphenyl borate (2-APB, 40 µM) were incubated 30 minutes with the indicated agent, before treatment with PKHB1 (CC_{50}), epirubicin (42.5 µM for MCF-7 and MDA-MB-231 and 5 µM for 4T1 for 24 h), or H_2O_2 (25 µM for all cell lines for 24 h) when indicated.

Intracellular Ca^{2+} levels assay

5×10^4 cells/well in 24 wells dishes (Life Science) were left untreated or pre-incubated with 2.5 mM BAPTA, and then treated for 2 h with PKHB1 (CC_{50}) or left untreated in medium. Then, cells were detached, washed with RINGER buffer without Ca^{2+}, and resuspended in 200 µL of the same RINGER buffer with 0.001 µg/mL of Fluo-4 AM (Life Technologies) and 0.001 µg/mL of Pluronic F-127 (Life Technologies), incubated 37°C for 30 min. Next, cells were washed with RINGER buffer w/o Ca^{2+} and assessed by BD Accuri C6 flow cytometer (BD Biosciences, Franklin Lakes, NJ, USA) (total population 10,000 cells), and data was analyzed using FlowJo software (LLC, Ashland, OR, USA).

In vivo model

This study was approved by The Animal Research and Welfare Ethics Committee (CEIBA), of the College of Biological Sciences, number: CEIBA-2018-003. All experiments were conducted according to Mexican regulation NOM-062-ZOO-1999. Female BALB/c mice (6- to 8-week-old; 22 ± 2 g weight) were maintained in controlled environmental conditions (25°C and 12 h light/dark cycle) and supplied with rodent food (LabDiet, St. Louis, MO, USA) and water *ad libitum*, and they were monitored daily for health status. Mice were randomly assigned to different groups for all studies. All experiments were designed in accordance with the ARRIVE guidelines for animal care and protection (supplemental material).[15]

Tumor establishment

5×10^5 live 4T1 cells in 100 µL of PBS were injected subcutaneously in the left hind. Tumor volume and mice weight were measured three times per week using a caliper (Digimatic Caliper Mitutoyo Corporation, Japan) and a digital scale (American Weigh Scale-600-BLK, USA), respectively. Tumor volume was determined with the formula: tumor volume (mm^3) = (Length × width²)/2. When tumor reached 70–120 mm^3, 3 days after inoculation with tumor cells, mice were treated daily with 400 µg of PKHB1 in 200 µL of sterile water by intraperitoneal injection, control mice were treated with 200 µL of sterile water. Sixteen days after inoculation with tumor cells, mice were anesthetized with ketamine (i.p. 80 mg/kg body weight) and xylazine (i.p. 10 mg/kg body weight) and were euthanized by cervical dislocation. Tumors from Control or PKHB1-treated mice, were obtained and fixed in 3.7% neutral formalin, embedded in paraffin, sectioned (5 µm thickness) and stained with H&E (MERCK). Histopathological analyses were done by an external veterinarian pathologist (National professional certificate 2,593,012).

T cells evaluation

Sixteen days after tumor inoculation, mice treated (n = 6) or untreated (n = 6) were anesthetized and sacrificed as described above. Blood was obtained by cardiac puncture and isolation of the peripheral blood mononuclear cells (PBMCs) was

performed by density gradient centrifugation using Ficoll-Hypaque-1119 (Sigma-Aldrich, St Louis, MO, USA). The spleen, lymph node, and tumor were harvested and filtered through a cell strainer (70 μM) with PBS (PBMCs were obtained from the spleen as described above), then 1×10^6 cells/mL were plated and the percent of CD3+, CD4+ and CD8 + T cells was observed by flow cytometry with the Mouse T lymphocyte subset antibody cocktail CD3 (clone 145–2C11), CD4 (clone RM4-5), and CD8 (clone 53–6.7) (from BD Bioscience) following the manufacturer's instructions.

Myeloid-derived suppressor cells (MDSCs) and Tregs evaluation

For MDSCs assessment, PBMCs were obtained from the blood of mice as described above. Cells were labeled with a cocktail of CD11b-PE (clone M1/70), Gr-1-APC (clone RB6/8C5), and Ly-6 G-FITC (clone 1A8) using the Mouse MDSC Flow kit (from Biolegend) following the manufacturer's instructions.

For Tregs evaluation, PBMCs were obtained from the blood of mice as described above. Cells were labeled using a True Nuclear One Step Staining Mouse Treg Flow kit (FOXP3-AlexaFluor488, CD25-PE, CD4-PerCP; Biolegend) following the manufacturer's instructions.

Cells were assessed in a BD Accuri C6 flow cytometer (BD Biosciences, Franklin Lakes, NJ, USA), and data was analyzed using FlowJo software (LLC, Ashland, OR, USA).

Calreticulin, HSP70, and HSP90 exposure

5×10^4 cells/well were plated in 24-well plates and treated with PKHB1 (CC_{50}) for 2 h or epirubicin (42.5 μM for MCF-7 and MDA-MB-231 and 5 μM for 4T1 for 24 h). Then, cells were detached, washed, and incubated for 1 h at room temperature (RT) with 2 μg/mL of anti-Calreticulin (FMC-75, Enzo Life Science), 0.8 μg/mL anti-HSP70 (F-3, Santa Cruz Biotechnology), and 0.8 μg/mL anti-HSP90 (F-8, Santa Cruz Biotechnology) in FACS buffer; cells were washed and incubated for 30 min in darkness at RT with goat anti-mouse IgG (Alexa Fluor 488) (H + L, Life Technologies) (1:1500) in FACS buffer; cells were then washed and incubated in the dark for 10 min at RT with 7-AAD (Life Technologies) (1:1000) in FACS buffer. The surface exposure of CALR, HSP70 and HSP90 was determined by flow cytometry in non-permeabilized (7-AAD-negative) cells.

Immunofluorescence microscopy

2.5×10^5 cells/well in 6-well dishes were left untreated (Control) or treated with PKHB1 (CC_{50}) and incubated for 2 h. Then, cells were washed with PBS and stained with Calreticulin-PE antibody (FMC-75, 2 μg/ml) and Hoechst 33,342 (0.5 μg/ml) (Thermo Scientific Pierce, Rockford, IL, USA), incubated for 1 h in FACS buffer at RT, washed twice, maintained in PBS, and assessed by confocal microscopy (Olympus X70; Olympus, Tokyo, Japan).

ATP and High-mobility group box 1 release assay

2.5×10^5 cells/well in 6-well dishes were left untreated (Control) or treated with PKHB1 (CC_{50}) for 2 h. Supernatants were recovered, centrifuged at 1600 rpm/10 minutes and used to assess extracellular ATP by a luciferase assay (ENLITEN kit, Promega, Madison, WI, USA), or HMGB1 using the HMGB1 ELISA kit for MDA-MB-231, MCF-7 and 4T1 cells (BioAssay ELISA kit human or mouse, respectively; US Biological Life Science Salem, MA, USA) following the manufacturer's instructions. Bioluminescence was assessed in a microplate reader (Synergy HT, Software Gen5; BioTek, Winooski, VT, USA) at 560 nm, and absorbance was assessed at 450 nm.

T cell isolation

Mice were anesthetized and sacrificed as described above, and blood was obtained by cardiac puncture. PBMCs isolation was performed as described above. Murine CD3+ cells were isolated from total PBMCs by positive selection using magnetic-activated cell sorting (MACS) microbead technology with anti-CD3ε-biotin and anti-biotin microbeads (Miltenyi Biotech; >98% purity and >98% viability), as stated by manufacturer's instructions.

Differentiation of bone marrow-derived dendritic cells (BMDCs)

After sacrifice of anesthetized mice (n = 6), bone marrow was removed from the femur and tibia by flushing into RPMI-1640. Eluted cells were cultured for 5 days with 20 ng/mL of IL-4 and GM-CSF (R&D Systems, Minneapolis, MN, USA) until approximately 70% of the cells were CD11c+.

Evaluation of DCs maturation

CD11c, MHC-II, CD80, and CD86 were evaluated by flow cytometry with the fluorescent label-conjugated antibodies, antiCD11c-Alexa-fluor 488 (N418, R&D Systems), anti-MHC Class II-PE (REA813, Miltenyi Biotec), anti-CD80-FITC (16–10A1, R&D Systems), and antiCD86-APC (GL1) from BD Biosciences (San Jose, CA, USA). In brief, 1×10^6 DCs /mL were stained in 100 μL of FACS buffer with the indicated antibodies at RT for 30 minutes and then were washed twice with PBS, centrifugated at 1600 rpm/10 min, resuspended in 100 μl of FACS buffer and assessed by Flow Cytometer as described previously. For MHC-II and CD80 evaluation by flow cytometry, CD11c was added with MHC-II or CD86, we then gated CD11c+ cells and we next assessed MHC-II or CD86 MFI.

PKHB1-KC and EPI-KC preparation

4T1 cells (1.5×10^6 cells/mL per mice) were plated and, after adherence, cells were then treated with 400 μM of PKHB1 for 2 h or 10 μM of EPI for 24 h, to obtain 80–90% of killed cells (KC). After treatments, cells were obtained, centrifuged at 1600 rpm/10 min and resuspended in 100 μL of serum-free

medium/mice. Cell death was confirmed using Trypan blue staining and flow cytometry. Finally, the PKHB1-KC or EPI-KC were inoculated by subcutaneous injection in the right flank.

Freeze and thaw-killed cells preparation

4T1 cells (3×10^6 cells/mL per mice) were first frozen at $-80°C$ for 15 min, then thawed 10 min at $37°C$ in a water bath. The freeze–thaw (F-T) cycles were repeated three times in rapid succession. After the final thaw, killed cells were resuspended in PBS.

DCs' co-culture with PKHB1-KC, EPI-KC, or FT-KC

DCs were resuspended in fresh medium (1×10^6 cells/mL), left untreated (control) or incubated with 3×10^6 4T1 killed cells/mL obtained after treatment with PKHB1, EPI, or FT, to give a range of 1:3 (DCs to killed cells); co-culture was left for 24 h. Then the supernatant was obtained, and the well was washed twice with PBS before the next co-culture.

DCs + T lymphocytes co-culture

Control DCs or DCs previously co-cultured with PKHB1-KC, EPI-KC, or FT-KC were maintained in fresh medium at 1×10^6 cells/mL. Then, allogeneic BALB/c mCD3+ cells were added at 3×10^6 cells/mL to give a range of 1:3 (DCs to CD3+ cells), co-culture was left for 96 h. Then, lymphocytes were collected (in the supernatant), washed with PBS, and resuspended in fresh medium at 5×10^6 cells/mL for their use in the next co-culture.

T-Lymphocytes + 4T1 cells co-culture

1×10^5 cells/mL viable 4T1 cells were plated. Then, allogeneic BALB/c mCD3+ cells were added to each well at 5×10^5 cells/mL, unprimed (previously co-cultured with control DCs) or primed (previously co-cultured with DCs-PKHB1-KC, EPI-KC, or FT-KC) to give a range of 1:5 (tumor to effector). Co-culture was left for 24 h.

Cytokine release assay

Supernatants from the indicated co-cultures were obtained for the assessment of IL-2, IL-4, IL5, and TNFα (BD CBA Mouse Th1/Th2 Cytokine Kit, San Jose, CA, USA) by flow cytometry following manufacturer's instructions. IFNγ was assessed using an ELISA kit (Sigma-Aldrich) and the Synergy HTTM (BioTek Instruments, Inc., Winooski, VT, USA) plate reader at 570 nm wavelength, following manufacturer's instructions.

Calcein assay

4T1 cells (1×10^6 cells/mL) were stained with (0.1 mL/mL) Calcein-AM from BD Biosciences (San Jose, CA) in FACS buffer at $37°C$ and 5% CO_2 for 30 min, washed twice with PBS. Thus, primed or unprimed T cells were added in a 1:5 (tumor to effector) ratio. Co-culture was incubated at $37°C$ and 5% CO_2 for 24 h. Finally, calcein

positive or negative 4T1 cells were assessed in a BD AccuryC6 flow cytometer (BD Biosciences) (total population 10,000 cells). Data was then analyzed using FlowJo software.

Prophylactic vaccination

Vaccination was carried out as follows: PKHB1-KC (n = 10) or EPI-KC (n = 10) were obtained as previously described, and then inoculated s.c. in 100 µL of serum-free medium into the right hind leg (day −7), 7 days later, viable (5×10^5) 4T1 cells were inoculated into the left hind leg (day 0). Tumor volume and weight were measured as described above.

PKHB1-KC and EPI-KC treatment

Tumor was established by subcutaneous injection of 5×10^5 4T1 cells in 100 µL of PBS, in the left hind. Tumor volume and mice weight were measured as described above. When tumor reached $70–120$ mm^3 the first treatment of PKHB1-KC (n = 10) or EPI-KC (n = 10) was applied. Killed cells were inoculated subcutaneously in 100 µl of serum-free medium, in the right hind, twice a week for a total of four applications in a 2-week period. Control mice were treated with 100 µl of serum-free medium.

Long-term antitumor effect evaluation

Mice in complete remission after prophylactic (n = 9) or therapeutic (n = 9) 4T1-PKHB1-KC application were re-challenged with 5×10^5 4T1 viable cells in 100 µL of PBS in the left hind and tumor volume was measured as described above.

Long-term splenocytes-cytotoxicity

Mice in complete remission after prophylactic (n = 4) or therapeutic (n = 4) PKHB1-KC application were re-challenged with 5×10^5 4T1 viable cells in 100 µL of PBS in the left hind. Three days after tumor inoculation mice were sacrificed, spleens were harvested, filtered through a cell strainer (70 µM) with PBS, and PBMCs were obtained as described above. Splenocytes were recovered and co-cultured with 4T1 cells (previously stained with calcein-AM) at 44:1 ratio (respectively). Finally, calcein positive or negative cells were assessed as described above.

Statistical Analysis

Mice were randomly assigned to different groups for all *in vivo* studies. At least three independent experiments were repeated three independent times. Mann-Whitney tests and two-tailed unpaired Student's *t*-tests were performed using GraphPad Prism Software (San Diego CA, USA) and presented as mean values $\pm$ SD. The *p* values were considered significant as follows: $p < 0.05$.

Results

PKHB1 induces breast cancer cell death

Although the potency of PKHB1was previously demonstrated in hematopoietic malignancies,[9,11] its effectiveness was not yet evaluated for solid tumors *in vivo*. Thus, after peptide synthesis and characterization (Supplemental material and methods, table sup.1 and figure sup.1), we evaluated here its effect in two types of human breast cancer cell lines, I) MCF-7 (luminal subtype) and II) MDA-MB-231 (triple negative subtype), as well as on the murine 4T1 cell line (mimics triple negative subtype).[16] We observed that PKHB1 induces cell death in a concentration-dependent way in MCF-7 (Figure 1(a)), MDA-MB-231 (Figure 1(b)), and 4T1 (Figure 1(c)) cells, as they showed an increase in the percentage of double-positive Ann-V-APC/PI staining (figure sup. 2). We determined that the cytotoxic concentration that induces approximately 50% of cell death (CC$_{50}$) in MDA-MB-231 and MCF-7 is 200 μM whereas in 4T1 is 300 μM.

Next, we evaluated mitochondrial damage and cytosolic Ca^{2+} augmentation, and observed that PKHB1 (CC$_{50}$) induced loss of mitochondrial membrane potential (Figure 1(d)), ROS production (Figure 1(e)) and increase of intracellular Ca^{2+} (Figure 1(f)) in all cell lines. Afterwards, we searched to determine the cell death effectors and evaluated ROS-dependence, also, we used inhibitors of caspases (Z-VAD), necroptosis (Nec-1), and the Ca^{2+}-chelator (BAPTA) and assessed cell death. We used epirubicin (EPI) and H$_2$O$_2$ as controls for inhibition. We found that Z-VAD inhibited the cell death induced by EPI but not PKHB1-induced cell death (Figure 1(g)), while NAC and NEC-1 inhibited the cell dead induced by H$_2$O$_2$ but not PKHB1-mediated cell death (Figure 1(h,i)). Finally, we observed that the Ca^{2+} chelator BAPTA inhibited the Ca^{2+} augmentation (figure sup. 3) and cell death (Figure 1(j)), induced by PKHB1. This Ca^{2+} dependence was previously observed for leukemic cells,[9,11] suggesting a similar cell death mechanism and common signaling pathway among solid and liquid cancers.

To assess this hypothesis, we used a phospholipase C (PLC) inhibitor (U73122) and ER receptor inhibitors (dantrolene, for ryanodine receptors, and 2-APB, for IP$_3$ receptors). We determined that PKHB1-cell death is significatively inhibited when blocking the ER-Ca^{2+}-channels with U73122, dantrolene and 2-APB (Figure 1(j,k) and Figure 1(l)) in breast cancer cells, confirming a similar cell death pathway induced by PKHB1 in breast cancer cells, as previously found in leukemic cells.

PKHB1 has antitumor effects in breast cancer and promotes intratumorally CD8 + T cell infiltration

To evaluate *in vivo* the potential antitumor effect of PKHB1, 4T1 breast cancer cells were grafted into BALB/c mice. Daily treatments were initiated when tumor volume reached approximately 100 mm^3, and 16 days after the cell transplant, tumor volume of the control mice had reached 1500 mm^3, requiring the sacrifice of the animals, while the tumor volume of the PKHB1-treated mice reached a maximum volume of 890 mm^3 (at day 8) which started to decrease, reaching a volume of 570 mm^3 at day 16 (Figure 2(a)) (individual growth curves in figure sup. 4). Also, daily treatment with PKHB1 did not affect mice weight (figure

sup. 5). The decrease in tumor volume was correlated with the decrease in tumor weight, going from 1.5 grams in the controls to 0.40 grams in PKHB1-treated mice (Figure 2(b)). The decrease of tumor volume in mice treated with PKHB1, led us to evaluate the involvement of T cells in the observed effect. First, we analyzed histological sections of tumors from control (Figure 2(c)) or PKHB1-treated mice (Figure 2(d)); results revealed that tumors from control mice showed tumor cells (black arrows) with moderate mitotic activity (blue arrows), whereas the PKHB1-treated mice showed sporadic mitotic activity, extensive necrosis with abundant accumulation of cellular debris (green arrows), and abundant inflammatory exudate, composed of polymorphonuclear elements, eosinophils, and lymphoplasmacytic cells (red arrows).

Additionally, we evaluated if the cell number and distribution of T lymphocytes in peripheral blood, spleen, lymph nodes, and tumor site, changed after PKHB1 treatment. We observed (Figure 2(e)) that the percentage of CD3+ cells increased in blood, lymph nodes, and tumors of PKHB1-treated mice, while it was maintained in spleen. When we assessed CD4+ cells, the percentage of cells significantly augmented in lymph nodes, whereas it was significantly diminished in the tumor site (Figure 2(f)). Furthermore, CD8 + T cells significantly increased in peripheral blood and specially in tumor site (gating strategy in figure sup. 6), while they significantly diminished in lymph nodes (Figure 2(g)). To extend this analysis, we evaluated the proportion of myeloid-derived suppressor cells (MDSCs) and Tregs in peripheral blood of control and PKHB1-treated mice. We found a significant decrease in the percent of MDSCs (mean from 48% to 23%) and Tregs (mean from 12% to 3%) in mice treated with PKHB1, when compared with control mice (Figure 2(h,i)). Additionally, we determine a significant increase in the ratio of CD8/Tregs (mean 2% to 14%) in mice treated with PKHB1, when compared with control mice (Figure 2(j)). Finally, we determined whether splenocytes from PKHB1-treated mice could induce an antitumor cell cytotoxicity. For this purpose, we evaluated the calcein negative 4T1 cells after co-culture with splenocytes obtained from control or PKHB1-treated mice. In Figure 2(k), results show that splenocytes from PKHB1-treated mice induced a significant increase in calcein negative 4T1 cells (75%) in comparison with control mice (40%). These results improve the knowledge of the immune system-involvement in the antitumor effect mediated by PKHB1 treatment.

PKHB1 induces DAMPs exposure and release in breast cancer cell lines

As we observed that PKHB1 induced cell death in breast cancer cell lines and CD8 + T lymphocyte-recruitment in tumor site and the decrease of immunosuppressive cells, we wondered if cell death induced by PKHB1 was able to induce DAMPs' exposure/release in breast cancer cells. The first step was to evaluate the exposure of CALR (one of the principal DAMPs related with ICD).[17] Our results show that PKHB1-treatment and EPI-treatment were able to induce a significant increase of CALR positive cells in MCF-7 (Figure 3(a)), MDA-MB-231 (Figure 3(b)), and 4T1 (Figure 3(c)) cells. The CALR exposure induced by PKHB1 was confirmed by immunofluorescence microscopy,
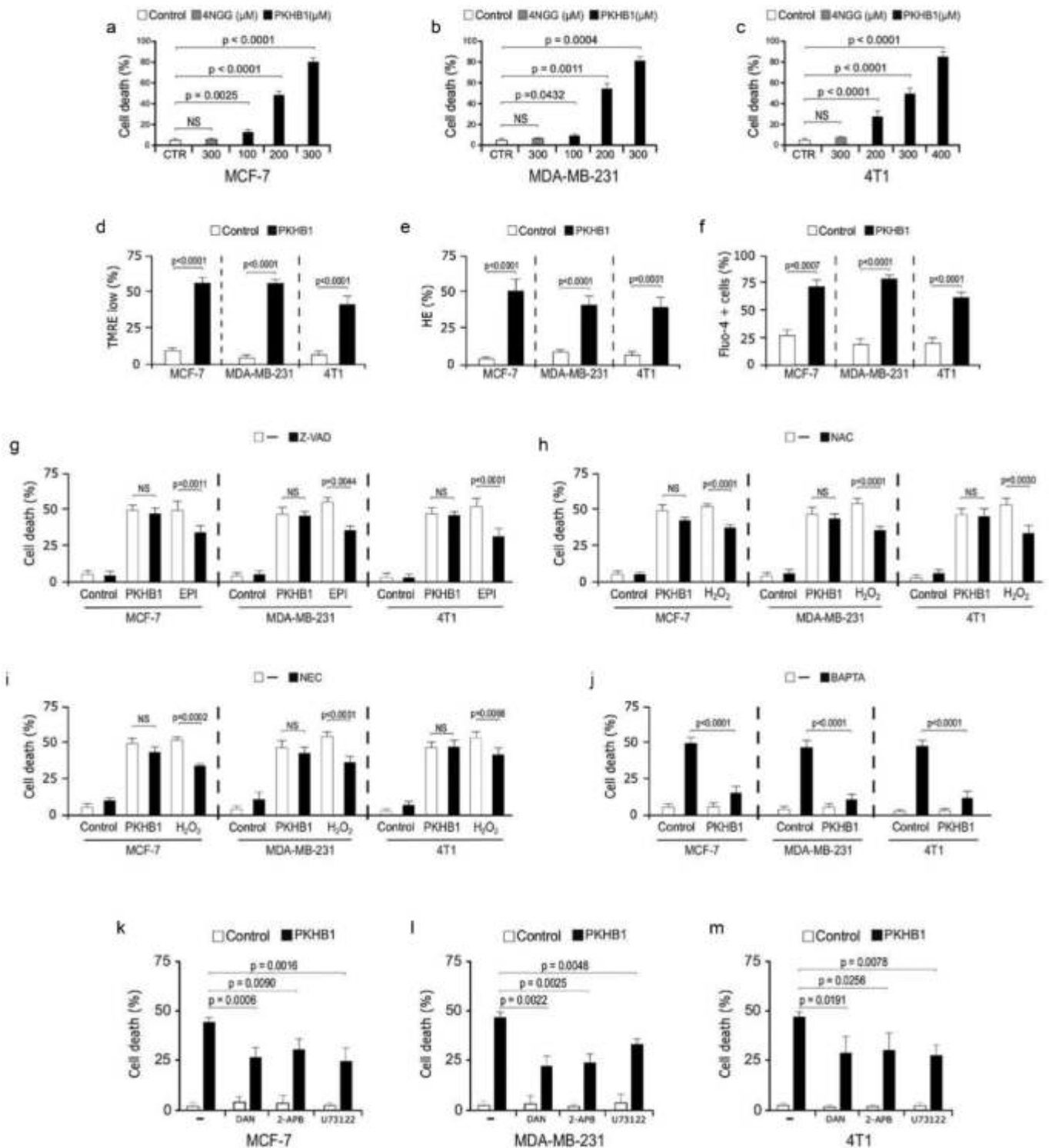
Figure 1. PKHB1 induces cell death in breast cancer cell lines. Cell death analysis in (A) MCF-7, (B) MDA-MB-231 and (C) 4T1 cells, without treatment (Control), treated with the control peptide 4NGG (300 µM) or PKHB1 (100, 200, 300, or 400 µM) for 2 h. (D) Representative graphs and quantification of the loss of ΔΨm measured through TMRE, (E) ROS levels measured through Hydroethidine staining and (F) intracellular Ca^{2+} by Fluo-4 staining, by flow cytometry in cells left alone or treated with the CC_{50} of PKHB1 (200 µM for MCF-7 and MDA-MB-231 and 300 µM for 4T1) for 2 h. (G-I) Cell death induced by PKHB1 (CC_{50}), Epirubicin (42.5 µM for MCF-7 and MDA-MB-231 and 5 µM for 4T1) and H2O2 (25 µM for all cell lines) was assessed in cells left without pre-treatment (-) or pre-treated (30 minutes) with Z-VAD-FMK (Z-VAD), N-Acetyl Cysteine (NAC) and Necrostatin-1 (NEC-1). (J) Cell death induced by PKHB1 (CC_{50}) was assessed in cells left without pre-treatment (-) or pre-treated (30 minutes) with BAPTA. Cell death induced by PKHB1 (CC_{50}) was assessed as in J in cells left without pre-treatment (-) or pre-treated (30 minutes) with dantrolene, 2-APB or U73122. Graph represents the means (±SD) of triplicates of three independent experiments. NS = Not significant.

where we observed that PKHB1 induced CALR exposure in all the cases Figure 3(d,e) and Figure 3(f). Additionally, PKHB1 treatment induced 24 ± 3, 3.2 ± 1.3 and 4.23 ± 2-fold of HSP70 exposure (Figure 3(g)), 2.7 ± 0.6, 2 ± 0.6, and 7 ± 1.85-fold of HSP90 exposure (Figure 3(h)) in MCF-7, MDA-MB-231 and 4T1 cells, respectively, when compared with untreated cells.
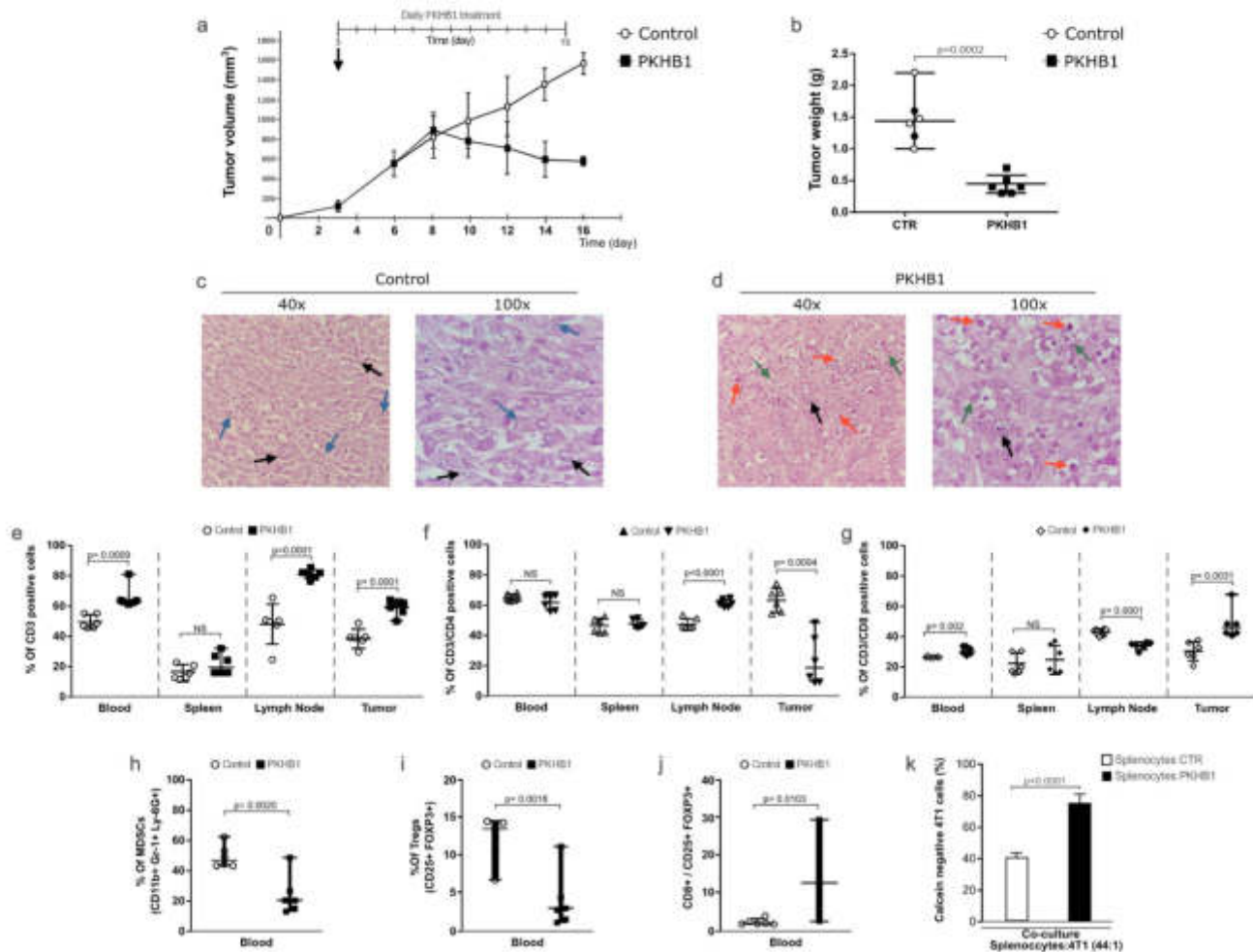
Figure 2. PKHB1 treatment induces tumor reduction and T cells distribution. Mice were inoculated s.c. with 5×10^5 4T1 viable cells and when tumor reached 70–120mm^3 were treated with sterile water (Control, n = 6) or PKHB1 (400 μg of PKHB1 daily, n = 6), tumor volume was measured three times per week. (A) Graphs indicate the mean of the tumor volume in PBS-treated group (Control, n = 6) or PKHB1-treated group (PKHB1, n = 6). (B) Graphs indicate the tumor weight of control and treated mice at day 16. (C,D) Histology from tumors of control or PKHB1-treated mice stained with H&E. Tumor cells (black arrows), mitotic cells (blue arrows), cellular debris (green arrows) and immune system cells infiltration (red arrows). (E, F, and G) Graphs show the percent of CD3+, CD4+, and CD8+ cells in blood, spleen, lymph node, and tumor of control or PKHB1-treated mice at day 16. (H-I) Graphs show the percent of MDSCs and Tregs in blood of control or PKHB1-treated mice at day 16. (J) Graph show the ratio of CD8/Tregs cells of control or PKHB1-treated mice at day 16. (K) Graphs show the percent of calcein negative 4T1 cells after the co-culture with splenocytes of control (n = 4), or PKHB1-treated mice (n = 4). NS = Not significant.

Finally, we wondered if PKHB1 induced the release of HMGB1 and ATP, two important DAMPs related with ICD.[7] Therefore, the presence of HMGB1 and ATP was assessed in the supernatants of treated and untreated breast cancer cells. In Figure 3, results showed a significant release of HMGB1 (Figure 3(i)) and ATP (Figure 3(j)) in the supernatants of PKHB1-treated cells, when compared with untreated cells.

PKHB1-KC induce maturation of bone marrow-derived DCs and antitumor T cell responses

To assess the immunogenicity of the dead cells obtained upon treatment with PKHB1, 4T1 cells were treated with 400 μM of PKHB1, epirubicin (EPI) or freeze and thaw cycles (FT) as positive or negative controls (respectively) of ICD. The PKHB1-killed cells (PKHB1-KC), EPI-KC, or FT-KC were then prepared as described in the methods section, and its ability to induce DCs maturation was

evaluated as we show in the schema of Figure 4(a). Thus, bone marrow-derived murine DCs were left untreated (Control) or pulsed for 24 h with the PKHB1-KC, EPI-KC, FT-KC, or LPS (1 μg/mL). After co-culture, DCs pulsed with the different stimulus (killed cells or LPS) maintained the expression of the DCs marker CD11c (Figure 4(b)), while only LPS induced a significative increase of the MHC-II in cell surface (Figure 4(c)). However, the PKHB1-KC, EPI-KC, and LPS induced a significant increase of the co-stimulatory molecule CD86 while no difference was observed in the DCs stimulated with the FT-KC (Figure 4(d)). Additionally, DCs pulsed with PKHB1-KC show a significant increase in CD80 cell surface expression and TNFα release in comparison with unstimulated DCs (figure sup. 7A-C).

Once we determined DCs markers after co-culture with killed cells, we assessed if the DCs pulsed with the different killed cells (PKHB1-KC, EPI-KC or FT-KC) were able to prime T cells. First, primary T lymphocytes (CD3+ cells) were co-
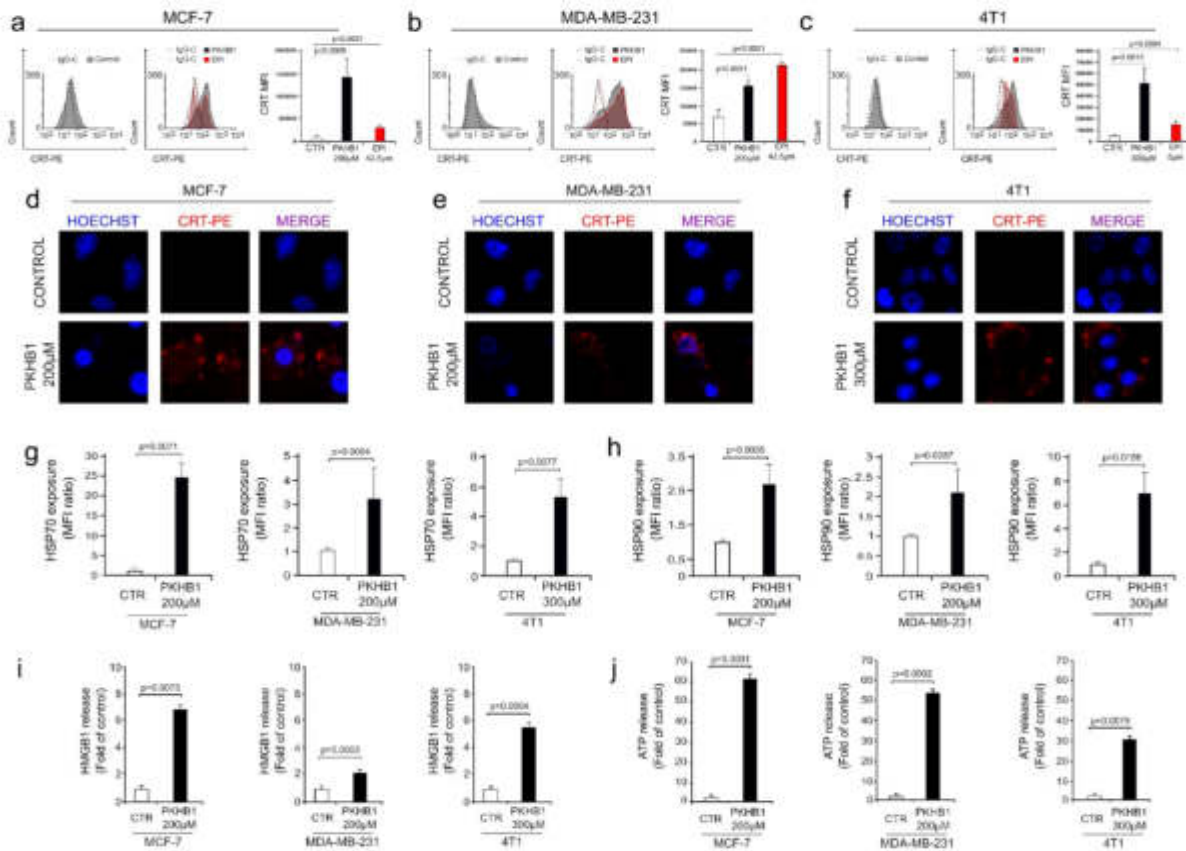
Figure 3. PKHB1 induces exposure and release of DAMPs in breast cancer cells. Representative FACS histograms of CALR exposure (filled histograms) and IgG isotype antibodies (open histograms) in non-permeabilized (7-AAD negative cells) (A) MCF-7, (B) MDA-MB-231, and (C) 4T1 cells, untreated (Control) or treated with the CC_{50} of PKHB1 (in gray) (200 μM for MCF-7 and MDA-MB-231 and 300 μM for 4T1) for 2 h or EPI (in red) (42.5 μM for MCF-7 and MDA-MB-231 and 5 μM for 4T1) for 24 h. Calreticulin exposure observed by confocal microscopy in (D) MCF-7, (E) MDA-MB-231, and (F) 4T1 cells untreated (Control) or treated with PKHB1 (CC_{50}) using CALR-PE staining and Hoechst 33,342. Representative graphs of the ratio of HSP70 (G) or HSP90 (H) exposure in non-permeabilized cells (7-AAD negative cells), untreated (Control) or treated with PKHB1 (CC_{50}) for 2 h. Representative graphs of the (I) HMGB1 or (J) ATP release in the supernatants of control or PKHB1 (CC_{50}) treated cells. Graphs shown are means (± SD) of triplicates of three independent experiments. CALR-PE = Calreticulin-PhycoErythrin.

cultured for 96 h with pulsed or unpulsed DCs, and we observed the release of TNFα, IFNγ, and IL-2 in the co-culture of CD3+ and DCs-PKHB1-TCL (table sup. 2). Next, primed (co-cultured with pulsed DCs-PKHB1-KC, EPI-KC, or FT-KC) or unprimed (co-cultured with unstimulated DCs) T lymphocytes were collected and co-cultured during 24 h with viable 4T1 cells (previously stained with calcein-AM). To assess antitumor cell cytotoxicity, we evaluated the increase in calcein negative 4T1 cells after co-culture with primed or unprimed T lymphocytes. Results showed that only T lymphocytes co-cultured with pulsed DCs-PKHB1-KC and DCs-EPI-KC induced a significant increase in calcein negative 4T1 cells (Figure 4(e)), in comparison with the lymphocytes co-cultured with DCs-FT-KC or unprimed T lymphocytes. Additionally, lymphocytes stimulated with DCs-PKHB1-KC show a significant increase in IFNγ and IL-2 release in the co-culture with 4T1 cells in comparison with lymphocytes stimulated with control DCs (figure sup. 7D and E).

Prophylactic vaccination with PKHB1-KC prevented tumor establishment of 4T1 cells

Considering that PKHB1 treatment induces tumor decline, infiltration of CD8+ cells into the tumor, DAMPs' exposure and release, and the antitumor immune response *ex vivo*, the

next step was to carry out the *Gold Standard* of ICD (prophy-lactic vaccination)[18,19] to confirm whether PKHB1 induced ICD. The vaccine was based in the subcutaneous inoculation of the 4T1-PKHB1-KC, 7 days before the transplantation of viable 4T1 cells, while mice were inoculated with 4T1-EPI-KC used as a positive control, and controls without KC were injected with serum-free medium (Figure 5(a)). Results showed that vaccination with PKHB1-KC prevented tumor establishment in 80% (8/10) of mice compared to 70% (7/10) of mice treated with EPI-KC. No survival (0%) was observed in the Control group inoculated with serum-free medium (Figure 5(b)) (individual growth curves in figure sup. 8 A-C). Additionally, survival rates of mice in each group were consistent with tumor growth, observing, respectively, 80% and 70% of survival in mice vaccinated with PKHB1-KC and EPI-KC by day 60, while control mice perished by day 21 (Figure 5(c)).

Treatment with PKHB1-KC induces tumor regression

After *ex vivo* and *in vivo* results, we evaluated if the immu-nogenicity of PKHB1-KC was able to diminish tumor growth and improve overall survival in syngeneic mice bearing 4T1 tumors. First, 4T1 viable cells were inoculated in BALB/c mice. When tumor reached 70–120 mm³,
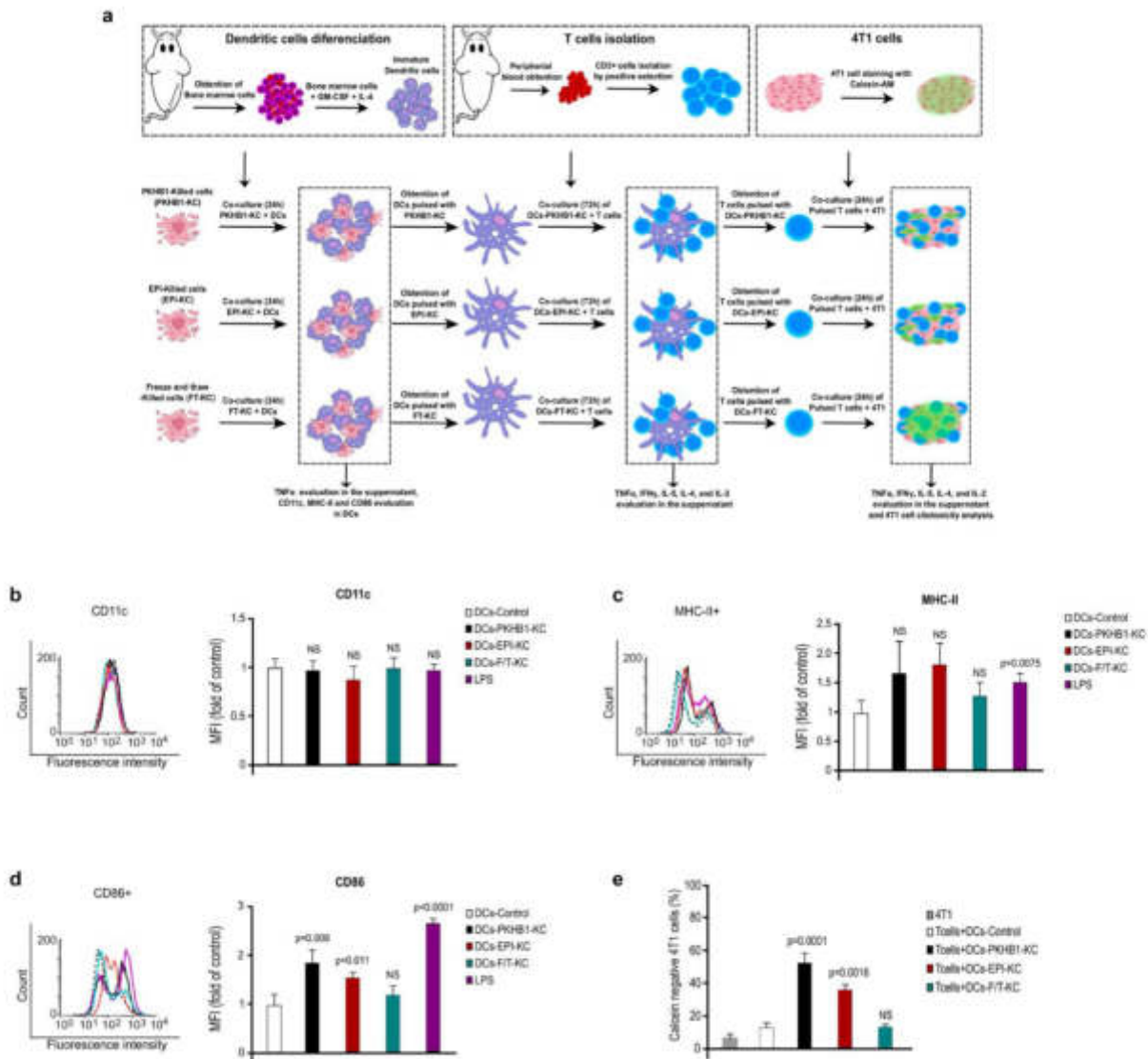
Figure 4. PKHB1-Killed cells induce antitumor immune responses *ex vivo*. (A) Schema of the ex vivo experiments. (B) Representative histograms from flow cytometry analyses of CD11c expression on DCs left with medium (CTR) or pulsed 24 h with a PKHB1-KC, EPI-KC, FT-KC, or LPS, graphs of the means obtained by FACS (right side). (C) Representative histograms from flow cytometry analyses of MHC-II expression on DCs treated as in A, graphs of the means obtained by FACS (right side). (D) Representative histograms from flow cytometry analyses of CD86 expression on DCs treated as in A, graphs of the means obtained by FACS (right side). (E) Graphs shown are means (± SD) of triplicates of three independent experiments from flow cytometry analyses of 4T1 cells stained with calcein-AM and co-cultured with T lymphocytes (unprimed or primed). NS = Not significant.

a control group was treated with serum-free medium, a second group was treated with PKHB1-KC and the third group was treated with EPI-KC. All mice were treated two times per week for a total of four treatments (Figure 5 (d)). Tumor growth measurements show that PKHB1-KC-treated mice had diminished tumor growth after day 10 (7 days after the first treatment), which continued to decrease until no tumor was detected by day 18, in the group of EPI-KC the tumor diminished after day 10 (7 days after the first treatment) which continued to decrease until no tumor was detected by day 16 (Figure 5(e)). Tumor growth diminution was reflected in overall mice survival, as PKHB1-KC-treated mice presented a 78% (7/9) of survival, while the EPI-KC-treated mice presented 67% (6/9) of survival, and all control mice perished by day 23 (Figure 5 (f)) (individual growth curves in figure sup. 8D-F).

PKHB1-KC prophylactic and therapeutic vaccinations induce long-term antitumor effect

To assess the long-term antitumor response against 4T1 breast cancer cells induced by PKHB1-KC in a prophylactic or therapeutic application, mice in complete remission (tumor free >60 days) were re-challenged with living 4T1 cells. Tumor volume analysis showed that, contrary to naïve mice (Control), which showed a correct 4T1 tumor establishment, mice in remission after PKHB1-KC prophylactic or therapeutic application showed a slight increase in tumor volume at day 3, which immediately disappears by day 6 (Figure 6(a)). These results correlate with mice survival, where we observed that compared to naïve mice, in which a primary 4T1 cells challenge resulted in a 0% (0/9) of survival by day 23, those that were in remission after prophylactic or therapeutic application of PKHB1-KC were completely resistant to a re-challenge with
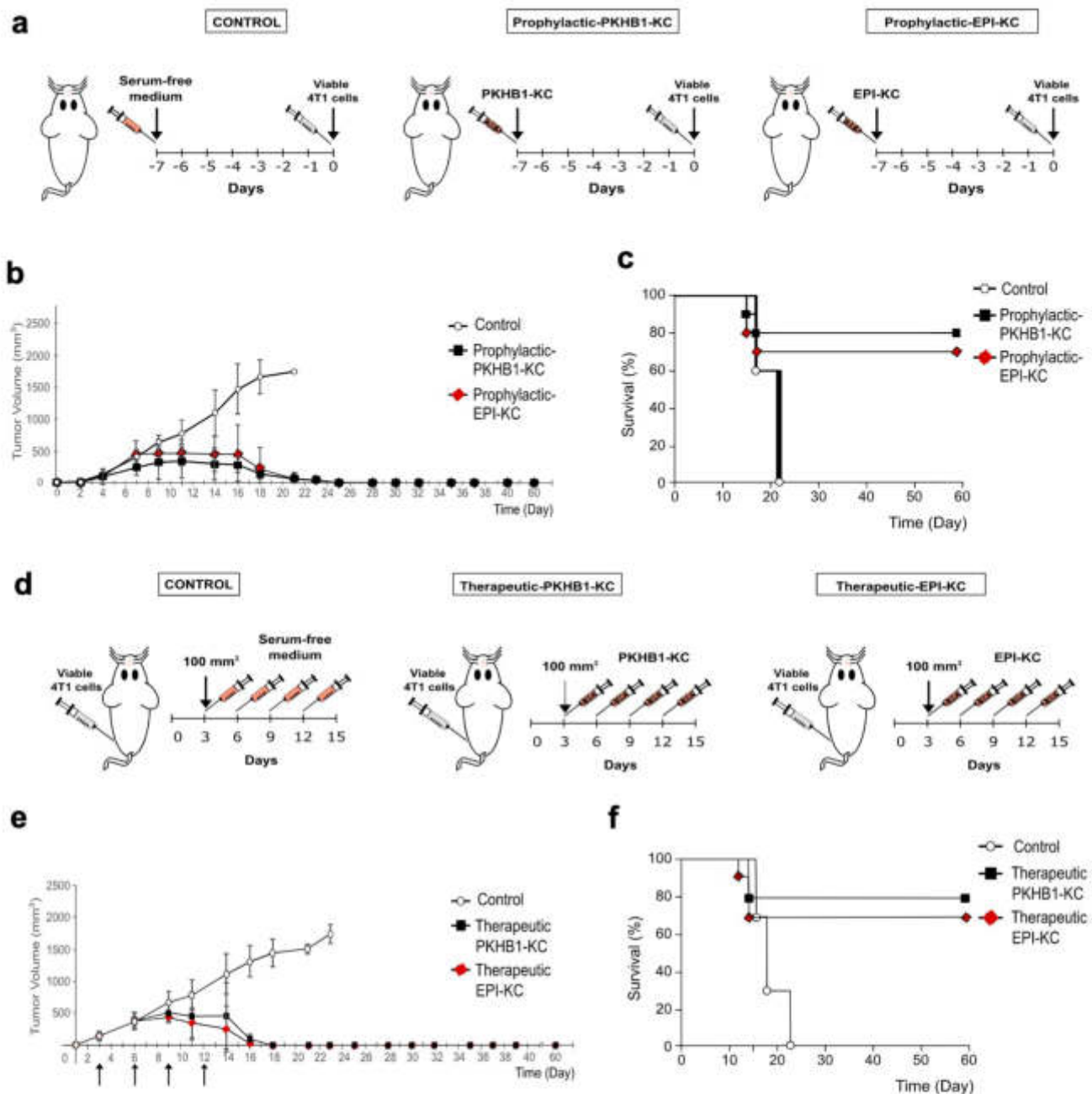
Figure 5. PKHB1-KC induce tumor elimination in a prophylactic and therapeutic application. (A) Schema of PKHB1-KC or EPI-KC prophylactic application. (B) Graph indicates the mean of the tumor growth in mice treated with serum-free medium (Control; n = 10) or mice receiving a prophylactic vaccination with PKHB1-KC (Prophylactic-PKHB1-KC, n = 10) or EPI-KC (Prophylactic-EPI-KC, n = 10). (C) Kaplan–Meier survival graph of mice treated as in B over time. (D) Schema of PKHB1-KC or EPI-KC therapeutic application. (E) Graph indicates the mean of the tumor growth in mice treated with serum-free medium (Control; n = 9), PKHB1-KC (Therapeutic-PKHB1-KC, n = 9) or EPI-KC (Therapeutic-EPI-KC, n = 9), arrows indicate days of KC or serum-free medium inoculation. (F) Kaplan–Meier survival graph of mice treated as in E over time.

4T1 cells, resulting in a 100% (9/9) of survival (Figure 6(b)). Furthermore, we determined if splenocytes from re-challenged mice can induce an antitumor cell cytotoxicity. For this purpose, we evaluated the increase in calcein negative 4T1 cells after co-culture with splenocytes obtained from naïve or re-challenged mice. In Figure 6 (d), results showed that splenocytes from re-challenged mice induced a significant increase in calcein negative 4T1 cells (60%) in comparison with naïve mice (30%).

Discussion

Here, we assessed for the first time the characteristics of the cell death induced by PKHB1 in breast cancer cells, including the triple negative phenotype, which conserves the principal molecular characteristics of cell death (caspase-independent, calcium-dependent, PLC-dependent, and IP_3 R and RYR receptor-dependent cell death with the presence of ROS, loss of mitochondrial membrane potential and the intracellular accumulation of Ca^{2+}) reported mainly in
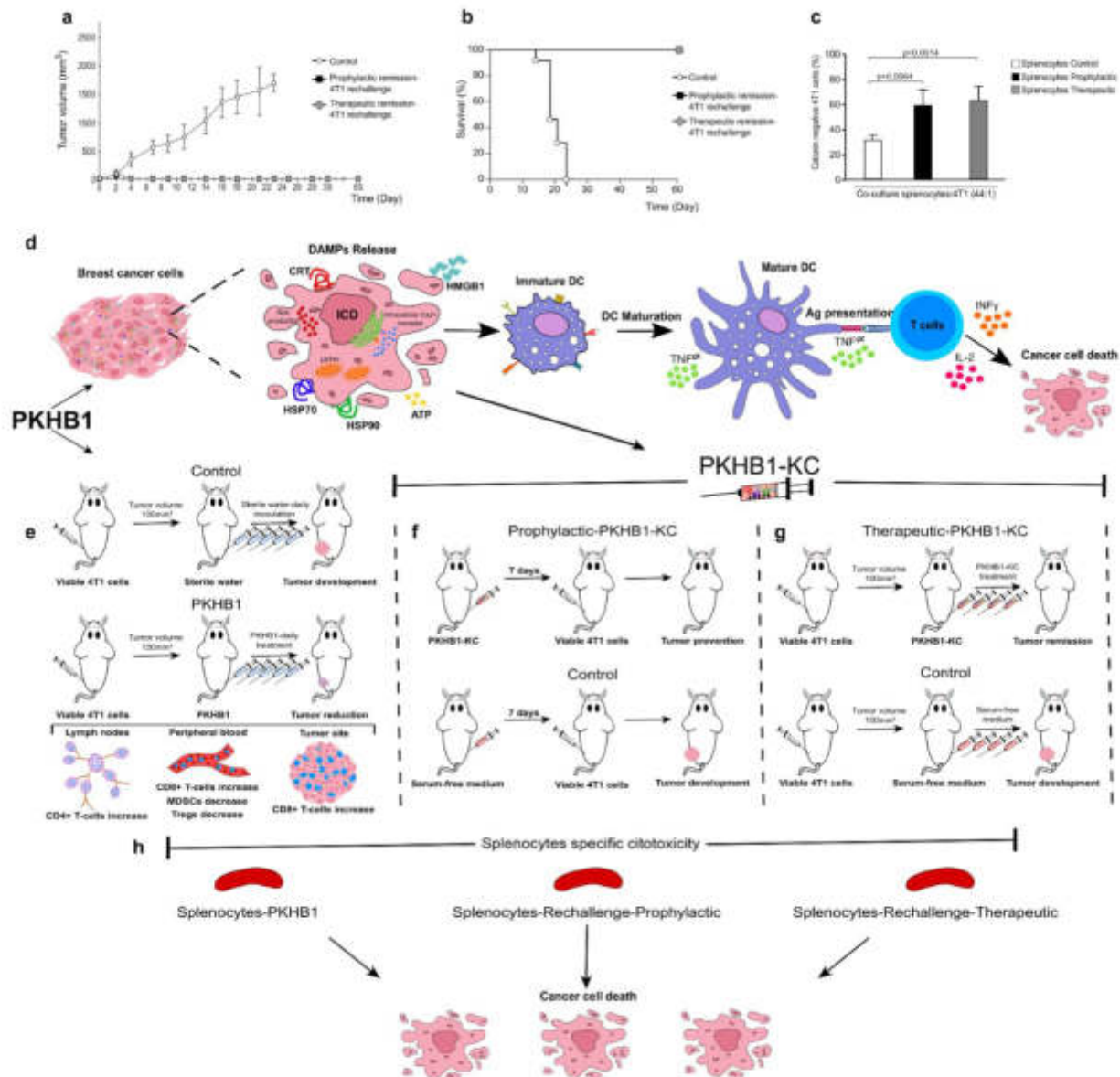
Figure 6. PKHB1-KC prophylactic and therapeutic application induces long-term antitumor effect, schematic representation of the PKHB1-effect. Mice in remission (30 days) after PKHB1 prophylactic or therapeutic PKHB1-KC application were re-challenged with 5×10^5 4T1 viable cells. (A) Graph indicates the mean of the tumor growth in PBS-treated group (Control; n = 9), prophylactic re-challenged group (Prophylactic remission-4T1 re-challenge, n = 9) or therapeutic re-challenged group (Therapeutic remission-4T1 re-challenge, n = 9). (B) Kaplan–Meier survival graph of mice treated as in A over time. (C) Graphs show the percent of calcein negative 4T1 cells after co-culture with splenocytes control (n = 4), prophylactic (n = 4) or therapeutic (n = 4) re-challenged mice. (D) PKHB1 induces ROS production, intracellular Ca^{2+} accumulation, loss of mitochondrial membrane potential ($\Delta\Psi m$), leading to DAMPs exposure and release in breast cancer cells. Neoantigens and DAMPs exposure/release induced by PKHB1 promotes DCs maturation, which triggers T cell activation to induce cancer cytotoxicity. (E) However, PKHB1-treatment *in vivo* induces T cell redistribution in lymph nodes, peripheral blood and intratumorally, leading to tumor reduction. (F) PKHB1-KC prophylactic vaccination prevented tumor establishment. (G) PKHB1-KC therapeutic application induced tumor remission. (H) PKHB1-treatment, PKHB1-KC prophylactic or therapeutic application induced tumor-specific splenocytes' cytotoxicity.

leukemic cells.[9,11,12,14] We recently reported the overexpression of PLCγ1 and its importance in the cell death induced by PKHB1 in CLL cells,[9] but although here we did not assess specially this isoform, it has been demonstrated the the overexpression of PLCγ1 in breast cancer patients is correlated with poor clinical outcome,[20] and the overexpression of PLC-β,[1-2]PLC-ε, and PLC-δ has negative outcomes.[21] Thus, the involvement of PLC in the mechanism of PKHB1-cell death, might have an advantage in the cancer cells that overexpress these proteins.

Our results also revealed the antitumor effect of PKHB1 against 4T1-breast cancer cells *in vivo*, as PKHB1-treatment diminished tumor volume and weight. Furthermore, we observed the distribution of T cells in PKHB1-treated mice that involves the increase of T cells (in blood, lymph node, and tumor), trafficking of CD4+ cells to lymph nodes, and tumor CD8+ cells infiltration that its associated to an antitumor response.[22] Additionally, PKHB1 induced the decrease of immunosuppressive cells such as MDSCs and Tregs in blood, also, we observed an increase in the

ratio of CD8+/Tregs, which has been related with an enhanced antitumor immune activity.[23,24] Overall, our results are promising, and indicate that PKHB1 promote a robust antitumor immune response as it has been reported that extensive tumor infiltration by cytotoxic CD8 + T cells, the decrease of MDSCs and Tregs, and the increase in the ratio CD8+/Tregs are strongly associated with patient's survival and response to therapy, even in different phenotypes of breast cancer.[23–27] Finally, splenocytes from PKHB1-treated mice were more cytotoxic against breast cancer cells than splenocytes from control mice, probably due to the immunogenicity of the cell death triggered by PKHB1.[22,28]

The low immunogenicity of tumor cells is a main obstacle of antitumor therapies; therefore, a way to reactivate potent antitumor immune responses is through the emission of DAMPs[29] and dead cells-derived antigens, which can be achieved in the ICD.[5,30] Here, we demonstrated that PKHB1 is capable of inducing CALR, HSP70, and HSP90 exposure, HMGB1 and ATP release, which can promote the uptake of dying cells, and the recruitment, maturation and cross-presentation activity of antigen-presenting cells (APCs).[28,31] In this sense, we demonstrated that the cell death induced by PKHB1 and epirubicin (our positive control of ICD)[32–34] are able to promote a mature phenotype of DCs,[35] both induced a significant increase in the co-stimulatory molecule CD86, such as different ICD inductors.[36] Additionally, we observed that DCs pulsed with the PKHB1-KC and EPI-KC promote the antitumor specific cytotoxicity of T cells, which confirm the phenotypic and functional maturation of DCs. Additionally, we observed that the freeze and thaw-killed cells do not stimulate the DCs, as other studies have demonstrated that freeze and thaw-killed cells suppress DCs maturation and function.[37]

However, vaccination assays involving syngeneic models are the gold standard to formally identify ICD inducers, since this demonstrates the tumor rejection capacity of the immunized host.[29,38] Our results show that the prophylactic application of EPI-KC and PKHB1-KC prevented tumor establishment and increased survival in 70 and 80% (respectively) of the mice, without using adjuvants and with only one vaccination, in comparison with other strategies of prophylactic KC-vaccines.[39–41] Also, we used Epirubicin, a well-known ICD inductor with major side-effects in human[32,42] as a positive control, highlighting its ability to prevent the establishment of breast cancer in 70% of the mice. Our results are in line with the protective potential of established ICD inducers including oxaliplatin, doxorubicin, idarubicin, mitoxantrone, and specific forms of radiotherapy (in colon cancer) which presented between 80% and 90% of tumor-free mice[17,43,44] while the antibody 7A7 (anti-EGFR) induced 50% of survival (lung cancer),[45] and especially with the fact that an ICD inductor should display elevated tumor-free survival (>50%).[19]

The therapeutic application of the dead cells killed by a potential ICD inducer can be used as a confirmatory trial for ICD inductors, to evaluate their ability to mediate therapeutic effects depending on the immune system against established neoplasms.[38] In this sense, our results show that when we treated tumor bearing mice with only four applications of PKHB1-KC,

tumor volume decreased 7 days after the first administration, reaching tumor regression on day 18 in approximately 80% of mice, while in the group of EPI-KC the tumor diminished 7 days after the first treatment which continued to decrease until tumor regression on day 16. Our results highlight the immunogenicity of the PKHB1-induced cell death, because the therapeutic application of the PKHB1-KC induced tumor remission even in the absence of adjuvants. Additionally, we determined the therapeutic potential of the EPI-KC for the first time, as a novel strategy for the application of chemotherapy-ICD inductors. These results differentiate the PKHB1-KC from other therapeutic strategies with tumor lysates against melanoma, prostate and ovarian cancer, which have been poorly evaluated and were mainly used in combination with adjuvants.[46,47] The success of the therapeutic application of PKHB1-KC in breast cancer was similar to the T-ALL model,[14] despite their intrinsic molecular differences.[16,48–50]

The perspectives for cell therapy against cancer are based on the development of T cell responses, resulting in effective rejection of tumors and long-term protection.[51,52] From this fact, the induction of ICD eventually results in long-lasting protective antitumor immunity.[53] Our results demonstrate that PKHB1-KC induces long-term antitumor effect since 100% of mice in remission after PKHB1-KC prophylactic or therapeutic application survived at the re-challenge with 4T1 cells. Although immunotherapy with pulsed DCs, primed T lymphocytes or CAR-T cells is the main approach used to stimulate antitumor immune responses, they represent greater technical complexity, higher cost, among other disadvantages regarding the use of crude PKHB1-KC.[54–56]

Overall, our results demonstrate that PKHB1 is an ICD inductor in breast cancer cells and highlight a new approach for TSP-1 peptides mimic, which could induce ICD as a conserved mechanism of cell death in different types of tumor cells, including solid cancers, additionally, our results provide evidence for a novel strategy in the obtention and application of killed cancer cells against breast cancer.

Authors' contributions

KMCR, ACUP and RMR carried out cell death, TMRE, and ROS assessment. KMCR and RMR carried out Ca^{2+} assessment. LGM carried out peptide synthesis. KMCR performed *ex vivo* and *in vivo* experiments. ACMT and PK conceived and supervised the work. KMCR and ACMT prepared the figures and wrote the manuscript. KMCR, LGM, RMR,

ACUP, PK, ACMT, and CRP designed experiments, analyzed and interpreted data, and read and approved the final manuscript.

ORCID

Kenny Misael Calvillo-Rodríguez http://orcid.org/0000-0001-7289-6166
Philippe Karoyan http://orcid.org/0000-0003-1525-6474
Ana Carolina Martínez-Torres http://orcid.org/0000-0002-6183-0089

References

1. Sung H, Ferlay J, Siegel RL, Laversanne M, Soerjomataram I, Jemal A, Bray F. Global cancer statistics 2020: GLOBOCAN estimates of incidence and mortality worldwide for 36 cancers in 185 countries. CA Cancer J Clin. 2021 May 1 Internet]. [cited 2022 Feb 7];71(3):209–249. Available from: https://onlinelibrary.wiley.com/doi/full/10.3322/caac.21660
2. Fortis SP, Sofopoulos M, Sotiriadou NN, Haritos C, Vaxevanis CK, Anastasopoulou EA, Janssen N, Arnogiannaki N, Ardavanis A, Pawelec G, et al. Differential intratumoral distributions of CD8 and CD163 immune cells as prognostic biomarkers in breast cancer. J Immunother Cancer. 2017 Apr 18 Internet]. [cited 2020 Jul 15];5(1):39. Available from: http://jitc.bmj.com/lookup/doi/10.1186/s40425-017-0240-7
3. Groenendijk FH, Bernards R. Drug resistance to targeted therapies: déjà vu all over again [Internet]. Vol. 8:Molecular Oncology. Elsevier. 2014. cited 2020 Jul 15 1067–1083. Available from: https://febs.onlinelibrary.wiley.com/doi/full/10.1016/j.molonc.2014.05.004
4. Galluzzi L, Humeau J, Buqué A, Zitvogel L, Kroemer G. Immunostimulation with chemotherapy in the era of immune checkpoint inhibitors. Nat Rev Clin Oncol. 2020 Internet]. 2020 Aug 5 [cited 2022 Feb 7];17(12):725–741. Available from: https://www.nature.com/articles/s41571-020-0413-z
5. Garg AD, More S, Rufo N, Mece O, Sassano ML, Agostinis P, Zitvogel L, Kroemer G, Galluzzi L. Trial watch: Immunogenic cell death induction by anticancer chemotherapeutics.

OncoImmunology. 2017 Oct 4;6(12):e1386829. doi: 10.1080/2162402X.2017.1386829. PMID: 29209573 Available from: https://www.tandfonline.com/doi/full/10.1080/2162402X.2017.1386829
6. Galluzzi L, Buqué A, Kepp O, Zitvogel L, Kroemer G. Immunogenic cell death in cancer and infectious disease. Nat Rev Immunol. 2017. Feb;17(2):97–111. doi:10.1038/nri.2016.107.
7. Kroemer G, Galluzzi L, Kepp O, Zitvogel L. Immunogenic cell death in cancer therapy. Annu Rev Immunol. 2013;31(1):51–72. doi:10.1146/annurev-immunol-032712-100008.
8. Stanton SE, Disis ML. Clinical significance of tumor-infiltrating lymphocytes in breast cancer [Internet]. Journal for ImmunoTherapy of Cancer BioMed Central Ltd. 2016 [cited 2020 Jul 15];4(1):59. Available from http://jitc.bmj.com/lookup/doi/10.1186/s40425-016-0165-6
9. Martinez-Torres AC, Quiney C, Attout T, Boullet H, Herbi L, Vela L, Barbier S, Chateau D, Chapiro E, Nguyen-Khac F, et al. CD47 agonist peptides induce programmed cell death in refractory chronic lymphocytic leukemia B cells via PLCγ1 activation: evidence from mice and humans. PLoS Med. 2015;12(3). doi:10.1371/journal.pmed.1001796
10. Denèfle T, Boullet H, Herbi L, Newton C, Martinez-Torres A-C, Guez A, Pramil E, Quiney C, Pourcelot M, Levasseur MD, et al. Thrombospondin-1 mimetic agonist peptides induce selective death in tumor cells: design, Synthesis, and structure–activity relationship studies. J Med Chem. 2016 Sep 22 Internet]. [cited 2018 Dec 21];59(18):8412–8421. Available from http://pubs.acs.org/doi/10.1021/acs.jmedchem.6b00781
11. Uscanga-Palomeque AC, Calvillo-Rodríguez KM, Gómez-Morales L, Lardé E, Denèfle T, Caballero-Hernández D, Merle-Béral H, Susin SA, Karoyan P, Martínez-Torres AC, et al. CD 47 agonist peptide PKHB 1 induces immunogenic cell death in T-cell acute lymphoblastic leukemia cells. Cancer Sci. 110:1. 256–268. Internet]. 2018 Dec 14 [cited 2018 Dec 21];cas.13885. Available from https://onlinelibrary.wiley.com/doi/abs/10.1111/cas.13885
12. Denèfle T, Pramil E, Gómez-Morales L, Levasseur MD, Lardé E, Newton C, Herry K, Herbi L, Lamotte Y, Odile E, et al. Homotrimerization approach in the design of thrombospondin-1 mimetic peptides with improved potency in triggering regulated cell death of cancer cells. J Med Chem. 2019 Sep 12 Internet]. [cited 2019 Sep 26];62(17):7656–7668. Available from: https://pubs.acs.org/doi/10.1021/acs.jmedchem.9b00024
13. Martinez-Torres A-C, Quiney C, Attout T, Boullet H, Herbi L, Vela L, Barbier S, Chateau D, Chapiro E, Nguyen-Khac F, et al. CD47 agonist peptides induce programmed cell death in refractory chronic lymphocytic leukemia B cells via PLCγ1 activation: evidence from mice and humans. PLOS Med. 12:3. e1001796. Internet]. 2015 Mar 1 [cited 2021 Aug 26];():. Available from https://journals.plos.org/plosmedicine/article?id=10.1371/journal.pmed.1001796
14. Martínez-Torres AC, Calvillo-Rodríguez KM, Uscanga-Palomeque AC, Gómez-Morales L, Mendoza-Reveles R, Caballero-Hernández D, Karoyan P, Rodríguez-Padilla C. PKHB1 tumor cell lysate induces antitumor immune system stimulation and tumor regression in syngeneic mice with tumoral T lymphoblasts. J Oncol. Internet]. 2019 Jun 4 [cited 2019 Sep 23];2019:1–11. Available from:. https://www.hindawi.com/journals/jo/2019/9852361/
15. Kilkenny C, Brown WJ, Cuthill IC, Emerson M, Altman DG. Animal research: reporting in vivo experiments: the ARRIVE guidelines. Br J Pharmacol. 2010 Aug;160(7):1577–9. doi:10.1111/j.1476-5381.2010.00872.x.
16. Pulaski BA, Ostrand-Rosenberg S. Mouse 4T1 breast tumor model. Current Protocols in Immunology. 2001;Chapter 20. doi:10.1002/0471142735.im2002s39.
17. Obeid M, Tesniere A, Ghiringhelli F, Fimia GM, Apetoh L, Perfettini JL, Castedo M, Mignot G, Panaretakis T, Casares N, et al. Calreticulin exposure dictates the immunogenicity of cancer cell death. Nat Med. 2007;13(1):54–61. doi:10.1038/nm1523.

18. Garg AD, Krysko D V, Verfaillie T, Kaczmarek A, Ferreira GB, Marysael T, Rubio N, Firczuk M, Mathieu C, Roebroek AJM, et al. A novel pathway combining calreticulin exposure and ATP secretion in immunogenic cancer cell death. EMBO J. 2012;31 (5):1062–1079. doi:10.1038/emboj.2011.497.

19. Humeau J, Lévesque S, Kroemer G, Pol JG. Gold Standard Assessment of Immunogenic Cell Death in Oncological Mouse Models. In: López-Soto A, Folgueras A. (eds) Cancer Immunosurveillance. Methods in Molecular Biology, vol 1884. Humana Press, New York, NY; 2019. https://doi.org/10.1007/978-1-4939-8885-3_21

20. Lattanzio R, Iezzi M, Sala G, Tinari N, Falasca M, Alberti S, Buglioni S, Mottolese M, Perracchio L, Natali PG, et al. PLC-gamma-1 phosphorylation status is prognostic of metastatic risk in patients with early-stage luminal-A and -B breast cancer subtypes. BMC Cancer. 2019 Dec 30 Internet]. [cited 2021 Mar 4];19(1):747. Available from: https://bmccancer.biomedcentral.com/articles/10.1186/s12885-019-5949-x

21. Cai S, Sun P-H, Resaul J, Shi L, Jiang A, Satherley LK, Davies EL, Ruge F, Douglas-Jones A, Jiang WG, et al. Expression of phospholipase C isozymes in human breast cancer and their clinical significance. Oncol Rep. 2017 Mar 1 Internet]. [cited 2021 Aug 10];37(3):1707–1715. Available from: http://www.spandidos-publications.com/10.3892/or.2017.5394/abstract

22. Krekorian M, Fruhwirth GO, Srinivas M, Figdor CG, Heskamp S, Witney TH, Aarntzen EHJG. Imaging of T-cells and their responses during anti-cancer immunotherapy. Theranostics 2019; 9(25):7924–7947. doi:10.7150/thno.37924. Available from https://www.thno.org/v09p7924.htm.

23. Law AMK, Valdes-Mora F, Gallego-Ortega D. Myeloid-derived suppressor cells as a therapeutic target for cancer. Cells. 2020 Feb 27 Internet]. [cited 2022 Jan 27];9(3). Available from:561. /pmc/articles/PMC7140518/

24. Markowitz J, Wesolowski R, Papenfuss T, Brooks TR, Carson WE. Myeloid derived suppressor cells in breast cancer. Breast Cancer Res Treat. 2013; Jul Internet]. [cited 2022 Jan 27];140(1):13. Available from: /pmc/articles/PMC3773691/

25. Peng GL, Li L, Guo YW, Yu P, Yin XJ, Wang S, Liu CP. CD8+ cytotoxic and FoxP3+ regulatory T lymphocytes serve as prognostic factors in breast cancer. Am J Transl Res. 2019 Aug 15;11 (8):5039–5053. Available from: https://www.ncbi.nlm.nih.gov/pmc/articles/PMC6731430/

26. Salgado R, Denkert C, Demaria S, Sirtaine N, Klauschen F, Pruneri G, Wienert S, Van den Eynden G, Baehner FL, Penault-Llorca F, et al. The evaluation of tumor-infiltrating lymphocytes (TILs) in breast cancer: recommendations by an International TILs Working Group 2014. Annal Oncol. 2015;26(2):259–271. https://doi.org/10.1093/annonc/mdu450. Available from: https://www.sciencedirect.com/science/article/pii/S0923753419313699.

27. Catacchio I, Silvestris N, Scarpi E, Schirosi L, Scattone A, Mangia A. Intratumoral, rather than stromal, CD8+ T cells could be a potential negative prognostic marker in invasive breast cancer patients. Transl Oncol. Internet]. 2019 Mar 1 [cited 2020 Jul 15];12 (3):585–595. Available from: /pmc/articles/PMC6350084/?report=abstract: 10.1016/j.tranon.2018.12.005.

28. Krysko DV, Garg AD, Kaczmarek A, Krysko O, Agostinis P, Vandenabeele P. Immunogenic cell death and DAMPs in cancer therapy. Nat Rev Cancer. 2012;12(12):860–875. doi:10.1038/nrc3380.

29. Garg AD, Dudek-Peric AM, Romano E, Agostinis P. Immunogenic cell death. Int J Dev Biol. Internet]. 2015 Sep 2 [cited 2018 Dec 21];59(1–3):131–140. Available from: http://www.ncbi.nlm.nih.gov/pubmed/26374534

30. Garg AD, Galluzzi L, Apetoh L, Baert T, Birge RB, Bravo-San Pedro JM, Breckpot K, Brough D, Chaurio R, Cirone M, et al. Molecular and translational classifications of DAMPs in immunogenic cell death. Front Immunol. 2015;6. doi:10.3389/fimmu.2015.00588

31. Galluzzi L, Vitale I, Warren S, Adjemian S, Agostinis P, Martinez AB, Chan TA, Coukos G, Demaria S, Deutsch E, et al. Consensus guidelines for the definition, detection and interpretation of immunogenic cell death. J Immunother Cancer. 2020 Mar;8(1): e000337. doi:10.1136/jitc-2019-000337. Available from: https://jitc.bmj.com/content/8/1/e000337

32. Li L, Li Y, Yang C, Radford DC, Wang J, Janát-Amsbury M, Kopeček J, Yang J. Inhibition of immunosuppressive tumors by polymer-assisted inductions of immunogenic cell death and multivalent PD-L1 crosslinking. Adv Funct Mater. 2020 Mar 3 Internet]. [cited 2021 Mar 4];30(12):1908961. Available from: https://onlinelibrary.wiley.com/doi/abs/10.1002/adfm.201908961

33. Vanmeerbeek I, Sprooten J, De Ruysscher D, Tejpar S, Vandenberghe P, Fucikova J, Spisek R, Zitvogel L, Kroemer G, Galluzzi L, et al. Trial watch: chemotherapy-induced immunogenic cell death in immuno-oncology. OncoImmunology. 9:1. https://doi.org/101080/2162402X20191703449 Internet]. 2020 Jan 1 [cited 2022 Jan 27];9(1):1703449. Available from: https://www.tandfonline.com/doi/abs/10.1080/2162402X.2019.1703449

34. Reyes-Ruiz A, Calvillo-Rodriguez KM, Martínez-Torres AC, Rodríguez-Padilla C. The bovine dialysable leukocyte extract IMMUNEPOTENT CRP induces immunogenic cell death in breast cancer cells leading to long-term antitumour memory. Br J Cancer. 2021 Internet]. 2021 Feb 3 [cited 2021 Aug 26];124 (8):1398–1410. Available from: https://www.nature.com/articles/s41416-020-01256-y

35. Dudek AM, Martin S, Garg AD, Agostinis PI. Semi-mature, and fully mature dendritic cells: toward a DC-cancer cells interface that augments anticancer immunity. Front Immunol. Internet]. 2013 Dec 11 [cited 2018 Dec 21];4:438. Available from:. http://www.ncbi.nlm.nih.gov/pubmed/24376443.

36. Montico B, Nigro A, Casolaro V, Dal Col J. Immunogenic apoptosis as a novel tool for anticancer vaccine development [Internet]. International Journal of Molecular Sciences MDPI AG. 2018 [cited 2021 Jun 22]. Available from; 19. /pmc/articles/PMC5855816/.

37. Abdellateif MS, Shaarawy SM, Kandeel EZ, El-Habashy AH, Salem ML, El-Houseini ME. A novel potential effective strategy for enhancing the antitumor immune response in breast cancer patients using a viable cancer cell-dendritic cell-based vaccine. Oncol Lett. 2018 Jul 1 Internet]. [cited 2022 Jan 27];16 (1):529–535. Available from: http://www.spandidos-publications.com/10.3892/ol.2018.8631/abstract.

38. Kepp O, Tartour E, Vitale I, Vacchelli E, Adjemian S, Agostinis P, Apetoh L, Aranda F, Barnaba V, Bloy N, et al. Consensus guidelines for the detection of immunogenic cell death. OncoImmunology. 2014;3(9):e955691. doi:10.4161/21624011.2014.955691.

39. Fan Y, Kuai R, Xu Y, Ochyl LJ, Irvine DJ, Moon JJ. Immunogenic cell death amplified by co-localized adjuvant delivery for cancer immunotherapy. Nano Lett. 2017 Dec 13 Internet]. [cited 2021 Aug 10];17(12):7387–7393. Available from: https://pubs.acs.org/doi/abs/10.1021/acs.nanolett.7b03218 .

40. Lin B, Zhao H, Fan J, Xie F, Wang W, Ding X. B16 cell lysates plus polyinosinic-cytidylic acid effectively eradicate melanoma in a mouse model by acting as a prophylactic vaccine. Mol Med Rep. 2014 Aug 1 Internet]. [cited 2021 Aug 10];10(2):911–916. Available from: http://www.spandidos-publications.com/10.3892/mmr.2014.2241/abstract

41. Salewski I, Gladbach YS, Kuntoff S, Irmscher N, Hahn O, Junghanss C, Maletzki C. In vivo vaccination with cell line-derived whole tumor lysates: neoantigen quality, not quantity matters. J Transl Med. 2020 Oct 21;18(1):402. doi:10.1186/s12967-020-02570-y.

42. De Azambuja E, Ameye L, Diaz M, Vandenbossche S, Aftimos P, Hernández SB, Shih-Li C, Delhaye F, Focan C, Cornez N, et al. Cardiac assessment of early breast cancer patients 18 years after treatment with cyclophosphamide-, methotrexate-, fluorouracil- or epirubicin-based chemotherapy. Eur J Cancer. 2015 Nov 1, 51 (17):2517–2524. doi:10.1016/j.ejca.2015.08.011.

43. Tesniere A, Schlemmer F, Boige V, Kepp O, Martins I, Ghiringhelli F, Aymeric L, Michaud M, Apetoh L, Barault L, et al. Immunogenic death of colon cancer cells treated with oxaliplatin. Oncogene. 2010;29(4):482–491. doi:10.1038/onc.2009.356.

44. Gorin JB, Ménager J, Gouard S, Maurel C, Guilloux Y, Faivre-Chauvet A, Morgenstern A, Bruchertseifer F, Chérel M, Davodeau F, Gaschet J. Antitumor immunity induced after α irradiation. Neoplasia. 2014 Apr;16(4):319–328. doi:10.1016/j.neo.2014.04.002.

45. Garrido G, Rabasa A, Sánchez B, López MV, Blanco R, López A, Hernández DR, Pérez R, Fernández LE. Induction of immunogenic apoptosis by blockade of epidermal growth factor receptor activation with a specific antibody. J Immunol. 2011 Nov 15;187 (10):4954–4966. doi:10.4049/jimmunol.1003477.

46. Chiang CL, Coukos G, Kandalaft LE. Whole Tumor Antigen Vaccines: Where Are We? Vaccines (Basel). 2015 Apr 23;3 (2):344–72. doi:10.3390/vaccines3020344.

47. Wu A, Oh S, Gharagozlou S, Vedi RN, Ericson K, Low WC, Chen W, Ohlfest JR. In vivo vaccination with tumor cell lysate plus CpG oligodeoxynucleotides eradicates murine glioblastoma. J Immunother. 2007 Nov-Dec;30(8):789–797. doi:10.1097/CJI.0b013e318155a0f6.

48. Irvin BJ, Williams BL, Nilson AE, Maynor HO, Abraham RT. Pleiotropic contributions of phospholipase C-gamma1 (PLC-gamma1) to T-cell antigen receptor-mediated signaling: reconstitution studies of a PLC-gamma1-deficient Jurkat T-cell line. Mol Cell Biol. 2002 Dec;20(24):9149–9161. doi:10.1128/MCB.20.24.9149-9161.2000

49. McAndrew D, Grice DM, Peters AA, Davis FM, Stewart T, Rice M, Smart CE, Brown MA, Kenny PA, Roberts-Thomson SJ, et al. ORAI1-mediated calcium influx in lactation and in breast cancer. Mol Cancer Ther. 2011;10(3):448–460. doi:10.1158/1535-7163.MCT-10-0923.

50. Abalsamo L, Spadaro F, Bozzuto G, Paris L, Cecchetti S, Lugini L, Iorio E, Molinari A, Ramoni C, Podo F, et al. Inhibition of phosphatidylcholine-specific phospholipase C results in loss of mesenchymal traits in metastatic breast cancer cells. Breast Cancer Res. 2012;14(2). doi:10.1186/bcr3151.

51. Henry F, Bretaudeau L, Hequet A, Barbieux I, Lieubeau B, Meflah K, Grégoire M. Role of antigen-presenting cells in long-term antitumor response based on tumor-derived apoptotic body vaccination. Pathobiology. 1999;67(5–6):306–310. doi:10.1159/000028086.

52. Farkona S, Diamandis EP, Blasutig IM. Cancer immunotherapy: the beginning of the end of cancer? BMC Med. 2016;14(1). doi:10.1186/s12916-016-0623-5.

53. Zhou J, Wang G, Chen Y, Wang H, Hua Y, Cai Z. Immunogenic cell death in cancer therapy: present and emerging inducers. [Internet]. Vol. 23, Journal of Cellular and Molecular Medicine Blackwell Publishing Inc; 2019 [cited 2020 Jul 21]. p. 4854–4865. Available from: /pmc/articles/PMC6653385/?report=abstract. ;23:8. 10.1111/jcmm.14356.

54. Calmeiro J, Carrascal MA, Tavares AR, Ferreira DA, Gomes C, Falcão A, et al. Dendritic cell vaccines for cancer immunotherapy: the role of human conventional type 1 dendritic cells [Internet]. Vol. 12:Pharmaceutics. MDPI AG. 2020. [cited 2020 Jul 22]. Available from: /pmc/articles/PMC7076373/?report=abstract

55. Papaioannou NE, Beniata OV, Vitsos P, Tsitsilonis O, Samara P. Harnessing the immune system to improve cancer therapy. Ann Transl Med. 2016 Jul;4(14):261. doi:10.21037/atm.2016.04.01 Available from: https://atm.amegroups.com/article/view/10188/11634

56. Lee Ventola C. Cancer immunotherapy, part 1: current strategies and agents. P T. Internet]. 2017 Jun 1 [cited 2020 Jul 22];42(6):375–383. Available from: /pmc/articles/PMC5440098/?report=abstract

CHAPTER 2

2. Study of the mechanism and immunogenicity of the cell death induced by Immunepotent-CRP.

The results in the present chapters gave rise to a patent: 102966 filed by the Universidad Autónoma de Nuevo León.

2.1 Article 2. IMMUNEPOTENT-CRP induces DAMPs release and ROS-dependent cell autophagosome formation in HeLa and MCF-7.

2.2 Article 3. IMMUNEPOTENT-CRP increases intracellular calcium leading to ROS production and cell death through ER-calcium channels in breast cancer and leukemic cell lines

2.3 Article 4. The bovine dialysable leukocyte extract IMMUNEPOTENT CRP induces immunogenic cell death in breast cancer cells leading to long-term anti-tumor memory

BMC Cancer

RESEARCH ARTICLE

Open Access

IMMUNEPOTENT CRP induces DAMPS release and ROS-dependent autophagosome formation in HeLa and MCF-7 cells

Ana Carolina Martínez-Torres[1*] , Alejandra Reyes-Ruiz[1†], Kenny Misael Calvillo-Rodriguez[1†], Karla Maria Alvarez-Valadez[1†], Ashanti C. Uscanga-Palomeque[1], Reyes S. Tamez-Guerra[1] and Cristina Rodríguez-Padilla[1,2]

Abstract

Background: IMMUNEPOTENT CRP (ICRP) can be cytotoxic to cancer cell lines. However, its widespread use in cancer patients has been limited by the absence of conclusive data on the molecular mechanism of its action. Here, we evaluated the mechanism of cell death induced by ICRP in HeLa and MCF-7 cells.

Methods: Cell death, cell cycle, mitochondrial membrane potential and ROS production were evaluated in HeLa and MCF-7 cell lines after ICRP treatment. Caspase-dependence and ROS-dependence were evaluated using QVD.oph and NAC pre-treatment in cell death analysis. DAMPs release, ER stress (eIF2-α phosphorylation) and autophagosome formation were analyzed as well. Additionally, the role of autophagosomes in cell death induced by ICRP was evaluated using SP-1 pre-treatment in cell death in HeLa and MCF-7 cells.

Results: ICRP induces cell death, reaching CC_{50} at 1.25 U/mL and 1.5 U/mL in HeLa and MCF-7 cells, respectively. Loss of mitochondrial membrane potential, ROS production and cell cycle arrest were observed after ICRP CC_{50} treatment in both cell lines, inducing the same mechanism, a type of cell death independent of caspases, relying on ROS production. Additionally, ICRP-induced cell death involves features of immunogenic cell death such as P-eIF2α and CRT exposure, as well as, ATP and HMGB1 release. Furthermore, ICRP induces ROS-dependent autophagosome formation that acts as a pro-survival mechanism.

Conclusions: ICRP induces a non-apoptotic cell death that requires an oxidative stress to take place, involving mitochondrial damage, ROS-dependent autophagosome formation, ER stress and DAMPs' release. These data indicate that ICRP could work together with classic apoptotic inductors to attack cancer cells from different mechanisms, and that ICRP-induced cell death might activate an immune response against cancer cells.

Keywords: Autophagy, DAMPs, Bovine dialyzable leukocyte extract, ROS, Immunotherapy, Transfer factor

---

* Correspondence: ana.martinezto@uanl.edu.mx
†Alejandra Reyes-Ruiz, Kenny Misael Calvillo-Rodriguez and Karla Maria Alvarez-Valadez contributed equally to this work.
[1]Universidad Autonoma de Nuevo Leon, Facultad de Ciencias Biologicas, Laboratorio de Inmunologia y Virologia, San Nicolás de los Garza, Mexico
Full list of author information is available at the end of the article

Background

Among the different types of cancer, breast and cervical cancer remain the principal causes of women death worldwide [1]. Main treatments consist of surgical removal of the tumor, chemotherapy, radiation therapy, hormonal therapy, and immunotherapy. However, these treatments still have limited success, and the develop-ment of new therapies to improve existing ones is a major challenge.

IMMUNEPOTENT CRP (ICRP), a bovine dialyzable leukocyte extract (DLE) obtained from disintegrated spleen, is cytotoxic to several cancer cell lines, including those from lung cancer [2] cervical cancer [3] and breast cancer [4, 5], while sparing noncancerous cells [6]. In murine melanoma, it prevented cell growth and diminished VEGF release [7]. In the cervical cancer cell lines HeLa and SiHa, and the non-small cell lung cancer cell lines A549, and A427, it induced cell cycle arrest and caspase-independent but ROS-dependent cell death [2, 3]. Additionally, its administration promoted a decrease in tumor volume and an increase in the survival of mice bearing 4 T1 tumors without visibly affecting vital or-gans, or hematological and biochemical parameters [8]. Additionally, ICRP induced immunogenic cell death (ICD) alone or in combination with oxaliplatin in the murine model B16F10 [9]; this immunogenicity ofcancer cell death relies on the antigenicity of the neoan- tigens expressed by dead cancer cells and the release of damage-associated molecular patterns (DAMPs) such as calreticulin (CRT), ATP and HMGB1 [10]. Until today, every ICD inductor causes endoplasmic reticulum (ER) stress, which implies several cellular processes as eIF2α phosphorylation (P-eIF2α) and exposure of chaperone proteins like CRT [11]. Besides ER stress, production of reactive oxygen species (ROS) is an essential component that instigates the intracellular danger-signallingpathways that govern ICD. ROS and other reactive species are the main intracellular signal transducers sustaining autophagy, thus, several studies have shownan autophagy-ROS dependence for the release of DAMPs [12, 13].

Autophagy is a primary survival mechanism activated in cells subjected to stress. However, if cellular stress continues, autophagy often becomes associated with features of cell death. This dual role of autophagy has been associated with the resistance of cancer cells to treatments (as a pro-survival process) or the inductionof cell death (as a pro-death process) depending on the stimulus. Moreover, autophagy can be dispensable for the induction of cell death but required for its immuno-genicity [14, 15].

The purpose of this study was to analyze the molecu- lar pathways by which ICRP exerts its cytotoxicity. We used HeLa and MCF-7 cell lines to further characterize

its mechanism of cytotoxicity evaluating cell cycle, mitochondrial membrane potential, caspase and ROS dependence for cell death, autophagosome formation, eIF2-α phosphorylation, DAMPs release and the role of autophagy in the mechanism of ICRP-induced cell death.

Methods

Cell culture

Human cervix adenocarcinoma HeLa (ATCC® CCL-2™) and human breast adenocarcinoma MCF-7 (ATCC® HTB-22™) cells were obtained from the American Type Culture Collection (2015), mycoplasma tested (last test August 2019), and maintained in a humidified incubator containing 5% CO_2 at 37 °C. Cells were cultured in DMEM-F12 supplemented with 10% fetal bovine serum (FBS) and 1% penicillin-streptomycin (Life Technologies,Grand Island, NY), and were routinely grown in plastic tissue-culture dishes (Life Sciences, Corning, NY).

Peripheral blood mononuclear cells (PBMC) extraction.

After obtaining written informed consent, PBMC were isolated from healthy donors by density gradient centri-fugation with Ficoll-Paque™ PLUS (GE Healthcare, Chicago, Ilinois, USA) and maintained at $4X10^6$ cells/ mL in cell culture plates at 37 °C in 5% CO_2 atmosphere, using RPMI 1640 medium (GIBCO Thermofisher, Waltham, Massachusetts, USA) supplemented with 1 µg/ mL amphotericin B, 1 µg/mL penicillin and $2.5X10^{-3}$ µg/mL streptomycin (GIBCO Thermofisher, Waltham, Massachusetts, USA) and 10% of FBS (GIBCO Thermo-fisher, Waltham, Massachusetts, USA). The study was approved by the Institutional Ethics Committee at the Universidad Autonoma de Nuevo León, College of Biological Sciences.

Cell death analysis

Cell death was determined by staining cells with 2.5 µg/ mL APC Annexin V (BD Pharmingen, San Jose, CA) and 0.5 µg/mL propidium iodide (PI) (Sigma-Aldrich, ST. Louis, MO). In brief, 5×10^4 cells were seeded in 24- well plates and were incubated with IMMUNEPOTENT CRP for 24 h, with or without pre-incubation with QVD.oph (10 µM), N-acetyl-L-cysteine (NAC) (5 mM) or Spautin-1 (Sp-1) (15 µM). Cells were then recuper-ated, washed with PBS (Phosphate-buffered saline) and then resuspended in 100 µl of binding buffer (10 mM HEPES/ NaOH pH 7.4, 140 mM NaCl, 2.5 mM $CaCl_2$).

Finally, cells were stained, incubated at 4 °C for 20 min and assessed with BD Accury C6 flow cytometer (Becton Dickinson, Franklin Lakes, NJ). The results were analyzed using FlowJo Software (LLC, Ashland, OR).

PBS, stained with CYTO-ID Autophagy Detection Kit (Enzo Life Science, Farmingdale, NY) and measured by flow cytometry as explained above.

Statistical analysis

The results presented here represent the mean of at least three independent experiments done in triplicate (mean ± SD). Statistical analysis was done using paired student T-test, and the statistical significance was defined as $p < 0.05$. The data was analyzed using Graph- Pad Prism (GraphPad Software, San Diego, CA, USA).

Results

IMMUNEPOTENT CRP induces cell death in HeLa and MCF-7 cells through cell cycle arrest, loss of mitochondrial membrane potential and ROS generation

ICRP induces regulated cell death in HeLa, SiHa, A549 and A427 cells [2, 3], while sparing noncancerous cells [6], however its effect on breast cancer derived-MCF-7 cell line, has not been assessed. Thus, to determine the effect of ICRP in MCF-7 cells, we evaluated cell death induced by different doses of ICRP after 24 h of treat- ment using HeLa cells and healthy-donor derived PBMC as a control. ICRP induced cell death in a concentration- dependent manner, in both cell lines, after 24 h of treatment (Fig. 1a), while PBMC were only slightly affected. Cell death was characterized by double-positive Annexin-V and PI staining, as previously reported forcervical cancer [3] and lung cancer cells [2]. In HeLa cells, ICRP provoked cell death (Annexin-V and/or PI staining) in 30% of the cells at 1 U/mL dose, reaching 50% at 1.25 U/mL and increasing near to 90% at 1.5 U/ mL. In MCF-7 cells, ICRP induced a slight cell death at 1.25 U/mL (less than 20% of the cells), and at 1.5 U/mL it induced cell death in 50% of the cells, reaching 80% at 1.75 U/mL. On the other hand, ICRP induced a slightcell death induction at 1.25 U/mL and at 1.5 U/mL (less than 20% of the cells), reaching 20% of cell death at 1.75 U/mL in PBMC (Fig. 1a).

Moreover, it is known that mitochondria play a central role in cell death signaling, as mitochondrial dysfunction leads to ROS generation which has been associated with many types of cell death [16]. Thus, loss of mitochon- drial membrane potential and ROS production were evaluated in HeLa, MCF-7, and PBMC after ICRP CC_{50} treatment for 24 h. As expected, loss of mitochondrial membrane potential (Fig. 1b) and ROS generation (Fig. 1c) were observed in 50% of the HeLa and MCF-7 cells after treatment in both cell lines, whereas in PBMC we could observe a slight and non-significant loss of mitochondrial membrane potential (Fig. 1b) and ROS production (Fig. 1c). Because we observed that ICRP did not generate a significant affectation in PBMC, further

studies were continued using only HeLa and MCF-7 cell lines.

ICRP is known to induce cell cycle arrest in HeLa cells in a time-dependent manner, reaching the maximum accumulation of cells in G2/M phase after 24 h of treatment [3]. Here we evaluated the cell cycle of MCF-7 cells after the treatment with ICRP using HeLa cells as a control. As seen in Fig. 1d and e, ICRP effectively induces cell cycle arrest in the G2/M phase in both cell lines after 24 h of treatment. Additionally, ICRP also induces cell cycle arrest in S phase in MCF-7 cells (Fig. 1d, e).

IMMUNEPOTENT CRP induces caspase-independent cell death but in a ROS-dependent manner in HeLa and MCF-7 cells

Once we confirmed that the principal cell death features induced by ICRP in HeLa cells were maintained in breast cancer cells, we next wondered if the cell death was also caspase-independent, as previously shown in HeLa cells [3]. To determine this, a pan-caspase inhibi- tor, QVD.oph, was used before treatment with ICRP. As shown in Fig. 2a, ICRP-mediated cell death was inde- pendent of caspase activation in HeLa and MCF-7 cells.

Then, as ROS generation has been associated with caspase-independent types of cell death [17], the antioxi- dant NAC was used to determine if ROS were playing a role in ICRP-induced cell death. NAC was able to inhibit ICRP-mediated cell death (Fig. 2b) by reducing ROS production in both cell lines (Fig. 2c).

IMMUNEPOTENT CRP induces eIF2α phosphorylation and DAMPS release in HeLa and MCF-7 cells

Recently, our research group found that ICRP induced the release of several DAMPs (CRT, ATP, HSP70, HSP90 and HMGB1), and ICD in B16F10 murine mel- anoma cells [9]. However, these features have not been assessed in human cancer cells. Considering that one ofthe first steps in the induction of ICD is the activation of an ER stress response, which involves the phosphoryl- ation of eIF2α (P-eIF2α) [11]; this parameter was evalu- ated in human cancer cell lines by flow cytometry after 18 h of treatment. As shown in Fig. 3a and b, ICRP was able to induce eIF2α phosphorylation in 47 and 57% of HeLa and MCF-7 cells treated with ICRP, respectively; this was confirmed by confocal microscopy (Fig. 3c and Fig. 3d). Because DAMPs exposure and release has been implicated in cell death involving ER stress [10], the next step was to evaluate if treatment with ICRP could induce the exposure or release of the principal DAMPs in the human cancer cell lines HeLa and MCF-7.

First, CRT exposure was assessed by flow cytometry and the results showed that 50% of HeLa (Fig. 3e) and MCF-7 (Fig. 3f) cells treated with ICRP exposed CRT,

Fig. 1 IMMUNEPOTENT CRP induces RCD through mitochondrial and cell cycle alterations in HeLa and MCF-7 cells. a. Cell death was measured by flow cytometry through Annexin-V and PI staining and graphed, in HeLa (left) and MCF-7 cells (center), and PBMC (right) treated with different concentrations of ICRP for 24 h. b. Loss of $\Delta\Psi$m induced by ICRP was measured by flow cytometry using TMRE staining in HeLa (1.25 U/mL, 24 h) (left), MCF-7 cells (1.5 U/mL, 24 h) (center), and PBMC (1.5 U/mL, 24 h) (right). c. ROS levels were measured by flow cytometry through DCFDA staining in HeLa (1.25 U/mL, 24 h) (left), MCF-7 cells (1.5 U/mL, 24 h) (center), and PBMC (1.5 U/mL, 24 h) (right). d. Schematic representation of changes in cellular DNA content measured by flow cytometry through PI staining in HeLa (1.25 U/mL, 24 h) (left) and MCF-7 cells (1.5 U/mL, 24 h) (right). e. The results obtained as in (D) were analyzed using Flowjo software and graphed. The graphs represent the means (± SD) of triplicates of at least three independent experiments

which was confirmed by confocal microscopy (Fig. 3g and Fig. 3h). Furthermore, as observed in Fig. 4, ICRP induced 393- and 114-fold ATP release, and 2.7- and2.4-fold HMBG1 release in HeLa and MCF-7 cells, respectively, as compared with untreated control. These results indicate that ICRP induces ER stress and DAMPs release in cervical and breast cancer cell lines.

IMMUNEPOTENT CRP induces ROS-dependent autophagosome formation in HeLa and MCF-7 cells

ROS production and autophagosome formation have been related with the release of DAMPs. For this reason, evaluation of both characteristics was assessed in cervical and breast cancer cell lines. Morphological assessment of cells treated with ICRP indicated the presences of vacuoles in HeLa (Fig. 5a) and MCF-7 (Fig. 5b) cells. Additionally, intracellular formation of vacuoles depended of ROS production in cells treated with ICRP (Fig. 5a and Fig. 5b), thus, the next step was to evaluate if autophagy was taking place after ICRP treatment and if this was dependent of ROS production. We demonstrated that ICRP effectively induced autophagosome formation in approximately 40% of Hela (Fig. 5c) and 50% of MCF-7 (Fig. 5d) cells. Furthermore, autophago- some formation was ROS-dependent, as the use of the antioxidant NAC completely inhibits autophagosomes in cells treated with ICRP (Fig. 5c-e).

71

Fig. 2 IMMUNEPOTENT CRP induces caspase-independent cell death in a ROS-dependent manner in HeLa and MCF-7 cells. a. Cell death was evaluated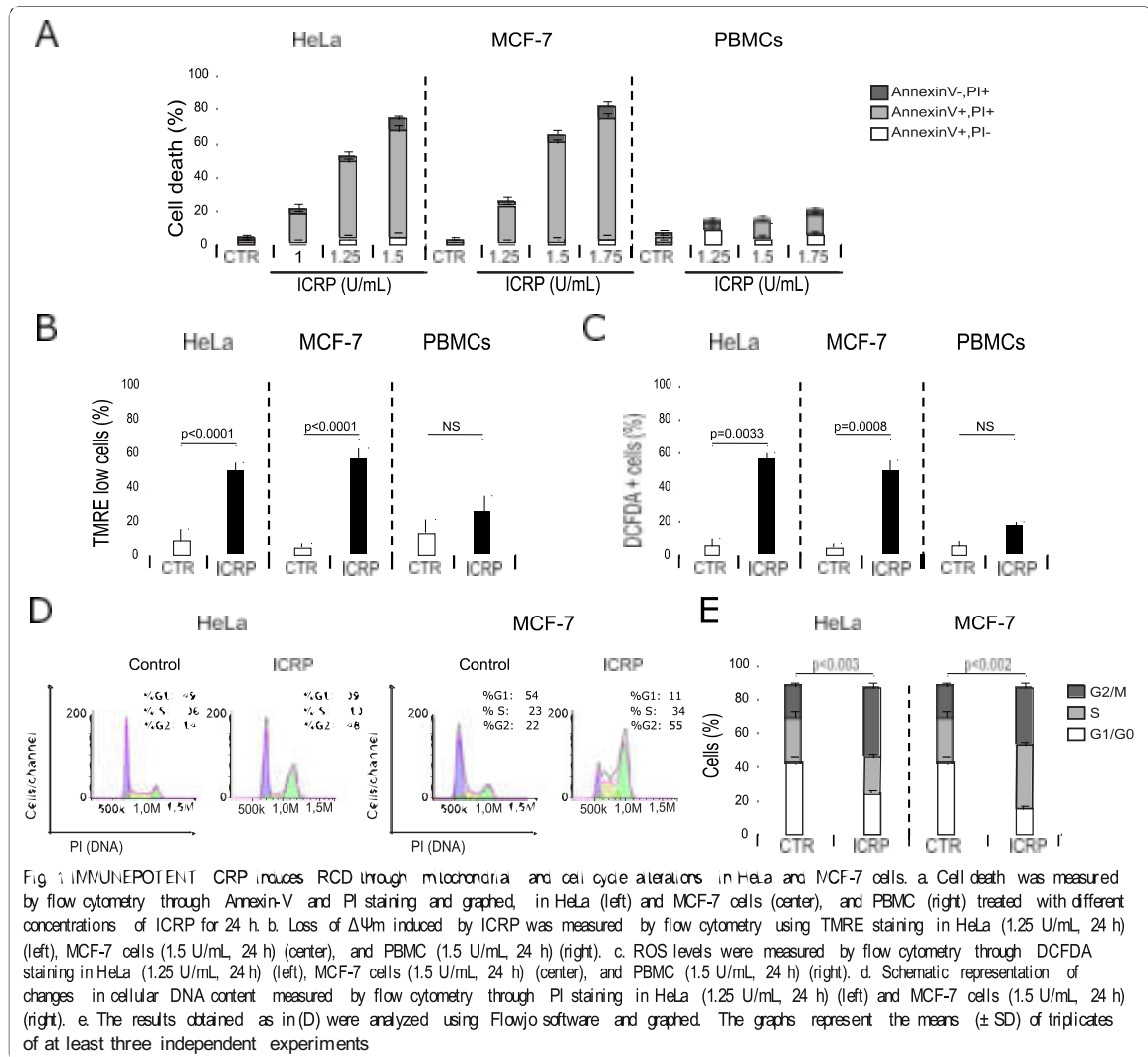 in HeLa (left) and MCF-7 cells (right) left alone or pretreated with QVD.oph before ICRP treatment (24 h). b. Effect on cell death of HeLa (left) and MCF-7 cells (right) left alone or pretreated with NAC before ICRP treatment (24 h). c. ROS production was measured in HeLa (left) and MCF-7 cells (right) left alone or pretreated with NAC before ICRP treatment (24 h), through DCFDA staining. The charts represent the means (± SD) of triplicates of at least three independent experiments
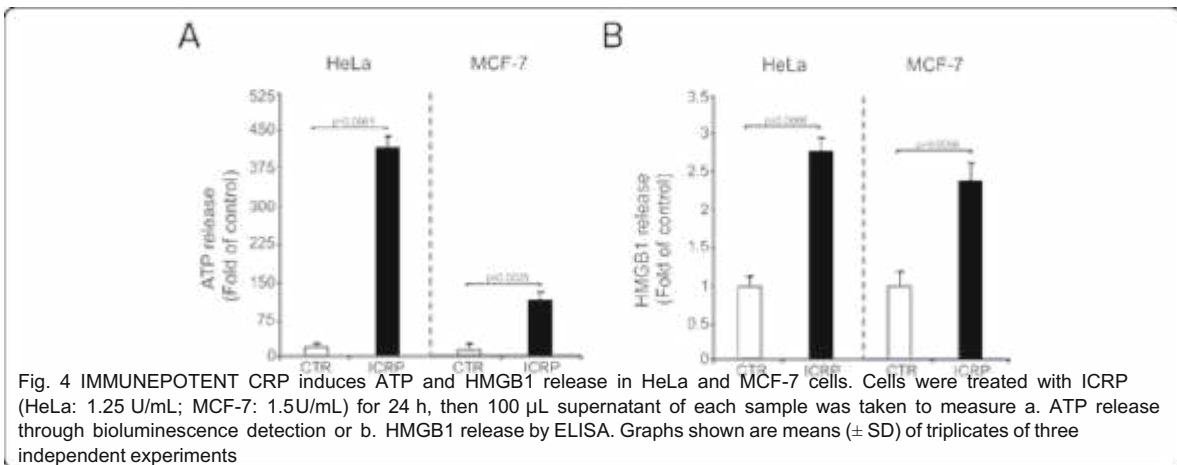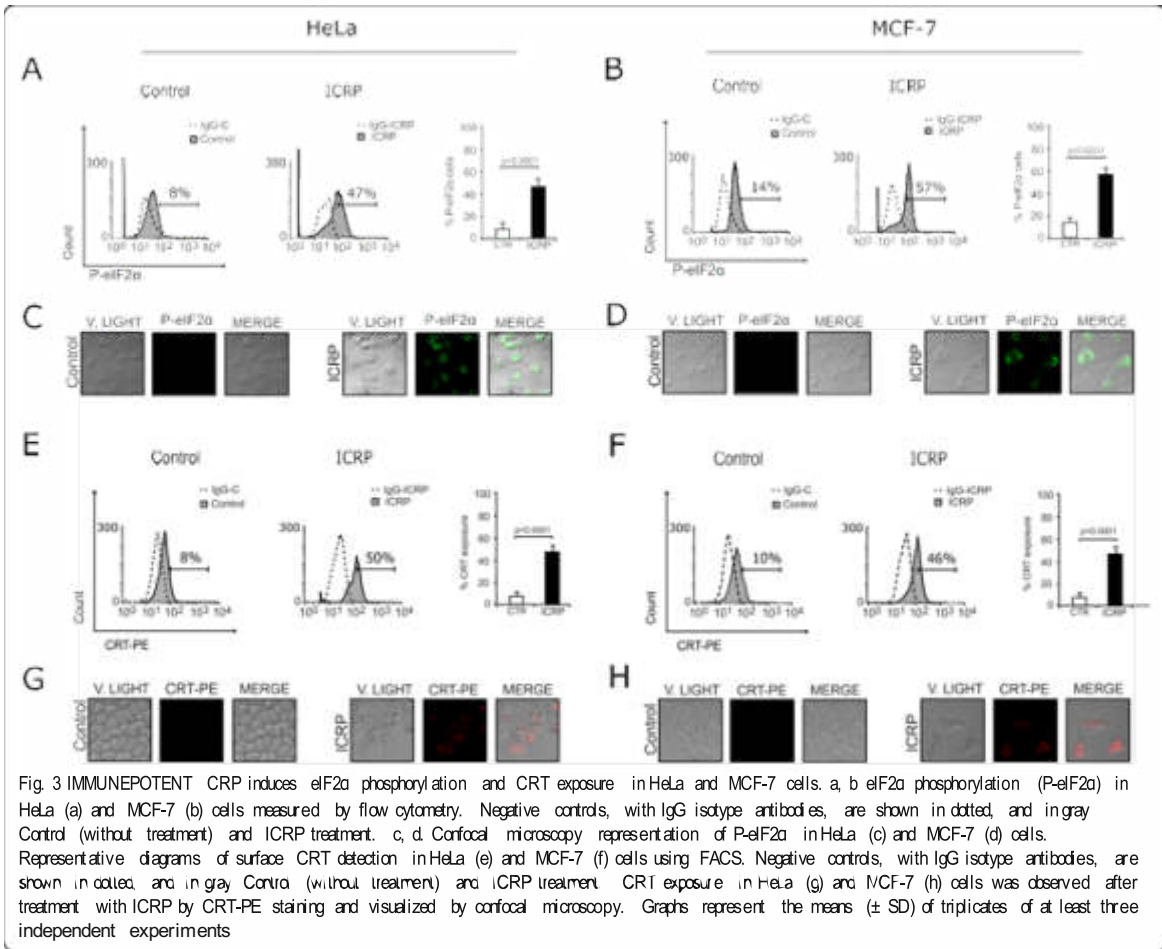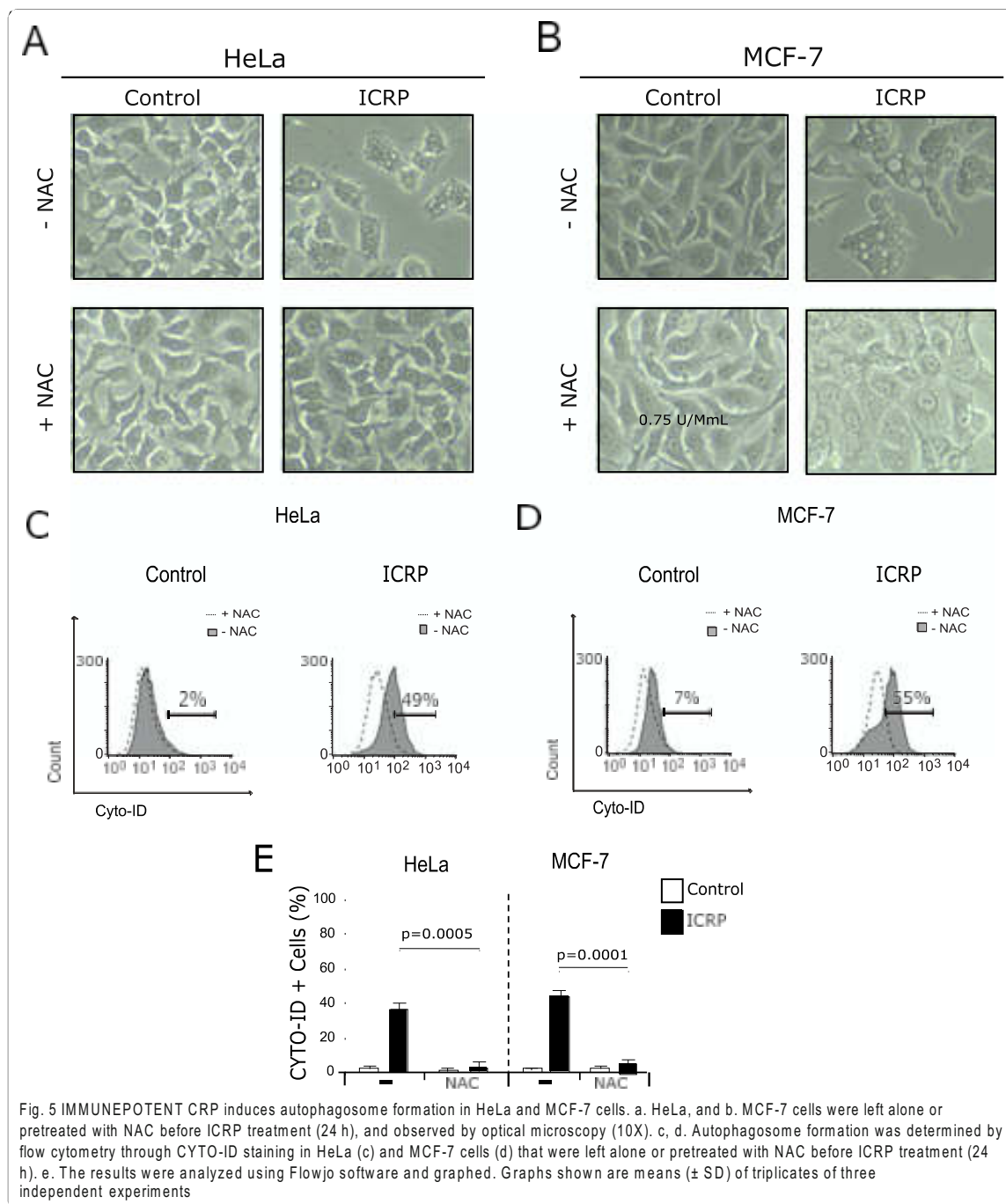
IMMUNEPOTENT CRP induces pro-survival autophagosomes in HeLa and MCF-7 cells

Autophagy can be pro-survival or pro-death [18]. Indeed, there is a type of regulated cell death that relies on the autophagic machinery (or components) called "autophagic cell death" which is characterized by being caspase-independent [14, 17]. We observed autophagosome formation and caspase-independent cell death after ICRP treatment in HeLa and MCF-7 cells, the next question was whether the mechanism of death induced by ICRP relied on autophagy. Therefore, the autophagic inhibitor Spautin-1 (SP-1) was used to analyze if autophagosome formation was pro-survival or pro-death. For this purpose, autopha- gosome formation was assessed with or without SP-1 pre-treatment. In Fig. 6, SP-1 was able to completely inhibit autophagosome formation in HeLa (Fig. 6a)and MCF-7 cells (Fig. 6b). Then, the role of autopha- gosomes in the cell death induced by ICRP was evaluated. Results show that cell death was not inhib- ited with SP-1 (Fig. 6c), furthermore, cell death signif- icatively augmented when autophagy was inhibited. Through these results we can conclude that ICRPinduces pro-survival autophagosome formation in both cell lines.

Discussion

Cancer is a heterogeneous disease, and one of the challenges of cancer treatment is that each type of cancer has different molecular features. Here, we use two different cell lines, human cervix adenocarcinoma HeLa and human breast adenocarcinoma MCF-7 cells,and show that ICRP induces cell death, loss of mito- chondrial membrane potential, ROS production and cell cycle arrest. Both cell lines exhibit the same mechanism, that is to say, a type of caspase-independent cell death that relies on ROS production. The observation of a conserved cell death mechanism in both cell lines hasbeen reported in studies with other agents. For instance, Khazaei et al. demonstrated that broadleaf wild leek (*Allium atroviolaceum*) bulb extract induces cell death in HeLa and MCF-7 cells, sharing some features of the cell death mechanism induced by this treatment, such as Bcl-2 downregulation, DNA degradation and caspase activation on both cell lines [19]. On the other hand, Martinez-Torres et al., found that chitosan gold nano- particles (CH-AuNPs) induce cell death in HeLa and MCF-7 cells though different cell death mechanisms. In HeLa cells they observed that the cell death induced by CH-AuNPs was dependent of caspase activation,whereas it was caspase independent in MCF-7 cells.

Fig. 3 IMMUNEPOTENT CRP induces eIF2α phosphorylation and CRT exposure in HeLa and MCF-7 cells. a, b eIF2α phosphorylation (P-eIF2α) in HeLa (a) and MCF-7 (b) cells measured by flow cytometry. Negative controls, with IgG isotype antibodies, are shown in dotted, and in gray Control (without treatment) and ICRP treatment. c, d. Confocal microscopy representation of P-eIF2α in HeLa (c) and MCF-7 (d) cells. Representative diagrams of surface CRT detection in HeLa (e) and MCF-7 (f) cells using FACS. Negative controls, with IgG isotype antibodies, are shown in dotted, and in gray Control (without treatment) and ICRP treatment. CRT exposure in HeLa (g) and MCF-7 (h) cells was observed after treatment with ICRP by CRT-PE staining and visualized by confocal microscopy. Graphs represent the means (± SD) of triplicates of at least three independent experiments

Fig. 4 IMMUNEPOTENT CRP induces ATP and HMGB1 release in HeLa and MCF-7 cells. Cells were treated with ICRP (HeLa: 1.25 U/mL; MCF-7: 1.5U/mL) for 24 h, then 100 μL supernatant of each sample was taken to measure a. ATP release through bioluminescence detection or b. HMGB1 release by ELISA. Graphs shown are means (± SD) of triplicates of three independent experiments

73

Fig. 5 IMMUNEPOTENT CRP induces autophagosome formation in HeLa and MCF-7 cells. a. HeLa, and b. MCF-7 cells were left alone or pretreated with NAC before ICRP treatment (24 h), and observed by optical microscopy (10X). c, d. Autophagosome formation was determined by flow cytometry through CYTO-ID staining in HeLa (c) and MCF-7 cells (d) that were left alone or pretreated with NAC before ICRP treatment (24 h). e. The results were analyzed using Flowjo software and graphed. Graphs shown are means (± SD) of triplicates of three independent experiments

However, they also proved that ROS production seems to be a conserved feature of the cell death mechanism induced by CH-AuNPs [20]. In another study, Green tea polyphenols (GTP) were evaluated in vitro in different cell lines, where they found that MCF-7 cells where more sensitive to the treatment with GTP than HeLa cells [21]. These variable mechanisms observed in HeLa and MCF-7 cells rely on the similarities and differences between the molecular machinery existing on each cell line. Here, we have proved that ICRP could induce a
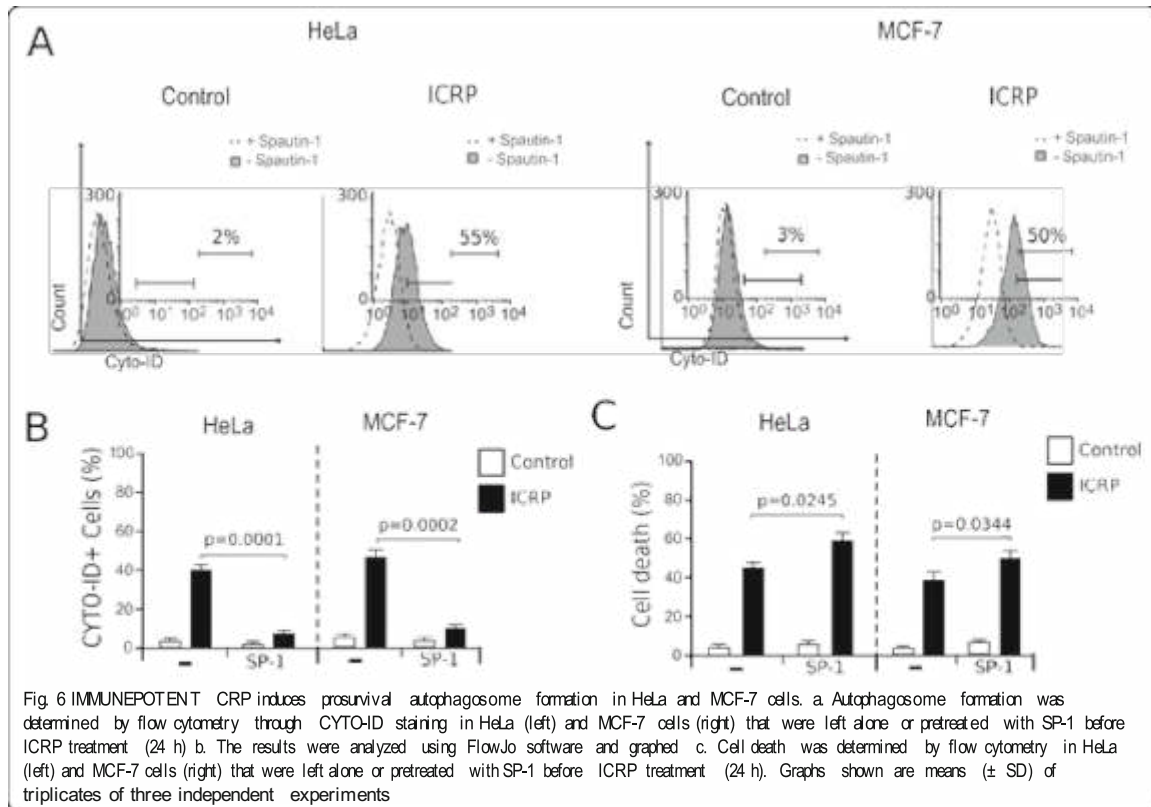
Fig. 6 IMMUNEPOTENT CRP induces prosurvival autophagosome formation in HeLa and MCF-7 cells. a. Autophagosome formation was determined by flow cytometry through CYTO-ID staining in HeLa (left) and MCF-7 cells (right) that were left alone or pretreated with SP-1 before ICRP treatment (24 h) b. The results were analyzed using FlowJo software and graphed c. Cell death was determined by flow cytometry in HeLa (left) and MCF-7 cells (right) that were left alone or pretreated with SP-1 before ICRP treatment (24 h). Graphs shown are means (± SD) of triplicates of three independent experiments

conserved mechanism of cell death in these two cell lines, as observed before in non-small cell lung cancercell lines (A549 and A427 cells) where ICRP induced DNA degradation, mitochondrial damage, ROS produc- tion, and cell death independent of caspases but relianton ROS production [2]. This indicates that the treatment with ICRP can overcome the mechanisms of cell death resistance existing in different types of cancer cells. However, it is important to mention, that differences in the cell death mechanism induced by ICRP in HeLa and MCF-7 cells could be observed in further analyses.

There is still much to understand about the mecha- nisms by which ICRP exerts these effects, nevertheless,in this work, we have shown that the cytotoxic effect in- duced by ICRP in HeLa and MCF-7 cells relies on the increase of ROS production. Interestingly, in our previ- ous work, we observed that, in HeLa cells, the increase of ROS formation is one of the first steps of cell death induced by ICRP, even before caspase activation [3]. This ROS-dependent cell death has been induced by other treatments. For example, Wu et al. demonstratedthat the protein kinase C inhibitor, Chelerythrine, could induce cell death through ROS-dependent ER stress in human prostate cancer cells [22]. Furthermore, Kim

et al. observed that Resveratrol-induced cell death in ovarian cancer cells was attenuated by the antioxidant NAC, and there was a ROS-dependent decrease of Notch1 signaling on these cells after treatment [23]. However, despite the implication of ROS in cell death, there are some agents that induce cell death without relying in ROS production [24–26].

Additionally, ROS production has been related with the induction of ICD, considering that DAMPs release is either accompanied or triggered by ROS [27]. Recently, our research group found that ICRP induces ICD in a murine melanoma model [9]. Here, we observed that ICRP induces the exposure and release of the principal DAMPs (CRT, ATP and HMBGB1) and eIF2α phos- phorylation, a process known as an ER stress indicatorand biomarker of ICD [11], in the human cancer cells, HeLa and MCF-7 cells, indicating that ICRP could in- duce ICD in these models. Caspase-independent ICD has been observed in studies with other treatments, for instance, the CD47-agonist peptide PKHB1-induced caspase-independent and Ca^{2+}-dependent cell death, pursing an immunogenic mechanism of cell death in leukemic cells [28, 29]; in addition, Giampazolias et al. demonstrated that in contrast to apoptosis, cells

undergoing caspase-independent cell death generated apro-inflammatory and immunogenic anti-tumour response through the activation of nuclear factor-κB (NF-κB) [30].

Furthermore, recent studies argue that ROS and other reactive species are the main intracellular signal trans-ducers sustaining autophagy, because the ROS scavenger NAC attenuated induced autophagy by citreoviridin[31], hydroxysafflor yellow A-sonodynamic therapy [32], ergosterol peroxide from marine fungus Phoma sp. [33], patulin [34], dimethylaminomicheliolide [35] and many other agents. In this work, we proved that ICRP induces ROS-dependent autophagosome formation in both cell lines. This ROS-Autophagy interplay has been related with the induction of ICD as well, because these pro- cesses can play a central role in the exposure and release of DAMPs [12]. ROS production, autophagosome formation, DAMPs release and ER stress have been ob- served in the induction of ICD by other treatments, in- cluding mitoxantrone, doxorubicin, oxaliplatin and photodynamic therapy [10, 27, 36–38]. However, it will be necessary to perform gold-standard vaccination ex-periments to determine whether ICRP is a bona fide ICD inducer in these cancer models [39].

Moreover, autophagy has been referred to as a double-edge sword because it helps maintain cell homeostasis but, in certain contexts, excessive or sustained cell autophagy may be pro-death [18]. Furthermore, autoph- agy may not be necessary for the induction of cell death but may be required for its immunogenicity [40], thus, we evaluated the role of autophagosome formation in the mechanism of cell death induced by ICRP, finding that it induces prosurvival autophagosomes in HeLa and MCF-7 cells. This role of autophagy as a cancer cell's pro-survival response to therapeutics has been observed in many treatments, including trastuzumab [41], epiribi- cin [42], tamoxifen [43], paclitaxel [44] and radiation [45]. Thus, it will be important to evaluate the role of autophagy in the induction of DAMPs release by ICRP to have a better understanding of the mechanism of action of this treatment.

Here we demonstrate that ICRP is able to induce a se-lective non-apoptotic cell death that promotes ER-stress and DAMP's release. These characteristics shed light into the therapeutic potential of the combination of ICRP with traditional chemotherapies, which seems encouraging, as observed in murine melanoma where ICRP increased the immunogenicity of oxaliplatin treatment [9]. Additionally, in the 4 T1 murine model it was observed that ICRP improved the antitumor effects of doxorubicin/cyclophosphamide treatment [8]. Thus, further assessments to describe the cell death mechan- ism and the potential immunogenic mechanism of the combination of ICRP with classical chemotherapies will undoubtedly straighten its applicability and advantage against cervical and breast cancer.

Conclusions

Overall our results show that IMMUNEPOTENT CRP induces cell cycle arrest, mitochondrial damage, ROS-dependent autophagosome formation with a pro-survival role, ER stress and DAMPs release, pursing a non-apoptotic cell death, relying on ROS production in HeLa and MCF-7 cells. These data postulate ICRP as a treat-ment that could execute a conserved mechanism of cell death, in spite of the heterogeneity of cancer cells, open-ing the gate to the study of the immunogenic potential of ICRP-induced cell death in cervical and breast cancer models.

Author details
[1] Universidad Autonoma de Nuevo Leon, Facultad de Ciencias Biologicas, Laboratorio de Inmunologia y Virologia, San Nicolás de los Garza, Mexico. [2] Longeveden, SA de CV, Monterrey, Mexico.

References

1. Siegel RL, Miller KD, Jemal A. Cancer statistics, 2019. CA Cancer J Clin. Jan. 2019;69(1):7–34.
2. Martinez-Torres AC, Gomez-Morales L, Martinez-Loria AB, Uscanga-Palomeque AC, Vazquez-Guillen JM, Rodriguez-Padilla C. Cytotoxic activity of IMMUNEPOTENT CRP against non-small cell lung cancer cell lines. PeerJ. 2019;2019(9)e7759:1-18.
3. Martínez-Torres AC, Reyes-Ruiz A, Benítez-Londoño M, Franco-Molina MA, Rodríguez-Padilla C. IMMUNEPOTENT CRP induces cell cycle arrest and caspase-independent regulated cell death in HeLa cells through reactive oxygen species production. BMC Cancer. 2018;18:13.
4. Franco-Molina MA, et al. In vitro effects of bovine dialyzable leukocyte extract (bDLE) in cancer cells. Cytotherapy. 2006;8(4):408–14.
5. Mendoza-Gamboa E, et al. Bovine dialyzable leukocyte extract modulates AP-1 DNA-binding activity and nuclear transcription factor expression in MCF-7 breast cancer cells. Cytotherapy. 2008;10(2):212–9.
6. Lorenzo-Anota HY, et al. Bovine dialyzable leukocyte extract IMMUNEPOTENT-CRP induces selective ROS-dependent apoptosis in T-acute lymphoblastic leukemia cell lines. J. Oncol. 2020;2020:1–17.
7. Franco-Molina MA, et al. Antiangiogenic and antitumor effects of IMMUNEPOTENT CRP in murine melanoma. Immunopharmacol Immunotoxicol. 2010;32(4):637–46.
8. Santana-Krímskaya SE, et al. IMMUNEPOTENT CRP plus doxorubicin/cyclophosphamide chemotherapy remodel the tumor microenvironment in an air pouch triple-negative breast cancer murine model. Biomed Pharmacother. 2020;126:110062.
9. Rodríguez-Salazar MDC, et al. The novel immunomodulator IMMUNEPOTENT CRP combined with chemotherapy agent increased the rate of immunogenic cell death and prevented melanoma growth. Oncol Lett. 2017;14(1):844–52.
10. Krysko DV, Garg AD, Kaczmarek A, Krysko O, Agostinis P, Vandenabeele P. Immunogenic cell death and DAMPs in cancer therapy. Nature Reviews Cancer. 2012;12(12):860–75.
11. Kepp O, et al. EIF2α phosphorylation as a biomarker of immunogenic cell death. Seminars in Cancer Biol. 2015;33:86–92.
12. Hou W, et al. Strange attractors: DAMPs and autophagy link tumor cell death and immunity. Cell Death Dis. 2013;4(12):e966.
13. Zhang Q, Kang R, Zeh HJ, Lotze MT, Tang D. DAMPs and autophagy: Cellular adaptation to injury and unscheduled cell death. Autophagy. 2013;9(4) Taylor and Francis Inc.:451–8.
14. Doherty J, Baehrecke EH. Life, death and autophagy. Nature Cell Biol. 2018;20(10) Nature Publishing Group:1110–7.
15. Kroemer G, Galluzzi L, Kepp O, Zitvogel L. Immunogenic cell death in Cancer therapy. Annu Rev Immunol. 2013;31:51–72.
16. Vakifahmetoglu-Norberg H, Ouchida AT, Norberg E. The role of mitochondria in metabolism and cell death. Biochem Biophys Res Communications. 2017;482(3) Elsevier B.V:426–31.
17. Galluzzi L, et al. Molecular mechanisms of cell death: Recommendations of the Nomenclature Committee on Cell Death 2018. Cell Death and Differentiation. 2018;25(3) Nature Publishing Group:486–541.
18. Das CK, Mandal M, Kögel D. Pro-survival autophagy and cancer cell resistance to therapy. Cancer Metastasis Rev. 2018;37(4) Springer New York LLC:749–66.
19. Khazaei S, et al. In vitro antiproliferative and apoptosis inducing effect of Allium atroviolaceum bulb extract on breast, cervical, and liver cancer cells. Front. Pharmacol. 2017;8(JAN):5.
20. Martínez-Torres AC, Zarate-Triviño DG, Lorenzo-Anota HY, Ávila-Ávila A, Rodríguez-Abrego C, Rodríguez-Padilla C. Chitosan gold nanoparticles induce cell death in hela and MCF-7 cells through reactive oxygen species production. Int J Nanomedicine. 2018;13:3235–50.
21. Liu S m, Ou S y, Huang H h. Green tea polyphenols induce cell death in breast cancer MCF-7 cells through induction of cell cycle arrest and mitochondrial-mediated apoptosis. J Zhejiang Univ Sci B. 2017;18(2):89–98.
22. Wu S, et al. Chelerythrine induced cell death through ROS-dependent ER stress in human prostate cancer cells. Onco Targets Ther. 2018;11:2593–601.
23. Kim TH, Park JH, Woo JS. Resveratrol induces cell death through ROS-dependent downregulation of Notch1/PTEN/Akt signaling in ovarian cancer cells. Mol Med Rep. 2019;19(4):3353–60.
24. Conway GE, et al. Non-thermal atmospheric plasma induces ROS-independent cell death in U373MG glioma cells and augments the cytotoxicity of temozolomide. Br J Cancer. 2016;114(4):435–43.
25. Seong M, Lee DG. Reactive oxygen species-independent apoptotic pathway by gold nanoparticles in Candida albicans. Microbiol Res. 2018;207:33–40.
26. Wang H, Zhang X. ROS reduction does not decrease the anticancer efficacy of X-Ray in two breast cancer cell lines. Oxid Med Cell Longev. 2019;2019. Article ID 3782074:1-12.
27. Li X. The inducers of immunogenic cell death for tumor immunotherapy. Tumori. 2017;104(1) SAGE Publications Ltd:1–8.
28. Uscanga-Palomeque AC, et al. CD47 agonist peptide PKHB1 induces immunogenic cell death in T-cell acute lymphoblastic leukemia cells. Cancer Sci. 2019;110(1):256–68.
29. Martínez-Torres AC, et al. PKHB1 tumor cell lysate induces antitumor immune system stimulation and tumor regression in syngeneic mice with Tumoral T Lymphoblasts. J Oncol. 2019;2019:1–11.
30. Giampazolias E, et al. Mitochondrial permeabilization engages NF-κB-dependent anti-tumour activity under caspase deficiency. Nat Cell Biol. Sep. 2017;19(9):1116–29.
31. Liu YN, et al. Citreoviridin induces ROS-dependent autophagic cell death in human liver HepG2 cells. Toxicon. Mar. 2015;95:30–7.
32. Jiang Y, et al. ROS-Dependent Activation of Autophagy through the PI3K/Akt/mTOR Pathway Is Induced by Hydroxysafflor Yellow A-Sonodynamic Therapy in THP-1 Macrophages. Oxid Med Cell Longev. 2017;2017. Article ID 8519169:1-16.
33. Wu HY, et al. Ergosterol peroxide from marine fungus Phoma sp. induces ROS-dependent apoptosis and autophagy in human lung adenocarcinoma cells. Sci Rep. 2018;8(1):1–4.
34. Yang G, et al. Patulin induced ROS-dependent autophagic cell death in human Hepatoma G2 cells. Chem Biol Interact. 2018;288:24–31.
35. Wang Y, et al. ROS generation and autophagosome accumulation contribute to the DMAMCL-induced inhibition of glioma cell proliferation by regulating the ROS/MAPK signaling pathway and suppressing the Akt/mTOR signaling pathway. Onco Targets Ther. 2019;12:1867–80.
36. Dudek AM, Garg AD, Krysko DV, De Ruysscher D, Agostinis P. Inducers of immunogenic cancer cell death. Cytokine Growth Factor Rev. 2013;24(4):319–33.
37. Garg AD, et al. Molecular and translational classifications of DAMPs in immunogenic cell death. Front Immunol. 2015;6:588.
38. Rapoport BL, Anderson R. Realizing the clinical potential of immunogenic cell death in cancer chemotherapy and radiotherapy. Int J Mol Sci. 2019;20(4):959 MDPI AG.
39. Kepp O, et al. Consensus guidelines for the detection of immunogenic cell death. OncoImmunology. 2014;3(9):e955691.
40. Michaud M, et al. Autophagy-dependent anticancer immune responses induced by chemotherapeutic agents in mice. Science (80-). 2011;334(6062):1573–7.
41. Vazquez-Martin A, Oliveras-Ferraros C, Menendez JA. Autophagy facilitates the development of breast cancer resistance to the anti-HER2 monoclonal antibody trastuzumab. PLoS One. 2009;4(7):e6251.
42. Sun WL, Chen J, Wang YP, Zheng H. Autophagy protects breast cancer cells from epirubicin-induced apoptosis and facilitates epirubicin-resistance development. Autophagy. 2011;7(9):1035–44.
43. Qadir MA, et al. Macroautophagy inhibition sensitizes tamoxifen-resistant breast cancer cells and enhances mitochondrial depolarization. Breast Cancer Res Treat. 2008;112(3):389–403.
44. Wen J, et al. Autophagy inhibition re-sensitizes pulse stimulation-selected paclitaxel-resistant triple negative breast cancer cells to chemotherapy-induced apoptosis. Breast Cancer Res Treat. 2015;149(3):619–29.
45. Han MW, et al. Autophagy inhibition can overcome radioresistance in breast cancer cells through suppression of TAK1 activation. Anticancer Res. Mar. 2014;34(3):1449–55.

Publisher's Note

IMMUNEPOTENT CRP INCREASES INTRACELLULAR CALCIUM THROUGH ER-CALCIUM CHANNELS, LEADING TO ROS PRODUCTION AND CELL DEATH IN BREAST CANCER AND LEUKEMIC CELL LINES

Helen Y. Lorenzo-Anota[1,2,+] , Alejandra Reyes-Ruiz[1,+] , Kenny M. Calvillo-Rodríguez[1] , Rodolfo Mendoza-Reveles[1] , Andrea P. Urdaneta-Peinado[1] , Karla M. Alvarez-Valadez[1] , Ana Carolina Martínez-Torres[1,^,*] , Cristina Rodríguez-Padilla[1,3,^]

[1] Laboratorio de Inmunología y Virología, Facultad de Ciencias Biológicas, Universidad Autónoma de Nuevo León, San Nicolás de los Garza, México
[2] Tecnológico de Monterrey, The Institute for Obesity Research, Monterrey, México
[3] LONGEVEDEN S.A. de C.V.

+ Co-first authors
^ Co-senior authors

* Corresponding author: Ana Carolina Martínez-Torres. Laboratorio de Inmunología y Virología, Facultad de Ciencias Biológicas, Universidad Autónoma de Nuevo León, San Nicolás de los Garza, México. E-mail: ana.martinezto@uanl.edu.mx

Figure 1: Graphical abstract

ABSTRACT

IMMUNEPOTENT CRP (ICRP) is an immunotherapy that induces cell death in cancer cell lines. However, the molecular mechanisms of death are not completely elucidated. Here, we evaluated the implication of intracellular Ca^{2+} augmentation in the cell death induced by ICRP on T-ALL and breast cancer cell lines. Cell death induction and the molecular characteristics of cell death were evaluated in T-ALL and breast cancer cell lines by assessing autophagosome formation, ROS production, loss of mitochondrial membrane potential, ER stress and intracellular Ca^{2+} levels. We assessed the involvement of extracellular Ca^{2+}, and the implication of the ER-receptors, IP_3R and RyR, in the cell death induced by ICRP, by using an extracellular calcium chelator and pharmacological inhibitors. Our results show that ICRP increases intracellular Ca^{2+} levels as the first step of the cell death mechanism that provokes ROS production and loss of mitochondrial membrane potential. In addition, blocking the IP_3 and ryanodine receptors inhibited ER-Ca^{2+} release, ROS production and ICRP-induced cell death. Taken together our results demonstrate that ICRP triggers intracellular Ca^{2+}-increase leading to different regulated cell death modalities in T-ALL and breast cancer cell lines.
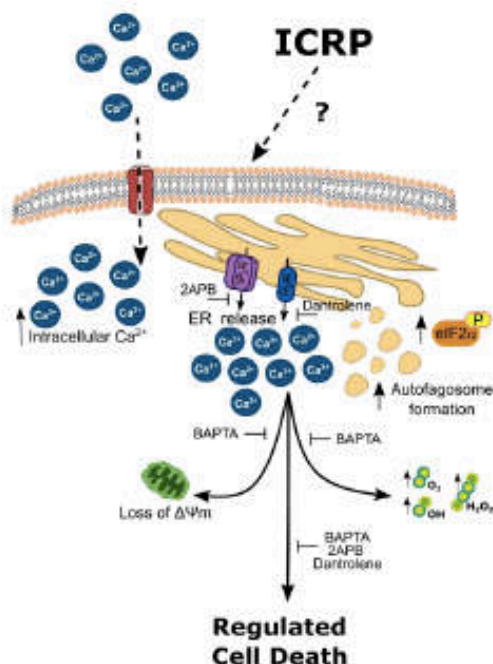
INTRODUCTION

Despite the pivotal advances in the treatment of breast cancer and T-cell acute lymphoblastic leukemia (T-ALL), breast cancer is one of the leading causes of death among women (Siegel et al., 2019), whereas T-ALL is the most diagnosed cancer in children worldwide (Karman and Johansson, 2017; Terwilliger and Abdul-Hay, 2017). One of the reasons is the ability of cancer cells to develop different mechanisms of resistance to the current therapies including cell death inductors.

IMMUNEPOTENT CRP (ICRP) is a bovine dialyzable leukocyte extract (DLE) obtained from disrupted spleen; it has shown immunomodulatory properties and cytotoxic activity against cancer cell (Arnaudov, 2017; Kirkpatrick 2000). It is cytotoxic in solid cancer cell lines, including melanoma, cervical, lung and breast cancer (Martinez-Torres et al., 2018, 2019; Reyes-Ruiz et al., 2021; Rodríguez-Salazar et al., 2017) and hematological malignances, such as T-ALL (Lorenzo-Anota et al., 2020). Despite the molecular differences between the cancer cell linages evaluated, some characteristics of the ICRP-mediated cell death mechanism remain conserved among the different cancer types studied. In all cancer cell lines ICRP has demonstrated to enhance reactive oxygen species (ROS) production leading to loss of mitochondrial membrane potential, DNA damage that promotes cell cycle arrest and finally, DNA degradation (Lorenzo-Anota et al., 2020; Martinez-Torres et al., 2018, 2019a, b; Reyes-Ruiz et al., 2021). Interestingly, solid cancer cells exposed to ICRP succumb to a caspase-independent but ROS-dependent cell death, whereas this same agent induces caspase activation leading to ROS and caspase-dependent cell death in leukemic cells.

We recently reported that ICRP induces characteristics related with endoplasmic reticulum (ER) stress such as autophagosome formation, translocation of ER chaperones to the cell surface, and eIF2a phosphorylation (P-eIF2a) (Almanza et al., 2019) in cervical and breast cancer (Martinez-Torres et al., 2020; Reyes-Ruiz et al., 2021). Yet, these mechanisms have not been previously dilucidated in hematological malignances.

It has been shown that the depletion of the ER Ca^{2+} pool or ER-Ca^{2+} overload results in disturbances that can lead to ER stress (Zhivotovsky and Orrenius, 2011). As Ca^{2+} is a highly versatile second messenger, it regulates broad cellular functions, and disturbances in Ca^{2+} homeostasis can lead to cell death (Monteith et al., 2017). Ca^{2+} alterations can lead to distinct types of regulated cell death mechanisms, such as caspase-dependent and caspase-independent cell death modalities, in different cancer types (Danese et al., 2021). However, it is unknown if there are alterations in ER-Ca^{2+} homeostasis after I-CRP-treatment in solid or liquid cancers. To better understand the mechanism of action of ICRP, the purpose of this study was to evaluate for the first time the role of Ca^{2+} in the mechanism of cell death induced by ICRP in T-ALL and breast cancer cells.

MATERIALS AND METHODS

Cell culture

MCF-7 human breast adenocarcinoma (ATCC® HTB-22TM), 4T1 murine mammary adenocarcinoma (ATCC® CRL2539TM), and T-acute lymphoblastic leukemia cell lines CEM (ATCC® CCL-119TM) and MOLT-4 (ATCC CRL-1582) were obtained from the American Type Culture Collection. MCF-7 cells were cultured in DMEM-F12 while 4T1, CEM and MOL-4 cells were cultured in RPMI-1640, all were supplemented with 10 % fetal bovine serum (FBS) and 1 % penicillin-streptomycin (Life Technologies, Grand Island, NY) and maintained in a humidified incubator in 5 % CO_2

at 37 °C. Cell count was performed using 0.4 % trypan blue (MERCK, Darmstadt, Germany) in a Neubauer chamber.

Cell death induction and inhibition

IMMUNEPOTENT CRP (ICRP) was produced as previously described (Coronado-Cerda et al., 2016; Franco-Molina et al., 2006), and dissolved in cell culture media. One unit (U) of ICRP is defined as 24 mg of peptides obtained from 15×10^8 leukocytes. We used different pharmacological inhibitors to determine the cell death mechanism of ICRP in cancer cell lines. QVD-OPh (QVD, 10 μM) as a general caspase inhibitor, N-acetylcysteine (NAC, 5 mM) was used as a ROS inhibitor, Spautin-1 (Sp-1, 15μM) as autophagosome inhibitor, BAPTA (50 μM) as extracellular calcium chelator, Dantrolene (30 μM) as ryanodine receptors (RyR) inhibitor, and 2-APB (30 μM) as inositol triphosphate receptor (IP3R) inhibitor. The inhibitors were added 30 minutes before ICRP (CC50) treatment.

Cell death analysis

Cell death quantification was determined by analyzing phosphatidylserine exposure using annexin V-allophycocyanin (APC) (AnnV, 0.25 μg/mL; BD Biosciences Pharmingen, San Jose, CA, USA) and cell membrane permeability with propidium iodide (PI; 0.5 μg/mL; MilliporeSigma, Eugene, OR, USA) staining. In brief, 5×10^4 cells were seeded and exposed to different concentrations of ICRP in subsequent assays; this allowed to define the median cytotoxic concentration of ICRP required to induce 50 % of cell death (CC50). After 24 h of treatment, cells were recollected and washed with phosphate-buffered saline (PBS), then resuspended in binding buffer (10 mM HEPES/NaOH pH 7.4, 140 mM NaCl, 2.5 mM CaCl2), and stained during 20 minutes at 4 °C. Finally, cells were assessed in BD Accury C6 flow cytometer (Becton Dickinson, Franklin Lakes, NJ) and analyzed in FlowJo Software (LLC, Ashland, OR).

Autophagosome formation assay

Autophagosome formation was assessed using Autophagy Detection Kit (Cyto-ID; Abcam, Cambridge, UK). In brief, 5×10^4 breast cancer cells were cultured in 24-well plates (Life Sciences) and 1×10^5 leukemia cells were cultured in 96-well plates (Life Sciences). Cells were treated with ICRP (CC50) for 24 h and then detached, washed with PBS, recovered, and stained following the manufacturer's instructions. Measurement was determined by flow cytometry and analyzed using Flowjo Software as mentioned previously.

EIF2α phosphorylation assay

Breast cancer cells (5×10^4) and T-acute lymphoblastic leukemic cells (1×10^6) were plated in 6-well dishes (Life Sciences) and incubated with ICRP (CC50) for 18 h. Cells were then collected and fixed with methanol for 1 h at 4 °C, washed with 2 %-FACS Buffer (PBS 1× and 2 % FBS) and centrifuged twice at 1,800 rpm during 20 min. Next, cells were suspended in 50 μL of 10 %-FACS Buffer (PBS 1× and 10 % FBS), incubated for 30 min, and shaken at 400 rpm and 25 °C. After this, 0.5 μL of anti-EIF2S1 (phospho S51) antibody [E90] (Abcam, ab32157) was added, incubated for 2 h, and washed with 2 %-FACS Buffer. Cells were suspended in 100 μL of 10 %-FACS Buffer), incubated for 15 min, and shaken at 400 rpm and 25 °C, 0.5 μL of goat anti-rabbit IgG H&L (Alexa Fluor® 488) (Abcam, ab150077) was then added and incubated for 1 h in darkness. Cells were washed with 2 %-FACS Buffer and eIF2α phosphorylation was measured by flow cytometry, as mentioned before.

Intracellular Ca²⁺ levels analysis

Intracellular calcium was assessed using Fluo-4 AM (Life Technologies). Breast cancer cells (5×10^4) and T-acute lymphoblastic leukemic cells (1×10^6) were plated in 6-well dishes (Life Sciences) and incubated with ICRP CC50 for 18 h. After treatment, cells were washed twice with KREBS buffer, resuspended in RINGER buffer with 0.001 μg/mL of Fluo-4 AM (Life Technologies) and

0.001 µg/mL of Pluronic F-127 (Life Technologies), and incubated at 37 °C for 30 min in darkness. Next, cells were washed twice with RINGER buffer. For fluorescence microscopy, cells were placed on microscopy slides with coverslips, assessed by confocal microscopy (OLYMPUS X70) and analyzed with Image-J software.

For intracellular calcium quantification cells were collected, washed, and assessed by flow cytometry and results were analyzed using FlowJo Software (LLC, Ashland, OR).

Mitochondrial membrane potential assessment

To determine mitochondrial damage, we tested loss of mitochondrial membrane potential by tetramethylrhodamine ethyl ester stain (TMRE, 50 nM; Sigma, Aldrich, Darmstadt, Germany). In brief, 5×10^4 cells were incubated with ICRP (CC_{50}) for 24 h in presence or absence of 1.5 mM BAPTA (MERCK). Cells were then harvested, washed with PBS, stained, incubated at 37 °C for 30 min, and measured by flow cytometry as described above.

ROS generation analysis

ROS levels were determined by staining cells with 2',7'-Dichlorofluorescin diacetate (DCFDA; 2.5 µM; MERCK). In brief, 5×10^4 cells/well were incubated with ICRP (CC_{50}) during 24 h in presence or absence of BAPTA (1.5 mM; MERCK). Cells were then detached, washed with PBS, stained, incubated at 37 °C for 30 min, and measured using a flow cytometer, as mentioned before.

Cleaved caspase-3 analysis

We used a specific detection kit, FITC-DEV-FMK (ABCAM; Cambridge, UK) to assess caspase-3 activation. In brief, 1×10^5 cells/well were incubated with ICRP (CC_{50}) for 24 h, then cells were recovered and stained following the manufacturer's instructions. Results were measured using a flow cytometer, as mentioned before.

Statistical analysis

Data were analyzed using GraphPad Prism Software (GraphPad Software Inc., San Diego, CA) and showed as mean ± SD of triplicates from three independent experiments. Statistical analyses were done using the paired Student's t-test. The statistical significance was defined as $p < 0.05$.

RESULTS

IMMUNEPOTENT-CRP triggers different ROS-dependent cell death modalities depending on the cancer cell lineage

ICRP is cytotoxic in a concentration-dependent manner on breast cancer (MCF-7 and 4T1) (Figure 2A) and T-ALL (CEM and MOLT-4) (Figure 2B) cell lines provoking phosphatidyl serine exposure and cell membrane permeabilization. Cell death in 30 % of cells (CC_{30}) was reached at 1 U/mL, 50 % (CC_{50}) at 1.25 U/mL, 80 % (CC_{80}) at 1.5 U/mL, and 100 % (CC_{100}) at 2 U/mL in MCF-7 cells (Figure 2A above). In 4T1 cells 30 % of cell death (CC_{30}) was reached at 0.1 U/mL, 50 % (CC_{50}) at 0.15 U/mL, 80 % (CC_{80}) at 0.2 U/mL, and 100 % (CC_{100}) at 0.5 U/mL (Figure 2A down). In T-ALL cell lines CEM and MOLT-4 30 % of cell death (CC_{30}) was reached at 0.4 U/mL, 50 % (CC_{50}) at 0.6 U/mL, 80 % (CC_{80}) at 0.8 U/mL, and 100 % (CC_{100}) 1 U/mL (Figure 2).

To further visualize the differences on cell death induced by ICRP on breast and leukemic cell lines, we next evaluated the dependence on caspases in ICRP-induced cell death. As shown in Figure 2C, the percentage of ICRP-induced cell death in MCF-7 cells did not change in presence of QVD (pan caspase inhibitor), passing from 49±4.6 % in control to 49.48±8.8 % in ICRP-treated cells (p>0.05). Interestingly in 4T1 cells QVD significantly potentiated the cell death induced by ICRP, passing from 49.6±5.9 % to 59.5±7.1 % (p=0.005). On T-ALL cell lines the cell death induced by ICRP diminishes in the presence of QVD, passing in CEM from 47±5.1 % to 26.15±8.8 % (p=0.001) and in MOLT-4 from 49.5±4.9 % to 22.8±4.3 % (p=0.001). These results indicate that ICRP
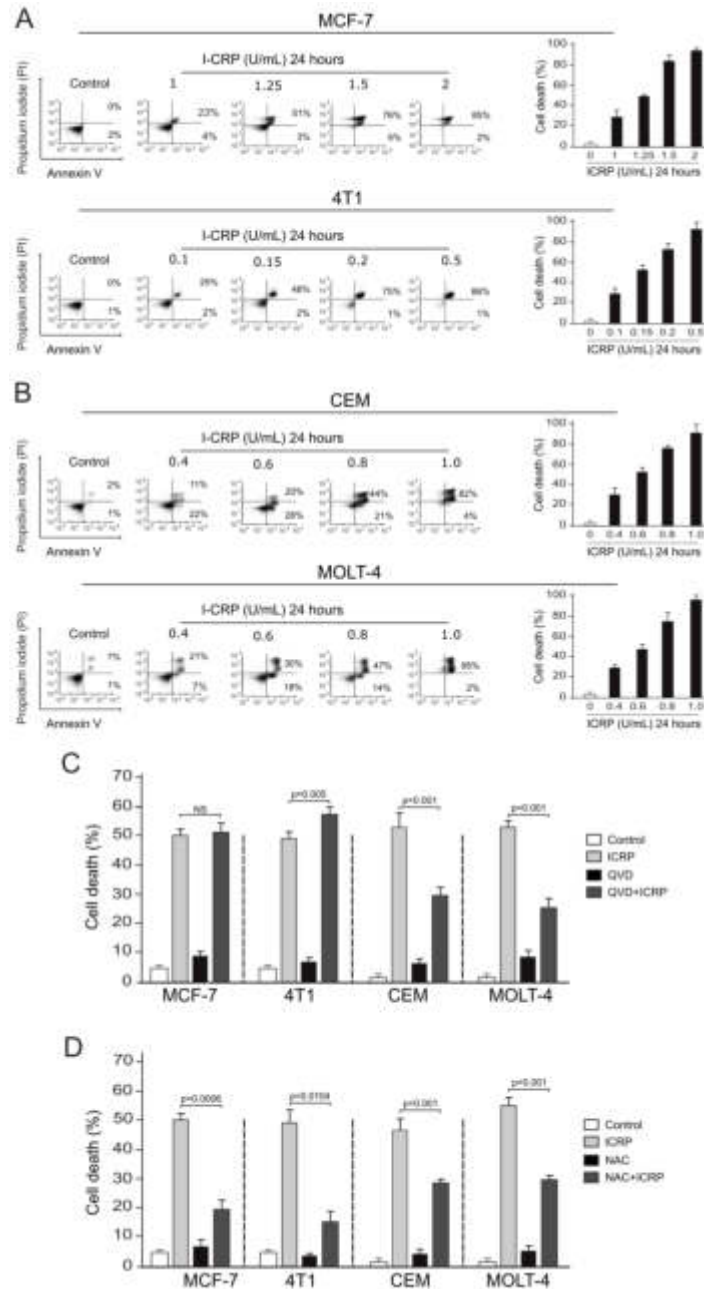
Figure 2: IMMUNEPOTENT CRP induces different regulated cell death modalities concentration and ROS-dependent manner on breast cancer and in T-ALL cell lines. A-B. Representative dot plots and quantification of cell death measured by flow cytometry using Annexin-V and PI staining in breast cancer cell lines MCF-7 (above) and 4T1 (down) (A) and in T-acute lymphoblastic leukemia cells lines CEM (above) and MOLT-4 (down) (B) treated with different concentrations of ICRP for 24 h. C. Cell death quantification of MCF-7, 4T1, CEM and MOLT-4 cell lines left alone or pretreated with a pan-caspase inhibitor QVD before ICRP CC_{50} treatment (24 h). D. Cell death quantification in MCF-7, 4T1, CEM and MOLT-4 cell lines left alone or pretreated with the antioxidant NAC before ICRP CC_{50} treatment (24 h). The means (± SD) of triplicates of at least three independent experiments were graphed.

82

induces a caspase-independent cell death on breast cancer cell lines, but caspase-dependent cell death on leukemic cells.

It is known that ICRP-induced cell death relies on ROS production in solid and leukemic cancer cell lines (Lorenzo-Anota et al., 2020; Martinez-Torres et al., 2018, 2019[a], b; Reyes-Ruiz et al., 2021). The ROS implication on ICRP-induced cell death was assessed here on breast and leukemic cell lines. First, we determined that N-Acetylcysteine (NAC) prevents ROS production by I-CRP in MCF-7, 4T1, CEM and MOLT-4 cell lines (Supplementary Figure 2). Then, in Figure 2D we show that cell death triggered by ICRP diminished from 49±4.6 % to 18.9±9 % in MCF-7 cells (p=0.0006), from 49.6±5.9 % to 15.65±11.7 % in 4T-1 cells (p=0.0104), from 47±5.1 % to 24.1±6.3 % in CEM cells (p=0.001), and from 49.5±4.9 % to 26.4±5.6 % in MOLT-4 cells (p=0.001) in presence of the ROS scavenger NAC. These data demonstrate that ICRP induces different ROS-dependent cell death modalities on breast cancer and T-ALL cell lines.

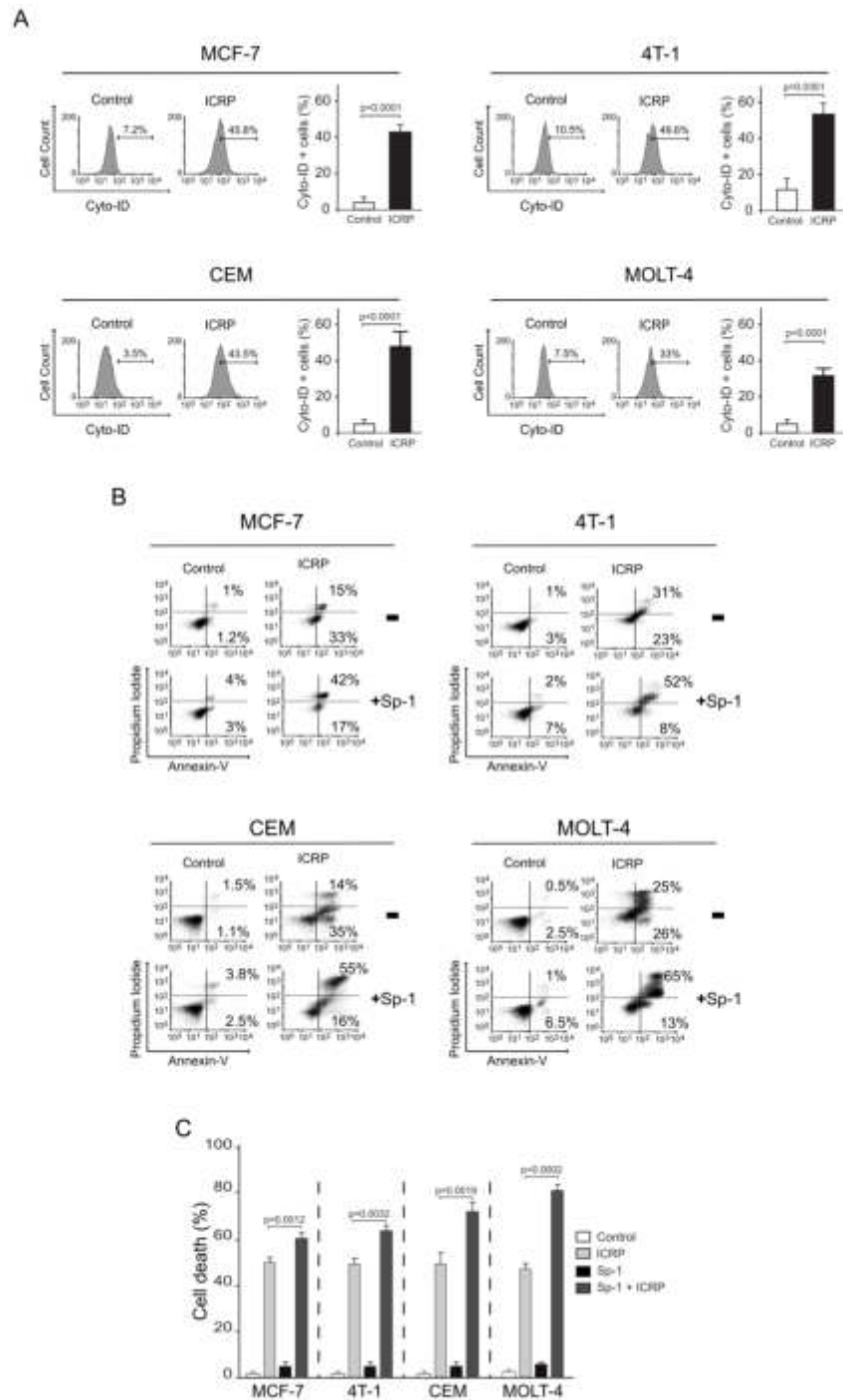*IMMUNEPOTENT-CRP induces ROS-dependent autophagy on breast cancer and T-ALL cells*

It has been reported that intracellular ROS augmentation could induce autophagy, which plays an important role on cell survival (Inguscio et al., 2012). Thus, we evaluated if ICRP could induce autophagy on leukemic cell lines as in breast cancer cells. In Figure 3A we can depict representative histograms (left) and quantification (right) of autophagosome formation. As shown, ICRP increased autophagosome formation in breast cancer cell lines passing from 7.5±2.6 % to 45.8±4.1 % in MCF-7 (p<0.0001) and from 10.5±11.7 % to 49.6±5.9 % in 4T1 (p=0351), and in leukemic cells from 3.5±11.7 % to 43.5±2 % in CEM (p<0.0001), and from 7.6±4.0 % to 33±9.1 % (p<0.0001) in MOLT-4 cells. Interestingly, as previously indicated for breast cancer cells, NAC was able to completely inhibit autophagosome formation in leukemic cell lines (Supplementary Figure 2),

indicating that the exacerbated ROS production provoked by ICRP increases autophagosome formation.

During specific circumstances autophagy could play two principal roles, one as a cell survival strategy or cell death (Inguscio et al., 2012). For this, the next step was to evaluate if autophagosome formation produced by an exacerbated ROS production could play a fundamental role on survival or death. For this, we tested cell death in presence of Sp-1, an autophagic inhibitor that effectively inhibited autophagosomes induced by ICRP in breast cancer and leukemic cell lines (Supplementary Figure 3). In Figure 3B we observe the representative dot plots obtained from cell death analyses in the four cell lines assessed, while in Figure 3C we can observe the quantification in the graph. Cell death increased significantly when autophagy was inhibited (in the presence of Sp-1). In MCF-7 cells, cell death increased from 49.6±4.6 % to 59.3±3.8 % (p=0.0012), in 4T1 cells from 49.7±5.9 % to 60.5±7.9 % (p=0.0032), from 48.1±4.1 % to 71.8±6.8 % (p=0.0019) in CEM cells and from 51±9.1 % to 78±6.0 % (p=0.0002) in MOLT-4 cells. Taken together, the increase of ROS production induced by ICRP treatment provokes ROS-dependent autophagy in breast cancer and leukemic cell lines.

IMMUNEPOTENT-CRP induces ER stress and increases cytoplasmic Ca²⁺ levels in breast cancer and T-ALL cells

ROS generation is strongly associated with endoplasmic reticulum alterations which lead to a stress condition in this organelle (Zeeshan et al., 2016), promoting eIF2α-phosphorylation (P-eIF2α) (Rashid et al., 2015). In this context, autophagy could play a crucial role during ER stress as a protective mechanism (Deegan et al., 2013). ER stress and autophagy are two cross-talking processes (Orrenius et al., 2003). As previously shown, ICRP induces ROS augmentation promoting autophagosome formation. Hence, we evaluated eIF2α phosphorylation (P-eIF2α) in breast cancer and leukemic cell lines by flow

Figure 3: IMMUNEPOTENT-CRP induces prosurvival autophagosome formation on breast cancer and in T-ALL cell lines. A. Representative histograms (left) and quantification (right) of autophagosome formation measured by flow cytometry using Cyto-ID staining in breast cancer MCF-7 and 4T1 cells, and leukemic CEM and MOLT-4 cell lines treated with ICRP CC$_{50}$ (24 h). B. Representative dot plots (left) of cell death analysis in MCF-7, 4T1, CEM and MOLT-4 cell lines left alone or pretreated with the autophagy inhibitor Sp-1 before ICRP treatment CC$_{50}$ (24 h) and quantification (C). The means (± SD) of triplicates of at least three independent experiments were graphed.

84

cytometry. As observed in Figure 4A, ICRP causes P-eIF2α in MCF-7 (58±8.7 %), 4T1 (31±4.2 %), CEM (35±7.9 %), and MOLT-4 (40±6.5 %) cell lines, revealing, that ICRP induced P-eIF2α, one of the principal biomarkers of ER stress on breast and leukemic cell lines.

In earlier stages of ER stress conditions, intracellular alterations could induce ER-calcium (Ca^{2+}) release, increasing the cytosolic Ca^{2+} concentration (Zeeshan et al., 2016). The presence of autophagy and P-eIF2α suggested alterations in the ER, therefore we evaluated the increase in cytosolic calcium. Results indicated that treatment with ICRP induced an augmentation of Ca^{2+} levels in the cytoplasm in comparison with untreated cells (control) in breast cancer (MCF-7 and 4T1) (Figure 4B) and leukemic (CEM and MOLT-4) (Figure 4C) cell lines. The increase in cytosolic Ca^{2+} levels was confirmed by flow cytometry as shown in Figure 4D and 4E, where we show a representative histogram (left) and quantification (right). We observed that ICRP increases cytosolic level of Ca^{2+} in breast cancer cells MCF-7 10.7±3.4 % to 54.2±4.9 % (p<0.0001) and 4T1 17.5±3.4 % to 50.8±6.0 % (p<0.0001) and in T-ALL cell lines CEM 9.8±2.2 % to 54.2±5.4 % (p<0.0001) and MOLT-4 5.6±3.1 % to 44.7±4.4 % (p<0.0001). Additionally, in all cancer cell lines (Supplementary Figure 4) the extracellular Ca^{2+} chelator (BAPTA) significantly inhibited the augmentation of cytoplasmic Ca^{2+} levels, revealing, that ICRP induces calcium alterations on cancer cell lines.

Calcium alterations induced by IMMUNEPOTENT CRP promote mitochondrial damage, ROS production and calcium-dependent cell death on breast cancer and T-ALL cells

Cytoplasmic Ca^{2+} overload is associated with different cell death modalities (Orrenius and Zhivotovsky, 2015; Zhivotovsky and Orrenius, 2011). As an increase of cytosolic Ca^{2+} levels were observed in all cancer cells after ICRP-treatment, we assessed the impli-
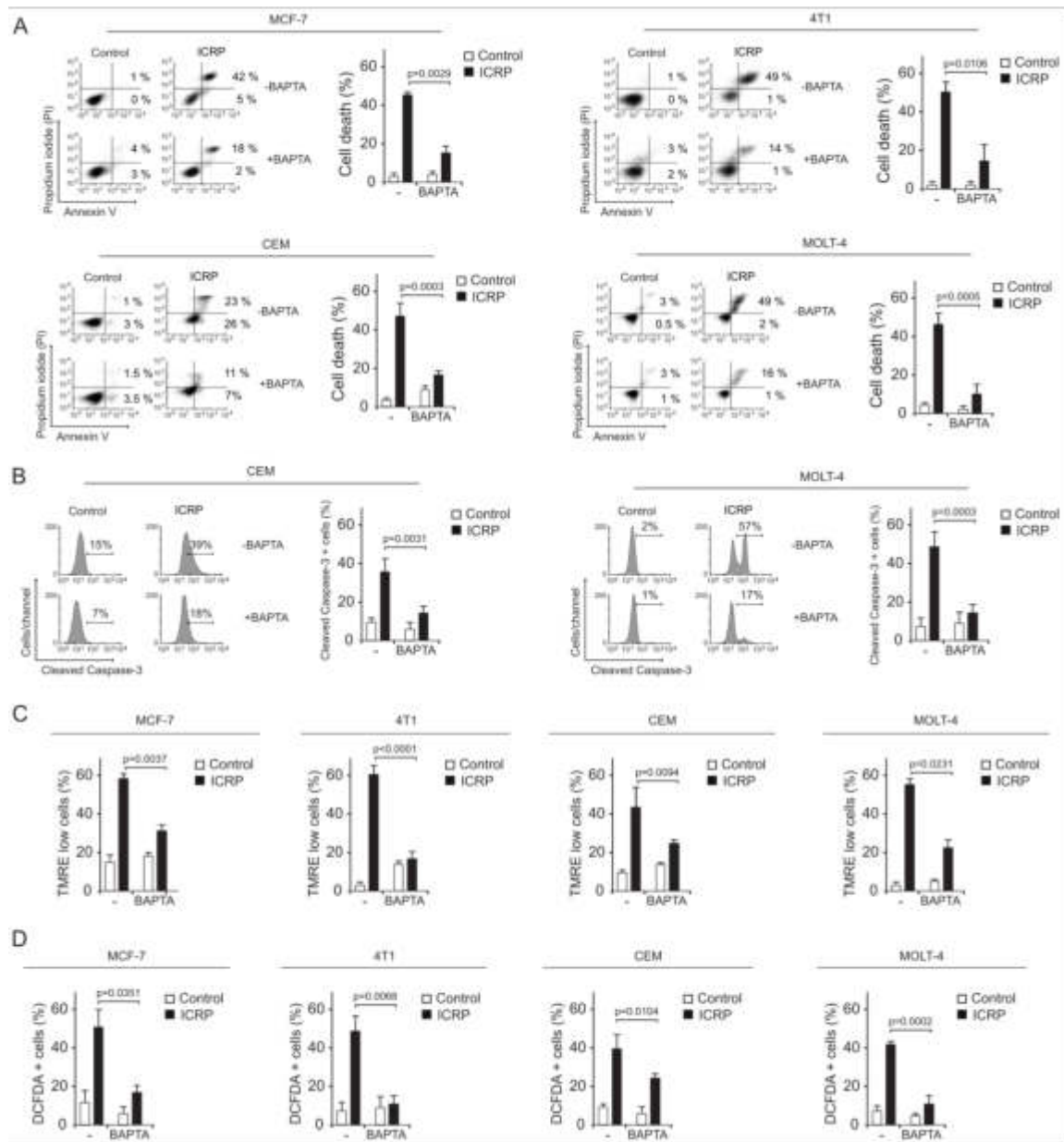
cation of Ca^{2+} augmentation on cell death induced by ICRP. First, cell death was evaluated in presence or absence of BAPTA. As observed in Figure 5A, ICRP induced cell death in up to 50 % of cells after 24 h of treatment, and the ICRP cytotoxicity was significantly inhibited in presence of BAPTA from 47.3±4.8 % to 20.1±3.9 % in MCF-7 (p=0029), since 49.8±5.2 % to 14.2±8.7 % in 4T1 (p=0.0106), from 45.5±9.0 % to 20.9±7.0 % in CEM (p=0.0003) and in MOLT-4 from 48.9±9.3 % to 17.3±3.4 % (p=0.0005). These results indicate that ICRP induces calcium-dependent cell death on breast and leukemic cell lines.

As previously shown, ICRP treatment induces caspase-independent cell death in breast cancer cells (Martínez-Torres et al., 2020; Reyes-Ruiz et al., 2021), however it triggers apoptosis involving caspase-3 cleavage (a principal effector caspase) on leukemic cell lines (Lorenzo-Anota et al., 2020). Thus, we tested cleaved caspase-3 on CEM, and MOLT-4 cell lines treated with ICRP. In Figure 5B we showed representative histograms (left) and quantification of cleaved caspase-3. As shown, the pre-treatment with BAPTA prevented caspase-3 cleavage on CEM (39±12.1 % to 18.37±5.4 %) (p=0.0031) and MOLT-4 (57±3.8 % to 17±3.6 %) (p=0.0003) cell lines, suggesting that calcium alteration induced by ICRP promotes caspase-3 activation that culminates in apoptosis pathway in leukemic cells.

The cytoplasmic Ca^{2+} overload has been associated with mitochondrial alterations in different cell death pathways (Orrenius and Zhivotovsky, 2015; Zhivotovsky and Orrenius, 2011). Thus, the loss of mitochondrial membrane potential and ROS production in presence of BAPTA, were analyzed. ICRP treatment induced loss of mitochondrial membrane potential in all cell lines (Figure 5C) and was inhibited in presence of calcium chelator BAPTA from 59±5.4 % to 33±3.4 % (p=0.0037) in MCF-7, from 60.5±4.8 % to 18.4±2.4 % (p<0.0001) in 4T1, from 41.1±10.8 % to 22±7.2 % (p=0.0094), and from 56.2±2.6 % to 21.6±6.2 % (p=0.0231).
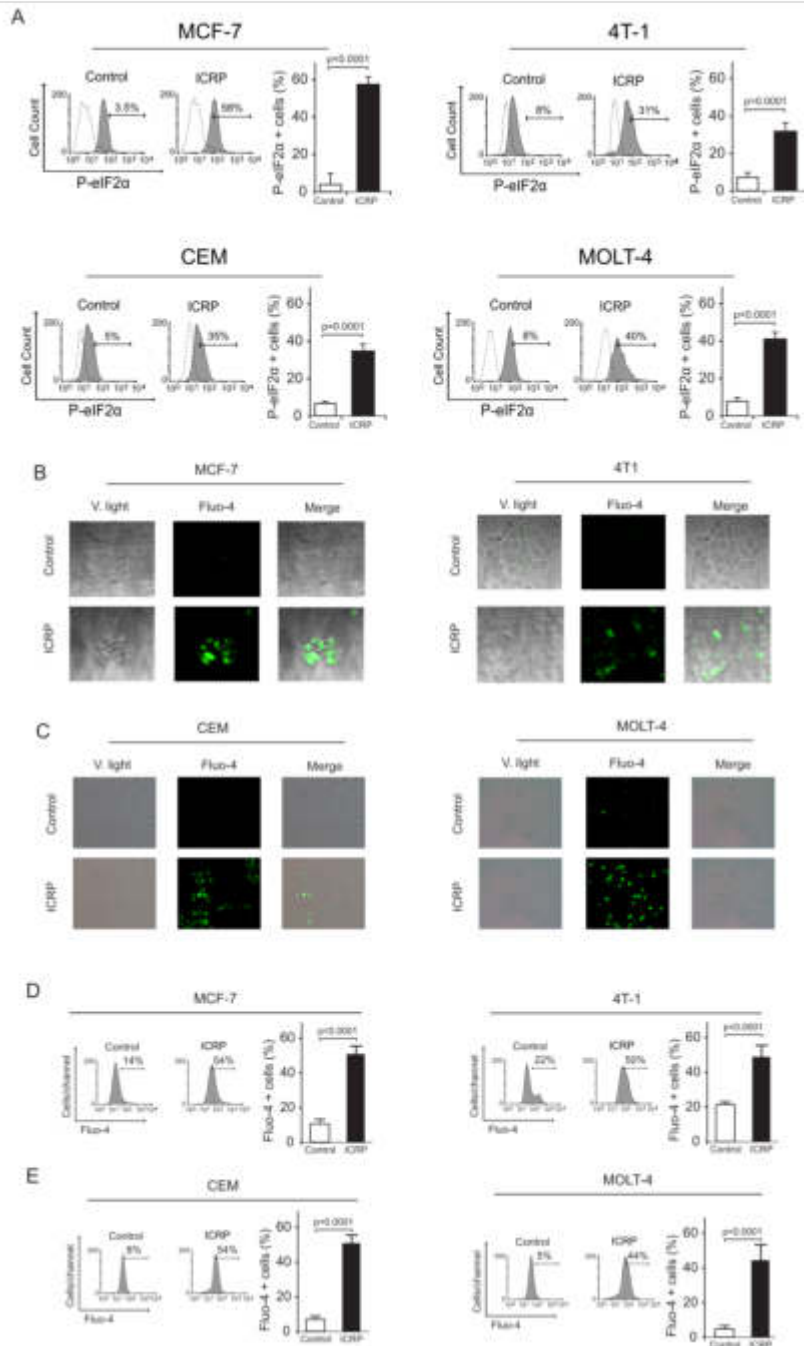
Figure 4: IMMUNEPOTENT-CRP induces eIF2α phosphorylation and increases in the cytoplasmic Ca²⁺ levels. A. Representative histograms and quantification of eIF2α phosphorylation measured by flow cytometry using anti-EIF2S1 monoclonal antibody in breast cancer cell lines MCF-7 and 4T1 (left), and leukemic cells lines CEM and MOLT-4 (right). B. Confocal microscopy representation of Ca²⁺ cytoplasmic levels measured by Fluo-4AM staining in breast cancer cell lines MCF-7 (left) and 4T1 (right) in absence (control) or presence of ICRP CC₅₀ for 18 h and visualized using fluorescence microscopy (OLYMPUS X70) (40×). C. Fluorescence microscopy representation of Ca²⁺ cytoplasmic levels measured trough Fluo-4AM staining in leukemic cell lines CEM (left) and MOLT-4 (right) in absence (control) or presence of ICRP CC₅₀ for 18 h and visualized using fluorescence microscopy (OLYMPUS IX70) (40×). D-E. Representative histograms and quantification of Ca²⁺ cytoplasmic levels assessed through Fluo-4AM staining by flow cytometry in breast cancer cell lines MCF-7 and 4T1 (above) (D), and in T-ALL cell lines CEM and MOLT-4 (down) (E) treated with ICRP CC₅₀ for 18 h. Graphs represent

86

Figure 5: IMMUNEPOTENT CRP induces Ca²⁺-dependent cell death in tumoral and leukemic cell lines. A. Representative dot plots and quantification of cell death measured by flow cytometry through Annexin-V and PI staining in breast cancer cell lines MCF-7 and 4T1 (above), and in T-ALL cell lines CEM and MOLT-4 (down) treated with ICRP CC₅₀ for 24 h in presence or absence of BAPTA. B. Representative histograms and quantification of caspase-3 cleaved by flow cytometry using FITC-DEVD-FMK staining in T-ALL cell lines CEM (left) and MOLT-4 (right) treated with ICRP CC₅₀ for 24 h in presence or absence of BAPTA. C-D. Quantification of loss of mitochondrial membrane potential (C) and ROS production (D) evaluated through TMRE and DCFDA staining, respectively, by flow cytometry in breast cancer cell lines MCF-7 and 4T1, and in T-ALL cell lines CEM and MOLT-4 treated with ICRP CC₅₀ for 24h in presence or absence of BAPTA. Graphs represent the mean (± SD) of triplicates of at least three independent experiments.

ICRP treatment-induced ROS production at MCF-7 (49.7±9.7 %), 4T1 (47.7±8.3 %), CEM (38.6±7.3 %), and MOLT-4 (41.6±3.5 %) also decreased in the presence of BAPTA to 19.4±6.9 %, 10.1±4.7 %, 26.2±2.7 %, and 13.6±7.1 %, respectively

87

(Figure 5D). These data demonstrate that ICRP-mediated cell death relies on the cytoplasmic increase of Ca2+ levels, being the first event observed during the ICRP-cytotoxic pathway. Moreover, Ca^{2+} deregulation is an invariable event that occurs in the caspase-independent or dependent pathways induced by ICRP.

Inhibition of ER-Ca^{2+} channels block ROS production and cell death induced by IMMUNEPOTENT-CRP

Inositol 1,4,5-trisphosphate receptors (IP_3R) and ryanodine receptors (RyR) are the principal mediators of Ca^{2+} release from intracellular stores (Hanson et al., 2004; Missiaen et al., 2001; Splettstoesser et al., 2007). We blocked IP_3R and RyR, using 2-APB (Splettstoesser et al., 2007) and Dantrolene (Zhao et al., 2001) respectively, to evaluate their implication on the mechanism induced by ICRP. We observed by fluorescent microscopy that in presence of 2-APB and Dantrolene, cytoplasmic Ca^{2+} was diminished in MCF-7, 4T1, CEM and MOLT-4 cell lines (Figure 6A).

ROS generation is strongly associated with Ca^{2+} leakage in ER (Zeeshan et al., 2016). Thus, we then determined if the IP_3R and RyR are involved on ROS production, the principal effectors on ICRP-cytotoxicity. In Figure 6B we can observe that ROS production induced by ICRP diminished in presence of 2-APB, the IP_3R inhibitor or Dantrolene, the RyR inhibitor. On MCF-7 ROS production passed from 49.7±9.7 % to 24±4.2 % and 23.6±4.5 %, respectively, in 4T1 from 44.6±5.6 % to 22.1±4.6 % and 15.8±2.7 %, respectively. T-ALL cell lines had a similar outcome, in CEM cells with ROS production passed from 38.6±7.3 % to 13.7±8.1 % and 6.25±2.3 %, respectively, and in MOLT-4 cells from 41.6±3.5 % to 19.9±8.1 % and 9.9±8.4 %, respectively. Taken together, these results revealed that ER Ca^{2+} release induces ROS production in breast cancer and leukemic cells.

Finally, we assessed the implication of these ER-Ca^{2+} release channels in cell death.

Our results in Figure 6C show that 2-APB diminished cell death on MCF-7 from 47.3 % to 25.3 % (p<0.0001), in 4T-1 from 48.6 % to 23.83 % (p<0.0001), in CEM from 50.9 % to 21.7 % (p=0.0135), and MOLT-4 from 52 % to 32 % (p=0.0009). Similar inhibition was observed using Dantrolene in cell death where it diminishes from 47.3 % to 27.4 % (p<0.0001) in MCF-7 cells, from 48.6 % to 24.01 % (p<0.0001) in 4T-1 cells, from 50.9 % to 25.8 % (p=0.0337) in CEM cells, and from 52 % to 30 % (p=0.0003) in MOLT-4 cells.

DISCUSSION

ROS-dependence has been the principal hallmark of ICRP-mediated cell death, independently of the cancer cell type assessed to date (Martinez-Torres et al., 2018, 2019a, b; Reyes-Ruiz et al., 2021). Here we show that ICRP induces calcium-dependent ROS production leading to cell death in T-ALL and breast cancer cell lines. Additionally, ICRP triggered caspase-dependent or caspase-independent cell death in different cancer cell lineages. This has been observed with other cell death inductors as gold nanoparticles or photodynamic treatments, which induce different cell death mechanisms in cancer cells, depending on the cancer cell type (Martínez-Torres et al., 2019b; Soriano et al., 2017). These treatments commonly induce mitochondrial damage and ROS production (Perillo et al., 2020), as we observed with ICRP.

ROS-induced stress can be sensed and activate autophagy, which plays a role on stress adaptation and cell death (Chang and Zou 2020; Cordani et al., 2019). In this work, we show that ICRP induces ROS-dependent autophagosome formation, as an adaptive mechanism to avoid cell death. Other agents such as Salinomycin, Oxaliplatin and Irinotecan induce ROS-dependent prosurvival autophagy in breast cancer cell lines MDA-MB-231 and MCF-7 (Kim et al., 2017), and gastric cancer cells (Shi et al., 2012; Zhu et al., 2020). The ROS-Autophagy-ER stress axis has been ex-

A
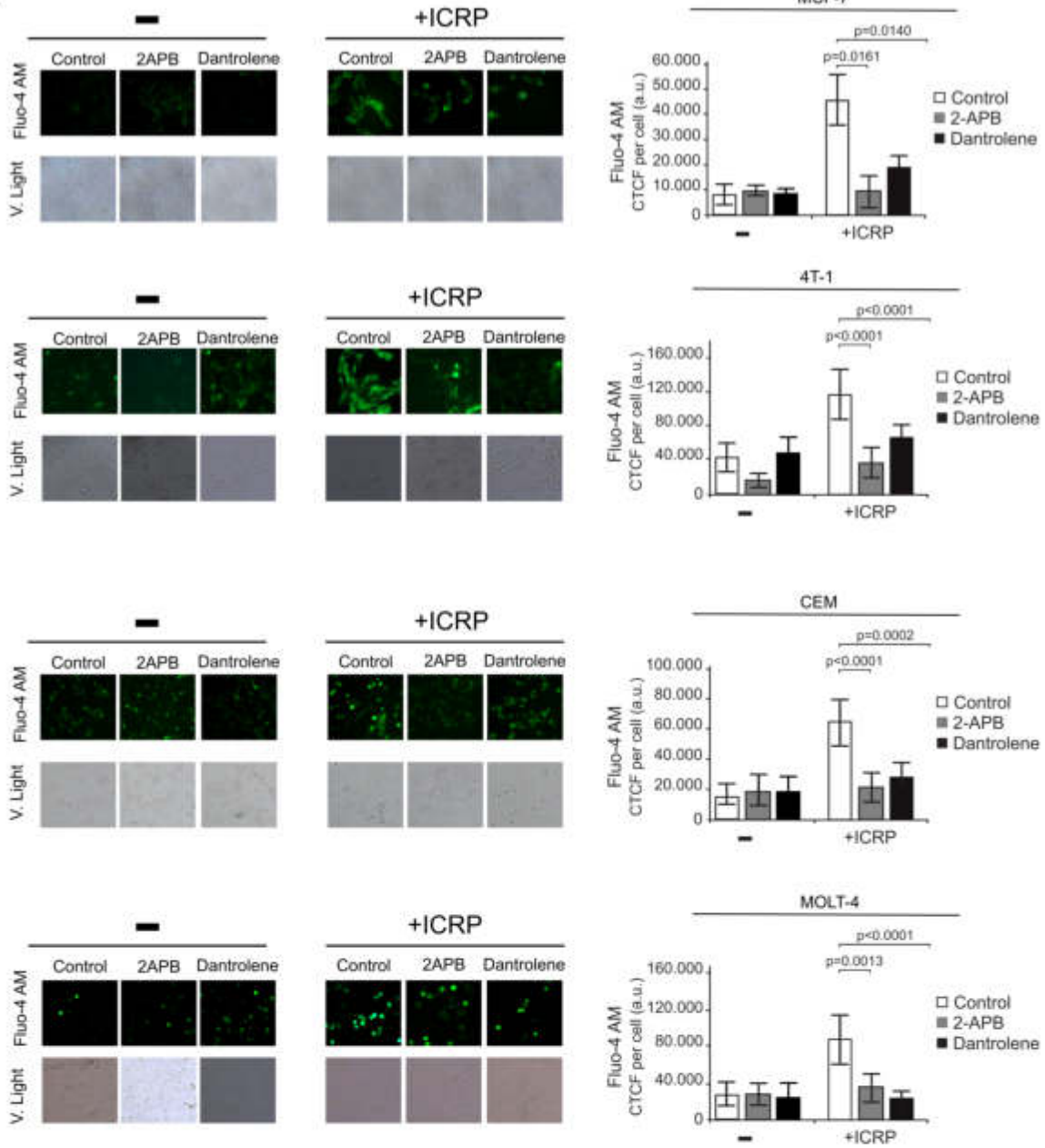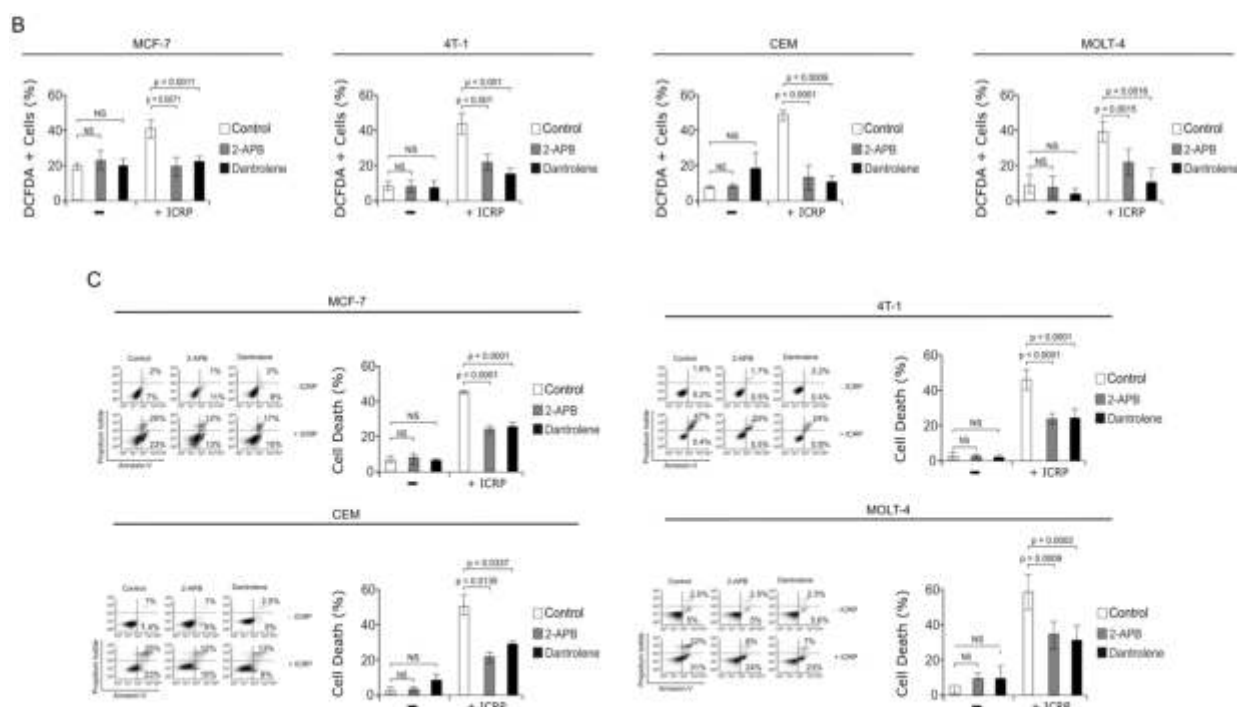
Figure 6: IMMUNEPOTENT-CRP induces Ca²⁺-dependent cell death in breast cancer and leukemic cell lines. A. Fluorescence microscopy representation (left) and quantification (right) of Ca²⁺ cytoplasmic levels measured through Fluo-4AM staining in breast cancer MCF-7 and 4T1 and leukemic cell lines CEM and MOLT-4 treated with ICRP CC₅₀ for 18 h and in presence or absence of 2-APB and Dantrolene, visualized using fluorescence microscopy (OLYMPUS IX70) (40×). B. Quantification of ROS production assessed by DCFDA staining by flow cytometry in breast cancer cell lines MCF-7 and 4T1, and in T-ALL cell lines CEM and MOLT-4 treated with ICRP CC₅₀ for 24 h in presence or absence of 2-APB and Dantrolene. C. Quantification of cell death measured by flow cytometry through Annexin-V and PI staining in breast cancer cell lines MCF-7 and 4T1 (above), and T-ALL cell lines CEM and MOLT-4 (down) treated with ICRP CC₅₀ for 24 h in presence or absence of 2-APB and Dantrolene. Graphs represent the mean (± SD) of triplicates of at least three independent experiments.

tensively linked, as ROS can promote ER-stress, mediating autophagy to abrogate cellular damage (Deegan et al., 2013; Rashid et al., 2015; Zeeshan et al., 2016). ER stress can mediate ROS cascades which in turn can activate autophagy as a protective mechanism (Cao and Kaufman 2014; Zhong et al., 2015; Zeeshan et al., 2016), explaining why ROS production induced by ICRP can lead to ER stress and autophagy on cancer cell lines. ER stress commonly involves P-eIF2α, which has also been linked to autophagy (Humeau et al.,

2020). In this sense, as I-CRP did in T-ALL and breast cancer cell lines, chemotherapeutics such as anthracyclines and oxaliplatin can induce P-eIF2α in U2OS and HCT 116 cancer cells (Bezu et al., 2018).

ER Ca²⁺ release is highly associated with ER stress conditions (Cioffi, 2011). It has been reported that during early stages of ER stress, oxidative stress forces Ca²⁺ out of ER (Li et al., 2009). High ER-Ca²⁺ release through RyR and IP₃R can provoke mitochon-

drial uptake generating ROS production, mitochondrial depolarization, and cell death (Kerkhofs et al., 2018). Here we show that extracellular Ca^{2+} chelation prevents the loss of mitochondrial membrane potential, ROS production, and cell death. It is well known that Ca^{2+} depletion from ER activates SOCE leading to high concentrations of Ca^{2+} inside the cell (Orrenius et al., 2003), explaining why BAPTA and ER-Ca^{2+} receptor inhibitors could decrease intracellular calcium augmentation. Moreover, we show that the inhibition of ER-calcium receptors (RyR and IP_3R) inhibits ROS production and death. Our results indicate that the increase of intracellular Ca^{2+} levels induced by ICRP is the first step on both cell death modalities described so far on breast and T-ALL cell lines.

These results are similar to the cell death pathways described with other treatments. For instance, menadione induces ER-Ca^{2+} release, accompanied by mitochondrial Ca^{2+} elevation, mitochondrial depolarization, and mitochondrial permeability transition pore (mPTP) opening, leading to cell death in pancreatic tumor cells (Baumgartner et al., 2009). Ceramide-induced cell death in HeLa cells involves ER-Ca^{2+} release and mitochondrial Ca^{2+} increase, accompanied by marked alterations in mitochondria morphology (Pinton et al., 2001). Also, cisplatin increased cytoplasmic and mitochondrial Ca^{2+} levels in HeLa cells, which further triggered mitochondrial-mediated and ER stress-associated cell death pathways, moreover, the inhibition of IP_3R decreased calcium release from the ER and inhibited cisplatin-induced cell death (Shen et al., 2016). In this context, an IP_3 receptor antagonist, 2-APB attenuates cisplatin induced $Ca2^+$-influx in HeLa-S3 cells and prevents activation of calpain and induction of apoptosis (Splettstoesser et al., 2007).

Overall, our results revealed that IMMUNEPOTENT CRP triggers endoplasmic reticulum stress accompanied by the increase of intracellular Ca^{2+} levels leading to mitochondrial damage and ROS production provoking regulated cell death on cancer cell lines. This work opens new possibilities to evaluate the cytotoxicity of ICRP in combination with other types of cell death inductors, and the immunogenicity of the cell death in hematological malignances and other solid cancers.

REFERENCES

Almanza A, Carlesso A, Chintha C, Creedican S, Doultsinos D, Leuzzi B, et al. Endoplasmic reticulum stress signalling - from basic mechanisms to clinical applications. FEBS J. 2019;286:241-78. doi: 10.1111/febs.14608.

Arnaudov A. Immunotherapy with dialyzable leukocyte extracts containing transfer factor. In: Metodiev K (ed) Immunotherapy - myths, reality, ideas, future. London: IntechOpen, 2017. doi: 10.5772/66524.

Baumgartner HK, Gerasimenko JV, Thorne C, Ferdek P, Pozzan T, Tepikin AV, et al. Calcium elevation in mitochondria is the main Ca2+ requirement for mitochondrial permeability transition pore (mPTP) opening. J Biol Chem. 2009;284:20796-803. doi: 10.1074/jbc.M109.025353.

Bezu L, Sauvat A, Humeau J, Gomes-da-Silva LC, Iribarren K, Forveille S, et al. eIF2α phosphorylation is pathognomonic for immunogenic cell death. Cell Death Differ. 2018;25:1375-93. doi: 10.1038/s41418-017-0044-9.

Cao SS, Kaufman RJ. Endoplasmic reticulum stress and oxidative stress in cell fate decision and human disease. Antioxid Redox Signal. 2014;21:396-413. doi: 10.1089/ars.2014.5851

Chang H, Zou Z. Targeting autophagy to overcome drug resistance: further developments. J Hematol Oncol. 2020;13(1):159. doi: 10.1186/s13045-020-01000-2.

Cioffi DL. Redox regulation of endothelial canonical transient receptor potential channels. Antioxid Redox Signal. 2011;15:1567-82. doi: 10.1089/ars.2010.3740.

Cordani M, Donadelli M, Strippoli R, Bazhin AV, Sánchez-Álvarez M. Interplay between ROS and autophagy in cancer and aging: from molecular mechanisms to novel therapeutic approaches. Oxid Med Cell Longev. 2019;2019:8794612. doi: 10.1155/2019/8794612.

Coronado-Cerda EE, Franco-Molina MA, Mendoza-Gamboa E, Prado-García H, Rivera-Morales LG, Zapata-Benavides P, et al. In vivo chemoprotective activity of bovine dialyzable leukocyte extract in mouse bone marrow cells against damage induced by 5-fluorouracil. J Immunol Res. 2016;2016:6942321. doi: 10.1155/2016/6942321.

Danese A, Leo S, Rimessi A, Wieckowski MR, Fiorica F, Giorgi C, et al. Cell death as a result of calcium signaling modulation: A cancer-centric prospective. Biochim Biophys Acta Mol Cell Res. 2021;1868(8):119061. doi: 10.1016/j.bbamcr.2021.119061.

Deegan S, Saveljeva S, Gorman AM, Samali A. Stress-induced self-cannibalism: on the regulation of autophagy by endoplasmic reticulum stress. Cell Mol Life Sci. 2013;70:2425-41. doi: 10.1007/s00018-012-1173-4.

Franco-Molina MA, Mendoza-Gamboa E, Miranda-Hernández D, Zapata-Benavides P, Castillo-León L, Isaza-Brando C, et al. In vitro effects of bovine dialyzable leukocyte extract (bDLE) in cancer cells. Cytotherapy. 2006;8:408-14. doi: 10.1080/14653240600847266.

Hanson CJ, Bootman MD, Roderick HL. Cell signalling: IP3 receptors channel calcium into cell death. Curr Biol. 2004;14:R933-5. doi: 10.1016/j.cub.2004.10.019.

Humeau J, Bezu L, Kepp O, Kroemer G. EIF2α phosphorylation: a hallmark of both autophagy and immunogenic cell death. Mol Cell Oncol. 2020;7(5):1776570. doi: 10.1080/23723556.2020.1776570.

Inguscio V, Panzarini E, Dini L. Autophagy contributes to the death/survival balance in cancer photodynamic therapy. Cells. 2012;1(3):464-91. doi: 10.3390/cells1030464.

Karrman K, Johansson B. Pediatric T-cell acute lymphoblastic leukemia. Genes Chromosomes Cancer. 2017;56:89-116. doi: 10.1002/gcc.22416.

Kerkhofs M, Bittremieux M, Morciano G, Giorgi C, Pinton P, Parys JB, et al. Emerging molecular mechanisms in chemotherapy: Ca^{2+} signaling at the mitochondria-associated endoplasmic reticulum membranes. Cell Death Dis. 2018;9(3):334. doi: 10.1038/s41419-017-0179-0.

Kim KY, Park KI, Kim SH, Yu SN, Lee D, Kim YW, et al. Salinomycin induces reactive oxygen species and apoptosis in aggressive breast cancer cells as mediated with regulation of autophagy. Anticancer Res. 2017;37:1747-58. doi: 10.21873/anticanres.11507.

Kirkpatrick CH. Transfer factors: identification of conserved sequences in transfer factor molecules. Mol Med. 2000;6:332-41.

Li G, Mongillo M, Chin KT, Harding H, Ron D, Marks AR, et al. Role of ERO1-alpha-mediated stimulation of inositol 1,4,5-triphosphate receptor activity in endoplasmic reticulum stress-induced apoptosis. J Cell Biol. 2009;186:783-92. doi: 10.1083/jcb.200904060.

Lorenzo-Anota HY, Martínez-Torres AC, Scott-Algara D, Tamez-Guerra RS, Rodríguez-Padilla C. Bovine dialyzable leukocyte extract IMMUNEPOTENT-CRP induces selective ROS-dependent apoptosis in T-acute lymphoblastic leukemia cell lines. J Oncol. 2020;2020:1598503. doi: 10.1155/2020/1598503.

Martínez-Torres AC, Reyes-Ruiz A, Benítez-Londoño M, Franco-Molina MA, Rodríguez-Padilla C. IMMUNEPOTENT CRP induces cell cycle arrest and caspase-independent regulated cell death in HeLa cells through reactive oxygen species production. BMC Cancer. 2018;18(1):13. doi: 10.1186/s12885-017-3954-5.

Martinez-Torres AC, Gomez-Morales L, Martinez-Loria AB, Uscanga-Palomeque AC, Vazquez-Guillen JM, Rodriguez-Padilla C. Cytotoxic activity of IMMUNEPOTENT CRP against non-small cell lung cancer cell lines. PeerJ. 2019a;7:e7759. doi: 10.7717/peerj.7759.

Martínez-Torres AC, Lorenzo-Anota HY, García-Juárez MG, Zarate-Triviño DG, Rodríguez-Padilla C. Chitosan gold nanoparticles induce different ROS-dependent cell death modalities in leukemic cells. Int J Nanomedicine. 2019b;14:7173-90. doi: 10.2147/IJN.S221021.

Martínez-Torres AC, Reyes-Ruiz A, Calvillo-Rodriguez KM, Alvarez-Valadez KM, Uscanga-Palomeque AC, Tamez-Guerra RS, et al. IMMUNEPOTENT CRP induces DAMPS release and ROS-dependent autophagosome formation in HeLa and MCF-7 cells. BMC Cancer. 2020;20(1):647. doi: 10.1186/s12885-020-07124-5.

Missiaen L, Callewaert G, De Smedt H, Parys JB. 2-Aminoethoxydiphenyl borate affects the inositol 1,4,5-trisphosphate receptor, the intracellular Ca2+ pump and the non-specific Ca2+ leak from the non-mitochondrial Ca2+ stores in permeabilized A7r5 cells. Cell Calcium. 2001;29:111-6. doi: 10.1054/ceca.2000.0163.

Monteith GR, Prevarskaya N, Roberts-Thomson SJ. The calcium-cancer signalling nexus. Nat Rev Cancer. 2017;17:367-380. doi: 10.1038/nrc.2017.18.

Orrenius S, Zhivotovsky B, Nicotera P. Regulation of cell death: the calcium-apoptosis link. Nat Rev Mol Cell Biol. 2003;4:552-65. doi: 10.1038/nrm1150.

Orrenius S, Gogvadze V, Zhivotovsky B. Calcium and mitochondria in the regulation of cell death. Biochem Biophys Res Commun. 2015;460(1):72-81. doi: 10.1016/j.bbrc.2015.01.137.

Perillo B, Di Donato M, Pezone A, Di Zazzo E, Giovannelli P, Galasso G, et al. ROS in cancer therapy: the bright side of the moon. Exp Mol Med. 2020;52:192-203. doi: 10.1038/s12276-020-0384-2.

Pinton P, Ferrari D, Rapizzi E, Di Virgilio F, Pozzan T, Rizzuto R. The Ca2+ concentration of the endoplasmic reticulum is a key determinant of ceramide-induced apoptosis: significance for the molecular mechanism of Bcl-2 action. EMBO J. 2001;20:2690-701. doi: 10.1093/emboj/20.11.2690.

Rashid HO, Yadav RK, Kim HR, Chae HJ. ER stress: Autophagy induction, inhibition and selection. Autophagy. 2015;11:1956-77. doi: 10.1080/15548627.2015.1091141.

Reyes-Ruiz A, Calvillo-Rodriguez KM, Martínez-Torres AC, Rodríguez-Padilla C. The bovine dialysable leukocyte extract IMMUNEPOTENT CRP induces immunogenic cell death in breast cancer cells leading to long-term antitumour memory. Br J Cancer. 2021; 124:1398–410. doi: 10.1038/s41416-020-01256-y.

Rodríguez-Salazar MDC, Franco-Molina MA, Mendoza-Gamboa E, Martínez-Torres AC, Zapata-Benavides P, López-González JS, et al. The novel immunomodulator IMMUNEPOTENT CRP combined with chemotherapy agent increased the rate of immunogenic cell death and prevented melanoma growth. Oncol Lett. 2017;14:844-52. doi: 10.3892/ol.2017.6202.

Shen L, Wen N, Xia M, Zhang YU, Liu W, Xu YE, et al. Calcium efflux from the endoplasmic reticulum regulates cisplatin-induced apoptosis in human cervical cancer HeLa cells. Oncol Lett. 2016;11:2411-9. doi: 10.3892/ol.2016.4278.

Shi Y, Tang B, Yu PW, Tang B, Hao YX, Lei X, et al. Autophagy protects against oxaliplatin-induced cell death via ER stress and ROS in Caco-2 cells. PLoS One. 2012;7(11):e51076. doi: 10.1371/journal.pone.0051076.

Siegel RL, Miller KD, Jemal A. Cancer statistics, 2019. CA Cancer J Clin. 2019;69(1):7-34. doi: 10.3322/caac.21551.

Soriano J, Mora-Espí I, Alea-Reyes M, Pérez-García L, Barrios L, Ibáñez E, et al. Cell death mechanisms in tumoral and non-tumoral human cell lines triggered by photodynamic treatments: apoptosis, necrosis and parthanatos. Sci Rep. 2017;7:41340. doi: 10.1038/srep41340.

Splettstoesser F, Florea AM, Büsselberg D. IP(3) receptor antagonist, 2-APB, attenuates cisplatin induced Ca2+-influx in HeLa-S3 cells and prevents activation of calpain and induction of apoptosis. Br J Pharmacol. 2007;151:1176-86. doi: 10.1038/sj.bjp.0707335.

Terwilliger T, Abdul-Hay M. Acute lymphoblastic leukemia: a comprehensive review and 2017 update. Blood Cancer J. 2017;7(6):e577. doi: 10.1038/bcj.2017.53.

Zeeshan HM, Lee GH, Kim HR, Chae HJ. Endoplasmic reticulum stress and associated ROS. Int J Mol Sci. 2016;17(3):327. doi: 10.3390/ijms17030327.

Zhao F, Li P, Chen SR, Louis CF, Fruen BR. Dantrolene inhibition of ryanodine receptor Ca2+ release channels. Molecular mechanism and isoform selectivity. J Biol Chem. 2001;276:13810-6. doi: 10.1074/jbc.M006104200.

Zhivotovsky B, Orrenius S. Calcium and cell death mechanisms: a perspective from the cell death community. Cell Calcium. 2011;50:211-21. doi: 10.1016/j.ceca.2011.03.003.

Zhong F, Xie J, Zhang D, Han Y, Wang C. Polypeptide from Chlamys farreri suppresses ultraviolet-B irradiation-induced apoptosis through restoring ER redox homeostasis, scavenging ROS generation, and suppressing the PERK-eIF2a-CHOP pathway in HaCaT cells. J Photochem Photobiol B. 2015;151:10-6. doi: 10.1016/j.jphotobiol.2015.06.016.

Zhu Q, Guo Y, Chen S, Fu D, Li Y, Li Z, et al. Irinotecan induces autophagy-dependent apoptosis and positively regulates ROS-related JNK- and P38-MAPK pathways in gastric cancer cells. Onco Targets Ther. 2020;13:2807-17. doi: 10.2147/OTT.S240803.

ARTICLE
Translational Therapeutics

The bovine dialysable leukocyte extract IMMUNEPOTENT CRP induces immunogenic cell death in breast cancer cells leading to long-term antitumour memory

Alejandra Reyes-Ruiz[1], Kenny Misael Calvillo-Rodriguez[1], Ana Carolina Martínez-Torres[1] and Cristina Rodríguez-Padilla[1,2]

BACKGROUND: Cancer recurrence is a serious problem in breast cancer (BC) patients, and immunogenic cell death (ICD) has been proposed as a strategy to overcome this recurrence. IMMUNEPOTENT CRP (ICRP) acts as an immunomodulator and can be cytotoxic to cancer cells. Thus, we evaluated if ICRP induces ICD in BC cells.
METHODS: Immunogenicity of ICRP-induced cell death was evaluated in vitro, analysing the principal biochemical characteristics of ICD in MCF-7, MDA-MB-231 and 4T1 cells. Ex vivo, we assessed the ability of killed cancer cells (KCC) obtained from ICRP-treated 4T1 cells (ICRP-KCC) to induce DC maturation, T-cell priming and T-cell-mediated cancer cytotoxicity. In vivo, we evaluated tumour establishment and antitumour immune memory after prophylactic ICRP-KCC vaccination in BALB/c mice.
RESULTS: ICRP induced caspase-independent, ROS-dependent cell death, autophagosome formation, P-eIF2α, chaperone protein exposure, CD47 loss, ATP and HMBG1 release in BC cells. Additionally, ICRP-KCC promoted DC maturation, which triggered T-cell priming and cancer cytotoxicity. Prophylactic vaccination with ICRP-KCC prevented tumour establishment and induced long-term antitumour memory in BALB/c mice, involving DC maturation in lymph nodes, CD8+ T-cell augmentation in lymph nodes, peripheral blood and tumour site and ex vivo tumour-specific cytotoxicity by splenocytes.
CONCLUSIONS: ICRP induces ICD in BC cells, leading to long-term antitumour memory.

British Journal of Cancer https://doi.org/10.1038/s41416-020-01256-y

BACKGROUND
Breast cancer is the most frequently diagnosed cancer and the leading cause of deaths in women.[1] One of the principal pitfalls leading to the mortality of this disease is associated with distant metastasis and its ability to recur up to 20 years after diagnosis,[2] these characteristics are related with the low immunogenicity of breast cancer cells, as a result of cancer cell release of immune-suppressive factors, which block the cancer-immunity cycle.[3] However, it is now being proposed that with appropriate immune response stimulation, cancer cells could become immunogenic.

In this regard, several studies indicate that immunogenic cell death (ICD) is a hopeful strategy to convert cancer cells into their own vaccine, promising a long-term success of anticancer therapies relying on memory immune response induction,[4,5] which could deal against high recurrence rate in breast cancer patients. It has been reported that a restricted number of chemotherapies induce ICD,[6] for instance, breast cancer patients treated with anthracyclines (ICD inducers) showed an increment in the ratio of CD8+ T cells over regulatory T cells intratumourally, and this predicts a favourable therapeutic response.[7]

IMMUNEPOTENT CRP (ICRP), a bovine dialysable leukocyte extract (DLE) obtained from disrupted spleen, is cytotoxic to several cancer cell lines,[8–11] without affecting the viability of non-cancer cells.[11] ICRP induces ICD in the murine melanoma model B16F10,[12] whereas in HeLa and MCF-7 cells, ICRP-mediated cell death involves CRT exposure, ATP and HMGB1 release, which are the principal damage-associated molecular patters (DAMPs) involved in ICD. In addition, ICRP leads to eIF2α phosphorylation (P-eIF2α), which indicates endoplasmic reticulum (ER) stress, an early ICD biomarker. Furthermore, ICRP has been reported to induce reactive oxygen species (ROS)-dependent autophagosome formation in HeLa and MCF-7 cells.[13]

ROS production, ER stress and autophagy stimulate intracellular danger signalling pathways that regulate the release of DAMPs and thus ICD.[14,15] These results suggest that ICRP might induce ICD in other cancer models, as a conserved mechanism. The aim of this study was to investigate the immunogenicity of ICRP-induced cell death in a panel of breast cancer models, using human and murine cell lines, as well as ex vivo and in vivo experiments using BALB/c mice.

METHODS
Cell culture
MCF-7 human breast adenocarcinoma (ATCC® HTB-22TM), MDA-MB-231 triple-negative breast adenocarcinoma (ATCC® HTB-26TM)

[1]Universidad Autónoma de Nuevo León, Facultad de Ciencias Biológicas, Laboratorio de Inmunología y Virología, San Nicolás de los Garza, México and [2]Longeveden, SA de CV, Monterrey, México
Correspondence: Ana Carolina Martínez-Torres (ana.martineztzo@uanl.edu.mx)
These authors contributed equally: Alejandra Reyes-Ruiz, Kenny Misael Calvillo-Rodriguez

The bovine dialysable leukocyte extract IMMUNEPOTENT CRP induces...
A Reyes-Ruiz et al.

1399

and 4T1 murine mammary adenocarcinoma (ATCC® CRL2539TM) cell lines were obtained from the American Type Culture Collection. MCF-7 and MDA-MB-231 cells were cultured in DMEM-F12 supplemented with 10% foetal bovine serum (FBS) and 1% penicillin–streptomycin (complete DMEM), and 4T1 cells were cultured in RPMI-1640 supplemented with 10% FBS and 1% penicillin–streptomycin (complete RPMI) (Life Technologies, Grand Island, NY) and routinely grown in plastic tissue-culture dishes (Life Sciences, Corning, NY). All cell cultures were maintained in a humidified incubator in 5% CO_2 at 37 °C. Cell count was performed in a Neubauer chamber, using 0.4% trypan blue (MERCK, Darmstadt, Germany).

Animals
The Animal Research and Welfare Ethics Committee (CEIBA), of the School of Biological Sciences approved this study: CEIBA-2019-006. All experiments were conducted according to Mexican regulation NOM-062-ZOO-1999. Female BALB/c mice (six-to-eight-week-old, 20 ± 2 g of weight) were provided by the animal house at the Universidad Autonoma de Nuevo Leon, Mexico. Animals were housed in plastic cages in groups of four and given seven days to acclimate to the housing facility. Environmental conditions were temperature 21 °C ± 3 °C, humidity 55% ± 10% and 12-h light/dark cycle. Animals were supplied with rodent maintenance food (LabDiet, St. Louis, MO) and water ad libitum, and they were monitored twice daily for health status, no adverse events were observed. Mice were randomly assigned to different groups for all studies. All experiments were designed in accordance to the Arrive guidelines for animal care and protection (Methods S1).[16]

Cell death assay
Cell death was measured using 1 μg/mL APC Annexin V (BD Pharmingen, San Jose, CA) and 0.5 μg/mL propidium iodide (PI) (MERCK). In brief, 5×10^4 cells/well in 24-well dishes (Life Sciences) were incubated in the presence or absence of different concentrations of IMMUNEPOTENT CRP (ICRP), epirubicin (EPI, Sigma-Aldrich, ST. Louis, MO) or cyclophosphamide (CPA, Sigma-Aldrich) for 24 h in complete DMEM or RPMI to a final volume of 400 μL to obtain the ICRP CC_{50}. For cell death inhibition assays, cells were pre-treated 30 min with or without 5mM N-acetyl-L-cysteine (NAC), 10 μM QVD.oph, 30 μM Necrostatin-1 (NEC-1) or 15 μM Spautin-1 (Sp-1), and then co-treated with or without ICRP CC_{50} for 24 h, as mentioned before. Cells were then detached, washed twice with PBS, suspended in 100 μL of binding buffer (10 mM HEPES/NaOH, pH 7.4, 140 mM NaCl and 2.5 mM $CaCl_2$), stained and assessed by BD Accury C6 flow cytometer (Becton Dickinson, Franklin Lakes, NJ). The results were analysed using FlowJo Software (LLC, Ashland, OR).

Loss of mitochondrial membrane potential analysis
For these assays, cells were stained with 500 nM TMRE (Sigma-Aldrich) to evaluate the loss of mitochondrial membrane potential. In brief, 5×10^4 cells/well in 24-well dishes (Life Sciences) were incubated in the presence or absence of ICRP CC_{50} for 24 h, as explained above. Cells were detached, washed with PBS, stained, incubated at 37 °C for 30 min and measured by flow cytometry as described above.

ROS generation analysis
ROS levels were determined by staining cells with 2.5 μM 2′,7′-dichlorofluorescin diacetate (DCFDA) (MERCK). In brief, 5×10^4 cells/well were incubated in the presence or absence of ICRP CC_{50} for 24 h, as explained above. Cells were then detached, washed with PBS, stained, incubated at 37 °C for 30 min and measured using a flow cytometer, as mentioned above.

Autophagosome formation assays
For flow cytometric assessment, 5×10^6 cells were cultured in 24-well plates (Life Sciences) in the presence or absence of ICRP CC_{50}

for 24 h. Cells were then detached, washed with PBS, stained with Autophagy Detection Kit (Abcam, Cambridge, UK) and measured by flow cytometry, as explained above.

For fluorescence microscopy, 5×10^4 cells were cultured in 24-well plates (Life Sciences), pre-treated 30 min with or without 15 μM Sp-1 and then co-treated with or without ICRP CC_{50} for 24 h, as mentioned above. Cells were then washed twice with PBS and stained with CYTO-ID Autophagy Detection Kit (Enzo Life Science, Farmingdale, NY) following the manufacturer's instructions. Nuclei were counterstained in blue with Hoechst 33342 dye (Enzo Life Science). Images were acquired with an InCellis Imager (BERTIN Instruments, Montigny-le-Bretonneux, France), fluorescence was measured using Image J (NIH Image, Bethesda, MD) to obtain the corrected total cell fluorescence (CTCF) using the following formula: CTCF = integrated density − (area of selected cell * mean fluorescence of background readings).

Western blot analysis
Cells were treated with ICRP CC_{50} for 24 h and were lysed in lysis buffer containing 20 mM Tris (pH 6.8), 2% SDS, 2 mM EDTA and 300 mM NaCl. The protein concentration for each sample was determined using a spectrophotometer in accordance with the manufacturer's recommendations. The proteins were separated by SDS-PAGE and transferred to nitrocellulose membranes. Western blotting was performed with anti-p62 (sc-48402, Santa Cruz Biotechnology, Dallas, TX) and anti-β-actin (BA3R, abm, Richmond, BC). After incubation with the anti-mouse secondary antibodies conjugated to horseradish peroxidase (ab6728, Abcam), blots were revealed using ECL western blotting substrate (Thermo Scientific, Waltham, MA).

EIF2α assay
For this assay, 5×10^5 cells were plated in 6-well dishes (Life Sciences) in complete DMEM or RPMI to a final volume of 2 mL, and incubated in the presence or absence of ICRP CC_{50} for 18 h or 1 μM thapsigargin (thaps) for 2 h. Cells were then collected and fixed with 80% methanol for 5 min at −20 °C, washed with PBS and permeabilized with 0.1% PBS-Tween for 20 min at 25 °C. The cells were then washed with PBS, suspended in 50 μL of 1× PBS/10% FSB/0.3 M glycine, incubated for 30 min and shaken at 400 rpm, 25 °C, followed by the addition of 0.2 μL of anti-EIF2S1 (phospho S51) antibody [E90] (ab32157, Abcam) (1:250) for eIF2α phosphorylation (P-eIF2α) analysis or 0.5 μL of anti-EIF2A (3A7A8, Santa Cruz Biotechnology) (1:100) for eIF2α total (T-eIF2α) assays, cells were incubated for 2 h and washed with 2% FACS Buffer (1× PBS and 2% FBS). Cells were then suspended in 100 μL of 1× PBS/10% FSB/0.3 M glycine, incubated for 15 min and shaken at 400 rpm and 25 °C; 0.2 μL of goat anti-rabbit IgG H&L (Alexa Fluor® 488) (ab150077, Abcam) (1:500) or 0.2 μL of goat anti-mouse IgG (Alexa Fluor® 488) (H+L, Life Technologies) (1:500) were then added for P-eIF2α or T-eIF2α analyses respectively, and incubated for 1 h in darkness. Cells were washed with 2% FACS Buffer and the fluorescence was measured by flow cytometry, as mentioned before.

Calreticulin, HSP70, HSP90 and CD47 exposure analyses
For this, 5×10^4 cells were seeded in 24-well plates and treated with ICRP CC_{50}, EPI CC_{50} or CPA CC_{50} for 24 h. Cells were detached, washed and incubated for 1 h at 25 °C with 2 μg/mL Calreticulin-antibody (FMC-75, Enzo Life Science), 0.8 μg/mL HSP70-antibody (F-3, Santa Cruz Biotechnology), 0.8 μg/mL HSP90-antibody (F-8, Santa Cruz Biotechnology), 3 μg/mL CD47 human-antibody (B6H12, Santa Cruz Biotechnology) or 3 μg/mL CD47 mouse-antibody (MIAP301, Santa Cruz Biotechnology), in 2% FACS buffer, cells were washed and incubated for 30 min in darkness at 25 °C with goat anti-mouse IgG (Alexa Fluor 488) (H+L, Life Technologies) (1:1500) or anti-rat IgG (Alexa Fluor 488) (H+L, Life Technologies) (1:1500) in 2% FACS buffer, cells were then washed, suspended in 2% FACS buffer with 7-AAD (Life Technologies)

95

The bovine dialysable leukocyte extract IMMUNEPOTENT CRP induces...
A. Reyes-Ruiz et al.

1400

(1:1000) or Fixable viability stain 780 (BD Biosciences) (1:1000) and incubated protected from light for 10 min at 25 °C. The surface exposure of CRT, HSP70, HSP90 and CD47 was determined by flow cytometry among viable (7-AAD-negative or Fixable viability stain 780-negative) cells.

ATP release assay
Supernatants of ICRP, EPI or CPA CC_{50}-treated cells (2×10^5) were used to assess extracellular ATP by a luciferase assay (ENLITEN kit, Promega, Madison, WI), following the manufacturer's instructions. Bioluminescence was determined in a Synergy HT microplate reader, using the Software Gen5 (BioTek, Winooski, VT) at 560 nm.

High-mobility group box 1 release assay
For this assay, 2×10^5 cells were treated with ICRP or EPI CC_{50} for 24 h or 48 h. Supernatants were used to assess extracellular HMGB1 using the HMGB1 BioAssay ELISA Kit (Human) for MCF-7 and MDA-MB-231 cells (US Biological Life Science, Salem, MA), and the HMGB1 BioAssay ELISA Kit (Mouse) for 4T1 cells (US Biological Life Science), following the manufacturer's instructions, in a spectrophotometer at a wavelength of 450 nm.

Generation of mouse BMDCs
To obtain bone marrow-derived dendritic cells (BMDCs), seven-to-eight-week-old BALB/c mice were anaesthetised with an intraperitoneal injection of ketamine (80 mg/kg body weight) and xylazine (10 mg/kg body weight) and were euthanised by cervical dislocation ($n = 5$ mice). Bone marrow was removed from femur and tibia after mouse death by flushing into complete RPMI (Life Technologies), as previously described.[17] Eluted cells were cultured at 37 °C in a controlled humidified atmosphere with 5% CO_2 for 5 days in complete RPMI and 20 ng/mL IL-4 and GM-CSF (R&D Systems, Minneapolis, MN), until approximately 50% of cells were CD11c+.

T-cell isolation
Seven-to-eight-week-old BALB/c mice were anaesthetised as mentioned above. Blood was obtained by cardiac puncture, and then cervical dislocation was performed. Peripheral blood mononuclear cell (PBMC) isolation was performed by density-gradient centrifugation, using Ficoll-Hypaque-1119 (MERCK). CD3+ cells were isolated from total PBMCs by positive selection using magnetic-activated cell sorting microbead technology with anti-CD3+-biotin and anti-biotin microbeads (Miltenyi Biotec, Bergisch Gladbach, Germany), following the manufacturer's instructions. Primary murine CD3+ cells were maintained in complete RPMI and incubated at 37 °C in a controlled humidified atmosphere with 5% CO_2.

Killed cancer cell (KCC) obtention
For the obtention of 4T1 killed cancer cells (KCC), we treated 4T1 cells with CC_{100} of ICRP (0.5 U/mL, ICRP-KCC), CC_{100} of EPI (10 μM, EPI-KCC) or CC_{100} of CPA (35 mM, CPA-KCC), and the dead cells obtained were then washed and detached; cell death (>90%) was confirmed using trypan blue staining and flow cytometry.

ICRP-KCC-mediated BMDC maturation
BMDCs were suspended in complete RPMI at a concentration of 1×10^6 cells/mL and stimulated with ICRP-killed cancer cells (ICRP-KCC) (3×10^6 cells/mL at a ratio of 1:3 BMDCs to ICRP-treated 4T1 cells (BMDC-ICRP-KCC)). Control BMDCs were left untreated or stimulated with 1 μg/mL lipopolysaccharide (LPS) (MERCK). After 24 h, culture supernatants were removed and stored at −80 °C to analyse TNF-α release by flow cytometry (BD CBA Mouse Th1/Th2 Cytokine Kit, BD Biosciences, San Jose, CA), and wells were washed twice with PBS before the next co-culture (with the addition of T lymphocytes). Additionally, some BMDC-Control and BMDC-ICRP-KCC wells were collected to analyse DC marker expression.

DC marker expression
For this assay, 1×10^5 BMDCs were suspended in 100 μL of 2% FACS buffer, and maturation was analysed by immunostaining using anti-CD11c-Alexa Fluor 488 (R&D Systems), anti-CD80-FITC and anti-CD86-APC (BD Biosciences) at 25 °C for 30 min, and washed twice with PBS. Cell surface markers were evaluated by flow cytometry, as mentioned above.

BMDC T-lymphocyte co-culture
BMDC-Control or BMDC-ICRP-KCC were maintained in complete RPMI at a concentration of 1×10^6 cells/mL. Allogeneic BALB/c mCD3+ cells were then added to each well at 3×10^6 cells/mL (at a ratio of 1:3 DCs to CD3+ cells), and incubated for 96 h at 5% CO_2 and 37 °C. Supernatants were then removed, stored at −80 °C to further analyse TNF-α, IFN-γ, IL-4 and IL-5 levels by flow cytometry (BD CBA Mouse Th1/Th2 Cytokine Kit, BD Biosciences), and lymphocytes were washed with PBS, and suspended in complete RPMI to be used in the next co-culture (T lymphocytes with cancer cells).

T lymphocyte–4T1 cell co-culture
Viable 4T1 cells were seeded at a concentration of 1×10^5 cells/mL. Cells were then stained with 0.1 μL/mL of calcein-AM (BD Biosciences) for 30 min and washed twice with PBS. Next, unprimed (previously co-cultured with BMDC-Control) or primed (previously co-cultured with BMDC-ICRP-KCC) allogeneic BALB/c CD3+ cells were added to each well at 5×10^5 cells/mL (at a ratio of 1:5 cancer cells to CD3+ cells); 4T1–T-lymphocyte co-culture was incubated at 37 °C and 5% CO_2 for 24 h. Supernatants were removed and stored at −80 °C to further analyse IFN-γ, IL-4 and IL-5 levels, as mentioned above. Cancer cells were then washed and detached to analyse 4T1-calcein-negative cells by flow cytometry, as described above.

Prophylactic vaccination
For this, 4T1 cells were treated with 0.5 U/mL ICRP, 10 μM EPI or 35 mM CPA for 24 h; cells were then washed, detached and cell death was confirmed using trypan blue staining and flow cytometry, as previously indicated to obtain the KCC. Seven-to-eight-week-old BALB/c mice were inoculated subcutaneously (s.c.) with 1.5×10^6 ICRP-killed 4T1 cells (ICRP-KCC, $n = 10$ mice), 1.5×10^6 EPI-killed 4T1 cells (EPI-KCC, $n = 10$ mice), 1.5×10^6 CPA-killed 4T1 cells (CPA-KCC, $n = 10$ mice) or with PBS ($n = 10$ mice) on the left flank side. On day 7 after vaccination, the mice were challenged s.c. on the opposite flank with 5×10^5 viable 4T1 cells.

Tumour volume measurements
Tumour volume was measured three times a week, using a calliper (Digimatic Calliper Mitutoyo Corporation, Japan), this was determined with the following formula: tumour volume (mm^3) $= 4 \div 3 * A$ (length) $* B$ (width) $* C$ (height). When the tumour reached the parameters that confine mouse pain and distress, or mice presented two or more parameters of pain and distress, as postulated by the Institutional Animal Research and Welfare Ethics Committee (CEIBA), mice were anaesthetised as described above and were euthanised by cervical dislocation.

Long-term memory assays
Mice in complete remission after ICRP-KCC prophylactic vaccination were rechallenged with 5×10^5 viable 4T1 cells in 100 μL of PBS into the opposite flank ($n = 9$ mice), and naive mice were used as control ($n = 9$ mice). Tumour volume and mice survival were evaluated, as described above.

Additionally, 3 days after tumour rechallenge, tissues from tumour-draining lymph nodes (TDLN) and tumour re-challenge sites were obtained from naive and ICRP-KCC mice, and fixed in 3.7% neutral formalin, embedded in paraffin, sectioned (5-μm thickness) and stained with H&E (MERCK). Histopathological

analyses were done by an external veterinarian pathologist (National professional certificate 2593012). Blood was obtained by cardiac puncture from anaesthetised mice as described above, and PBMC isolation was performed by density-gradient centrifugation, using Ficoll-Hypaque-1119 (MERCK). Cells from tumour rechallenge site, TDLN and spleen were isolated using 70-μm cell strainers (MERCK) and suspended in 2% FACS buffer. PBMCs, TDLN cells and tumour rechallenge site cells were stained with Mouse T lymphocyte antibody cocktail: PE-Cy7 CD3e, PE CD4 and FITC CD8 (BD Pharmingen) following the manufacturer's instructions. Maturation of DCs was analysed by immunostaining of cells from lymph nodes using anti-CD11c-Alexafluor 488 (R&D Systems), and anti-CD86-APC (BD Biosciences) at 25 °C for 30 min and washed twice with PBS. Cell surface markers were evaluated by flow cytometry, as mentioned above. Viable 4T1 cells were seeded at a concentration of 1×10^5 cells/mL, stained with 0.1 μL/mL of calcein-AM (BD Biosciences) for 30 min and washed twice with PBS. Next, splenocytes from naive or ICRP-KCC mice were added to each well at 40×10^5 cells/mL (at a ratio of 1:40 cancer cells to splenocytes); 4T1-splenocyte co-culture was incubated at 37 °C and 5% CO_2 for 24 h. Supernatants were removed and stored at −80 °C to further analyse IFN-γ, TNF-α, IL-2, IL-4 and IL-5 levels, as mentioned above. Cancer cells were then washed and detached to analyse 4T1-calcein-negative cells by flow cytometry, as described above ($n = 6$ mice per group).

Statistical analysis

Data were analysed using GraphPad Prism Software (GraphPad Software Inc., San Diego, CA) and shown as mean ± SD of triplicates from three independent experiments. For in vitro studies, statistical analyses were done using paired Student's t-test, and for in vivo and ex vivo studies, Mann–Whitney tests and two-tailed unpaired Student's t-tests were performed.

RESULTS

IMMUNEPOTENT CRP induces loss of mitochondrial membrane potential, pro-survival autophagosome formation and ROS-dependent cell death in MCF-7, MDA-MB-231 and 4T1 cells

ICRP induced cell death in all cell lines, in a concentration-dependent manner, as shown in Fig. 1a. Cell death in 30% of the cells (CC_{30}) was reached at 1 U/mL in MCF-7 and MDA-MB-231, and 0.1 U/mL in 4T1 cells. CC_{50} by ICRP was caused at 1.25 U/mL in MCF-7 and MDA-MB-231 cells, and 0.15 U/mL in 4T1 cells, whereas CC_{80} was induced at 1.5 U/mL in human breast cancer cells, and 0.2 U/mL in 4T1 cells, CC_{100} was reached at 2 U/mL in MCF-7 and MDA-MB-231, and 0.5 U/mL in 4T1 cells, where we observed more than 90% of cell death (Fig. 1a). The ICRP-killed 4T1 cells (ICRP-KCC) were generated with this CC_{100}. Loss of mitochondrial membrane potential was induced in 55–65% of MCF-7, MDA-MB-231 and 4T1 cells treated with ICRP CC_{50} for 24 h (Fig. 1b), also, this treatment generated an increase of ROS levels in 45–55% of MCF-7, MDA-MB-231 and 4T1 cells (Fig. 1c). Moreover, we observed autophagosome formation in 40–55% of MCF-7, MDA-MB-231 and 4T1 cells assessed by flow cytometry (Fig. 1d). This autophagosome formation was confirmed by fluorescence microscopy (Fig. 1e), which was inhibited in the presence of the autophagy inhibitor Sp-1 (Supplementary Fig. 1A). In addition, p62 downregulation was induced in MCF-7, MDA-MB-231 and 4T1 cells treated with ICRP CC_{50} for 24 h (Supplementary Fig. 1B).

The ROS scavenger NAC significantly inhibited ICRP-induced cell death, whereas the autophagy inhibitor Sp-1 significantly potentiated ICRP-mediated cell death (Fig. 1f). No significant changes were observed with the necroptosis inhibitor NEC-1 in MCF-7, MDA-MB-231 and 4T1 cells (Fig. 1f). Additionally, the caspase inhibitor QVD significantly potentiated ICRP-mediated cell death in MDA-MB-231 and 4T1 cells, whereas no significant changes were observed in MCF-7 cells (Fig. 1f).

IMMUNEPOTENT CRP causes eIF2α phosphorylation and DAMP emission in MCF-7, MDA-MB-231 and 4T1 cells

ICRP induced P-eIF2α in 40–60% of all cell lines treated with ICRP CC_{50} for 18 h; similar results were found when cells were treated with 1 μM Thaps for 2 h (Fig. 2a); importantly, no changes in total eIF2α expression (T-eIF2α) were found after treatments (Supplementary Fig. 2).

In addition, ICRP CC_{50} treatment for 24 h induced 3.73 ± 0.83-, 3.07 ± 0.97- and 3.20 ± 0.59-fold CRT exposure (Fig. 2b), 2.61 ± 0.82-, 1.63 ± 0.24- and 6.51 ± 1.74-fold HSP70 exposure (Fig. 2c), 2.55 ± 0.26-, 1.93 ± 0.31- and 6.23 ± 1.35-fold HSP90 exposure (Fig. 2d) and 135 ± 31.38-, 140.99 ± 50.38- and 7.30 ± 3.92-fold ATP release (Fig. 2e) in MCF-7, MDA-MB-231 and 4T1 cells, respectively, when compared with untreated cells. ICRP-treated cells also presented a decrease in CD47 exposure of 0.66 ± 0.21-, 0.79 ± 0.07- and 0.49 ± 0.17-fold in MCF-7, MDA-MB-231 and 4T1 cells, respectively, as compared with untreated control (Supplementary Fig. 3). Additionally, EPI CC_{50} treatment for 24 h induced 6.61 ± 1.61-, 2.69 ± 0.33- and 1.46 ± 0.20-fold CRT exposure (Fig. 2b), 3.41 ± 0.64-, 2.56 ± 0.45- and 1.66 ± 0.19-fold HSP70 exposure (Fig. 2c), 6.24 ± 0.28-, 2.98 ± 0.69- and 2.29 ± 0.95-fold HSP90 exposure (Fig. 2d) and 2.02 ± 0.92-, 12.61 ± 1.47- and 3.07 ± 0.66-fold ATP release (Fig. 2e) in MCF-7, MDA-MB-231 and 4T1 cells, respectively, in contrast with untreated cells.

Our results also revealed that ICRP CC_{50} treatment for 24 h induced 1.58 ± 0.07-, 1.65 ± 0.25- and 1.34 ± 0.28-fold HMGB1 release, and the same treatment for 48 h triggered 5.32 ± 0.83-, 4.94 ± 1.14- and 1.49 ± 0.04-fold HMGB1 release in MCF-7, MDA-MB-231 and 4T1 cells, respectively, as compared with untreated cells. Finally, EPI CC_{50} treatment for 24 h caused 7.51 ± 1.12-, 2.66 ± 0.61- and 1.13 ± 0.11-fold HMGB1 release, and this treatment for 48 h provoked 7.55 ± 0.89-, 2.87 ± 0.61- and 1.29 ± 0.08-fold HMGB1 release in MCF-7, MDA-MB-231 and 4T1 cells, respectively, in contrast with untreated cells (Fig. 2f).

Interestingly, CPA CC_{50} treatment for 24 h only induced significative DAMP emission in MCF-7 cells, but not MDA-MB-231 and 4T1 cells (Supplementary. Fig. 4)

Dead tumour cells obtained after ICRP treatment induce maturation of BMDCs

After determining that the principal biochemical characteristics of immunogenic cell death were evoked after ICRP treatment, we evaluated the capacity of the dead cells (obtained after ICRP (CC_{100}) treatment, ICRP-KCC) to mature BMDCs. As observed in Fig. 3a, b, the exposure of BMDCs to ICRP-KCC (BMDC-ICRP-KCC) significantly increased the expression of CD80 (57%), and CD86 (65%), whereas it maintained CD11c expression (48%), in comparison with unstimulated BMDCs (C80: 44%, CD86: 45% and CD11c: 49%). These results resemble the ones observed by our positive control, LPS, which significantly incremented CD80 (56%) and CD86 expression (70%), and also maintained CD11c expression (48%) in these cells. Furthermore, a significant increase in TNF-α release was observed in BMDCs stimulated with ICRP-KCC (760.68 ± 209.84 pg/mL) or LPS (7763.41 ± 1158.50 pg/mL), in comparison with unstimulated BMDCs (52.72 ± 1.66 pg/mL) (Fig. 3c). Thus, ICRP-KCC induced BMDC maturation.

Mature BMDCs exposed to ICRP-tumour cell lysate trigger anticancer immune responses

After the evaluation of ICRP-KCC-mediated BMDC maturation, the next step was to investigate if these mature cells could induce T-cell priming. Figure 3d, e shows a significant increase of TNF-α (380 ± 139.48 pg/mL) and IFN-γ (650.37 ± 12.86 pg/mL) release in the co-culture of BMDC-ICRP-KCC and T-cells, in contrast to the co-culture of BMDC-Control and T cells (TNF-α: 95.89 ± 71.63 pg/mL and IFN-γ: 185.67 ± 75.09 pg/mL). No significant differences were detected in TH-2 cytokines, IL-4 and IL-5 release (Supplementary. Table 1). Primed T cells obtained after co-culture with BMDC-ICRP-KCC caused a cytotoxic effect in up to 70% of 4T1 cells, whereas

The bovine dialysable leukocyte extract IMMUNEPOTENT CRP induces...
A. Reyes-Ruiz et al.

1402

the cytotoxicity induced by unprimed T cells was up to 19% of cancer cells; no cytotoxicity was detected in 4T1 cells without T cells (Fig. 3f and Supplementary. Fig. 5). In addition, a significant increase in IFN-γ release was observed in the co-culture of primed T cells with 4T1 cancer cells (192.29 ± 96.54 pg/mL), in comparison with the co-culture of unprimed T cells with 4T1 cells (8.44 ± 4.55 pg/mL) (Fig. 3g). No significant differences were detected in TH-2 cytokines, IL-4 and IL-5 release (Supplementary Table 1). These

data confirm the efficient antigen presentation by BMDC-ICRP-KCC to T cells and the immunocompetence of these T cells against 4T1 cells.

Prophylactic vaccination with ICRP-KCC prevents tumour establishment in BALB/c mice

In order to test the ability of ICRP-KCC to activate adaptive immune system in vivo, we performed a well-established

98

Fig. 1 IMMUNEPOTENT CRP induces loss of mitochondrial membrane potential, pro-survival autophagosome formation and ROS-dependent cell death in MCF-7, MDA-MB-231 and 4T1 cells. a Representative dot plots (left) and quantifications (right) of cell death measured by flow cytometry through Annexin-V and PI staining in MCF-7, MDA-MB-231 and 4T1 cells treated with different concentrations of ICRP for 24 h. **b–d** Quantifications of loss of mitochondrial membrane potential evaluated through TMRE staining (**b**) ROS levels assessed through DCFDA staining (**c**) or autophagosome formation measured through Green Detection Reagent staining (**d**) by flow cytometry in the absence (control, shown in white bar) or presence (shown in black bar) of ICRP CC_{50} for 24 h in MCF-7, MDA-MB-231 and 4T1 cells. **e** Representative immunofluorescence images of CYTO-ID staining in MCF-7, MDA-MB-231 and 4T1 cells left untreated (control) or treated with ICRP CC_{50} for 24 h. Nuclei were counterstained in blue with Hoechst 33342 dye. **f** Quantification of cell death (Annexin V−, PI+, Annexin V+, PI +, Annexin V+ and PI−) measured by flow cytometry through Annexin-V and PI staining in MCF-7, MDA-MB-231 and 4T1 cells in the absence (control, shown in white bar) or presence (shown in black bar) of ICRP CC_{50} for 24 h without co-treatment (−) or co-treated with N-acetyl cystein (NAC), QVD-OPH (QVD), Necrostatin-1 (NEC-1) or Spautin-1 (SP-1). The means (±SD) of triplicates of at least three independent experiments were graphed.

prophylactic tumour vaccination model in immunocompetent BALB/c mice[4,18] (Fig. 4). All unvaccinated (PBS) mice reached a correct tumour establishment on the challenge site (Fig. 4a), while immunisation of mice with ICRP-KCC prevented tumour growth at the challenge site in nine out of ten mice (Fig. 4b). Additionally, vaccinated mice with EPI-KCC induced tumour regression in 7/10 mice (Fig. 4c), while vaccination with CPA-KCC induced tumour regression at the challenge site in only 2/10 mice (Fig. 4d). These data confirmed that ICRP-KCC induced a potent immune response in vivo, reflected in 90% (9/10) of 60-day survival rates of mice in the ICRP-KCC group, whereas EPI induced 70% (7/10) 60-day survival, CPA induced 20% (2/10) survival and all PBS mice were euthanised by day 20 (10/10) (Fig. 4e).

Prophylactic vaccination with ICRP-KCC induces long-term antitumour memory in BALB/c mice
To investigate the effect of ICRP-KCC on the memory response in vivo, tumour-free mice that survived 150 days from a previous prophylactic vaccination with ICRP-KCC were rechallenged with viable 4T1 cancer cells, naive mice challenged with viable 4T1 cancer cells were used as control (Fig. 5a). The results show that tumour growth was prevented in rechallenged mice, while continuous tumour growth was observed in naive mice, challenged for the first time (Fig. 5b). This reflected in 100% (9/9) of survival in ICRP-KCC rechallenged mice, while naive mice perished by day 15 (9/9) (Fig. 5c). These results strongly suggest the stimulation of long-term antitumour immune memory by ICRP-KCC prophylactic vaccination.

To better characterise this immune response, we assessed tumour establishment, DC maturation, T-cell distribution and splenocyte–tumour-specific cytotoxicity after three days of tumour challenge (naive mice)/rechallenge (ICRP-KCC) (Supplementary Fig. 6). Histopathological analyses of tumour-draining lymph nodes showed a diffuse lymphoid hyperplasia in naive mice, whereas ICRP-KCC mice present a follicular lymphoid hyperplasia, indicating a modulated response associated with immunological memory (Fig. 5d). Due to these differences, we next evaluated the proportion of mature dendritic cells in tumour-draining lymph nodes. The results indicated that rechallenged ICRP-KCC group did not show significant difference in the percentage of DCs, but a higher proportion of mature DCs (CD11c+CD86+) were present when compared with challenged naive mice (Fig. 5e); on the other hand, studies of T-cell proportion in TDLNs revealed no differences in total CD3+ cells, a significant decrease of CD4+ T cells and an increase of CD8+ T cells in ICRP-KCC mice, when compared with naive mice (Fig. 5f).

Then, we assessed the proportion of T cells in peripheral blood, and no differences were detected in total CD3+ cells, while a significant decrease of CD4+ T cells and an increase of CD8+ T cells was observed in ICRP-KCC mice in contrast with naive mice (Fig. 5g).

Moreover, histopathological analyses of the tumour rechallenge site reveal that naive mice presented tumour establishment with an extensive infiltration of neoplastic cells in the striated muscle tissue and these cells demonstrated an intense mitotic

activity (Fig. 5h left). On the other hand, ICRP-KCC mice showed a discrete infiltration of neoplastic cells in the striated muscle tissue, observing a strong infiltration of lymphocytes and polymorphonuclear cells (Fig. 5h right). Additionally, we observed an increase in total CD3+ cells, a significant decrease in CD4+ T cells and a significant increase in CD8+ T cells in the tumour-rechallenged site of ICRP-KCC mice, when compared with naive mice (Fig. 5i). Furthermore, splenocytes from ICRP-KCC mice mediated a cytotoxic effect in 4T1 cells, inducing loss of cell viability in up to 50% of cancer cells, whereas no significant cytotoxic effect was detected in 4T1 cells co-cultured with splenocytes from naive mice (Fig. 5j and Supplementary. Fig. 7), indicating a tumour-specific cytotoxicity. Finally, a significant increase in IFN-γ (95.05 ± 40.01 pg/mL), TNF-α (4239.85 ± 784.34 pg/mL) and IL-2 (20.97 ± 0.68 pg/mL) release was observed in the co-culture of 4T1 cells with splenocytes from ICRP-KCC mice, in comparison with the co-culture of 4T1 cells with splenocytes from naive mice (IFN-γ: 27.66 ± 15.12 pg/mL, TNF-α: 3310.46 ± 422.46 pg/mL and IL-2: 10.69 ± 2.94 pg/mL) (Fig. 5k), and no significant differences were detected in TH-2 cytokines, IL-4 and IL-5 release (Supplementary Table 2).

DISCUSSION
IMMUNEPOTENT CRP is a promising immunotherapy that induces regulated cell death in cancer cells. In T-acute lymphoblastic leukaemia (T-ALLL) cells (Molt-4 and CEM), ICRP provokes ROS-dependent apoptosis accompanied by mitochondrial and nuclear alterations.[11] On the other hand, in cell lines from cervical (HeLa and SiHa cells) and lung cancer (A529 cells), ICRP induces non-apoptotic cell death (caspase-independent) that relies on ROS production, involving cell cycle arrest and loss of mitochondrial membrane potential.[9,10,13] In this work, we demonstrated that ICRP caused caspase- and necrosome-independent regulated cell death that relies on ROS production in MCF-7, MDA-MB-231 and 4T1 cells, suggesting a conserved mechanism of action in solid tumours, and with some shared characteristics in all the cell lines tested to this day. Other treatments also induce different cell death mechanisms, being specific for the type of cancer cell line tested with shared characteristics in the cytotoxic pathway.[19,20] In addition, no differences in cell death were observed in NEC-1 co-treated cells, which indicates that ICRP-mediated regulated cell death is different from necroptosis.

Moreover, inhibition of autophagy significantly potentiated ICRP-induced cell death, suggesting that ICRP induces pro-survival autophagosome formation in MDA-MB-231 and 4T1 cells, corresponding with our previous reports in MCF-7.[13] The induction of autophagy as a protective mechanism in cancer cells has also been demonstrated with other cancer treatments, including chemotherapy and radiation.[21] Furthermore, inhibition of caspases also resulted in a significant augmentation of ICRP-mediated cell death in MDA-MB-231 cells and 4T1 cells, but not MCF-7 cells. These results could be related with the "Phoenix Rising" pathway of cell death-induced tumour repopulation, in which caspase 3 plays key roles that have been demonstrated in 4T1 and MDA-MB-
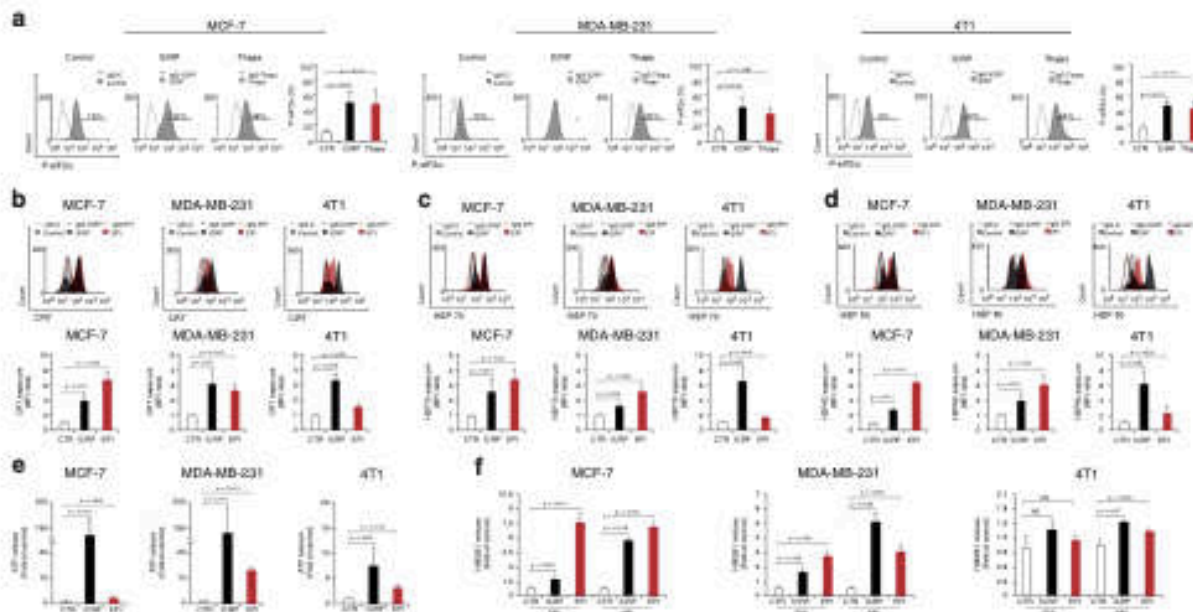
Fig. 2 IMMUNEPOTENT CRP causes eIF2α phosphorylation and DAMP emission in MCF-7, MDA-MB-231 and 4T1 cells. a Representative FACS histograms of P-eIF2α staining (in grey) and IgG isotype antibodies (dotted) of cancer cells left untreated (negative control) or treated with ICRP CC_{50} for 18 h or 1 μM Thaps for 2 h (positive control). Charts are the quantification of P-eIF2α staining in controls and cancer cells treated with ICRP or Thaps. **b–d** Representative FACS histograms of CRT (**b**), HSP70 (**c**) or HSP90 (**d**) exposure (filled histograms) and IgG isotype antibodies (open histograms) of cancer cells left untreated (negative control in grey) or treated with ICRP CC_{50} (in black), or EPI CC_{50} (positive control in red) for 24 h. Charts are the quantification of CRT (**b**), HSP70 (**c**) or HSP90 (**d**) exposure in cancer cells left untreated or treated with ICRP CC_{50} or EPI CC_{50} for 24 h. **e** Quantification of ATP release through bioluminescence detection in the supernatants of cancer cells in the absence (negative control) or presence of ICRP CC_{50} or EPI CC_{50} for 24 h. **f** Quantification of HMGB1 release assessed by ELISA in the supernatants of cancer cells in the absence (negative control) or presence of ICRP CC_{50} or EPI CC_{50} for 24 h and 48 h. Graphs represent the means (±SD) of triplicates of at least three independent experiments.

231 cells, and confirmed using MCF-7 cells, which are deficient in caspase 3 expression.[22]

Additionally, ICRP induced P-eIF2α (ER stress biomarker) in the three cell lines. The capacity of many agents to induce ICD relies on their ability to trigger ROS production and ER stress, being these two cellular processes essential components that initiate the intracellular danger signalling pathways that dictate ICD.[23,24]

ER stress response and ROS production have been associated with the induction of autophagy.[24,25] As we mentioned before, in this study, we proved that ICRP caused autophagosome formation in MCF-7, MDA-MB-231 and 4T1 cells, corresponding with the decrease in p62 levels observed after ICRP treatment, as p62 is itself degraded, when autophagy is induced.[26] The induction of ROS production, ER stress and autophagy has been observed in other studies, for instance, Shikonin induces cell death and pro-survival autophagy in human melanoma cells via ROS-mediated ER stress.[27] Furthermore, radiotherapy causes ROS generation, DNA damage, ER stress and autophagy in cancer cells.[28] The increase in ROS, ER stress and autophagy has been associated with cancer therapies that are classified as ICD inducers.[29,30]

P-eIF2α regularly antecedes chaperone protein exposure in the course of ICD; nonetheless, P-eIF2α is not necessarily followed by CRT exposure, particularly when the ER stress response re-establishes cell homoeostasis;[24,31] for this reason, we decided to evaluate P-eIF2α after 18 h of treatment, and surface-exposed chaperones after 24 h of treatment with ICRP. Here, we demonstrated that ICRP induced P-eIF2α and increased the "eat me signals" CRT, HSP70 and HSP90 on breast cancer cell surface, and also decreased the surface-associated "don't eat me" signal CD47. This constellation of surface signals then acts on phagocytic receptors of immune cells facilitating cellular engulfment.[32] The increased exposure of CRT, HSP70 and HSP90 proteins on cell surface was also observed after EPI treatment, a well-known inducer of ICD in breast cancer cells,[33] used here as positive control.

Higher levels of ATP release were observed after ICRP and EPI treatment in MCF-7 and MDA-MB-231 cells in comparison with 4T1 cells, this corresponds with previous studies in which it has been demonstrated that 4T1 is a p53-deficient cell line[34] and ATP is produced at higher levels using oxidative phosphorylation in cells expressing p53 versus cells lacking p53.[35] Besides, ICRP and EPI treatments triggered significant HMGB1 release in MCF-7 and MDA-MB-231, but partial HMGB1 release in 4T1 cells. This low ICRP-mediated HMGB1 release could be due to the exposure of cells to ICRP CC_{50} treatment, which was not sufficient for a significant release of HMGB1, as some agents induce the release of HMGB1 at CC_{100} but not CC_{50}.[36] Furthermore, as HMGB1 release has been observed at late times in the course of ICD,[37] we evaluated this parameter at 48 h, and we found a significant HMGB1 release after ICRP and EPI treatment on the three cell lines.

Another drug classified as ICD inducer is the alkylating agent CPA;[38,39] controversially, in our hands, this drug only triggered DAMP emission in MCF-7 cells but not in triple-negative MDA-MB-231 and 4T1 cells, this could be due to the fact that alkylating agents can induce NRF2 activation that blocks ER stress,[40] one of the principal parameters related to ICD.

DAMP emission induced by ICRP was also observed in MCF-7 cells, which are deficient in caspase 3 expression, suggesting that these processes do not require caspase 3 activation to take place. Although caspase activation plays a key role during DAMP emission and the immunogenicity of the cell death induced by several cancer treatments,[23,41,42] it has also been observed that a DAMP emission can be triggered in a caspase-independent fashion, for instance, Hyp-PDT-induced CRT exposure is caspase-
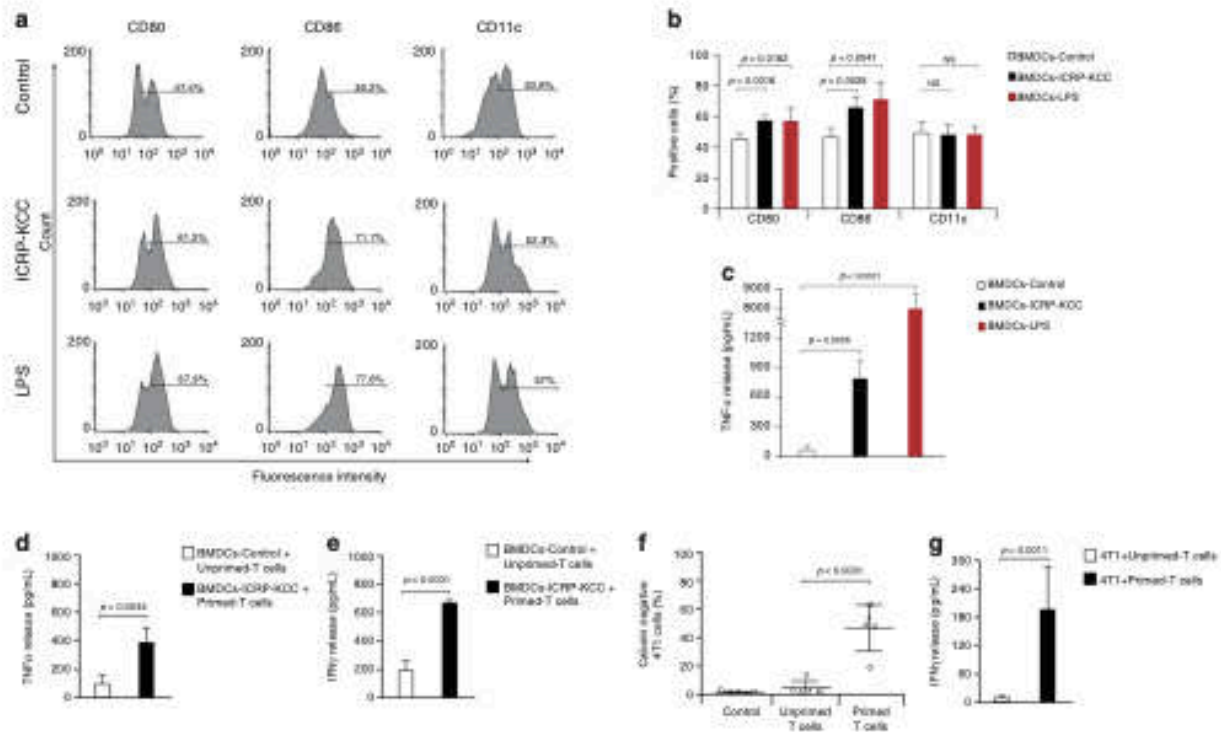
Fig. 3 ICRP-KCC triggers BMDC maturation and anticancer immune response. a Representative flow cytometry histograms showing the percentage of CD80+, CD86+ and CD11c+ BMDCs unstimulated (negative control), in co-culture ratio 1:3 with ICRP-treated 4T1 cells (ICRP-KCC) or stimulated with 1 μg/mL of LPS (positive control) during 24 h. **b** BMDCs were treated as in (**a**) and the means (±SD) obtained of five independent experiments were graphed. **c** Quantification of TNF-α concentration in supernatants of BMDCs treated as in (**a**). **d, e** Concentration of TNF-α (**d**) and IFN-γ (**e**) in supernatants of unstimulated BMDCs (BMDC-Control) or stimulated with ICRP-KCC (BMDC-ICRP-KCC), in co-culture ratio 1:3 with T cells for 96 h, expressed as the means (±SD) of five independent experiments. **f** Percentage of calcein-negative 4T1 cells left alone (Control) or after co-culture with unprimed T lymphocytes (previously co-cultured with BMDC-Control) or primed T lymphocytes (previously co-cultured with BMDC-ICRP-KCC) for 24 h (co-culture ratio 1:5). **g** Quantification of IFN-γ concentration in supernatants of 4T1 cells treated as in (**f**), expressed as the means (±SD) of five independent experiments. n = 5 mice per group.

independent,[43] and chemotherapeutic agents can activate an alternative caspase-insensitive mechanism for secretion of ATP.[44]

Nevertheless, it has been demonstrated that the release/exposure of all DAMPs is not determinant for immunogenic cell death;[45] thus, we further evaluated ex vivo and in vivo the immunogenicity of the cell death induced by ICRP. Cancer-dying cells by ICD inducers promote DC maturation, which strongly activates anticancer immunity. According to current models, only few treatments induce intracellular signalling pathways that lead to a cancer cell death able to stimulate fully mature DCs, including cyclophosphamide,[46] γ-irradiation,[47] doxorubicin, oxaliplatin,[48] bortezomib[49] and a CD47 agonist peptide.[50] Other therapies are only speculated to induce complete DC maturation, or use LPS, IFN type 1 or other stimulants in combination with tumour cell lysates (TCL) to promote DC maturation.[29,46] In addition, some cancer treatments may cause semi-mature DCs, namely DCs that lack phenotypic maturation markers or cytokine release, and thereby are unable to efficiently prime T cells.[51] Here, we demonstrated that ICRP-KCC obtained from ICRP-mediated 4T1 cell death induced maturation of BMDCs, which triggers a specific anticancer immune response against 4T1 cancer cells.

Furthermore, with the prophylactic tumour vaccination model, we demonstrated that ICRP-KCC activates the adaptive immune system in 90% BALB/c mice, leading to a long-term antitumour memory, which is desirable in cancer patients dealing with cancer recurrence. Usually, ICD inducers protect from 50% to 90% of individuals when used alone, without any type of adjuvants; such is the case of Hypericin-based photodynamic therapy (87%),[43]

mitoxantrone (80%),[52] oxaliplatin (80%)[53] and nanosecond pulsed electric fields (50%).[54] Other treatments need two previous vaccinations to induce slower tumour growth in vaccinated mice[55] or the use of combinational therapy to reach protection in 80% of the cases.[56] Moreover, agents classified as ICD inducers have been studied using TCL-loaded dendritic cell vaccines, but not TCL, and after several vaccine boosting, they reach up to 70% of survival.[29]

To test the potential of ICRP to trigger ICD on breast cancer cells in contrast to other well-known ICD inducers, we compared ICRP treatment with EPI and CPA (two drugs classified as ICD inducers[33,38,39]) in prophylactic vaccination assays. We found that whereas EPI-KCC vaccination protected 70% of individuals, CPA-KCC vaccination only protected 20% of individuals. These results are consistent with the observation of higher DAMP emission triggered by ICRP as compared to EPI, and the absence of DAMP emission after CPA treatment in 4T1 cells. Our results highlight the importance of evaluating the immunogenicity of the cell death provoked by ICD inducers in different biochemical contexts, as the immune effect of ICD drugs, such as CPA, can differ between cancer models.

It is known that T-cell responses generally peak ~1–4 days after a second antigen stimulation.[57,58] Here, we analysed tumour-draining lymph nodes after three days of tumour rechallenge and observed a follicular lymphoid hyperplasia in ICRP-KCC mice, which is associated with immunological memory; additionally, we observed an increase of mature DCs in ICRP-KCC mice in comparison to the naive group. Several studies have demonstrated that effector

The bovine dialysable leukocyte extract IMMUNEPOTENT CRP induces...
A Reyes-Ruiz et al.

06
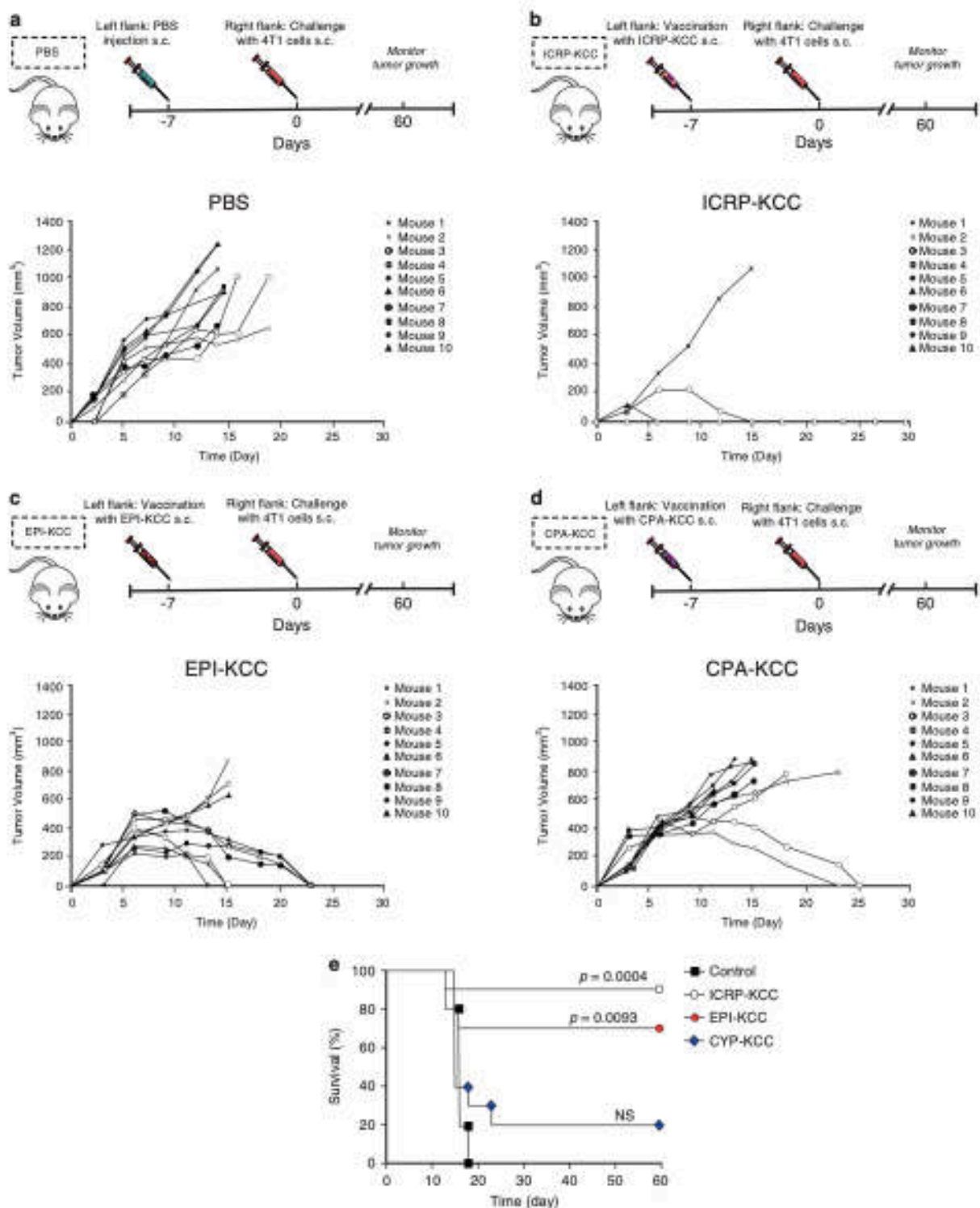
Fig. 4 Prophylactic vaccination with ICRP-KCC prevents tumour establishment in BALB/c mice. a–d Mice were inoculated s.c. with PBS, 1.5×10^6 ICRP-killed 4T1 cells (ICRP-KCC), 1.5×10^6 EPI-killed 4T1 cells (EPI-KCC) or 1.5×10^6 CPA-killed 4T1 cells (CPA-KCC) on the left flank side. On day 7 after vaccination, mice were challenged s.c. on the opposite flank with 5×10^5 viable 4T1 cells. Tumour growth on the challenge site was evaluated for up to 60 days after the challenge. Tumour volume on the challenge site of unvaccinated mice (PBS) (**a**) or vaccinated with ICRP-KCC (**b**), EPI-KCC (**c**) or CPA-KCC (**d**). Each line represents one mouse. **e** Kaplan–Meier graph with the percentage of survival in mice treated as in (**a–d**) (*n* = 10 mice per group).
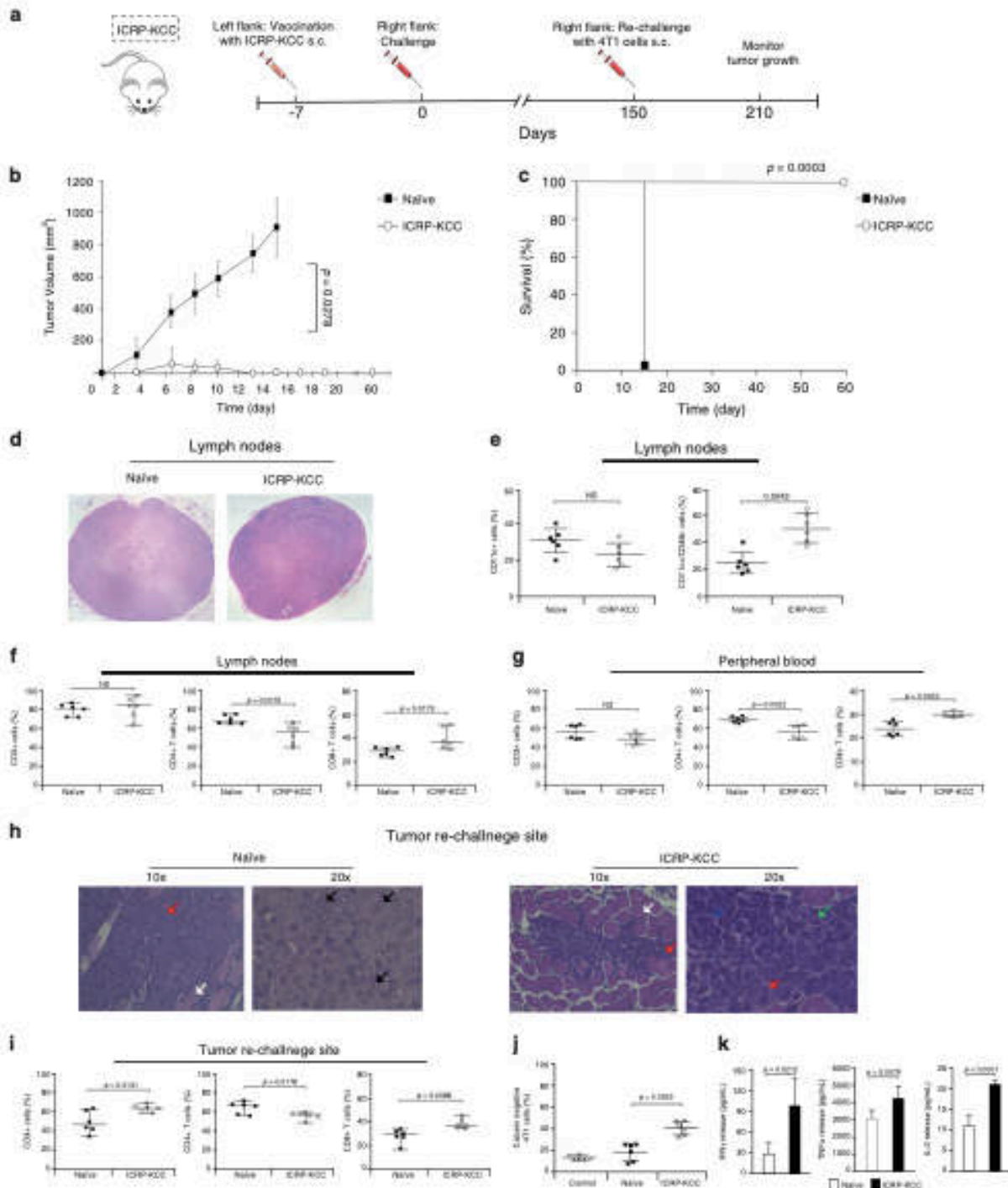
memory T cells potentiate the maturation of DCs, and in addition to T cells, BCR signalling is sufficient for memory B cells to induce complete activation of DCs.[59]

We also observed an increase of CD8+ T cells over CD4+ T cells in the TDLNs, peripheral blood and tumour rechallenge site of immunised mice; these results correspond with the observations that in the same host, memory assessments result in robust CD8+ T-cell responses, but poor boosting of CD4+ T-cell recall responses,[60] which is correlated with the demonstration that CD4+ memory cells proliferated for a shorter period of time than CD4+ naive cells because of their cytokine profile.[61]

Finally, we observed a tumour-specific cytotoxicity by splenocytes from immunised mice, whereas no cytotoxicity was observed in the co-culture of 4T1 with splenocytes from naive mice, indicating the activation of a rapid immune response triggered by the antitumour memory establishment. This

103

The bovine dialysable leukocyte extract IMMUNEPOTENT CRP induces...
A Reyes-Ruiz et al.

08

Fig. 5 ICRP-KCC prophylactic vaccination induces long-term antitumour memory, modulates tumour establishment, DC maturation, T-cell distribution and splenocyte–tumour-specific cytotoxicity after tumour rechallenge. a Mice in remission after ICRP-KCC prophylactic vaccination were rechallenged s.c. with 5×10^5 viable 4T1 cells after 150 days of prophylactic vaccination. Tumour growth on the challenge site was evaluated for up to 60 days after rechallenge. **b** Tumour volume on the challenge site of naive mice (black square, $n = 9$ mice) or mice in remission after a previous 1.5×10^6 ICRP-KCC vaccination (white circle, $n = 9$ mice). **c** Kaplan–Meier graph with the percentage of survival of mice treated as in (c). **d**, **k** Naive mice ($n = 6$) and mice in remission after ICRP-KCC prophylactic vaccination ($n = 6$) were challenged/rechallenged s.c. with 5×10^5 viable 4T1 cells. Three days later, tumour-draining lymph nodes, peripheral blood, the tumour rechallenge site and spleen were obtained. **d** Histology from lymph nodes of naive and ICRP-KCC mice stained with H&E. **e** Percentage of CD11c- and CD86-positive cells in TDLNs of naive and ICRP-KCC mice. **f**, **g** Proportion of CD3-, CD4- and CD8-positive cells in TDLNs (**f**) and peripheral blood (**g**) of naive and ICRP-KCC mice. **h** Histology from tumour rechallenge sites of naive and ICRP-KCC mice stained with H&E. Normal tissue (white arrows), tumour cells (red arrows), mitotic cells (black arrows), lymphocytes (blue arrows) and polymorphonuclear cells (green arrows). **i** Proportion of CD3-, CD4- and CD8-positive cells in tumour rechallenge sites of naive and ICRP-KCC mice. **j** Percentage of calcein-negative 4T1 cells left alone (Control), or co-cultured with splenocytes from naive or ICRP-KCC mice for 24 h (co-culture ratio 1:40). **k** Quantification of IFN-γ, TNF-α and IL-2 concentration in supernatants of co-cultures obtained as in (j), expressed as the means (±SD) of three independent experiments ($n = 6$ mice per group).
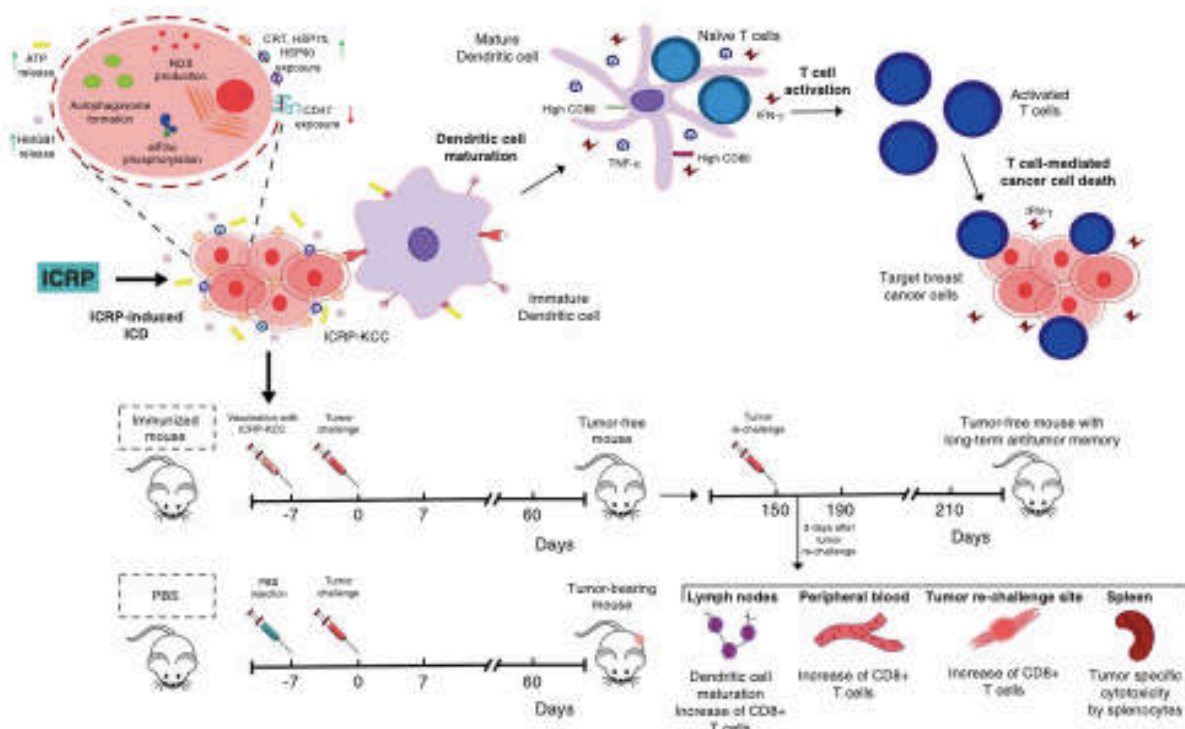
Fig. 6 Schematic depiction of IMMUNEPOTENT CRP-induced immunogenic cell death in breast cancer cells. IMMUNEPOTENT CRP induces ROS production, autophagosome formation and eIF2α phosphorylation in breast cancer cell lines leading to DAMP release. Neoantigens and the release of DAMPs promote DC maturation, which triggers T-cell activation to induce cancer cytotoxicity. Moreover, ICRP-KCC prophylactic vaccination prevented tumour establishment and induces long-term antitumour memory in BALB/c mice; this protection involves an increase of DC maturation in lymph nodes, CD8+ T cells in lymph nodes, peripheral blood and tumour rechallenge site, as well as tumour-specific cytotoxicity by splenocytes. ROS, reactive oxygen species; ER, endoplasmic reticulum; CRT, calreticulin; HSP70, 70-kDa heat shock protein; HSP90, 90-kDa heat shock protein; CD47, Cluster of Differentiation 47; HMGB1, high-mobility group box 1; ATP, adenosine triphosphate; TNF-α, tumour necrosis factor alpha; IFN-γ, interferon gamma.

evaluation corresponds with our ex vivo assessment where we observed an increase in Th1-type cytokines, which are associated with the generation of cytotoxic responses.[62]

The results in this work are supported by the recent demonstration that breast tumour-bearing mice treated with ICRP present a decrease in tumour volume and increase in survival in comparison with untreated mice.[61] Also, within the tumour, ICRP treatment decreased PD-L1, IDO and Gal-3 expression, IL-6, IL-10 and MCP-1 levels, and increased IFN-γ and IL-12 levels. Moreover, ICRP treatment increased CD8+ T cells, memory T cells and innate effector cells in peripheral blood, where an increase was also observed in IFN-γ and IL-12 levels,[63] indicating that these findings could be due to ICD induction in the tumour of these mice.

In conclusion, IMMUNEPOTENT CRP triggers loss of mitochondrial membrane potential, pro-survival autophagosome formation, eIF2α phosphorylation and caspase-independent but ROS-dependent cell death in breast cancer cells; these intracellular signalling pathways lead to alterations in the composition of the plasma membrane of dying cells (increased CRT, HSP70 and HSP90 exposure and decreased CD47 exposure), as well in their microenvironment (release of ATP and HMGB1), which stimulates DC maturation, priming of T cells, promoting an antitumour immune response ex vivo and in vivo and leading to a long-term antitumour memory (Fig. 6). Overall, our results show that ICRP may have the capacity to turn breast cancer cells into potential vaccines in vivo.

The bovine dialysable leukocyte extract IMMUNEPOTENT CRP induces...
A Reyes-Ruiz et al.

1

AUTHOR CONTRIBUTIONS
A.R.R. and K.M.R.C. designed and performed all the in vitro, ex vivo and in vivo experiments. K.M.C.R. established the ex vivo and in vivo models. A.C.M.T. directed, conceived and supervised the project. A.R.R. and A.C.M.T. wrote the paper with support of K.M.C.R, A.R.R, K.M.C.R and A.C.M.T. prepared the figures. A.R.R, K.M.C.R, A.C.M.T. and C.R.P. designed experiments, performed statistical analysis, analysed and interpreted data and read and approved the final paper.

ADDITIONAL INFORMATION
Ethics approval and consent to participate The Animal Research and Welfare Ethics Committee (CEIBA) of the School of Biological Sciences approved this study: CEIBA-2019/20-006. All experiments were conducted according to Mexican regulation NOM-062-ZOO-1999.

Consent to publish Not applicable.

Data availability The datasets that support the findings of this study are available from the corresponding author on reasonable request.

Competing interests The authors declare no competing interests.

Supplementary information is available for this paper at https://doi.org/10.1038/s41416-020-01256-y.

Publisher's note Springer Nature remains neutral with regard to jurisdictional claims in published maps and institutional affiliations.

REFERENCES
1. Siegel, R. L., Miller, K. D. & Jemal, A. Cancer statistics. *CA Cancer J. Clin.* **69**, 7–34 (2019).
2. Richman, J. & Dowsett, M. Beyond 5 years: enduring risk of recurrence in oestrogen receptor-positive breast cancer. *Nat. Rev. Clin. Oncol.* **16**, 296–311 (2019).
3. Pederzini, A. Immunotherapy in breast cancer. *Panminerva Med* **15**, 435–436 (1973).
4. Kroemer, G., Galluzzi, L., Kepp, O. & Zitvogel, L. Immunogenic cell death in cancer therapy. *Annu. Rev. Immunol.* **31**, 51–72 (2013).
5. Garg, A. D., More, S., Rufo, N., Mece, O., Sassano, M. L., Agostinis, P. et al. Trial watch: immunogenic cell death induction by anticancer chemotherapeutics. *OncoImmunology* https://doi.org/10.1080/2162402X.2017.1386829 (2017).
6. Galluzzi, L., Senovilla, L., Zitvogel, L. & Kroemer, G. The secret ally: immunostimulation by anticancer drugs. *Nat. Rev. Drug Discov.* **11**, 215–233 (2012).
7. Ladoire, S., Mignot, G., Dabakuyo, S., Arnould, L., Apetoh, L., Rébé, C. et al. In situ immune response after neoadjuvant chemotherapy for breast cancer predicts survival. *J. Pathol.* **224**, 389–400 (2011).
8. Franco-Molina, M. A., Mendoza-Gamboa, E., Zapata-Benavides, P., Castillo-Tello, P., Isaza-Brando, C. E., Zamora-Avila, D. et al. Antiangiogenic and antitumor effects of IMMUNEPOTENT CRP in murine melanoma. *Immunopharmacol. Immunotoxicol.* **32**, 637 646 (2010).
9. Martínez-Torres, A. C., Reyes-Ruiz, A., Benítez-Londoño, M., Franco-Molina, M. A. & Rodríguez-Padilla, C. IMMUNEPOTENT CRP induces cell cycle arrest and caspase-independent regulated cell death in HeLa cells through reactive oxygen species production. *BMC Cancer* **18**, 13 (2018).
10. Martínez-Torres, A. C., Gomez-Morales, L., Martinez-Loria, A. B., Uscanga-Palomeque, A. C., Vazquez-Guillen, J. M. & Rodríguez-Padilla, C. Cytotoxic activity of IMMUNEPOTENT CRP against non-small cell lung cancer cell lines. *PeerJ* **7**, e7759 (2019).
11. Lorenzo-Anota, H. Y., Martinez-Torres, A. C., Scott-Algara, D., Tamez-Guerra, R. S. & Rodríguez-Padilla, C. Bovine Dialyzable Leukocyte Extract IMMUNEPOTENT-CRP Induces Selective ROS-Dependent Apoptosis in T-Acute Lymphoblastic Leukemia Cell Lines. *J. Oncol.* https://doi.org/10.1155/2020/1598503 (2020).
12. Rodriguez-Salazar, M. D. C., Franco-Molina, M. A., Mendoza-Gamboa, E., Martinez-Torres, A. C., Zapata-Benavides, P., López-González, J. S. et al. The novel immunomodulator IMMUNEPOTENT CRP combined with chemotherapy agent increased the rate of immunogenic cell death and prevented melanoma growth. *Oncol. Lett.* **14**, 844–852 (2017).
13. Martinez-Torres, A. C., Reyes-Ruiz, A., Calvillo-Rodriguez, K. M., Alvarez-Valadez, K. M., Uscanga-Palomeque, A. C., Tamez-Guerra, R. S. et al. IMMUNEPOTENT CRP induces DAMPS release and ROS-dependent autophagosome formation in HeLa and MCF-7 cells. *BMC Cancer* **20**, 647 (2020).
14. Hou, W., Zhang, Q., Yan, Z., Chen, R., Zeh, H. J., Kang, R. et al. Strange attractors: DAMPs and autophagy link tumor cell death and immunity. *Cell Death Dis.* **4**, e966 (2013).
15. Zhang, Q., Kang, R., Zeh, H. J., Lotze, M. T. & Tang, D. DAMPs and autophagy: cellular adaptation to injury and unscheduled cell death. *Autophagy* **9**, 451–458 (2013).
16. Kilkenny, C., Browne, W. J., Cuthill, I. C., Emerson, M. & Altman, D. G. Improving bioscience research reporting: the arrive guidelines for reporting animal research. *PLoS Biol.* **8**, e1000412 (2010).
17. Meurer, S. K., Neß, M., Weiskirchen, S., Kim, P., Tag, C. G., Kauffmann, M. et al. Isolation of mature (Peritoneum-Derived) mast cells and immature (bone marrow-derived) mast cell precursors from mice. *PLoS ONE* **11**, e0158104 (2016).
18. Kepp, O., Tartour, E., Vitale, I., Vacchelli, E., Adjemian, S., Agostinis, P. et al. Consensus guidelines for the detection of immunogenic cell death. *OncoImmunology* **3**, 9 (2014).
19. Martinez-Torres, A. C., Zarate-Triviño, D. G., Lorenzo-Anota, H. Y., Ávila-Ávila, A., Rodriguez-Abrego, C. & Rodríguez-Padilla, C. Chitosan gold nanoparticles induce cell death in hela and MCF-7 cells through reactive oxygen species production. *Int. J. Nanomed.* **13**, 3235–3250 (2018).
20. Martinez-Torres, A. C., Lorenzo-Anota, H. Y., García-Juárez, Martin, G., Zarate-Triviño, D. G. & Rodríguez-Padilla, C. Chitosan gold nanoparticles induce different ROS-dependent cell death modalities in leukemic cells. *Int. J. Nanomed.* **14**, 7173–7190 (2019).
21. Das, C. K., Mandal, M. & Kögel, D. Pro-survival autophagy and cancer cell resistance to therapy. *Cancer Metastasis Rev.* **37**, 749–766 (2018).
22. Huang, Q., Li, F., Liu, X., Li, W., Shi, W., Liu, F. F. et al. Caspase 3-mediated stimulation of tumor cell repopulation during cancer radiotherapy. *Nat. Med* **17**, 860–866 (2011).
23. Krysko, D. V., Garg, A. D., Kaczmarek, A., Krysko, O., Agostinis, P. & Vandenabeele, P. Immunogenic cell death and DAMPs in cancer therapy. *Nat. Rev. Cancer* **12**, 860–875 (2012).
24. Kepp, O., Semeraro, M., Bravo-San Pedro, J. M., Bloy, N., Buqué, A., Huang, X. et al. EIF2α phosphorylation as a biomarker of immunogenic cell death. *Semin. Cancer Biol.* **33**, 86–92 (2015).
25. Sica, V., Galluzzi, L., Bravo-San Pedro, J. M., Izzo, V., Maiuri, M. C. & Kroemer, G. Organelle-specific initiation of autophagy. *Mol. Cell* **59**, 522–539 (2015).
26. Yoshii, S. R. & Mizushima, N. Monitoring and measuring autophagy. *Int. J. Mol. Sci.* **18**, 1865 (2017).
27. Liu, Y., Kang, X., Niu, G., He, S., Zhang, T., Bai, Y. et al. Shikonin induces apoptosis and prosurvival autophagy in human melanoma A375 cells via ROS-mediated ER stress and p38 pathways. *Artif. Cells, Nanomed., Biotechnol.* **47**, 626–635 (2019).
28. Kim, W., Lee, S., Seo, D., Kim, K., Kim, E. et al. Cellular stress responses in radiotherapy. *Cells* **8**, 1105 (2019).
29. Chen, H. M., Wang, P. H., Chen, S. S., Wen, C. C., Chen, Y. H., Yang, W. C. et al. Shikonin induces immunogenic cell death in tumor cells and enhances dendritic cell-based cancer vaccine. *Cancer Immunol. Immunother.* **61**, 1989–2002 (2012).
30. Obeid, M., Panaretakis, T., Joza, N., Tufi, R., Tesniere, A., van Endert, P. et al. Calreticulin exposure is required for the immunogenicity of γ-irradiation and UVC light-induced apoptosis. *Cell Death Differ.* **14**, 1848–1850 (2007).
31. Xu, C., Bailly-Maitre, B. & Reed, J. C. Endoplasmic reticulum stress: Cell life and death decisions. *J. Clin. Investig.* **115**, 2656–2664 (2005).
32. Garg, A. D., Romano, E., Rufo, N. & Agostinis, P. Immunogenic versus tolerogenic phagocytosis during anticancer therapy: mechanisms and clinical translation. *Cell Death Differ.* **23**, 938 951 (2016).
33. Li, L., Li, Y., Yang, C. H., Radford, D. C., Wang, J., Janát-Amsbury, M. et al. Inhibition of immunosuppressive tumors by polymer-assisted inductions of immunogenic cell death and multivalent PD-L1 crosslinking. *Adv. Funct. Mater.* **30**, 1–13 (2020).
34. Sang, H., Pisarev, V. M., Chavez, J., Robinson, S., Guo, Y., Hatcher, L. et al. Murine mammary adenocarcinoma cells transfected with p53 and/or Flt3L induce antitumor immune responses. *Cancer Gene Ther.* **12**, 427–437 (2005).

35. Puzio-Kuter, A. M. The role of p53 in metabolic regulation. Genes Cancer 2, 385–391 (2011).

36. Uscanga-Palomeque, A. C., Calvillo-Rodríguez, K. M., Gómez-Morales, L., Lardé, E., Denèfle, T., Caballero-Hernández, D. et al. CD47 agonist peptide PKHB1 induces immunogenic cell death in T-cell acute lymphoblastic leukemia cells. Cancer Sci. 110, 256–268 (2019).

37. Ocadlikova, D., Lecciso, M., Isidori, A., Loscocco, F., Visani, G., Amadori, S. et al. Chemotherapy-induced tumor cell death at the crossroads between immunogenicity and immunotolerance: focus on acute myeloid leukemia. Front Oncol. 9, 1–10 (2019).

38. Wu, J. & Waxman, D. J. Immunogenic chemotherapy: Dose and schedule dependence and combination with immunotherapy. Cancer Lett. 419, 210–221 (2018).

39. Rossi, A., Lucarini, V., Macchia, I., Sestili, P., Buccione, C., Donati, S. et al. Tumor-intrinsic or drug-induced immunogenicity dictates the therapeutic success of the PD1/PDL axis blockade. Cells 9, 1–21 (2020).

40. Zanotto-filho, A., Masamsetti, V. P., Loranc, E., Tonapi, S. S., Bernard, X., Bishop, A. J. R. et al. Alkylating agent induced NRF2 blocks endoplasmic reticulum stress-mediated apoptosis via control of glutathione pools and protein thiol homeostasis. Mol. Cancer Ther. 15, 3000–3014 (2017).

41. Yoon S., Park S. J., Han J. H., Kang J. H., Kim J. H., Lee J., et al. Caspase-dependent cell death-associated release of nucleosome and damage-associated molecular patterns. Cell Death Dis. https://doi.org/10.1038/cddis.2014.450 (2014).

42. Casares, N., Pequignot, M. O., Tesniere, A., Ghiringhelli, F., Roux, S., Chaput, N. et al. Caspase-dependent immunogenicity of doxorubicin-induced tumor cell death. J. Exp. Med. 202, 1691–1701 (2005).

43. Garg, A. D., Krysko, D. V., Verfaillie, T., Kaczmarek, A., Ferreira, G. B., Marysael, T. et al. A novel pathway combining calreticulin exposure and ATP secretion in immunogenic cancer cell death. EMBO J. 31, 1062–1079 (2012).

44. Boyd-Tressler, A., Penuela, S., Laird, D. W. & Dubyak, G. R. Chemotherapeutic drugs induce ATP release via caspase-gated pannexin-1 channels and a caspase/pannexin-1-independent mechanism. J. Biol. Chem. 289, 27246–27263 (2014).

45. Garg, A. D., Dudek, A. M., Ferreira, G. B., Verfaillie, T., Vandenabeele, P., Krysko, D. V. et al. ROS-induced autophagy in cancer cells assists in evasion from determinants of immunogenic cell death. Autophagy 9, 1292–1307 (2013).

46. Schiavoni, G., Sistigu, A., Valentini, M., Mattei, F., Sestili, P., Spadaro, F. et al. Cyclophosphamide synergizes with type I interferons through systemic dendritic cell reactivation and induction of immunogenic tumor apoptosis. Cancer Res. 71, 768–778 (2011).

47. Kim, S. K., Yun, C. H. & Han, S. H. Enhanced anti-cancer activity of human dendritic cells sensitized with gamma-irradiation-induced apoptotic colon cancer cells. Cancer Lett. 335, 278–288 (2013).

48. Ghiringhelli, F., Apetoh, L., Tesniere, A., Aymeric, L., Ma, Y., Ortiz, C. et al. Activation of the NLRP3 inflammasome in dendritic cells induces IL-1β-dependent adaptive immunity against tumors. Nat. Med. 15, 1170–1178 (2009).

49. Cirone M., Di Renzo L., Lotti L. V., Conte V., Trivedi P., Santarelli R. et al. Primary effusion lymphoma cell death induced by bortezomib and AG 490 activates dendritic cells through CD91. PLoS ONE https://doi.org/10.1371/journal.pone.0031732 (2012).

50. Martínez-Torres A. C., Calvillo-Rodríguez K. M., Uscanga-Palomeque A. C., Gómez-Morales L., Mendoza-Reveles R., Caballero-Hernández D. et al. PKHB1 tumor cell lysate induces antitumor immune system stimulation and tumor regression in syngeneic mice with tumoral T lymphoblasts. J. Oncol. https://doi.org/10.1155/2019/9852361 (2019).

51. Dudek, A. M., Martin, S., Garg, A. D. & Agostinis, P. Immature, semi-mature, and fully mature dendritic cells: Toward a DC-cancer cells interface that augments anticancer immunity. Front. Immunol. 4, 438 (2013).

52. Menger L., Vacchelli E., Adjemian S., Martins I., Ma Y., Shen S., et al. Cardiac glycosides exert anticancer effects by inducing immunogenic cell death. Sci. Transl. Med. https://doi.org/10.1126/scitranslmed.3003807 (2012).

53. Tesniere, A., Schlemmer, F., Boige, V., Kepp, O., Martins, I., Ghiringhelli, F. et al. Immunogenic death of colon cancer cells treated with oxaliplatin. Oncogene 29, 482–491 (2010).

54. Rossi, A., Pakhomova, O. N., Mollica, P. A., Casciola, M., Mangalanathan, U., Pakhomov, A. G. et al. Nanosecond pulsed electric fields induce endoplasmic reticulum stress accompanied by immunogenic cell death in murine models of lymphoma and colorectal cancer. Cancers 11, 2034 (2019).

55. Qin, J., Kunda, N., Qiao, G., Calata, J. F., Pardiwala, K., Prabhakar, B. S. et al. Colon cancer cell treatment with rose bengal generates a protective immune response via immunogenic cell death. Cell Death Dis. 8, e2584 (2017).

56. Liu, P., Zhao, L., Pol, J., Levesque, S., Petrazzuolo, A., Pfirschke, C. et al. Crizotinib-induced immunogenic cell death in non-small cell lung cancer. Nat. Commun. 10, 1486 (2019).

57. Pennock, N. D., White, J. T., Cross, E. W., Cheney, E. E., Tamburini, B. A. & Kedl, R. M. T cell responses: naïve to memory and everything in between. Adv. Physiol. Educ. 37, 273–283 (2013).

58. Punt J., Stranford S. A., Jones P. P. & Owen J. A. (eds). Kuby Immunology, 8th edn. (McGraw-Hill Education, New York, USA; 2019).

59. Maddur, M. S., Kaveri, S. V. & Bayry, J. Induction of human dendritic cell maturation by naïve and memory B-cell subsets requires different activation stimuli. Cell. Mol. Immunol. 15, 1074–1076 (2018).

60. Ravkov, E. V. & Williams, M. A. The magnitude of CD4+ T cell recall responses is controlled by the duration of the secondary stimulus. J. Immunol. 183, 2382–2389 (2009).

61. MacLeod, M. K. L., McKee, A., Crawford, F., White, J., Kappler, J. & Marrack, P. CD4 memory T cells divide poorly in response to antigen because of their cytokine profile. Proc. Natl Acad. Sci. USA 105, 14521–14526 (2008).

62. Berger, A. Science commentary: Th1 and Th2 responses: what are they? Br. Med. J. 321, 424 (2000).

63. Santana-Krímskaya, S. E., Franco-Molina, M. A., Zárate-Triviño, D. G., Prado-García, H., Zapata-Benavides, P., Torres-del-Muro, F. et al. IMMUNEPOTENT CRP plus doxorubicin/cyclophosphamide chemotherapy remodel the tumor microenvironment in an air pouch triple-negative breast cancer murine model. Biomed. Pharmacother. https://doi.org/10.1016/j.biopha.2020.110062 (2020).

CONCLUSIONS

From the results obtained in the present thesis work we can conclude that the treatment with PKHB1 and Immunepotent-CRP induces cell death and DAMPs' release breast cancer cells. Also, both treatments can induce the antitumor immune system activation (*ex vivo*) through the maturation of dendritic cells and the activation of specific T cells responses without the use of adjuvants. Furthermore, the gold standard for the immunogenic cell death inductors was confirmed for PKHB1 and Immunepotent-CRP in a breast cancer tumor model. Additionally, the PKHB1-ICD and ICRP-ICD induces tumor regression as a therapeutic antitumor strategy. Finally, it was observed for first time that PKHB1-ICD and ICRP-ICD can induce a long-lasting antitumor immunity.

The results obtained in this work provide the evidence of a new ICD inductors for breast cancer cells and highlight a new approach of Thrombospondin-mimic peptides and dialyzable leukocyte extracts, which could induce ICD in others cancer cells.

PERSPECTIVES

- To evaluate the immunogenicity of the cell death induced by PKHB1 and ICRP in resistant cancer cells from patients, to confirm their efficacy and possible application in clinical trials.

- DCs-vaccines are one of the main immunotherapies recently employed for different types of cancer. Thus, it's important to determine the immunogenicity of cell death induced by PKHB1 and ICRP in *ex vivo* experiments using cancer cells from patients and DCs differentiated from human monocytes, to demonstrate if the cell death induced by PKHB1 or ICRP could be used in DCs-vaccines for humans.

- To evaluate the role of the innate immune system in the immunogenic cell death induced by PKHB1 or ICRP, to find key regulators in the response triggered for the tumor elimination.

- As ICD could occur in response to infection, it's important to determine if PKHB1 or ICRP could induce immunogenic cell death in infected models using virus, bacteria, among other pathogens.

- To evaluate the combinatorial effect (antagonistic, additive or synergistic) of PKHB1 with chemotherapies or immunotherapies for to determine the potential application of PKHB1 in combinatorial strategies *in vivo*.

- Determine the maximum tolerated dose of PKHB1 in mice, to provide the basis for choosing the range of peptide that can be used without adverse effects.

- It has been evaluated that TSP-1-CD47 axis have different effects in the immune system, such as activation, proliferation, migration, and cell

death. Thus, it's important to determine if PKHB1 could have a direct effect in healthy and autoreactive immune system cells

REFERENCES

Ahmed, Asma, and Stephen W.G. Tait. 2020. "Targeting Immunogenic Cell Death in Cancer." *Molecular Oncology* 14(12).

Barclay, A. Neil. 2009. "Signal Regulatory Protein Alpha (SIRPα)/CD47 Interaction and Function." *Current Opinion in Immunology*.

Barclay, A Neil, and Timo K Van den Berg. 2014. "The Interaction between Signal Regulatory Protein Alpha (SIRPα) and CD47: Structure, Function, and Therapeutic Target." *Annual review of immunology* 32: 25–50.

Calippe, Bertrand et al. 2017. "Complement Factor H Inhibits CD47-Mediated Resolution of Inflammation." *Immunity*.

"Cancer." https://www.who.int/news-room/fact-sheets/detail/cancer (April 11, 2023).

Cha, Jong Ho, Li Chuan Chan, Min Sup Song, and Mien Chie Hung. 2020. "New Approaches on Cancer Immunotherapy." *Cold Spring Harbor Perspectives in Medicine* 10(8).

Chang, Renee B., and Gregory L. Beatty. 2020. "The Interplay between Innate and Adaptive Immunity in Cancer Shapes the Productivity of Cancer Immunosurveillance." *Journal of Leukocyte Biology* 108(1).

Chao, Mark P., Irving L. Weissman, and Ravindra Majeti. 2012. "The CD47-SIRPα Pathway in Cancer Immune Evasion and Potential Therapeutic Implications." *Current Opinion in Immunology*.

Danese, Alberto et al. 2021. "Cell Death as a Result of Calcium Signaling Modulation: A Cancer-Centric Prospective." *Biochimica et Biophysica Acta (BBA) - Molecular Cell Research* 1868(8): 119061.

Denèfle, Thomas et al. 2016. "Thrombospondin-1 Mimetic Agonist Peptides Induce Selective Death in Tumor Cells: Design, Synthesis, and Structure–Activity Relationship Studies." *Journal of Medicinal Chemistry* 59(18): 8412–21. http://pubs.acs.org/doi/10.1021/acs.jmedchem.6b00781 (December 21, 2018).

DePeaux, Kristin, and Greg M. Delgoffe. 2021. "Metabolic Barriers to Cancer Immunotherapy." *Nature Reviews Immunology* 21(12).

Dias, Ana S., Catarina R. Almeida, Luisa A. Helguero, and Iola F. Duarte. 2019. "Metabolic Crosstalk in the Breast Cancer Microenvironment." *European Journal of Cancer* 121: 154–71.

Dunn, Gavin P., Lloyd J. Old, and Robert D. Schreiber. 2004. "The Three Es of Cancer Immunoediting." *https://doi.org/10.1146/annurev.immunol.22.012703.104803* 22: 329–60. https://www.annualreviews.org/doi/abs/10.1146/annurev.immunol.22.012703.104803 (April 13, 2023).

Dunn, Gavin P et al. 2002. "Cancer Immunoediting: From Immunosurveillance to Tumor Escape." *Nature immunology*.

Elliott, Michael R. et al. 2009. "Nucleotides Released by Apoptotic Cells Act as a Find-Me Signal to Promote Phagocytic Clearance." *Nature*.

Franco-Molina, M. A. et al. 2006. "In Vitro Effects of Bovine Dialyzable Leukocyte Extract (BDLE) in Cancer Cells." *Cytotherapy* 8(4): 408–14.

———. 2008. "IMMUNEPOTENT CRP (Bovine Dialyzable Leukocyte Extract) Adjuvant Immunotherapy: A Phase I Study in Non-Small Cell Lung Cancer Patients." *Cytotherapy* 10(5): 490–96.

Franco-Molina, Moisés A. et al. 2004. "Bovine Dialyzable Leukocyte Extract Protects against LPS-Induced, Murine Endotoxic Shock." *International Immunopharmacology* 4(13): 1577–86.

———. 2010. "Antiangiogenic and Antitumor Effects of IMMUNEPOTENT CRP in Murine Melanoma." *Immunopharmacology and Immunotoxicology* 32(4): 637–46.

Franco-Molina, Moisés A et al. 2011. "Anti-Inflammatory and Antioxidant Effects of

IMMUNEPOTENT CRP in Lipopolysaccharide (LPS)-Stimulated Human Macrophages." *African Journal of Microbiology Research* 5(22): 3726–36.

Franco-Molina, Moisés Armides et al. 2005. "Bovine Dialyzable Leukocyte Extract Modulates the Nitric Oxide and Proinflammatory Cytokine Production in Lipopolysaccharide-Stimulated Murine Peritoneal Macrophages in Vitro." *Journal of Medicinal Food* 8(1): 20–26.

Galluzzi, L. et al. 2015. "Essential versus Accessory Aspects of Cell Death: Recommendations of the NCCD 2015." *Cell Death and Differentiation*.

Galluzzi, L et al. 2012. "Molecular Definitions of Cell Death Subroutines: Recommendations of the Nomenclature Committee on Cell Death 2012." *Cell death and differentiation*.

Galluzzi, Lorenzo et al. 2017. "Immunogenic Cell Death in Cancer and Infectious Disease." *Nature Reviews Immunology*.

———. 2018. "Molecular Mechanisms of Cell Death: Recommendations of the Nomenclature Committee on Cell Death 2018." *Cell Death and Differentiation* 25(3): 486–541.

Garg, Abhishek D., and Patrizia Agostinis. 2017. "Cell Death and Immunity in Cancer: From Danger Signals to Mimicry of Pathogen Defense Responses." *Immunological Reviews* 280(1).

Garg, Abhishek D, Aleksandra M Dudek-Peric, Erminia Romano, and Patrizia Agostinis. 2015. "Immunogenic Cell Death." *The International journal of developmental biology* 59(1–3): 131–40. http://www.ncbi.nlm.nih.gov/pubmed/26374534 (December 21, 2018).

Ghiringhelli, François et al. 2009. "Activation of the NLRP3 Inflammasome in Dendritic Cells Induces IL-1B-Dependent Adaptive Immunity against Tumors." *Nature Medicine*.

Gicobi, Joanina K., Whitney Barham, and Haidong Dong. 2020. "Immune Resilience in Response to Cancer Therapy." *Cancer Immunology, Immunotherapy* 69(11): 2165–67. https://link.springer.com/article/10.1007/s00262-020-02731-4 (April 12, 2023).

Gubin, Matthew M., and Matthew D. Vesely. 2022. "Cancer Immunoediting in the Era of Immuno-Oncology." *Clinical cancer research : an official journal of the American Association for Cancer Research* 28(18): 3917–28. /pmc/articles/PMC9481657/ (April 12, 2023).

Gutierrez, Linda S., Zenaida Lopez-Dee, and Kenneth Pidcock. 2011. "Thrombospondin-1: Multiple Paths to Inflammation." *Mediators of Inflammation*.

Hanahan, Douglas. 2022. "Hallmarks of Cancer: New Dimensions." *Cancer Discovery* 12(1): 31–46. https://aacrjournals.org/cancerdiscovery/article/12/1/31/675608/Hallmarks-of-Cancer-New-DimensionsHallmarks-of (April 11, 2023).

Hanahan, Douglas, and Robert A Weinberg. 2011. "Hallmarks of Cancer: The next Generation." *Cell*.

Hollingsworth, Robert E., and Kathrin Jansen. 2019. "Turning the Corner on Therapeutic Cancer Vaccines." *npj Vaccines* 4(1).

Isenberg, Jeff S. et al. 2006. "CD47 Is Necessary for Inhibition of Nitric Oxide-Stimulated Vascular Cell Responses by Thrombospondin-1." *Journal of Biological Chemistry*.

———. 2009. "Differential Interactions of Thrombospondin-1, -2, and -4 with CD47 and Effects on CGMP Signaling and Ischemic Injury Responses." *Journal of Biological Chemistry*.

Jaiswal, Siddhartha et al. 2009. "CD47 Is Upregulated on Circulating Hematopoietic Stem Cells and Leukemia Cells to Avoid Phagocytosis." *Cell* 138(2): 271–85.

Kanda, Shigeru et al. 1999. "Role of Thrombospondin-1-Derived Peptide, 4N1K, in FGF-2-Induced Angiogenesis." *Experimental Cell Research*.

Keenan, Bridget P., and Elizabeth M. Jaffee. 2012. "Whole Cell Vaccines - Past Progress and Future Strategies." *Seminars in Oncology* 39(3).

Kepp, Oliver et al. 2011. "Molecular Determinants of Immunogenic Cell Death Elicited by Anticancer Chemotherapy." *Cancer and Metastasis Reviews*.

———. 2014. "Consensus Guidelines for the Detection of Immunogenic Cell Death." *OncoImmunology*.

Kroemer, Guido, Lorenzo Galluzzi, Oliver Kepp, and Laurence Zitvogel. 2013. "Immunogenic Cell Death in Cancer Therapy." *Annual Review of Immunology*.

Land, Walter G. 2015. "The Role of Damage-Associated Molecular Patterns (DAMPs) in Human Diseases Part II: DAMPs as Diagnostics, Prognostics and Therapeutics in Clinical Medicine." *Sultan Qaboos University Medical Journal* 15(2): e157–70.

Lara, Humberto H. et al. 2010. "Clinical and Immunological Assessment in Breast Cancer Patients Receiving Anticancer Therapy and Bovine Dialyzable Leukocyte Extract as an Adjuvant." *Experimental and Therapeutic Medicine* 1(3): 425–31.

Leclair, Pascal et al. 2018. "CD47-Ligation Induced Cell Death in T-Acute Lymphoblastic Leukemia Article." *Cell Death and Disease* 9(5).

Li, Ming O. et al. 2021. "Innate Immune Cells in the Tumor Microenvironment." *Cancer Cell* 39(6).

Liu, Jian et al. 2022. "Cancer Vaccines as Promising Immuno-Therapeutics: Platforms and Current Progress." *Journal of Hematology & Oncology 2022 15:1* 15(1): 1–26. https://jhoonline.biomedcentral.com/articles/10.1186/s13045-022-01247-x (April 24, 2023).

Lussier, Danielle M., and Robert D. Schreiber. 2016. "Cancer Immunosurveillance: Immunoediting." *Encyclopedia of Immunobiology* 4: 396–405.

Ma, Yang, Galina V. Shurin, Zhu Peiyuan, and Michael R. Shurin. 2013. "Dendritic Cells in the Cancer Microenvironment." *Journal of Cancer* 4(1).

Maiorino, Laura, Juliane Daßler-Plenker, Lijuan Sun, and Mikala Egeblad. 2022. "Innate Immunity and Cancer Pathophysiology." *https://doi.org/10.1146/annurev-pathmechdis-032221-115501* 17: 425–57. https://www.annualreviews.org/doi/abs/10.1146/annurev-pathmechdis-032221-115501 (April 19, 2023).

Majeti, Ravindra et al. 2009. "CD47 Is an Adverse Prognostic Factor and Therapeutic Antibody Target on Human Acute Myeloid Leukemia Stem Cells." *Cell* 138(2): 286–99.

Manna, Partha Pratim, and William A. Frazier. 2004. "CD47 Mediates Killing of Breast Tumor Cells via Gi-Dependent Inhibition of Protein Kinase A." *Cancer Research*.

Martinelli, Roberta et al. 2013. "Novel Role of CD47 in Rat Microvascular Endothelium: Signaling and Regulation of T-Cell Transendothelial Migration." *Arteriosclerosis, Thrombosis, and Vascular Biology*.

Martinez-Torres, Ana-Carolina et al. 2015. "CD47 Agonist Peptides Induce Programmed Cell Death in Refractory Chronic Lymphocytic Leukemia B Cells via PLCγ1 Activation: Evidence from Mice and Humans" ed. Shigekazu Nagata. *PLOS Medicine* 12(3): e1001796. https://dx.plos.org/10.1371/journal.pmed.1001796 (December 21, 2018).

Martinez-Torres, Ana Carolina et al. 2019. "Cytotoxic Activity of IMMUNEPOTENT CRP against Non-Small Cell Lung Cancer Cell Lines." *PeerJ* 2019(9).

Martínez-Torres, Ana Carolina et al. 2018. "IMMUNEPOTENT CRP Induces Cell Cycle Arrest and Caspase-Independent Regulated Cell Death in HeLa Cells through Reactive Oxygen Species Production." *BMC Cancer* 18. https://www.ncbi.nlm.nih.gov/pmc/articles/PMC5753472/ (March 25, 2019).

———. 2020. "IMMUNEPOTENT CRP Induces DAMPS Release and ROS-Dependent Autophagosome Formation in HeLa and MCF-7 Cells." *BMC Cancer 2020 20:1* 20(1): 1–11. https://bmccancer.biomedcentral.com/articles/10.1186/s12885-020-07124-5 (August 26, 2021).

Mateo, V. et al. 1999a. "CD47 Ligation Induces Caspase-Independent Cell Death in Chronic Lymphocytic Leukemia." *Nature Medicine*.

———. 1999b. "CD47 Ligation Induces Caspase-Independent Cell Death in Chronic Lymphocytic Leukemia." *Nature Medicine* 5(11): 1277–84. http://www.nature.com/articles/nm1199_1277 (December 21, 2018).

Miao, Lei, Yu Zhang, and Leaf Huang. 2021. "MRNA Vaccine for Cancer Immunotherapy." *Molecular Cancer* 20(1).

Mirochnik, Y., A. Kwiatek, and O. Volpert. 2008. "Thrombospondin and Apoptosis: Molecular Mechanisms and Use for Design of Complementation Treatments." *Current Drug Targets*.

Mishra, Alok K. et al. 2022. "Emerging Trends in Immunotherapy for Cancer." *Diseases* 10(3).

Monteith, Gregory R., Natalia Prevarskaya, and Sarah J. Roberts-Thomson. 2017. "The Calcium–Cancer Signalling Nexus." *Nature Reviews Cancer 2017 17:6* 17(6): 373–80. https://www.nature.com/articles/nrc.2017.18 (August 30, 2021).

Morse, Michael A., William R. Gwin, and Duane A. Mitchell. 2021. "Vaccine Therapies for Cancer: Then and Now." *Targeted Oncology* 16(2).

Navarro-Alvarez, Nalu, and Yong Guang Yang. 2011. "CD47: A New Player in Phagocytosis and Xenograft Rejection." *Cellular and Molecular Immunology*.

Obeid, Michel et al. 2007. "Calreticulin Exposure Dictates the Immunogenicity of Cancer Cell Death." *Nature Medicine* 13(1): 54–61. http://www.nature.com/articles/nm1523 (December 21, 2018).

Oldenborg, Per-Arne. 2013. "CD47: A Cell Surface Glycoprotein Which Regulates Multiple Functions of Hematopoietic Cells in Health and Disease." *ISRN Hematology*.

Perez, Caleb R., and Michele De Palma. 2019. "Engineering Dendritic Cell Vaccines to Improve Cancer Immunotherapy." *Nature Communications* 10(1).

Riley, Rachel S., Carl H. June, Robert Langer, and Michael J. Mitchell. 2019. "Delivery Technologies for Cancer Immunotherapy." *Nature Reviews Drug Discovery* 18(3).

Roberts, David D. et al. 2012. "The Matricellular Protein Thrombospondin-1 Globally Regulates Cardiovascular Function and Responses to Stress via CD47." *Matrix Biology*.

Rodríguez-Salazar, Maria Del Carmen et al. 2017. "The Novel Immunomodulator IMMUNEPOTENT CRP Combined with Chemotherapy Agent Increased the Rate of Immunogenic Cell Death and Prevented Melanoma Growth." *Oncology Letters* 14(1): 844–52.

Sabado, Rachel L., Sreekumar Balan, and Nina Bhardwaj. 2017. "Dendritic Cell-Based Immunotherapy." *Cell Research* 27(1).

Sadeghi Najafabadi, Seyed Amir, Azam Bolhassani, and Mohammad Reza Aghasadeghi. 2022. "Tumor Cell-Based Vaccine: An Effective Strategy for Eradication of Cancer Cells." *Immunotherapy* 14(8).

Santana-Krímskaya, Silvia Elena et al. 2020. "IMMUNEPOTENT CRP plus Doxorubicin/Cyclophosphamide Chemotherapy Remodel the Tumor Microenvironment in an Air Pouch Triple-Negative Breast Cancer Murine Model." *Biomedicine and Pharmacotherapy* 126: 110062.

Sarfati, Marika, Genevieve Fortin, Marianne Raymond, and Santos Susin. 2008. "CD47 in the Immune Response: Role of Thrombospondin and SIRP-α Reverse Signaling." *Current Drug Targets*.

Saumet, Anne et al. 2005. "Type 3 Repeat/C-Terminal Domain of Thrombospondin-1 Triggers Caspase-Independent Cell Death through CD47/Avβ3 in Promyelocytic Leukemia NB4 Cells." *Blood*.

Schreiber, Robert D., Lloyd J. Old, and Mark J. Smyth. 2011. "Cancer Immunoediting: Integrating Immunity's Roles in Cancer Suppression and Promotion." *Science* 331(6024): 1565–70. https://www.science.org/doi/10.1126/science.1203486 (April 13, 2023).

Shihab, Israa et al. 2020. "Understanding the Role of Innate Immune Cells and Identifying Genes in Breast Cancer Microenvironment." *Cancers* 12(8).

Showalter, Anne et al. 2017. "Cytokines in Immunogenic Cell Death: Applications for Cancer Immunotherapy." *Cytokine*.

Sierra-Rivera, Crystel A. et al. 2016. "Effect of Bovine Dialyzable Leukocyte Extract on Induction of Cell Differentiation and Death in K562 Human Chronic Myelogenous Leukemia Cells." *Oncology Letters* 12(6): 4449–60.

Sjostrom, J. 2001. "How Apoptosis Is Regulated, and What Goes Wrong in Cancer." *BMJ*.

Smyth, Mark J., Gavin P. Dunn, and Robert D. Schreiber. 2006. "Cancer Immunosurveillance and Immunoediting: The Roles of Immunity in Suppressing Tumor Development and Shaping Tumor Immunogenicity." *Advances in Immunology* 90: 1–50.

Soto-Pantoja, David R., Sukhbir Kaur, and David D. Roberts. 2015. "CD47 Signaling Pathways Controlling Cellular Differentiation and Responses to Stress." *Critical Reviews in Biochemistry and Molecular Biology*.

Soysal, Savas D., Alexandar Tzankov, and Simone E. Muenst. 2015. "Role of the Tumor Microenvironment in Breast Cancer." *Pathobiology* 82(3–4).

Subramanian, Shyamsundar, Eric T. Boder, and Dennis E. Discher. 2007. "Phylogenetic Divergence of CD47 Interactions with Human Signal Regulatory Protein α Reveals Locus of Species Specificity: Implications for the Binding Site." *Journal of Biological Chemistry*.

Sung, Hyuna et al. 2021. "Global Cancer Statistics 2020: GLOBOCAN Estimates of Incidence and Mortality Worldwide for 36 Cancers in 185 Countries." *CA: A Cancer Journal for Clinicians* 71(3): 209–49. https://onlinelibrary.wiley.com/doi/full/10.3322/caac.21660 (February 7, 2022).

Tan, Shuzhen, Dongpei Li, and Xiao Zhu. 2020. "Cancer Immunotherapy: Pros, Cons and Beyond." *Biomedicine and Pharmacotherapy* 124.

Tang, Daolin et al. 2019. "The Molecular Machinery of Regulated Cell Death." *Cell Research* 29(5).

Tešić, Nataša, Primož Poženel, and Urban Švajger. 2021. "Overview of Cellular Immunotherapies within Transfusion Medicine for the Treatment of Malignant Diseases." *International Journal of Molecular Sciences* 22(10).

Tesniere, A. et al. 2008. "Molecular Characteristics of Immunogenic Cancer Cell Death." *Cell Death and Differentiation*.

Uno, Shinsuke et al. 2007. "Antitumor Activity of a Monoclonal Antibody against CD47 in Xenograft Models of Human Leukemia." *Oncology Reports*.

Uscanga-Palomeque, Ashanti Concepción et al. 2018. "CD 47 Agonist Peptide PKHB 1 Induces Immunogenic Cell Death in T-cell Acute Lymphoblastic Leukemia Cells." *Cancer Science*: cas.13885. https://onlinelibrary.wiley.com/doi/abs/10.1111/cas.13885 (December 21, 2018).

Vesely, Matthew D., Michael H. Kershaw, Robert D. Schreiber, and Mark J. Smyth. 2011. "Natural Innate and Adaptive Immunity to Cancer." *https://doi.org/10.1146/annurev-immunol-031210-101324* 29: 235–71. https://www.annualreviews.org/doi/abs/10.1146/annurev-immunol-031210-101324 (April 12, 2023).

Wright, Jordan J., Alvin C. Powers, and Douglas B. Johnson. 2021. "Endocrine Toxicities of Immune Checkpoint Inhibitors." *Nature Reviews Endocrinology* 17(7).

Zhivotovsky, Boris, and Sten Orrenius. 2011. "Calcium and Cell Death Mechanisms: A Perspective from the Cell Death Community." *Cell Calcium* 50(3): 211–21.

Zitvogel, Laurence, Antoine Tesniere, and Guido Kroemer. 2006. "Cancer despite Immunosurveillance: Immunoselection and Immunosubversion." *Nature Reviews Immunology 2006 6:10* 6(10): 715–27. https://www.nature.com/articles/nri1936 (April 17, 2023).